OPTOGENETIC ANALYSIS OF EXCITATORY AND INHIBITORY NEUROTRANSMISSION IN THE ENTERIC NERVOUS SYSTEM

By

Alberto L. Perez-Medina

A DISSERTATION

Submitted to
Michigan State University
in partial fulfillment of the requirements
for the degree of

Pharmacology and Toxicology-Doctor of Philosophy

2019

ABSTRACT

OPTOGENETIC ANALYSIS OF EXCITATORY AND INHIBITORY NEUROTRANSMISSION IN THE ENTERIC NERVOUS SYSTEM

By

Alberto L. Perez-Medina

The enteric nervous system (ENS) is embedded within the gastrointestinal (GI) tract and controls GI function. Impaired ENS function leads to altered patterns of motility and secretion, causing GI disease. For instance, functional gastrointestinal disorders (FGID) are caused by poorly understood alterations in the structure and function of nerves and other cell types in the GI tract. These disorders comprise about 41% of the total GI complications in the United States, and altered patterns of motility that occur in the GI muscles is a hallmark characteristic of FGIDs. Although the ENS is fairly understood, further elucidation of the enteric circuitry that governs GI motility would help to understand the pathophysiology of FGID. For that reason, identifying the contributions of classes of enteric neurons that control GI motility and secretion could aid in the identification of novel therapeutic targets for the treatment of FGIDs. A widely used method to study neural control of GI motility is sharp-electrode electrophysiological recordings from the smooth muscle or enteric neurons. Conventional electrophysiological recordings rely on electrical stimulation of enteric neurons which will activate all neurons in an ex vivo preparation of the ENS, and does not allow cell-specific activation of individual subpopulations of myenteric neurons. To overcome this problem, we used immunohistochemical methods to identify subpopulations of myenteric neurons and the optogenetically activated protein channelrhodopsin-2 (ChR2) that can be selectively expressed in subsets of enteric neurons. In Chapter 3, immunohistochemical studies of the mouse enteric nervous system are performed using the purinergic neuronal marker, vesicular nucleotide transporter (VNUT) along with markers for specific subsets of myenteric neurons and nerve fibers (e.g., neuronal nitric oxide synthase, choline acetyltransferase, calretinin, calbindin, and tyrosine hydroxylase). Chapter 4 compares electrical and optogenetic

electrophysiology recordings from myenteric neurons of mice that express ChR2 in nNOS neurons. The studies described in Chapter 5 use ChAT-ChR2-YFP-BAC transgenic mice which have eYFP tagged ChR2 expressed in cholinergic neurons. Optogenetics was used to isolate the cholinergic component of the ENS. The findings discussed in this dissertation provides evidence of a more sophisticated enteric circuitry of GI motility. (1) Purinergic neurons are likely a separate subpopulation of enteric neurons. VNUT is only expressed in the form of punctate varicosities at the nerve fibers and is not endogenously expressed in the soma of enteric neurons. VNUT also does not colocalize with other of the tested neuronal immunoreactive markers. (2) BLS of ChR2 expressed in nNOS neurons induced a purinergic/nitrergic biphasic IJP, suggesting that nNOS IMNs co-releases a purine as a neurotransmitter. Expression of ChR2 in non-nNOS neurons could explain the biphasic IJP responses during electrophysiology recordings. Hence, the existence of separate subset populations of IMN populations (e.g., nNOS only and purinergic only IMNs) can't be ruled out. (3) BLS of ChR2 expressed in ChAT positive neurons induced EJPs and IJP responses. Inhibition of the nicotinic ACh receptor (nAChR) with mecamylamine significantly reduced the light-evoked IJP. Bath application of the purinergic $P2Y_1$ antagonist, MRS 2179, was sufficient to abolish the IJP response, while the muscarinic ACh receptor antagonist, Scopolamine, abolished the EJP response. The data suggest that BLS of ChR2 activates cholinergic EMNs and cholinergic interneurons, and that activation of the cholinergic interneurons activates purinergic only IMNs that supply the smooth muscle, resulting in a predominant purinergic only IJP. Taken together, this work provides evidence for a diverse and more complex enteric neural circuit of GI motility. Future experiments should, however, focus on studying these enteric circuits at the level of the neuron, as these studies can provide a more in-depth analysis of the enteric circuitry.

ACKNOWLEDGMENTS

My growth as a scientist would have never come into fruition without the overwhelming support from some exceptional individuals. First, I would like to thank my advisor/mentor Dr. James J. Galligan, whom I have great respect and admiration. It's inconceivable for me to think that I would have come this far without his help. Thank you for your guidance, support, kindness, and endless positivism during my training. I also want to thank Dr. William Atchison, for taking a chance on me and allowing me to participate in the Bridge to Ph.D. in Neuroscience Program (BPNP). At that time, I was uncertain if I wanted to pursue a career as a scientist. However, the BPNP program reignited my spark for scientific curiosity and allowed me to meet incredible people such as my former mentor Dr. Alexandra (Alex) Colon-Rodriguez. Alex, thank you for your unconditional support, you were firm and sometimes harsh, but you were always fair and had my best interest in mind, and for that I thank you.

I want to thank Dr. Colleen Hegg for being a member of my committee. She also offered much guidance and support through my candidacy. Therefore, thank you for the valuable input in interpreting my results. I want to thank also Dr. Brian D. Gulbransen for being a member of my committee as well, for your valuable input regarding my data and training, and for allowing me to collaborate in some of the projects in your lab, in which I was able to work with Dr. Vladimir (Vlado) Grubisic in a recent publication. Vlado, thank you so much for allowing me to work with you on your project. I will always appreciate your insightful guidance, as well as your friendship.

My family has always been a pillar of support in my life. My mom, dad, brother, sister, and my wife have given me unconditional love, and the motivation in times where I need it the most. Most importantly, my wife, Carla, she is my rock, who always tries to keep my feet on the ground, make

me laugh and cheer me up. I consider myself fortunate to be in the daily presence of an amazing and beautiful human being she is.

I consider myself also fortunate to be surrounded by amazing friends that have supported me these years. My lab members Eileen, Nadine, Yogesh, Ryan, Marion, Roxanne, Xiaochun, Kibrom, Krishna, Emilie, and Emmy, thank you all for being my friends and making every day as unique as the day before. Thank you to my undergraduate students: Harim Delgado and Jazmin Sotomayor-Ortiz for allowing me to be your mentor and for your hard work. They demonstrated to be dedicated students, research scientist, and they challenge me every day to try to become a better mentor. I wish you all the best of success where ever life takes you. Lastly, I want to thank the great people that make up the Pharmacology and Toxicology department: Dr. Richard Neubig, Dr. Anne Dorrance, faculty, and the administration for all the guidance and assistance during these five years.

TABLE OF CONTENTS

LIST OF TABLES

LIST OF FIGURES

KEY TO ABBREVIATIONS

Gastrointestinal	GI
Enteric nervous system	ENS
Irritable bowel syndrome	IBS
Irritable bowel syndrome-constipation	IBS-C
Irritable bowel syndrome-diarrhea	IBS-D
Irritable bowel syndrome-mixed	IBS-M
Immunohistochemistry	IHC
Immunoreactive	ir
Fast inhibitory junction potential	fIJP
Slow inhibitory junction potential	sIJP
Neuronal nitric oxide synthase	nNOS; NOS
Resting membrane potential	RMP
Area under the curve	AUC
Wildtype	WT
Functional Gastrointestinal disorder	FGID
Interstitial cells of Cajal	ICC
Interstitial cells of Cajal-Myenteric plexus	ICC_{MY}
Interstitial cells of Cajal-submucosal plexus	ICC_{SM}
Interstitial cells of Cajal- deep muscular plexus	ICC_{DMP}
Interstitial cells of Cajal- circular smooth muscle layer	ICC_{IM}
Voltage-gated Ca^{2+} channels	VGCC
Complementary DNA	cDNA
fast excitatory postsynaptic potential	fEPSP

Tetrodotoxin	TTX
Early after-hyperpolarization	Early-AHP
Inward-rectifying K^+ channels	K_{ir}, IRK
Choline acetyltransferase	ChAT
Excitatory motor neuron	EMN
Inhibitory motor neuron	IMN
Longitudinal muscle myenteric plexus	LMMP
Electrical field stimulation	EFS
Blue light stimulation	BLS
5-Hydroxytrypyophan	5-HT
Tachykinins	TK
Nitric oxide	NO
Vesicular nucleotide transporter	VNUT
Adenosine triphosphate	ATP
Phospholipase C-β	PLC-β
Diacylglycerol	DAG
Inositol 1,4,5-triphosphate	IP_3
Muscarinic ACh receptor 2	M_2
Muscarinic ACh receptor 3	M_3
Ribonucleic acid	RNA
Adenyl cyclase / cyclic adenyl monophosphate	AC/cAMP
Calcium	Ca^{2+}
Tertiary plexus	tp
After-hyperpolarization	AH
After-hyperpolarizing potential	AHP

Synaptic	S
Motor neurons	MN
Interneurons	IN
Alpha1	α1
Tetraethylammonium	TEA
After-depolarizing potential	ADP
Intrinsic primary afferent neurons	IPAN
Extrinsic primary afferent neurons	EPAN
Myoelectric migrating motor complex	MMC
Colonic migrating motor complex	CMMC
High amplitude propagating contractions	HAPC
Enterochromaffin cells	EC
Platelet-derived growth factor positive-α-receptors	PDGFR*α*+
Platelet-derived growth factors	PDGF
Smooth muscle cell	SMC
Ca^{2+} activated K^{+} channel 3	SK3
SMC-ICC-PDGFR*α*+	SIP
small intestinal bacterial overgrowth	SIBO
Channelrhodopsin	ChR
Channelrhodopsin-1	ChR1
Channelrhodopsin-2	ChR2
Excitatory yellow fluorescent protein	eYFP
Adeno associated virus	AAV
Recombinant AAV	rAAV
Light-emitting diode	LED

Causes recombination	Cre
Locus of crossing (x) over, P1	LoxP
Bacteriophage	P1
Calcium translocating channelrhodopsin	CatCh

CHAPTER 1: GENERAL INTRODUCTION

THE ENTERIC NERVOUS SYSTEM

General Description

Embedded within the gastrointestinal tract (GI) wall is a network of 200-600 million neurons known as the enteric nervous system (ENS) (Langley, 1921). As a division of the autonomic nervous system, the ENS regulates secretion, electrolyte and water transport, and local blood flow and GI motility. GI motility enhances nutrient and water absorption and propels luminal content for defecation. ENS malfunction alters normal GI activity, resulting in changes in bowel habits, which often lead to constipation, diarrhea, nausea, vomiting, and abdominal pain. These symptoms are common among patients diagnosed with inflammatory bowel disease (IBD) or functional /motility disorders such as gastroparesis and the irritable bowel syndrome (IBS) (Antonioli *et al.*, 2013; Goyal *et al.*, 1996). The estimated annual health care expenditure for GI disease totals $135.9 billion. Moreover, a total of $5.9 billion are aggregates charges billed to patients diagnosed with abdominal pain and functional/motility disorders, and an estimated $4.0 billion for those diagnosed with IBD (Peery *et al.*, 2019). Treatments for GI motility disorders are only helpful in improving the symptoms; it does not offer a cure, and too often present side effects that can sometimes exacerbate GI complications. For instance, 5-HT_3 receptor antagonist and 5-HT_4 receptor agonist are only useful in treating the symptoms of IBS related to diarrhea and constipation, respectively (Gershon, 2012), (Heredia *et al.*, 2013). In addition, adverse side effects are often too common, which have led researchers to discover novel therapeutic alternatives in treating GI motility disorders.

Structure of the enteric nervous system

The ENS is composed of 20 classes of enteric neurons along with multiple types of glia cells grouped together in myenteric (Auerbach's) and submucosal (Meissner's) plexuses a (Figure 1.1).

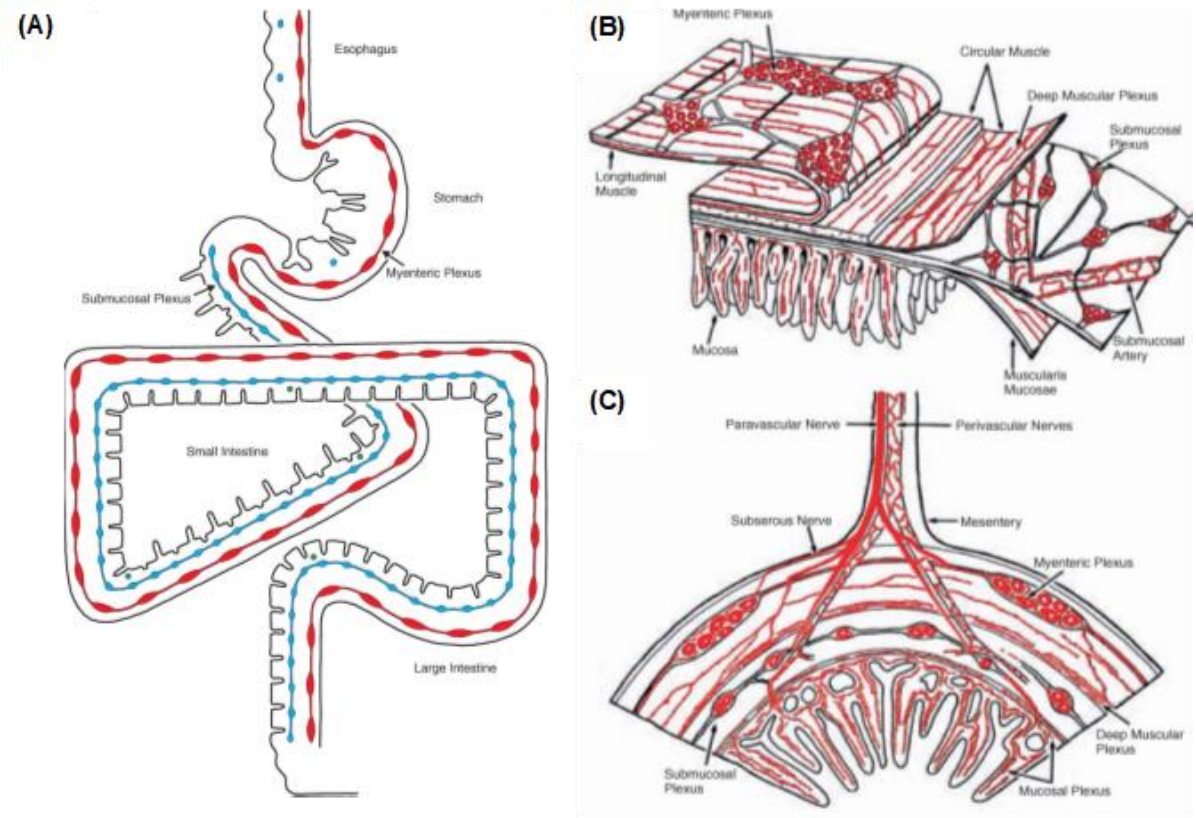

Figure 1.1: Distribution and organization of the enteric nervous system. (A) Diagram depicting the distribution of the ENS in the GI tract. The Submucosal (Meissner's) plexus (blue) is restricted to the small and large intestine, while the myenteric (Auerbach's) plexus (red) is continuous along the GI tract. (B) Wholemount and (C) transverse section drawing depicts the submucosal and myenteric plexus in addition to the nerve fibers that innervate the smooth muscle, mucosa, and blood vessels.
Modified From Furness, JB. The Enteric Nervous System (Blackwell, Oxford, 2006).

The number of enteric neurons in each ganglion varies; however, ganglia are interconnected with each other via interconnecting nerve fiber tracts allowing the formation of a sophisticated nerve network. The submucosal plexus lies between the intestinal lumen and circular smooth muscle layers and is found only in the small and large intestines. Neurons from this plexus primarily

project to the mucosa layer to regulate glandular secretion, alter electrolyte and water transport, and regulate local blood flow. Conversely, the myenteric plexus is a network of nerve strands and small ganglia that lie between the circular and longitudinal smooth muscle. This network is continuous along the GI tract and spans around the circumference of the intestinal tube; however, patterns of the ganglia do differ between regions. Moreover, the size, shape, and orientation of the myenteric ganglia also change among species. Nevertheless, the meshwork and fiber tracts of the myenteric plexus is a universally conserve marker, making it very useful for identifying the myenteric plexus in different animal species (Furness, 2006).

There are three components that make up the myenteric plexus: primary, secondary, and tertiary plexus (Figure 1.2). The ganglia and intermodal strands or interconnecting fiber tracks make up the primary meshwork of the myenteric plexus.

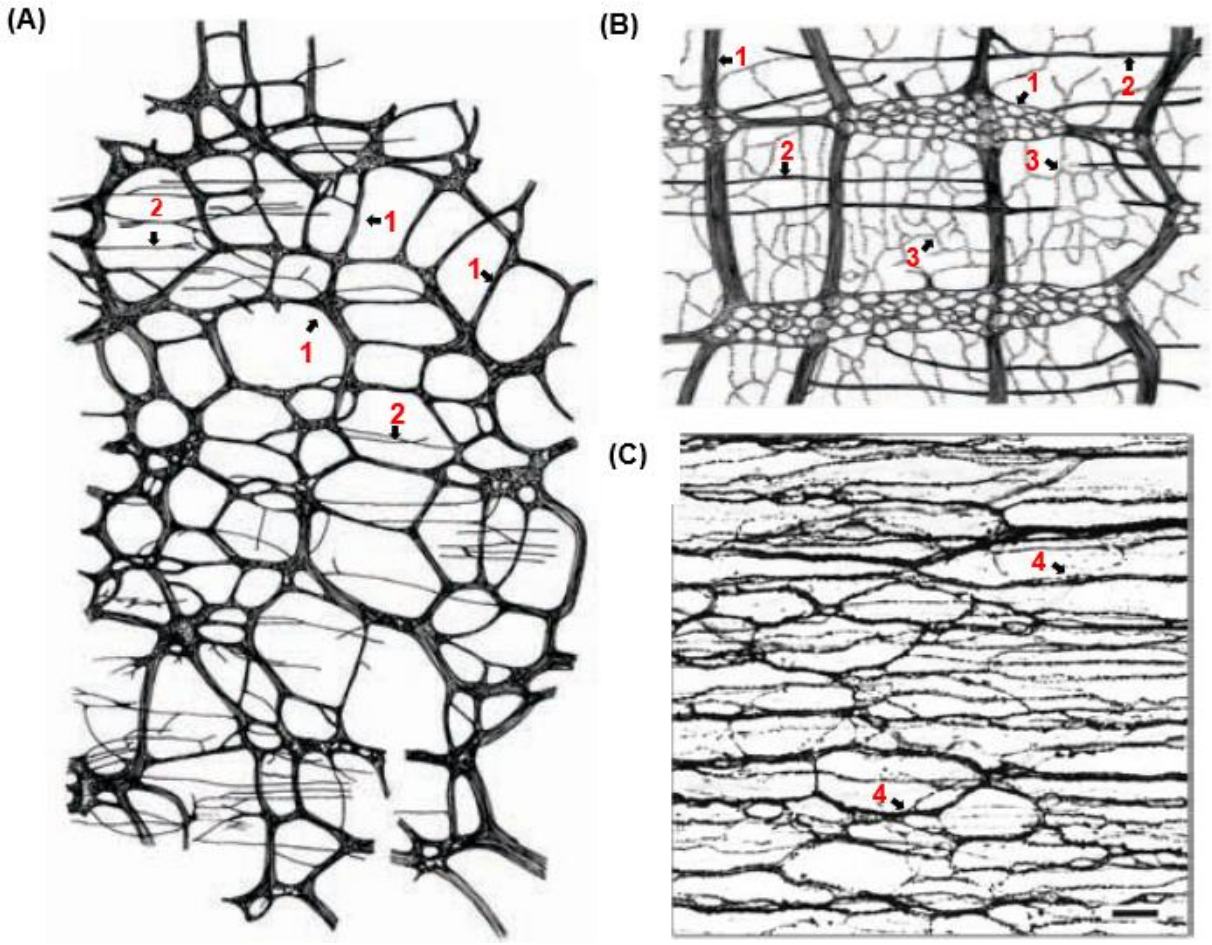

Figure 1.2: Drawing depicting myenteric nerves innervating the muscle layers. Wholemount preparation drawings of the (A) human and (B) guinea pig small intestine showing the (1) myenteric ganglia and intermodal strands (primary plexus), and the secondary components (2), which are nerve strands parallel to the circular muscle. The tertiary plexus (3) are thin nerve fiber that project to the longitudinal muscle and are depicted in the guinea pig small intestine. (B)White ovals in the ganglia are depicted as neurons. (C) Circular muscle wholemount micrograph in guinea-pig small intestine reveals the deep muscular plexus which are interconnections of nerve bundles (4) that projected along the axes of the circular muscle layer.
Modified from Furness, JB. The Enteric Nervous System (Blackwell, Oxford, 2006).

Some of the nerve fibers found in the intermodal strand enter the ganglia while others continue onward to reach other intermodal strands. The secondary plexus comprises of thin nerve fiber bundles that branch from the intermodal strands or from the ganglia. These fiber bundles run parallel to the circular muscle bundles. The tertiary plexus make up fine nerve bundles that meander in spaces between the meshwork formed by the primary plexus. This tertiary meshwork

can be traced back to the intermodal strands, ganglia, and secondary strands, and are known to project to the longitudinal smooth muscle. Fine nerve bundles are also found running parallel to the circular smooth muscles; these are called deep-muscular plexus. Most of the nerve fibers that project to the longitudinal muscle and deep-muscular plexus comes from subpopulations of myenteric derive motor neurons which have an essential role in coordinating GI patterns of motility. Some of these nerve fibers may also derive from vagal and lumbosacral sympathetic and parasympathetic neurons. These nerves, on the other hand, may as well alter GI motility, but their influence varies among GI segments. For instance, the autonomic nervous system has more influence on gastric motility compared to the small and large intestine. Nevertheless, ablation of any extrinsic input still renders the gut functional, as the ENS alone is efficient to maintain gut activity (Furness, 2006).

Microscopy, immunohistochemistry, and electrophysiological studies were crucial in the discovery of several enteric cell populations. As a result of these studies, scientists were encouraged to classify enteric neurons and interstitial cell populations based on their morphology, electrophysiological properties, and functional roles in the GI tract.

Morphology of enteric neurons

The morphology of enteric neurons was first studied by the Russian histologist and neuroscientist Alexandre Dogiel (Clerc *et al.*, 1998; Dogiel, 1985; Dogiel, 1989; Furness, 2006; Lomax *et al.*, 1999). He described three classes of enteric neurons, which he identified as Dogiel type I, II, and III neurons.

Dogiel type I

Dogiel type I neurons contain one axon, 4 to 20 dendrites, and a cell body that can reach up to 35 µm in length and up to 22 µm in width (Figure 1.3). These processes of these neurons project from one ganglion to another or can span through up to four ganglia before reaching their

final destination at the smooth muscle layer (Dogiel, 1985; Dogiel, 1989; Furness, 2006). This shows that not all neurons with Dogiel type I morphology are directly involved in neuromuscular transmission. Furthermore, immunohistochemical analysis of these neurons led researchers to classify them as the motor neurons and interneurons of the ENS (Brehmer *et al.*, 1999).

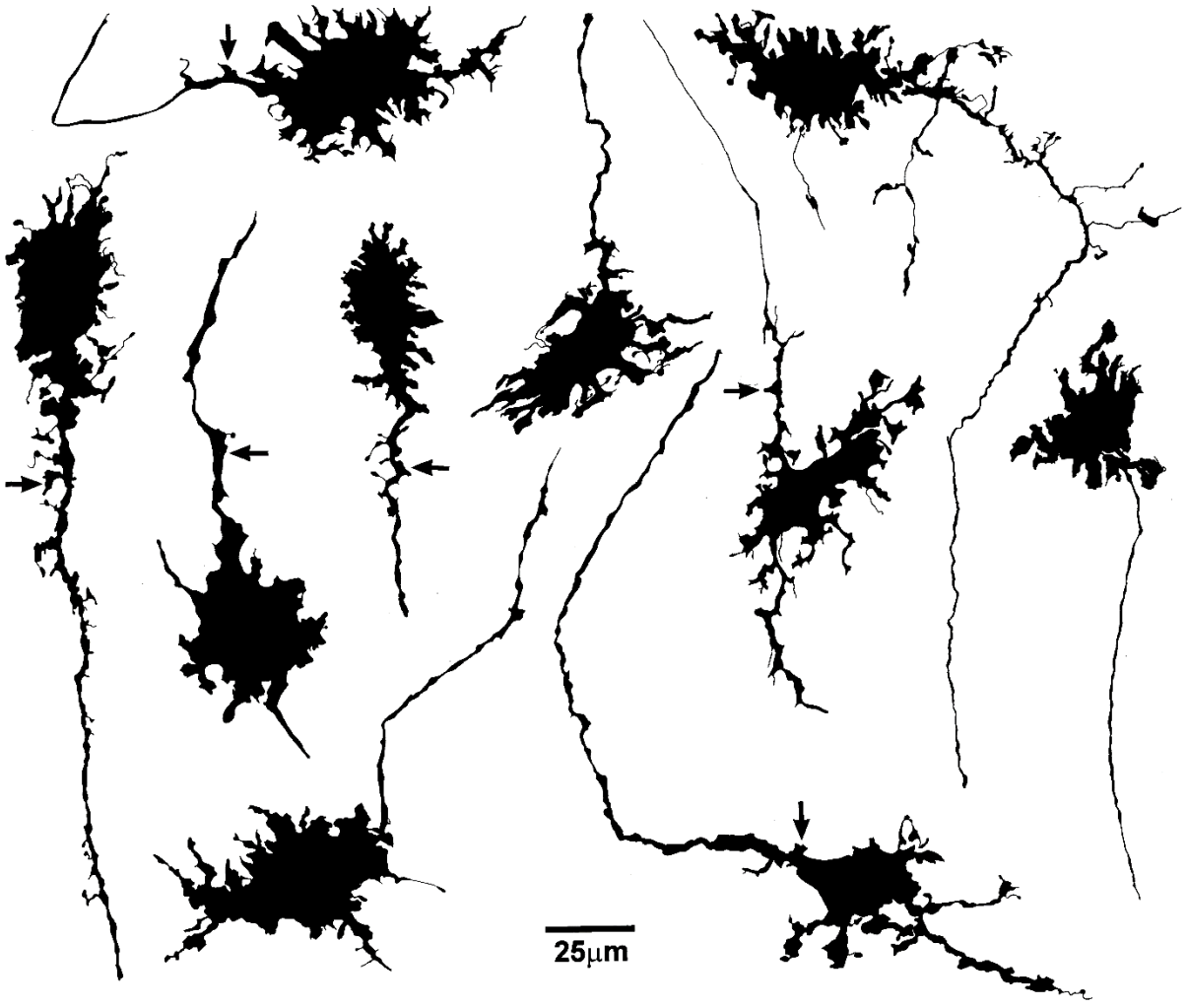

Figure 1.3: Drawing of various Dogiel type I neurons. Various forms of the Dogiel type I neurons located in the guinea pig distal colon that were injected with biocytin and drawn with a camera lucida. These cells have many dendrites (4-20) but only one axon.

Modified from Lomax et al., 1999.

Dogiel type II

Dogiel type II neurons have large round cell bodies that can reach up to 47 µm in diameter, and have a large number of mitochondria and lysosomes that make them conspicuous and easy to discern from the rest of the enteric neuron population (Pompolo *et al.*, 1988) (Figure 1.4). They are commonly found in the submucosal and myenteric plexus of the large and small intestine; however, they are a rarity in the stomach (Furness, 2006). Some Dogiel type II neurons are further classified as multipolar cells, as they have multiple long axons that arise from the nerve cell body (Stach, 1981) (Hendriks *et al.*, 1990) or pseudounipolar neurons because they contain a single process that branches into subsidiary axons at a short distance from the cell body (Furness, 2006). In general, Dogiel type II neurons have axonal projections to the mucosa (Song *et al.*, 1991), (Brookes, 2001), giving rise to extensive varicose branching within their own and neighboring ganglia (Bornstein *et al.*, 1991); (Brookes, 2001) furthermore, they project circumferentially (Bornstein *et al.*, 1991). However, in the guinea pig myenteric plexus, there are Dogiel type II neurons with short dendrite-like processes that project mainly aborally (Brookes, 2001; Stach, 1981). About 90% of the Dogiel type II neurons are immunoreactive for the calcium-binding protein, calbindin (Iyer *et al.*, 1988) (Song *et al.*, 1991) with limited immunoreactivity with other cell markers, suggesting that the overall function of Dogiel type II neurons in the ENS is overwhelmingly conserved and may not vary among individual Dogiel type II cell types.

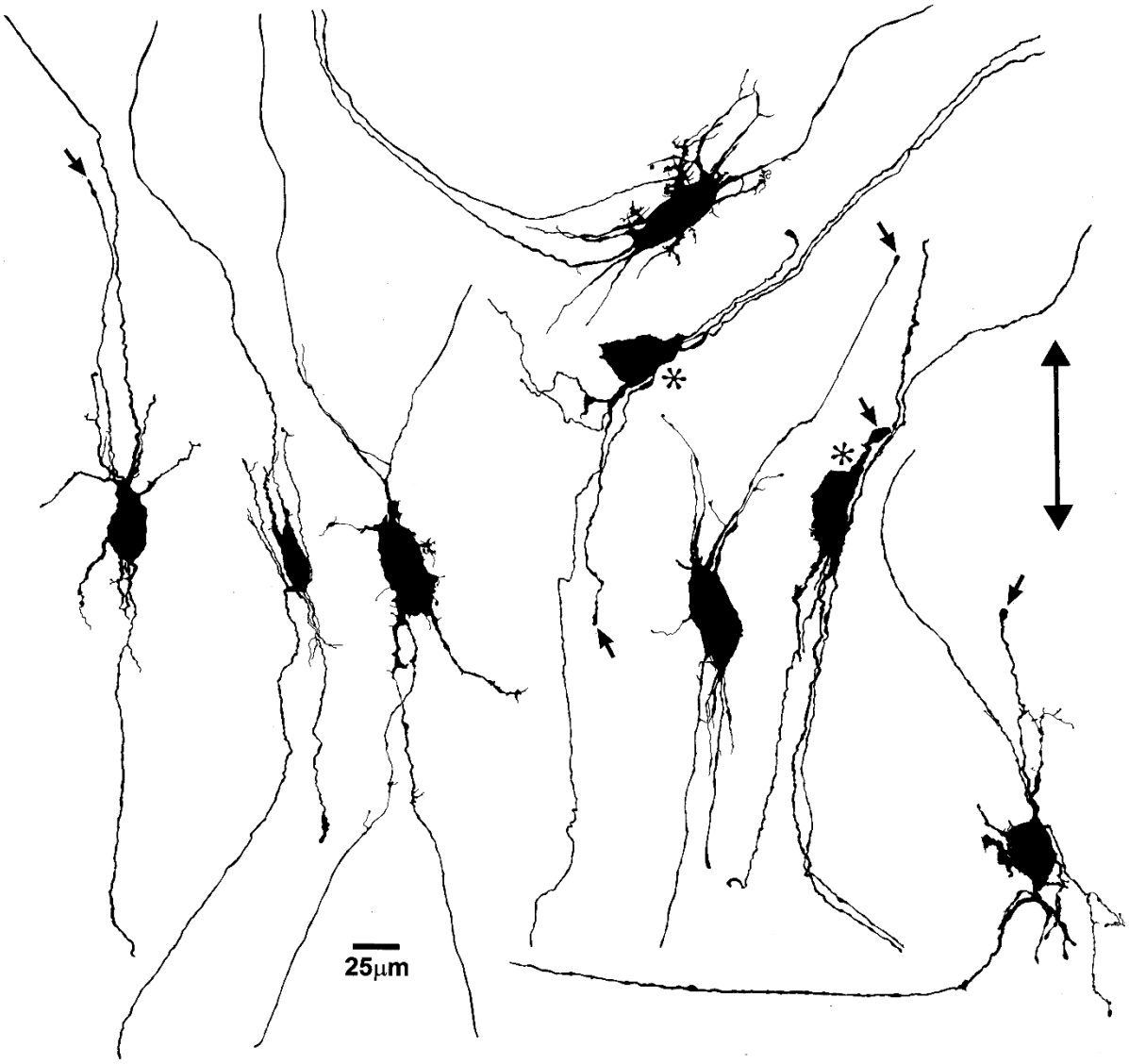

Figure 1.4: Drawing of various Dogiel type II neurons. Examples of Dogiel type II neurons in the guinea pig distal colon. Dogiel type II neurons shown in camera lucida drawings of myenteric neurons that had been electrophysiologically characterized and injected with the intracellular marker biocytin via recording electrode. These neurons are classified as multipolar cells due to the multiple long axons that originate from their cell body.

Modified from Lomax et al., 1999.

Dogiel type III

Dogiel type III neurons have 2 to 10 dendrites that become thin as they branch. Compared to Dogiel type II, Dogiel type III dendrites are short and end within the ganglion of origin (Figure 1.5). Their axon derives from a small conical protrusion of the cell body or a dendrite. Despite that more than 100 years has passed since their discovery (Dogiel, 1989; Furness, 2006), it is still unclear which neuron population correspond to Dogiel type III neurons

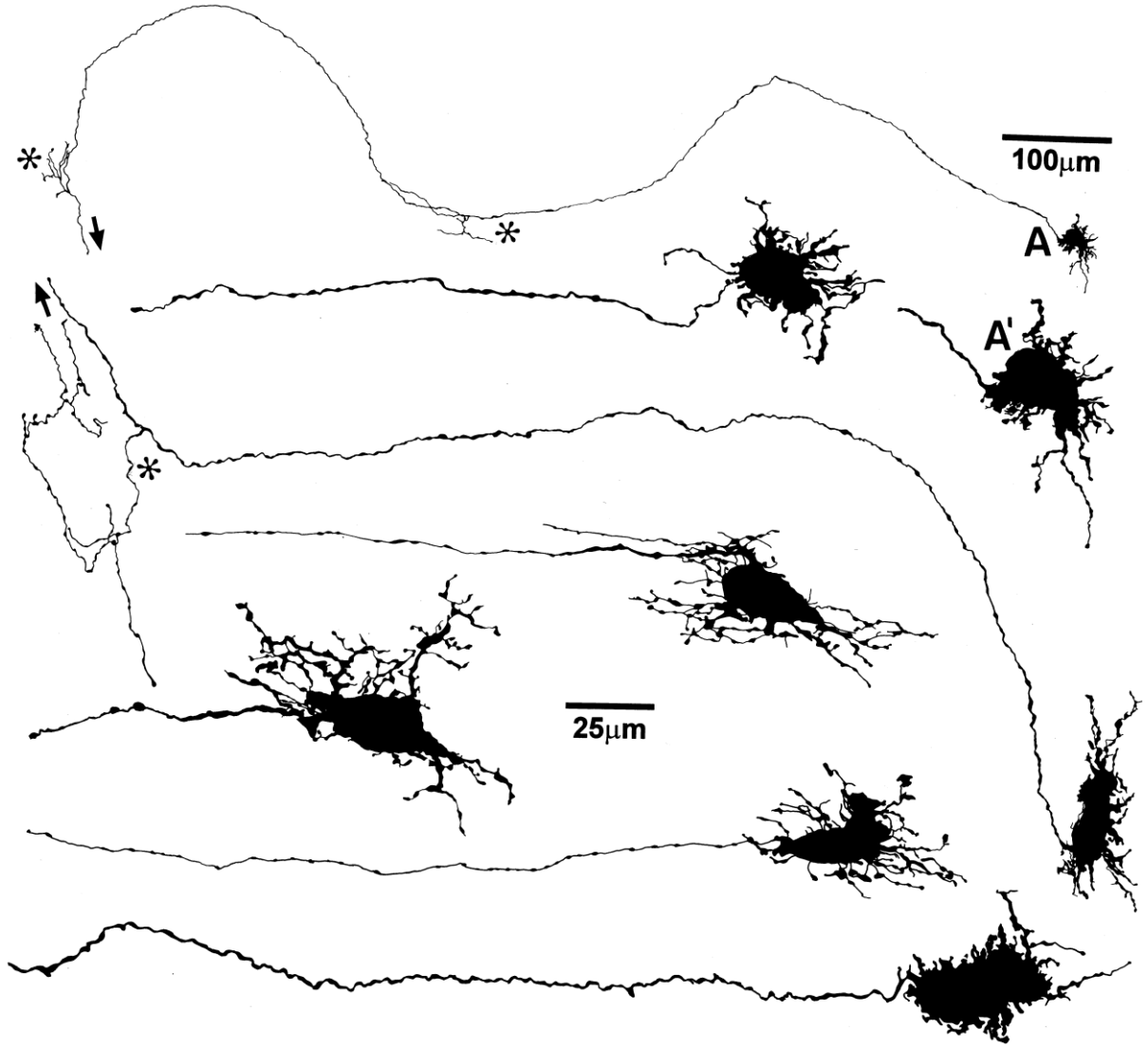

Figure 1.5: Drawing of Dogiel type III neurons. Dogiel type III cells depicted in this drawing come from the guinea pig distal colon, and shows similar characteristics described for filamentous neurons. These neurons have numerous fine dendrites and short ends compared to Dogiel type

Figure 1.5 (cont'd)

I and II cells, and their axons originate from small conical protrusions. These fine dendrites give rise to varicose collaterals that branched within the myenteric ganglia close to the cell body (asterisk). Classification of this third Dogiel type form using current methods of identification has shown to be difficult.

Modified from Lomax et al., 1999.

Physiology of enteric neurons

The study published by Nishi and North was the first to reveal the existence of different classes of enteric neuron classified by electrophysiological properties. These excitable cells were classified as type I, type II, and type III neurons, the formal being non-excitable cells (Nishi *et al.*, 1973). The following year, the Hirst group narrow the populations to S and AH cells, which were distinguishable by their different responses to transmural stimulation and the mechanism by which each cell type generates an action potential (Hirst *et al.*, 1974; Hirst *et al.*, 1973).

S neurons

The letter "S" in S neurons refers to the word synaptic, as S neurons are distinguishable by their capacity to generate fast excitatory postsynaptic potential (fEPSP) following transmural electrical stimulation (Hirst *et al.*, 1974). These neurons can reach a state of continuous action potential firing in response to 50 ms intracellular depolarizing pulses (Furness, 2006; Tamura *et al.*, 1989) and exhibit short duration after-hyperpolarization that last 20 to 100 ms following the brief action potential (Figure 1.6A). Application of the sodium channel blocker TTX inhibits the action potentials of S neurons, showing that TTX-sensitive Na+ channels are the main conductors of the S neuron action potential (Hirst *et al.*, 1974). In the case of cell morphology, all S neurons are Dogiel type I neurons, and none have type II morphology. This is because all S neurons have a single axon and short lamellar dendrites (Furness, 2006).

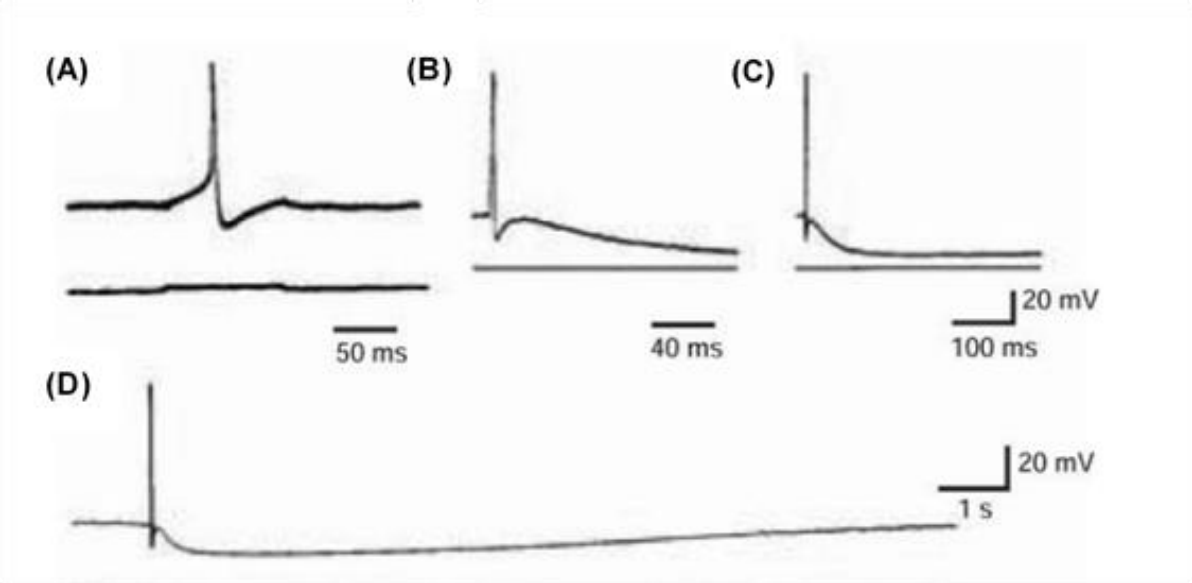

Figure 1.6: The action potentials of S and AH neurons. S neurons (A) and AH neurons (B, C, and D) action potentials are generated following a current pulse. Following the action potential, S neurons generates a fast after-hyperpolarization (20 to 100 ms in duration), and AH neurons exhibit a slow after-hyperpolarization (2 to 30 s in duration). S neurons exhibit Dogiel type I morphology and AH cells are likely Dogiel type II neurons.

Modified from Furness, JB. The Enteric Nervous System (Blackwell, Oxford, 2006).

AH neurons

Neurons that exhibit a long after-hyperpolarization (2 to 30 s in duration) following their action potential are called AH neurons (Hirst *et al.*, 1974) (Figure 1.6B, C and D). The AH neuron action potential is the most studied and complex of the two types of neurons in the ENS. In the guinea pig small intestine, the action potential can reach an amplitude of 75-110 mV during electrophysiological recordings, greater than S neuron (Figure 1.7). The initial response of the action potential is mediated by the activation of TTX resistant Na^+ channels (Unknown α-subunit), TTX non-resistant Na^+ channels ($Na_v1.9$; SCN11A), and N-type voltage-gated Ca^{+2} channels (α1B, $Ca_v2.2$; CACNA1B), followed by a small falling phase called the hump, which is a residual response due to the long-lasting Ca^{2+} currents. The follow up are two distinct phases of after-

hyperpolarization that end the action potential response. The first phase or early after-hyperpolarization (early AHP) is triggered by K^+ efflux resulting from the activation of inward-rectifying K^+ channels (K_{ir}, IRK) and BK channels (Kca1.1). The second phase, or late AHP, also results in the efflux of K^+ via calcium-dependent activation of IK channels. This last hyperpolarization triggers HCN channels mediating a non-selective cation current (Ih current) that reduces the amplitude of the late AHP. Also, between the early and late AHP, an after-depolarizing potential (ADP) can be seen due to Ca^{2+} activation of cation channels (CAN). (Furness *et al.*, 2004b). It has been shown that this slow AHP event can last up to 30 s. (Hirst *et al.*, 1974) (Hirst *et al.*, 1985). The AH cell action potential is blocked by TTX, suggesting that Na^+ is the main driver of the action potential current in AH neurons (North & Nishi 1976, (Furness, 2006)). Although N-type channels are predominant in AH cells, other Ca^{2+} channels such as R-type (α1E; $Ca_v2.3$; CACNA1E) and P/Q (α1A; $Ca_v2.1$; CACNA1A) type Ca^{2+} channels may play a smaller roles in AH cells (Rugiero *et al.*, 2002), (Kirchgessner *et al.*, 1999). Regarding morphology, all AH cells possess Dogiel type II morphology in the guinea pig ileum, yet in the pig intestine, most Dogiel type II neurons lack the late AHP (Cornelissen *et al.*, 2000).

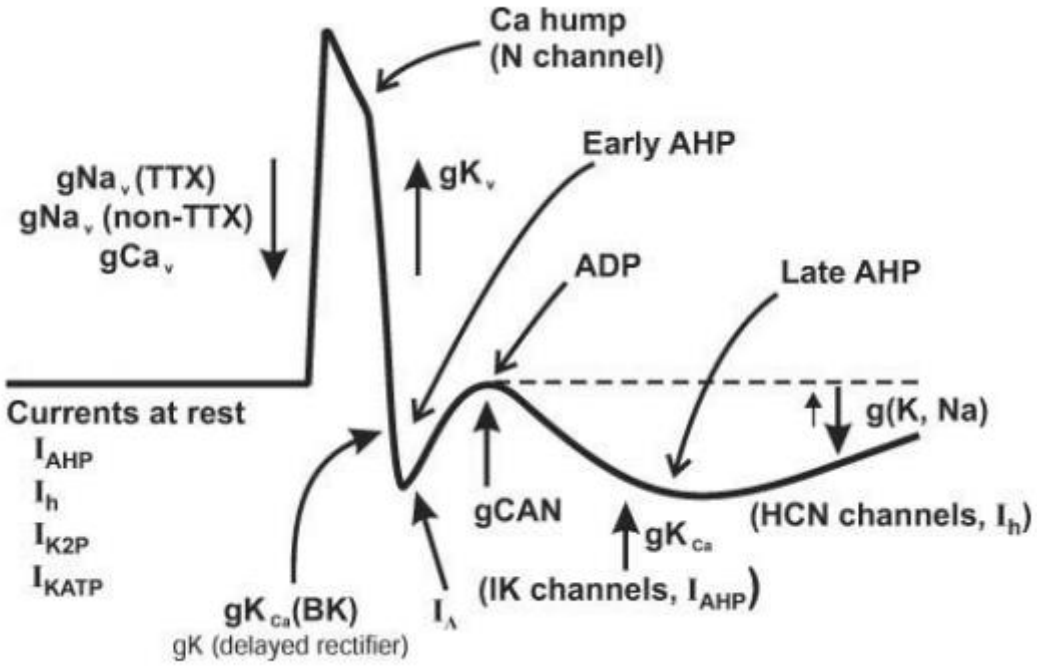

Figure 1.7: The different phases of the AH cell action potential. Referred to as intrinsic primary afferent neurons (IPANs), the action potential of AH cells is initiated after the opening of voltage-gated Na^+ channels and voltage-gated Ca^{2+} channels. Opening of these channels generates anNa^+ conductance (gNav) and Ca^{2+} conductance (gCa), which results in the depolarization of the cell from its resting state. Because Ca^{2+} channels remain open longer than Na^+ channels, it results in the hump response that occurs during the early repolarization phase. Once Ca^{2+} and Na^+ conductance declines the action potential is terminated, the early and then the late -hyperpolarization (AHP) response is initiated to drive the membrane potential of AH cells back to a resting state. The early AHP is initiated by Ca^{2+} activation of Ca^{2+} Channels (gCAN), and the following late AHP is driven by Ca^{2+} activation of K^+ channels (gKca).

Modified from Furness, JB. The Enteric Nervous System (Blackwell, Oxford, 2006).

Functional classification of enteric neurons

The classification of enteric neurons based on their functional role in GI motility was built on cumulative data obtained from studies focused on underlining the enteric reflexes, the morphology of enteric neuron populations, and studies that implemented neurochemical and pharmacological techniques. These different classes of enteric neurons are listed in Table 1.1.

Neuron type	Guinea-pig small intestine			Mouse small intestine		
	Code	Shape	Proportion	Code	Shape	Proportion
Intrinsic primary afferent neuron	ACh/NeuNcyt/IB4, 80% calbindin	Type II	26%	ACh/NF/CGRP/ calbindin +/- calretinin	Type II	26%
Inhibitory circular muscle motor neuron	NOS/VIP	Type I	16%	NOS/VIP +/- NPY	Type I	23%
Inhibitory longitudinal muscle motor neuron	NOS/VIP	Small Type I	2%	NOS/VIP	Small, no obvious dendrites	3%
Excitatory circular muscle motor neuron	ACh/TK	Medium Type I	12%	ACh/TK +/- calretinin	Small/medium, no obvious dendrites	21%
Excitatory longitudinal muscle motor neuron	ACh/TK/calretinin	Small Type I	25%	ACh/calretinin +/- TK	Small, no obvious dendrites	13%
Descending interneurons	ACh/NOS/VIP	Type I	5%	ACh/NOS	Type I	3%
Descending interneurons	ACh/5-HT	Type I	2%	ACh/5-HT	Type I	1%
Descending interneurons	ACh/SOM	Type III/ filamentous	4%	ACh/SOM/calretinin	Filamentous	4%
Ascending interneurons	ACh/TK/calretinin	Type I	5%	ACh/TK +/- calretinin	Type I	4% (estimated)
Intestinofugal neurons	ACh plus a range of peptides	Type I	<1%	Not identified	Not known	Not known
Tyrosine hydroxylase neurons	TH	–	Rare	TH	Type I	<0.5%

Table 1.1: Different functional classes of myenteric neurons in guinea pig and mouse small intestine. The three main classes of myenteric neurons are intrinsic primary afferent neurons (IPANs), Motor neurons, and interneurons. These populations of neurons are further defined by their functions, cell body morphologies, chemistries (code), and projections in the GI tract. All Dogiel type II neurons are IPNAs and are predominantly immunoreactive for calbindin a well-known Ca^{+2} binding protein. Motor neurons that cause the GI muscles to relax are inhibitory motor neurons (IMNs) and are predominately immunoreactive for the cell marker nNOS. Conversely, motor neurons that induces muscle contractility are called excitatory motor neurons and are overwhelmingly immunoreactive for the ChAT cell marker. Dogiel type I neurons which nerve fibers travel abnormally along the ganglia are ascending interneurons. These neurons trigger muscle contraction following synaptic activation of EMNs. Dogiel type I neurons that descends along the ganglia are called descending interneurons and innervate IMNs, hence have an important role in muscle relaxation. The main immunological markers for interneurons varies among subpopulation. Ascending interneurons are predominately cholinergic, while descending interneurons are also cholinergic but may co-express other types of markers depending on their sub-classification (e.g., 5-HT, nNOS, and SOM/calretinin)

Modified From Qu, Zheng-Dong et al., 2008.

Primary afferent neurons.

Primary afferent neurons detect changes in the chemical environment and physical state of the tissue they innervate and convey the information to a nerve circuit that modifies the functional state of that organ (Furness *et al.*, 2004c). These neurons are divided into three broad

classes: afferent neurons, which have cell bodies in the dorsal root ganglia (spinal afferents) or in the vagal (nodose and jugular) ganglia (vagal afferents) and afferent neurons whose cell bodies, are within the gut wall and include intrinsic primary afferent neurons whose processes remain within the ENS, and intestinofugal neurons that synapse with sympathetic neurons in the celiac, superior mesenteric and inferior mesenteric ganglia (Figure 1.8) (Furness *et al.*, 2004c; Szurszewski *et al.*, 2002). IPANs cell bodies are found in the submucosal and myenteric plexus of the small intestine and colon, and are rare in the stomach (Furness, 2006; Lawrentjew, 1931). These neurons have Dogiel type II morphology (Figure 1.4) (Dogiel, 1989) with AH cell electrophysiological characteristics (Figure 1.6B-D and Figure 1.7) (Hirst *et al.*, 1974; Iyer *et al.*, 1988). Retrograde tracers applied in the mucosa revealed that IPANs have extensive projections within the mucosa and submucosal ganglia (Brookes, 2001; Kirchgessner *et al.*, 1992) and axon terminals that synapse with other IPANs, interneurons, and motor neurons in the submucosal (Bornstein *et al.*, 1989; Evans *et al.*, 1994) and myenteric plexuses (Brookes, 2001; Kirchgessner *et al.*, 1992; Song *et al.*, 1997). In addition, myenteric IPANs project to the submucosal plexus, and submucosal IPANs project to the myenteric plexus. IPANs are immunoreactive for ChAT, substance P, and the calcium-binding protein known as calbindin (Brookes, 2001; Furness *et al.*, 1984). They comprise 13% of all neurons in the submucosal plexus of the guinea pig small intestine (Song *et al.*, 1992), and 26% of myenteric neurons in the guinea pig and mouse small intestine (Qu et al. 2008). IPANs respond to mechanical stimulation, distention of the gut, but also luminal chemical content such as inorganic acids, short-chain fatty acids, glucose, and most notable serotonin (5-HT) (Bertrand *et al.*, 1997; Kirchgessner *et al.*, 1996; Kunze *et al.*, 1995). 5-HT is synthesized and stored in the intestine (Bornstein, 2012) in fact, 5-HT is the most abundant signaling molecule in the gut, containing 95% of the body's 5-HT (Mawe *et al.*, 2013). Mechanical distortion of the mucosal villi leads to the EC cell release of 5-HT (Furness *et al.*, 1984; Gershon, 2012), which then binds to 5-HT_3 receptors, ligand-gated ion channels located at the mucosal terminals of IPANs (Bertrand *et al.*, 2002; Bertrand *et al.*, 2000), (Gwynne *et al.*, 2007) activating

local reflex pathways in the submucosal and myenteric plexus Gwynne *et al.*, 2007) (Gershon, 2012; Heredia *et al.*, 2013; Kirchgessner *et al.*, 1992; Tuladhar *et al.*, 1997). Hence, submucosal IPANs initiate the secretomotor and vasodilator reflexes that return water, electrolytes, and other fluids into the lumen (Furness *et al.*, 2003; Lomax *et al.*, 2001; Reed *et al.*, 2001), while myenteric IPANs enhances motility reflexes such as the peristatic reflex (Tuladhar *et al.*, 1997).

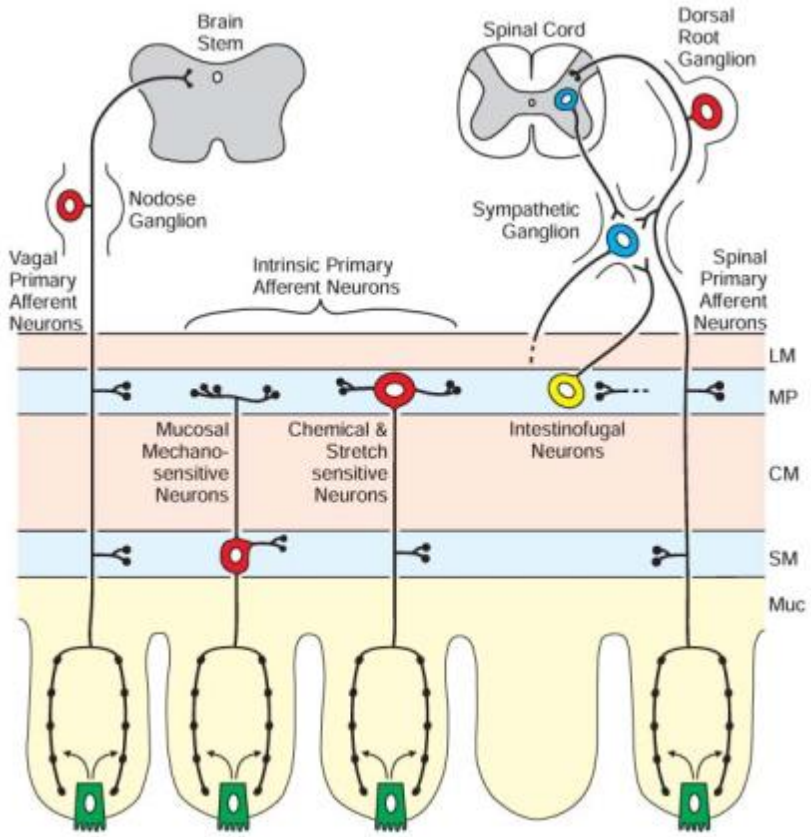

Figure 1.8: The afferent neurons of the digestive tract. Intrinsic primary afferent neurons (IPANs) are divided into two classes: myenteric IPANs which processes innervate the external muscle layers or project to the lumen, respond to mechanical and chemical stimuli, and IPANs that reside in the submucosal plexus (submucosal IPANs) which detect mechanical distortions at the mucosa and respond to changes to the luminal chemistry. The cell bodies of extrinsic primary afferent neurons (EPANs) reside in the dorsal root ganglia (spinal primary afferent neurons) and vagal (nodose and jugular) ganglia. Spinal primary afferent neurons supply collateral branches in sympathetic ganglia and the gut wall. Intestinofugal neurons are parts of the afferent limbs of entero-enteric reflex pathways. LM, longitudinal muscle; CM, circular muscle; MP, myenteric plexus; SM, submucosa; Muc, mucosa. Nerve endings in the mucosa are activated by hormones, most prominently 5-HT, released from entero-endocrine cells (Green cells).

Modified from Furness, JB. The Enteric Nervous System (Blackwell, Oxford, 2006).

Interneurons

Interneurons are neurons that relay sensory information from IPANs to motor neurons in the ENS. Hence, they are heavily involved in local motility reflexes. Interneurons that project orally are called ascending interneurons and are estimated to comprise 4 to 5% of the myenteric cell population while anally projecting interneurons are called descending interneurons and make up the 8 to 10% of the myenteric neurons in the ENS (Qu *et al.*, 2008b). All ascending and descending interneurons have smaller cell bodies than motor neurons, but maintain Dogiel type I morphology (Figure 1.3) and S cell electrophysiological characteristics (Figure 1.6A) (Bornstein *et al.*, 1984; Brookes, 2001). Ascending interneurons in the guinea pig and mouse small intestine, comprise of a single class of interneurons that contain the chemical coding for ChAT, calretinin, and SP (Brookes, 2001; Brookes *et al.*, 1997; Qu *et al.*, 2008b). These neurons mediate fEPSPs following ACh release and are heavily involved in local motility reflexes (Johnson *et al.*, 1996). Descending interneurons are divided into three classes: Nitrergic, serotonergic, and somatostatin-containing interneurons (Furness *et al.*, 1982; Li *et al.*, 1998). Somatostatin descending interneurons are distinctive from the other two classes as they contain prominent filamentous processes (Portbury *et al.*, 1995). These filamentous neurons represent ~4% of the myenteric neuron population and are suggested to have Dogiel type III morphology (Figure 1.5); however, their role in the ENS is still unclear as the cell targets are yet to be discovered (Qu *et al.*, 2008b). Serotonergic interneurons play an important role in maintaining the tonic inhibition during the colonic migrating motor reflex (Dickson *et al.*, 2010b).

Contrary to ascending interneurons, descending interneurons mediate both cholinergic and non-cholinergic fEPSP responses (LePard *et al.*, 1999). Following single myotomy of the ascending and descending pathways that lead to fEPSP generation, the amplitude of the non-cholinergic fEPSP recorded at the aboral side to the single myotomy was greatly reduced when compared to sham animals (LePard *et al.*, 1999). The P2X receptor antagonist suramin inhibits

the non-cholinergic fEPSP in the guinea pig small intestine (Johnson *et al.*, 1999a) of inhibitory motor neurons, suggesting that descending interneurons are likely to co-releases ACh and ATP during synaptic neurotransmission to inhibitory neurons or other neurons found in the descending inhibitory reflex.

Motor neurons

Myenteric neurons that innervate the circular and longitudinal smooth muscle layers and muscularis mucosae of the GI tract are divided into excitatory or inhibitory motor neurons. Retrograde labeling shows that all motor neuron populations contain Dogiel type I morphology (Figure 1.3) (Brookes *et al.*, 1991; Wattchow *et al.*, 1995; Wattchow *et al.*, 1997), many exhibit S cell electrophysiological properties (Figure 1.6A), and comprise about 60% of the myenteric cell population (Table 1.1) (Brookes, 2001; Qu *et al.*, 2008b). Motor neurons are distinguishable by the use of different immunological markers and their complex neuroeffector reflexes. In the guinea pig and mouse colon, excitatory motor neurons (EMNs) are Ir for ChAT, tachykinins (TK), and some, predominantly longitudinal projecting EMNs, contain the Ca^{2+} binding protein calretinin (Qu *et al.*, 2008b). These neurons release ACh as the predominant excitatory neurotransmitter to induce muscle contraction. The mechanism of contractions consists of ACh binding to the G-protein muscarinic ACh receptors (M_2 and M_3 types) in the muscle. M_3 receptors are coupled to a Gq protein. Hence, activation of this muscarinic receptor triggers PLC-β/DAG/IP3 mechanism that ends with the muscles contracting due to increasing concentrations of intracellular Ca^{2+} (Matsuyama *et al.*, 2013; Unno *et al.*, 2005). An opposite effect is seen with M2 receptor activation that obstructs smooth muscle relaxation by inhibiting an adenyl cyclase/cAMP mechanism (Candell *et al.*, 1990; Ehlert *et al.*, 1997; Sawyer *et al.*, 1998). Conversely, smooth muscle relaxation in the digestive tract is controlled by inhibitory motor neurons (IMNs). IMNs contain immunoreactivity for the vasoactive intestinal peptide (VIP), and for the rate-limiting enzyme that synthesizes nitric oxide (NO), the neuronal nitric oxide synthase (nNOS) (Qu *et al.*, 2008b). These

motor neurons release two inhibitory neurotransmitters for muscles relaxation to occur: a purine and NO. The purine, most suspected to be ATP, activates membrane-bound Gq purinergic $P2Y_1$ receptors in muscle, resulting in Ca^{2+} activation of SK channels that hyperpolarize the smooth muscles (Burnstock, 2014b; Castrichini *et al.*, 2014; Kurahashi *et al.*, 2014). NO binds to the endogenously expressed soluble guanylate cyclase (sGC) enzyme in muscle. This event triggers a cGMP/PKG mechanism that lowers intracellular concentrations of Ca^{+2} (Dhaese *et al.*, 2009; Lucas *et al.*, 2000). Together, ATP and NO control the relaxation component of GI motility.

Interstitial cells of gastrointestinal motility

Interstitial cells of Cajal (ICC) and platelet-derived growth factor positive-α-receptors (PDGFRα+) cells are two types of interstitial cell in the GI tract that receive myenteric motor neuron input to coordinate smooth muscle cell contractility and relaxation along the gastrointestinal tract. However, each class of interstitial cell is ir for different types of cell markers and ligand receptors (Figure 1.9A-C) and is suggested to receive neurogenic input from different motor neuron populations. Hence, each interstitial cell type may contribute to GI motility but via different mechanisms of action.

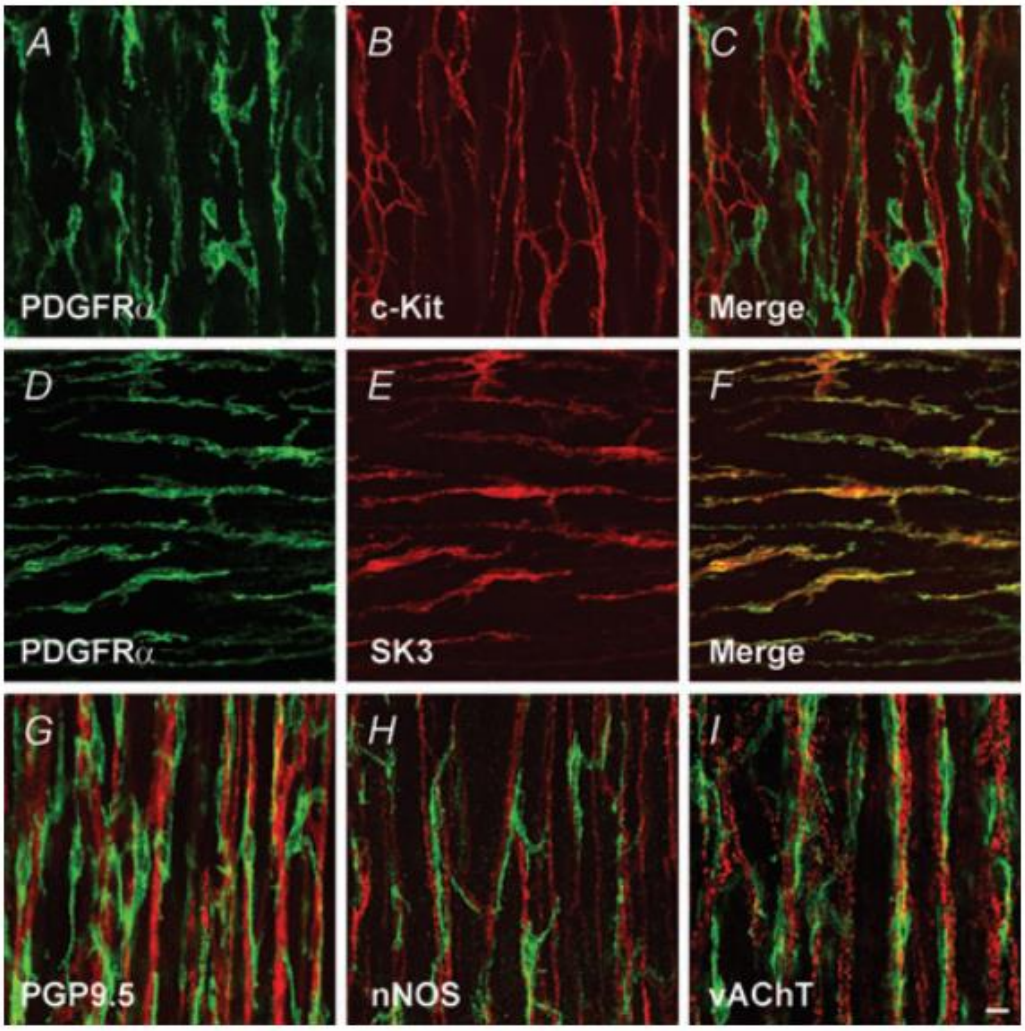

Figure 1.9: Relation of PDGFRα+ cells to ICC and enteric neurons in the murine mouse colon. No co-labeling of PDGFα+ cells (green) with c-Kit+ expressing ICC cells (red) was observed in the mouse colon circular muscle layer (A-C). The Ca^{+2} activated K^{+} channel (SK3) (Red) is highly expressed in PDGFα+ cells (green) in the mouse longitudinal muscle layer (D-F), also shown on circular muscle layer. PDGFα+ cells (red) are closely associated with the enteric cell marker (PGP9.5) (green) and with specific motor neuron classes: nNOS IMNs and ChAT EMNs (green). White bar is 10 µm.

Modified from Kurahashi et al., 2011.

Interstitial cells of Cajal

Slow waves are spontaneous electrophysiological events that lead to phasic contractions in the GI tract. Interstitial cells of Cajal (ICC) produce these slow waves and propagate the input

to electrically couple smooth muscle cells (SMCs) via gap junctions (Furness, 2006). The role of slow waves is to change the membrane potential of smooth muscles cells from a state of rest (resting membrane potential; RMP) to one that increases the probability of L-type voltage-gated Ca^{2+} channel (L-type VGCC) opening. Integration of input from the ENS, hormonal influences and paracrine factors cause the slow wave to reach the threshold (slow-wave-threshold) in the smooth muscle cell leading L-type VGCCs to open, increasing Ca^{+2} influx, and triggering smooth muscle contraction (Thorneloe *et al.*, 2005). Moreover, it has been shown that nitrergic and cholinergic motor neurons provide the predominant neurogenic input to ICC cells in the GI tract (Figure 1.10) (Alberti *et al.*, 2007; Kito *et al.*, 2003; Klein *et al.*, 2013; Suzuki *et al.*, 2003; Wang *et al.*, 2003) however, gastric slow wave mediated contractions do not require neurogenic intervention. In summary, these rhythmic contractions caused by ICC spontaneous electrical activity establishes the baseline potential for which many GI motility reflexes, such as peristalsis and migratory motor complex, can be a trigger (Sanders *et al.*, 2006).

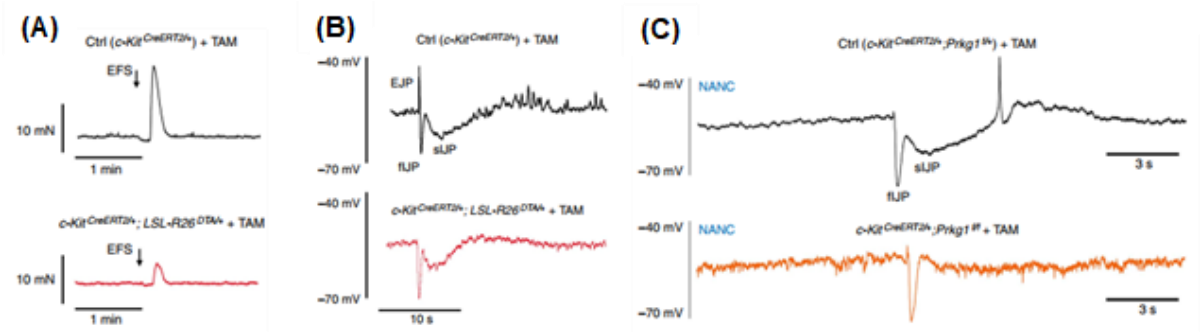

Figure 1.10: Loss of excitatory neuromuscular transmission and nitrergic component in ICC-deficient mice. Representative traces of circular muscle IJP recordings from mouse colon show that tamoxifen (TAM) induces recombination of the R26mTmG allele, carrying the latent diphtheria toxin A (DTA), into c-Kit (ICC) cells expressing the Cre recombinase enzyme (c-Kit$^{creERT2/+}$;LSL-R26$^{DTA/+}$ mice) diminishes the EJP response, compared to TAM-treated controls (c-Kit$^{creERT2/+}$ mice) (A and B). Deletion of the cGMP-dependent protein kinase I (Prkg1) in Cre recombinase expressing ICC cells by administering TAM to "floxed" Prkg1 mice (c-Kit$^{creERT2/+}$; Prkg1$^{f/f}$ mice) blocked the nitrergic, but not the purinergic, component of the IJP (C).

Modified from Klein et al., 2013.

PDGFRα+ cells

Platelet-derived growth factor receptor A (PDGFR$_A$) is a type III kinase receptor structurally similar to the c-kit receptor, the cell marker for ICC cells (Andrae *et al.*, 2008). These receptors, however, are not present in ICC cells (Iino *et al.*, 2009a; Peri *et al.*, 2013). Binding of platelet-derived growth factors (PDGF) to these receptors trigger signaling pathways, such as cell growth and differentiation, in fibroblast, smooth muscle cells, and glial cells (Kohler *et al.*, 1974; Westermark *et al.*, 1976). However, in the gut, these receptors are used to distinguish interstitial cells that have fibroblast-like characteristics (Komuro *et al.*, 1999) located at the gastrointestinal musculature, also known as platelet-derived growth factor positive-α-receptors (PDGFRα+) cells (Iino *et al.*, 2009a; Iino *et al.*, 2009c). Similar to ICC cells, PDGFRα+ cells form gap junctions with muscle cells of both the circular and longitudinal layers of the intestine (Horiguchi *et al.*, 2000). PDGFRα+ cells are distinguishable from ICC cells due to their differential expression of purinergic signaling genes. The gene that encodes for the purinergic $P2Y_1$ receptor of smooth muscle relaxation is highly expressed in PDGFRα+ cells, but not ICC cells (Peri *et al.*, 2013). Immunoreactivity for the Ca^{2+} activated K^+ channel 3 (SK3; Kcnn3) is also present in PDGFR containing cells, but almost entirely absent in c-kit staining ICC cells (Iino *et al.*, 2009c). Lastly, whole-cell intracellular recordings of isolated PDGFRα+ cells and smooth muscle cells showed that PDGFRα+ cells, but not smooth muscle cells, exhibited large hyperpolarization responses with P2Y1 receptor agonist (Kurahashi *et al.*, 2014). Hence, the data supports PDGFRα+ cells as the main target of purinergic innervation in the gastrointestinal tract. Hyperpolarization of these cells would later spread to electrically couple SMCs via gap junction.

A schematic drawing depicts the post-junctional relationship between SMCs, ICCs, and PDGFRα+ cells named the SMC-ICC- PDGFRα+ cells (SIP) syncytium. The SIP syncytium illustrates the plausible electrical coupling mechanism between these cell types, in which electrical changes in any of the cells of the SIP syncytium would affect the excitability of the greater

syncytium. As a result, neurotransmission to any of these cell types of the SIP syncytium will result in the regulation of motor function (Kurahashi *et al.*, 2014).

Slow waves of gastrointestinal motility

As previously mentioned, slow waves are rhythmic spontaneous depolarizations generated by specialize pacemaker cells, known as ICCs that influence the rhythmic contractions of the gastrointestinal (GI) muscles (Figure 1.11).

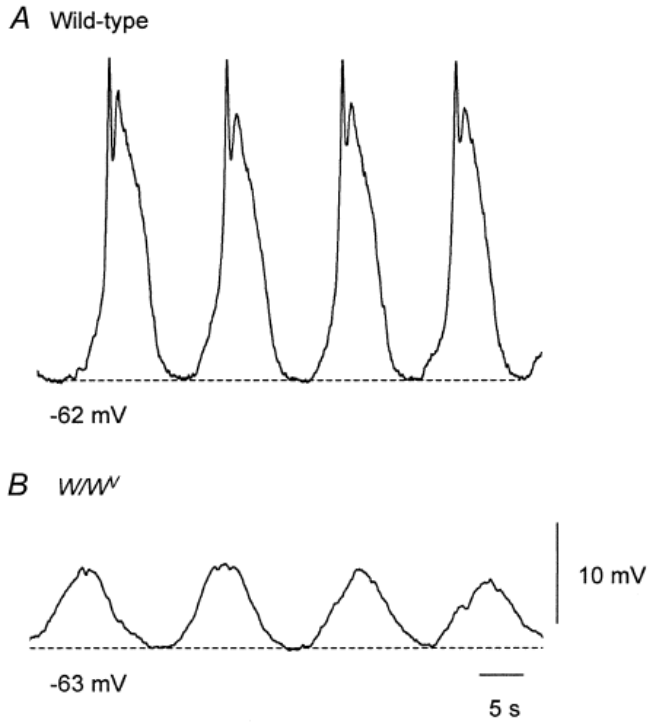

Figure 1.11: Intracellular recording of gastric slow waves. Intracellular recordings revealed slow wave responses recorded from the antral region of the stomach of wild-type (A) and W/W^v mutant mice (B). W/W^v mutant mice lack ICC$_{MY}$, as a results rhythmical slow waves have smaller amplitudes when compared to wild-type mice. Hence ICCs are responsible for influencing the rhythmic contractions of the gastrointestinal (GI) muscles.

Modified from (Dickens *et al.*, 2001)

There are three main subclasses of ICC cells that are important regulator of gastrointestinal motility; ICCs located at the myenteric plexus (ICC_{MY}), deep muscular plexus (ICC_{DMP}), and those found within the circular smooth muscle layer (ICC_{IM}). ICCs are connected to SMCs and one another via gap-junctions. Pacemaker potentials are therefore propagated to SMCs via gap junctions at a fraction of a second after initiation (Hirst *et al.*, 2003). Due to this coupling mechanism, each region of the intestinal smooth muscle is electrically connected; hence slow waves in one region will influence adjacent regions. ICC_{MY} are responsible for mediating most of the slow wave response, as studies performed in mice that lack the ICC marker c-kit show abolishment of the slow wave potential (Huizinga *et al.*, 1995; Ward *et al.*, 1995; Ward *et al.*, 1994). In some cases, slow waves require strong neurogenic input to initiate contraction. For instance, the small and large intestine requires excitatory neurogenic stimuli for the slow wave to reach threshold and the muscles to contract, while gastric slow waves can generate contractions without being influenced by neural activity. The muscarinic receptor antagonist atropine and the Na^+ channel inhibitor tetrodotoxin (TTX) substantially reduce the contraction response in the small intestine, yet do not eliminate the rhythmic activity of the slow wave (Liu *et al.*, 1969; Magnus, 1904), highlighting the important role enteric neurons have in regulating the patterns of smooth muscle contraction.

Slow wave patterns, including frequency and speed propagation, vary along the GI tract. Moreover, they occurs at greater frequency in smaller animals when compared to larger animals and humans. For instance, the duodenum rhythmic contractions occur at an 11-13 per min in humans, 18-19 per min in dogs, and 18 per min in cats (Alvarez *et al.*, 1922; Bayliss *et al.*, 1899; Ehrlein *et al.*, 1987). Contrast this to the small intestine of rats, in which the rhythmic contractions occur at 30 per min (Ruckebush, 1975; Scott *et al.*, 1976), or at a frequency of 25 per min in the guinea pig small intestine (Galligan *et al.*, 1985a).

Circuit of gastrointestinal motility: Peristaltic reflex

Some patterns of GI motility include mixing/segmentation, migratory motor complexes, and peristalsis. In the case of peristalsis, coordinated contraction and relaxation of the GI muscle allows luminal content to be propelled along the length of the GI tract from a proximal to distal direction. The peristaltic reflex is initiated when luminal content comes in contact with EC cells that reside within the epithelium lining of the lumen. These EC cells respond to mechanical and chemical stimuli causing the release of 5-hydroxytryptamine (5-HT) (Bertrand, 2004). 5-HT then activates $5HT_3$ and $5\text{-}HT_4$receptors located at the mucosal endings of IPANs (Dogiel type II/AH cells) that relay the signal to ascending and descending interneurons (Dogiel type I/S cells) in the myenteric plexus (Dickson *et al.*, 2010b; Grider *et al.*, 1996). In addition to mucosal input, the intestine has IPANs that can detect changes in muscle tension and receive input from mechanosensitive interneurons (Smith *et al.*, 2007; Spencer *et al.*, 2006). Ascending interneurons release acetylcholine (ACh) as the main excitatory neurotransmitter, activating nicotinic receptors of EMNs (Dogiel type I/S cells) (Johnson *et al.*, 1996; LePard *et al.*, 1999). Conversely, descending interneurons release ACh and a purine (likely ATP), activating cholinergic and purinergic receptors, respectively, of IMNs (Dogiel type I/S cell) (Gallego *et al.*, 2008a; Grider, 2003). Activation of EMNs releases ACh and substance P in the muscle layers, causing SMCs positioned orally to the luminal content to contract. At that same instant IMNs are activated, and release predominately nitric oxide and a purine, causing the muscles positioned at the aboral side of the luminal content to relax. This contractile and relaxation activity by the smooth muscles is synchronized and provides the necessary pressures to propel luminal content along the gut (Figure 1.12).

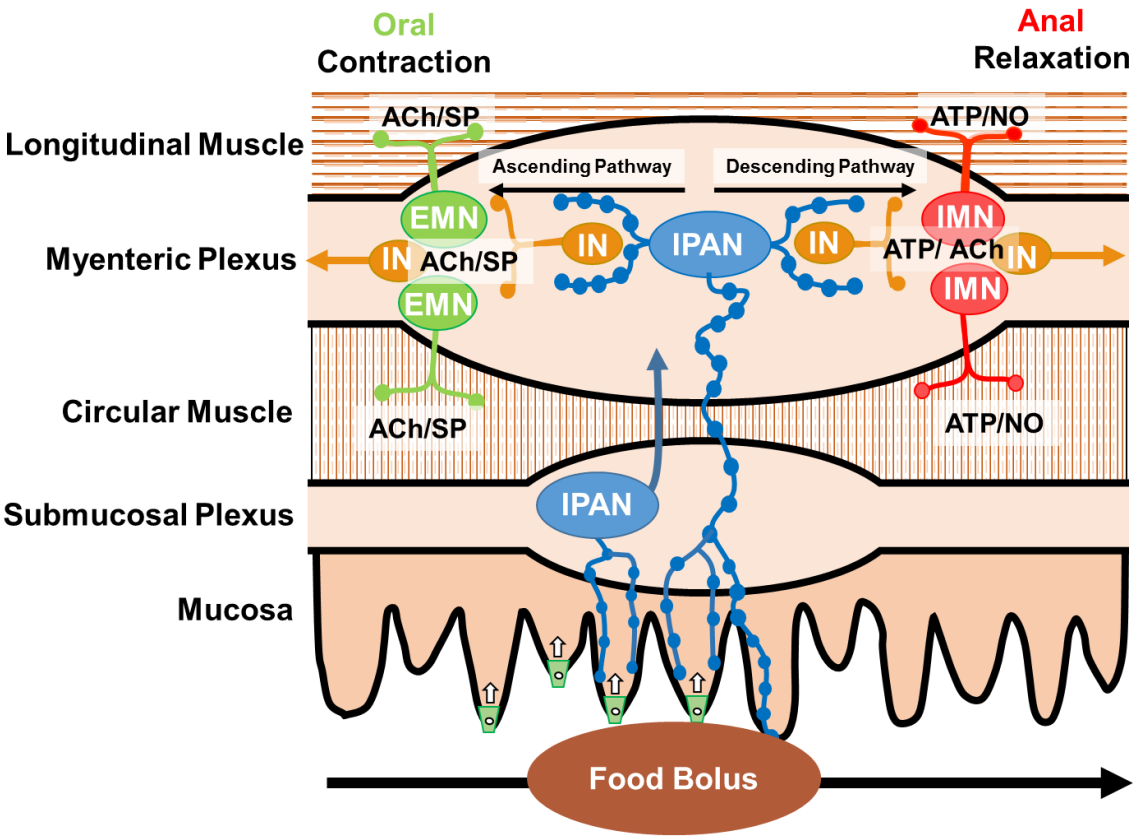

Figure 1.12: The peristaltic neuronal circuit of the GI tract. GI motility is initiated following the activation of IPANs. Mechanical distortion caused by food content (bolus) entering the intestinal milieu, and/ release of chemicals such as 5-HT (arrows) from EC cells (green) initializes the activation of receptors located the myenteric IPANs long processes that extend to the mucosal layer. Following activation IPANS relay the electrochemical signal to an ascending and descending pathway. The ascending pathway consists of predominately cholinergic INs that make synapse with EMNs. EMNs project to the muscle layers and release ACh and SP onto their respective receptors causing the muscles located oral to the food bolus to contract. Conversely, the descending pathway consist of mixed populations of cholinergic/purinergic descending IN that innervate IMNs that also project to the muscle layers, however this motor neuron population conduct relaxation of the muscles cells located anally to the food bolus. IMNs co-leases a purine (likely ATP) and NO as the primary neurotransmitters of smooth muscle relaxation. As a result, the synchronize contraction and relaxation of the muscles allows content to be propel along the GI tract. IPAN: intrinsic primary afferent neurons. (LePard and Galligan, 1999; Johnson et al. 1996; Grider, 2003; Gallego, 2008). IN: interneuron, EMN: excitatory motor neurons, IMN: inhibitory motor neuron, EC: enterochromaffin cells, ACh: acetylcholine, SP: substance P, NO: nitric oxide, ATP: adenosine triphosphate.

Patterns of gastrointestinal motility

Stomach (Gastric motility)

The stomach operates as a reservoir that accommodates the amount of content that enters its cavity and as a pump that pushes digesta towards the pylorus sphincter, first, to enhance the digestion of content and, second, to propel small amounts of digesta, into the duodenum. The reservoir incorporates the gastric fundus and gastric corpus of the stomach; its initial function is to increase its surface area when becoming full (Cannon, 1898). As food enters the stomach, inhibitory vagal pathways from the vago-vagal reflex innervate the enteric inhibitory pathway signaling the predominate release of NO, inducing the muscles to relax and increasing stomach capacity for food content. (Desai *et al.*, 1991; Hennig *et al.*, 1997; Tack *et al.*, 2002). In fact, these vagal afferents may activate myenteric 5-HT interneurons that synapse with IMNs that relax the stomach (Bulbring *et al.*, 1968). Once the volume in the stomach decreases, increased vagal activity causes the fundus to push content down to the corpus region of the stomach where digestion takes place (Wilbur *et al.*, 1973). Afterward, corpus SMCs depolarize causing the muscle to contract and propel content towards the antrum where most mixing and digestion of content takes place. In the stomach, slow wave potentials by themselves can reach threshold and induce smooth muscle cell contraction without intervention from enteric neurons (el-Sharkawy *et al.*, 1978). Slow waves in the stomach originate in the proximal corpus and propagate beyond the gastric pylorus. These same slow waves generated at the corpus that reach the pyloric canal are responsible for the gastric peristalsis ,.(Cannon, 1898; Kelly, 1969) (Fig. 5.7). Once food enters the stomach, the peristaltic waves stimulate contractions that allow the compression of content, mixing of solid content with gastric juices, and are responsible for the movement of small amounts of digesta into the duodenum (Andrews *et al.*, 1980; Cannon, 1911) Disruption of these patterns can lead to gastroparesis, or delayed gastric emptying (see below).

Symptoms of gastroparesis include nausea, vomiting, early satiety, and postprandial fullness, all which could result in weight loss, malnutrition, and dehydration.

Small intestine (Migrating myoelectric complex and peristalsis)

Chyme that enters the duodenum from the stomach is further digested in the small intestine. In fact, digestion, removal of epithelial cells and secretions, and nutrient absorption all occur in the small intestine. A pattern of motility in the small intestine is called the migrating myoelectric complex (MMC), also known as migrating motor complex, facilitates these functions. However, if the MMC rhythm is disrupted, it could lead to dysmotility at the small intestine, which, as a chain of events, increases the risk for small intestinal bacterial overgrowth (SIBO), causing bacteria to adhere and propagate in the small intestine. Patients with SIBO, then, run the risk of developing chronic diarrhea, malabsorption, and inflammation, exhibiting symptoms of abdominal pain, diarrhea, abnormal distension, flatulence, weakness, and weight loss (Dukowicz *et al.*, 2007).

The MMC corresponds to periods of intense contractile activity that occur at particular regions of the small intestine, and are predominantly observed during the fasted state. The MMC is comprised of four phases: Phase I (quiescent phase), phase II (an irregular phase), phase III (the phase corresponding to the MMC contraction), and phase IV (which is a brief cycle of irregular activity that occurs at the end of phase III) (Figure 1.13) (Soffer *et al.*, 1998). Once initiated, phase III of the MMC migrates slowly down the full length of the small intestine until it reaches the end of the ileum. Moreover, as phase III of the MMC traverse the small intestine, the contractions are strong enough to occlude the lumen. (Ehrlein *et al.*, 1987). These rapid sweeping occlusive contractions occur each time slightly more anally than before, hence, allowing luminal content to be slowly propelled along the small intestine (Galligan *et al.*, 1985b; Galligan *et al.*, 1986; Schemann *et al.*, 1986).

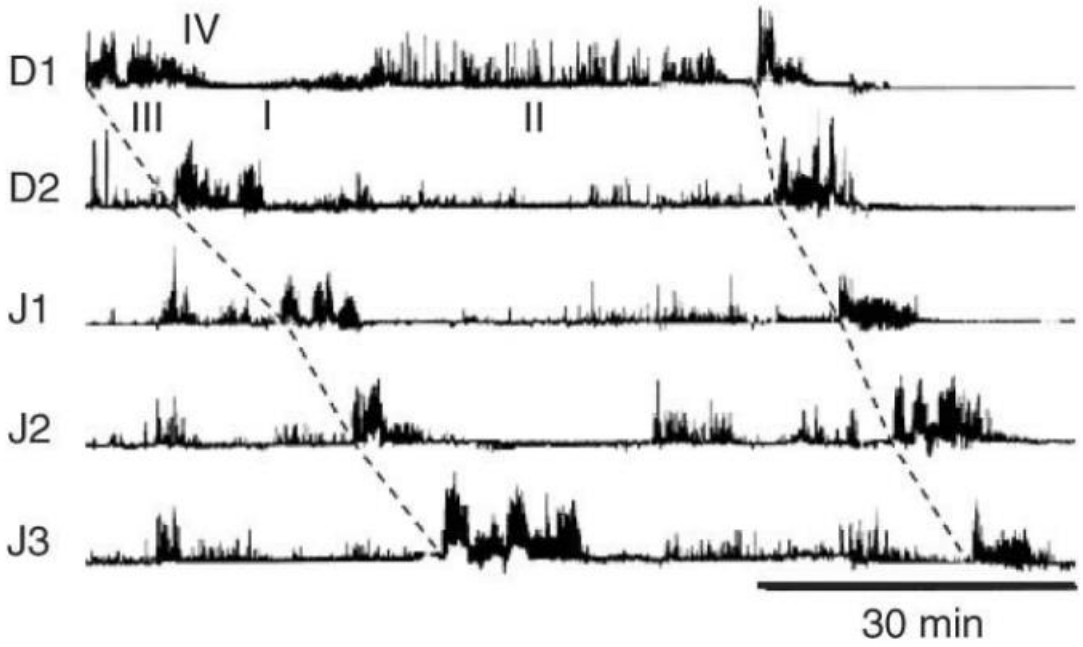

Figure 1.13: Migrating myoelectric complex (MMC) recordings from the human small intestine. The four phases of the MMC complex (I, II, III, and IV) were recorded by closely placing electrodes along the human duodenum (D1 and D2) and jejunum (J1, J2, and J3). The manometric recordings show a slow progression of the MMC (phase III) along the small intestine (dashed lines). Following phase III, we observe a brief cycle of irregular activity (phase IV) and then a phase were activity is quiescent (I). An irregular phase of activity (phase II) is then observed prior to initialization of another MMC (phase III) contraction.

Reproduced from Soffer (1998).

Severing the extrinsic nerves that project to the small intestine does not block the MMC, however does significantly prolong the duration of phase II (Aeberhard *et al.*, 1980; Bueno *et al.*, 1979; Galligan *et al.*, 1986; Marik *et al.*, 1975; Marlett *et al.*, 1979). Studies in the canine and guinea pig small intestine showed that the MMC is, however, blocked following application of nicotinic and muscarinic ACh receptor antagonist hexamethonium and atropine (El-Sharkawy *et al.*, 1982; Galligan *et al.*, 1986; Ormsbee *et al.*, 1979), and by the voltage-gated Na^+ channel antagonist tetrodotoxin (TTX). Hence. MMC progression is dependent on the ENS.

The phase III of the MMC speed of propagation travels at an average rate of 5.3 cm per min in the proximal end of the small intestine, and at an average rate of 1.5 cm per min at the distal end of the canine small intestine (Szurszewski, 1969). In contrast, the speed of propagation in the human small intestine also changes as seen in canines: 4.3 cm per min in the proximal jejunum, 1.3 cm per min at the proximal ileum, and 0.6 cm per min at the distal ileum (Kellow *et al.*, 1986). These propagation speeds are also similar to those recorded from the guinea pig small intestine (4 cm per min) (Galligan *et al.*, 1985a), and of the rabbit (2.5 to 10 cm per min) (Ruckebusch *et al.*, 1985).

Studies in the canine small intestine also reveal peristaltic reflexes that result from migrating clusters of contractions that occur in the fed state and in phase II of the MMC. These peristatic contraction clusters that move slowly along the intestine are generated by slow waves, they propagate up to 40 cm from an oral to anal trajectory, are preceded by relaxations, and as observed in phase III of the MMC, neurogenic innervation from the ENS modulates or enhance their peristaltic response (Dusdieker *et al.*, 1980; Ehrlein *et al.*, 1987).

Large intestine (Colonic migrating motor complex (CMMC)

The colonic migrating motor complex (CMMC), similar to the small intestine MMC, are neurally mediated, rhythmic, and spontaneous propulsive contractions that migrate along the length of the colon of small animals (Smith *et al.*, 2014), such as felines, canines and mice (Christensen *et al.*, 1974; Fida *et al.*, 1997; Sarna *et al.*, 1984). These CMMCs are dependent on the ENS, but not the CNS, since isolating the colon from extrinsic innervation still maintains the rhythmic functionality of the CMMC (Bywater *et al.*, 1989; Heredia *et al.*, 2009; Lyster *et al.*, 1995). In the human colon, the CMMC equivalents are called high amplitude propagation contractions (HAPC) (Bassotti *et al.*, 1988). Upon awakening, HAPCs resemble the murine CMMC in frequency and duration (Spencer *et al.*, 2012; Zarate *et al.*, 2011), therefore, it is proposed that

the basic physiology of colonic contractions (CMMCs and HAPCs) are conserved across animals and humans (Smith *et al.*, 2014).

CMMCs, and most likely the HAPCs, are responsible for the mass movement of fecal material in the colon (Bassotti *et al.*, 1988; Dickson *et al.*, 2010a). Changes in CMMC/HAPC patterns of motility could alter the transit of colonic content and lead to GI complications such as slow-transit constipation (STC), diarrhea and IBS. Reduced fecal pellet output and altered patterns of CMMC propagation are commonly observed in the partially obstructed STC mouse (POM-STC) model (Heredia *et al.*, 2012). Moreover, manometric studies performed in adults and children that suffer from STC also exhibit fewer HAPCs responses (Bharucha, 2012; Stanton *et al.*, 2005). Diarrhea and IBS, on the other hand, can be associated with an increase in HAPCs that can lead to symptoms of abdominal pain (Bharucha, 2012).

The mechanisms underlining the spontaneous CMMC consist of a relaxation phase followed by the CMMC contraction itself. During the initial phase of relaxation, known as tonic inhibition, IMNs are constantly active and releasing NO and ATP causing resting membrane hyperpolarization and spontaneous inhibitory potential in the circular muscles and pacemaker cells (ICC_{MY} and ICC_{IM}) (Bywater *et al.*, 1989; Dickson *et al.*, 2010a; Spencer *et al.*, 2001) (Dickson et al. 2010). Moreover, NO appears to act through pacemaker ICC cells, and purines through PDGFRα+ interstitial cells within the muscle syncytium (Blair *et al.*, 2012; Kurahashi *et al.*, 2014). It is suggested, however, that ongoing activity of descending serotonergic neurons are responsible for the continuous activation of IMNs. Serotonergic neurons periodically release 5-HT that activates $5HT_3$ receptors of myenteric IMNs resulting in tonic inhibition (Dickson *et al.*, 2010b; Qu *et al.*, 2008b). The spontaneous CMMC contraction follows after IMNs are switched off, and consists of fast electrical oscillations (frequency of 2 Hz) with action potentials (approximately 22 spikes per CMMC) superimposed on a slow depolarization (duration of 40-60 s), which contribute to the contraction (Bywater *et al.*, 1989; Dickson *et al.*, 2010a; Lyster *et al.*,

1995). These fast oscillations and slow depolarizations are generated by ACh and TK released from EMNs, which are activated by ascending nervous pathways (Dickson *et al.*, 2010a). Turning IMNs off during the CMMC contraction ensures that the EMNs maximally activate the pacemaker ICCs (ICC_{MY}) and the muscle, without being restricted by inhibitory neurotransmitters (Smith *et al.*, 2014). The spontaneous CMMC rhythmic pattern of contraction (duration of 39.5± 1.7 s) and relaxation (duration of 8.1 + 1.0 s) (tonic inhibition) then repeats momentarily (frequency of 0.3 cycles/ min) following cessation of the previous spontaneous CMMC (Dickson *et al.*, 2010a). Figure 1.14 shows a schematic depiction of the potential nerve pathway of the CMMC.

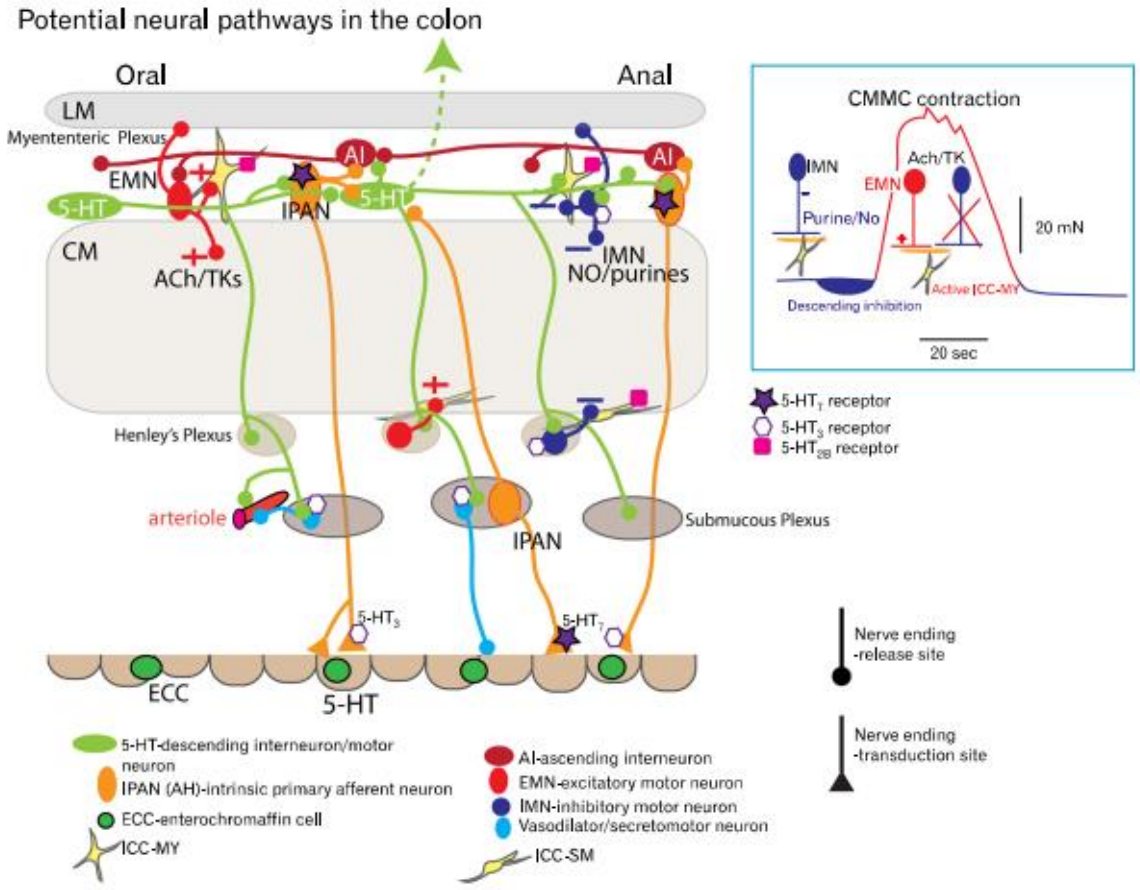

Figure 1.14: Schematic illustration depicting the potential nerve pathway of the colonic migratory motor complex. 5-HT released from mucosal EC cells (green) activates IPNAs (orange) which in turn activates myenteric 5HT neurons (light green) which make synapses with IMNs (blue) , and IPANs that project which synapse with ascending interneurons that activate EMNs (red) that connect and excite pacemaker interstitial cell of Cajal (ICC_{MY}) and the muscle layers (CM and LM). Myenteric 5-HT neurons (light green), make synapses with all types of

Figure 1.14 (cont'd)

myenteric and with the pacemaker network. The ongoing activity of descending serotonergic neurons are suggested to be responsible for the continuous activation of IMNs (blue) by periodically releasing 5-HT that activate receptors located on IMNs, which leads to NO and ATP mediated tonic inhibition at the muscle layers. In periods where IMNs are inactive or switch off, CMMC contractions fallows which consist of fast electrical oscillations with action

Modified from (Smith *et al.*, 2014)

OPTOGENETIC MANIPULATION OF THE ENTERIC NERVOUS SYSTEM

General Description

Investigatory methods such as immunostaining, electrophysiology, and genetic technologies have allowed us to identify neurophysiological properties of enteric neurons and their signaling pathways (Brookes, 2001; Qu *et al.*, 2008b). However, the contributions of individual ENS cell types are not well understood. Cre-lox recombination has allowed us to identify distinct cell populations in the ENS but it has been challenging to selectively activate each of these genetically-unique cell populations, and study their individual roles in enteric nerve circuits using traditional electrophysiological methods. Therefore, to identify specific types of enteric cells and underline their individual roles in the complex ENS circuitry, new techniques that combine genetic and stimulation technology are required to activate or silence the targeted cell population in a spatial and temporal manner (Wang, 2018). The development of optogenetic technology provides an approach to reshape the way we examine nerve circuits and synapses.

Optogenetics combines optical and genetic methods to either activate or silence genetically targeted neuronal circuits (Wang, 2018). The technique can be combined with electrophysiology and other technologies including Ca^{+2} and voltage-sensitive dye imaging to analyze neuronal activity (Boesmans *et al.*, 2015). Since the discovery of bacteriorhodopsin, found in *Halobacterium salinarum* in the late1960's (Grote *et al.*, 2014), and the full commercialization of optogenetic technologies in the last 15 years, researchers have been able

to discover new optogenetic actuators with improved photocurrent properties, and develop tools that advance site-specific delivery into living organisms (Wang, 2018). Optogenetics can be used to manipulate excitable cell activity (Bruegmann *et al.*, 2015; Hill *et al.*, 2015; Jia *et al.*, 2011; Park *et al.*, 2014), but most of all, it has been used to study nerve circuits controlling cognition, learning and memory (Liu *et al.*, 2012; Martinez *et al.*, 2015), fear (Martinez *et al.*, 2014b), and depression and anxiety (Martinez *et al.*, 2014a). Moreover, optogenetic techniques have recently been used to study ENS physiology and to develop non-pharmacological based alternatives to treat gastrointestinal motility disorders (Aad *et al.*, 2014; Gallegos *et al.*, 2014). Nevertheless, engineering better actuators, improving the technology for non-invasive site-specific gene delivery of actuators, as well as improving the light delivery system, would be beneficial if we are to consider using this technology for clinical applications.

Optogenetic Actuators

Microbial rhodopsin molecules with light-gating mechanisms are given the name of optogenetic actuators (Wang, 2018). These opsin-like proteins are either light-driven pumps or light-sensitive ion channels that can cause hyperpolarization or depolarization of excitable cells when exposed to a specific wavelength of light. Halorhodopsin (HR) is an example of a light-gated ion pump that is specific for chloride ions (Han *et al.*, 2007). Therefore, when light activates this inhibitory actuator, it silences neuron activity by causing chloride influx and an outward current. In contrast, light activation of the light-sensitive ion channel, channelrhodopsin (ChR), causes cation influx (Na^+, Ca^{2+}) and an inward photocurrent causing neuronal excitation (Nagel *et al.*, 2002; Nagel *et al.*, 2003). ChR2 is the most commonly used optogenetic actuator for studies of neurotransmission.

A brief history on channelrhodopsin

The discovery of channelrhodopsin (ChR) is based on years of scientific research focused on characterizing the swimming behavior and light response of the green microalgae *Chlamydomonas reinharditii* (Figure 1.15A). Light exposure to the eyespot of the microalgae induce phototaxis (positive phototaxis), and photophobic (evasive; negative phototaxis) responses resulting from exposure to harmful light wavelengths (e.g., UV) (Hegemann *et al.*, 1991; Lawson *et al.*, 1991) , or reactive oxygen species (ROS) (Ueki *et al.*, 2016). However, It was not until the early 2000's that ChR was established as the sensory photoreceptor responsible for microalgae locomotion (Figure 1.15B). In studies performed by Dr. Peter Hegemann and his collaborator Dr. George Nagel, cDNA sequences encoding for the microalgae opsin-related proteins (Chop1 and Chop2) were expressed in Xenopus oocytes and mammalian cells with the aim of performing voltage-clamp recordings and investigating the identity and ion specificity of the microalgae rhodopsin molecules. These experiments revealed two light-gated ion channels that were then given the names channelrhodopsin-1 (ChR1) and channelrhodopsin-2 (ChR2) due to their ion channel characteristics (Nagel *et al.*, 2002; Nagel *et al.*, 2003). ChR1 is permeable to protons (Nagel *et al.*, 2002), while ChR2 is cation permeable (Nagel *et al.*, 2003). ChR2 was improved for optogenetic applications and eventually implemented for light-induced depolarization of excitable cells. This assessment was backed by later studies that revealed that in cultured neurons could be depolarized by light following the introduction of the ChR2 gene (Chop2) into neurons (Boyden *et al.*, 2005; Ishizuka *et al.*, 2006; Li *et al.*, 2005). These studies paved the way for optogenetics to become a widely used technology to study neurotransmission in conjunction with traditional electrophysiology methods.

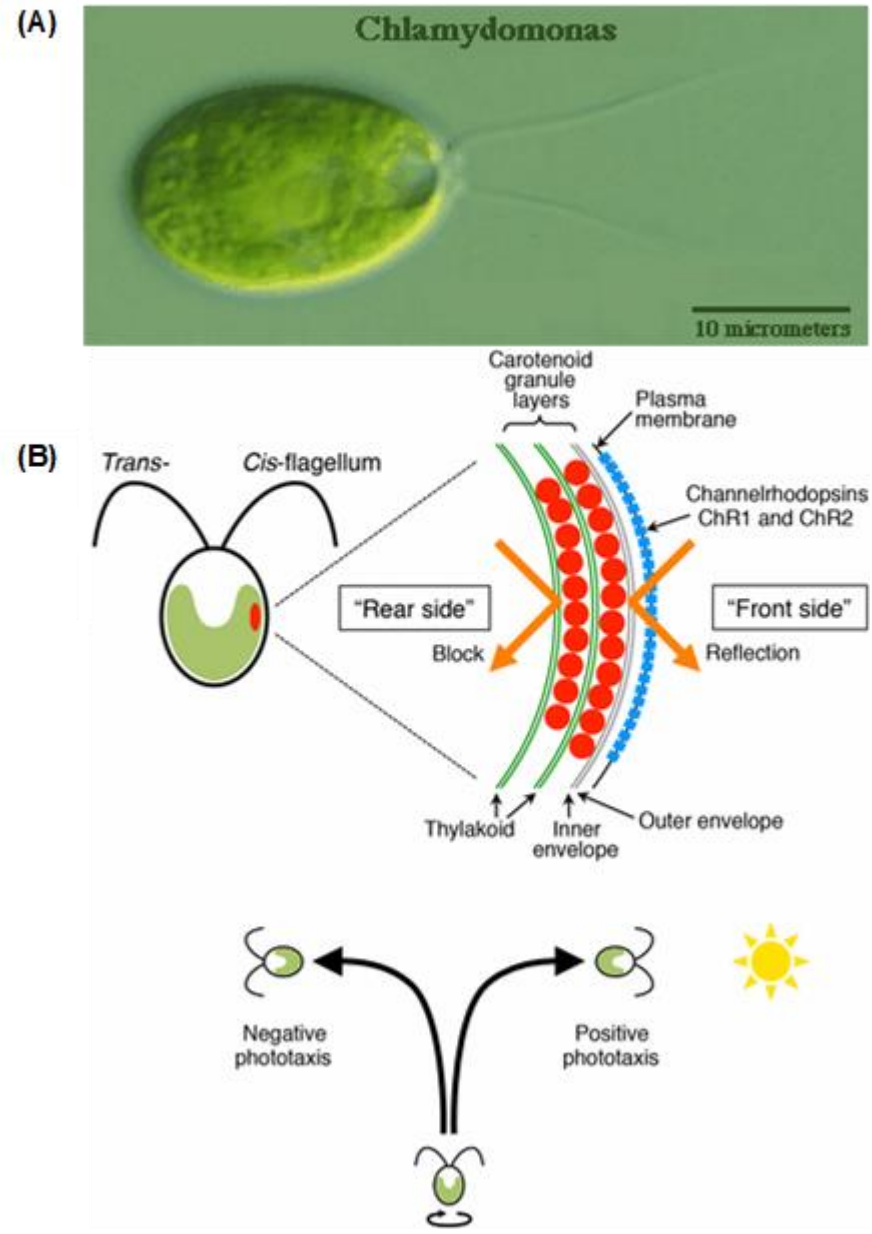

Figure 1.15: *Chlamydomonas reinharditii* and its phototactic behavior is driven by ChR activity. Brightfield image of the biflagellate green algae *C. reinharditii* with arrows pointing to the algaes two flagella. (A). A schematic diagram of *Chlamydomonas* cells and their phototactic behavior is depicted (B). The eyespot of the algae is located near the cell equator and contains the carotenoids granule layers (red) and the photoreceptor proteins known as channelrhodopsin (ChR1 and ChR2; blue). The carotenoid layer reflects light beams (orange arrows) and amplifies the signal from the outside of the cell on ChR (the “front side”) and blocks the light for the inside of the cell (the “rear side”). The flagella that is closest to the eyespot is called the cis-flagellum, and the other is called the trans-flagellum. Either way the algae self-rotates during swimming so that its eyespot can scan for different light intensities along its swimming path. The presence, absence, and intensity of light, as well the kind of wavelength of light that is being exposed to the channelrhodopsin molecules will then

Figure 1.15 (cont'd)

determine the swimming patterns of the cell by changing the beating rate of the flagella as well the direction the cell will swim, to sites where light is present (positive phototaxis) or absent (negative phototaxis).

Modified from (Caprette, 1995; Ueki *et al.*, 2016).

The structure and function of channelrhodopsin

ChR1 and ChR2 are seven transmembrane (7-TM) proteins that have no sequence homology to that of the animal rhodopsin, nor plays a crucial role in visual phototransduction (Figure 1.16) (Nagel *et al.*, 2002; Nagel *et al.*, 2003). These 7-TM proteins contain all-trans retinal chromophores that are covalently linked to the rest of the protein via a protonated Schiff base. Therefore, when the protein is exposed to blue light (470-480 nm) the all-trans-retinal chromophore absorbs the photon of light and induces an all-trans to a 13-cis-retinal conformation change (Bamann *et al.*, 2010). The outcome is the opening of the 7-TM pore region, and, in the case of ChR2, an increased inward rectifying current driven by H^+, Na^+, and Ca^{2+} ions and outward K^+ flux. Milliseconds after, the chromophore regains its all-trans conformation, causing the pore region of the protein to close, stopping the inward flow of cations (Nagel *et al.*, 2003).

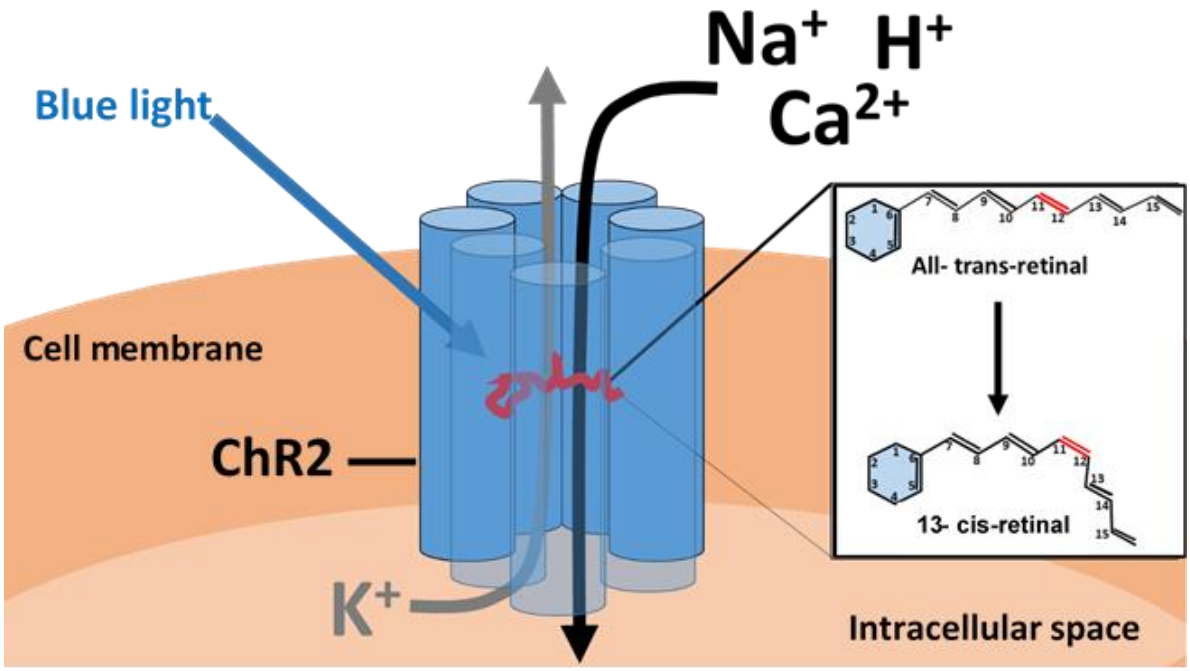

Figure 1.16: Schematic illustration depicting the structure and function of the Channelrhodopsin molecules. Channelrhodopsin is a seven-transmembrane (7-TM) protein, similar to G-protein-couple receptors, which contain the light-sensitive molecule retinal covalently linked to the rest of the protein via a protonated Sniff base. In the presence of blue light (470-480 nm) retinal shift from an all-trans-retinal state to a 13-cis-retinal conformation allowing monovalent and divalent cations to flow through its pore causing depolarization of the excitable cell.

ChR2 cation permeability is dependent on its gating mechanism, controlled by a cycle of light and darkness (photocycle). This photocycle of ChR2 is explained as a three-state model in which light activation of ChR2 from the ground (closed) state (C) leads to an excitation state of ChR2(C*). This is followed by slower dark reactions leading to an open state (O), a closed desensitized state (D), and recovery of the ground (closed) state (C) (Nagel *et al.*, 2003). However, in a study by Bamann and colleges, a more in-depth analysis of the molecular gating mechanism of ChR2 revealed that ChR2 photocycle consists of additional kinetic intermediates (P_0 to P_4) and spectral intermediates (P^{480}, P^{400}, and P^{520}) (Bamann *et al.*, 2008). (Figure 1.17). They explain that when ChR2 reaches its excitation state ($ChR2_{ex}$) following absorption of light at a wavelength of 480 nm, the intermediate spectral shifts from P_0^{480} to P_1^{400}, and in the span of

milliseconds goes into the red-shifted spectral intermediate state (P_2^{520}). During the transition of P_1^{400} to the P_2^{520} intermediate state, the channel begins to open ($ChR2_o$) and remains open until the remainder of the red-shifted spectral (P_3^{520}). Once the red-shifted spectral intermediate decays, the channel closes, and recovery of the ChR2-ground state begins. Bamann and colleagues summarize their findings as follows: opening of the channel occurs during the transition of the red-shifted spectral intermediates (P_2^{520} to P_3^{520}), transition from P_3^{520} to P_4^{480} which is coupled to channel closure and recovery of the ground state after a shift in the kinetic intermediates from P_1^{480} to P_0^{480}. The channel opens with a time constant of 200 µs and before it closes with a relaxation time of approximately 10 ms, hence, the full photocycle of ChR2 averages at roughly 11 ms. These findings provide further underlining of the molecular gating mechanism of ChR2 that can aid in the development of better ChR2 variants. For instance, ChR2 mutants with selective cation conductance (Bamann *et al.*, 2008), or ChR2 mutants that can be tailored to mimic a more endogenous spontaneous electrical response that could be implemented for therapeutic purposes.

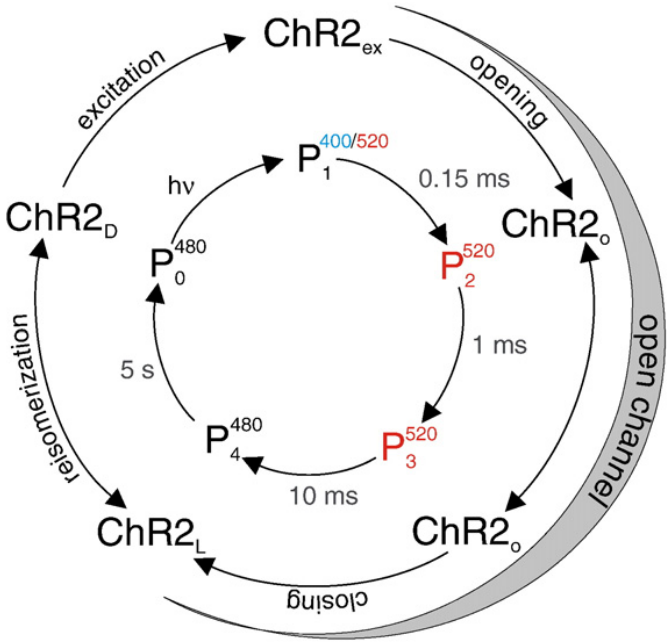

Figure 1.17: The proposed photocycle of ChR2. P^{400} is the blue-shifted intermediate, P^{520} is the red-shifted intermediate, and P^{480} represents the ground state of ChR2. The putative light and dark-adapted states, $ChR2_L$ and $ChR2_D$ respectively, switches between each other following isomerization. Light (480 nm) exposure to the channel during the dark-adapted state ($ChR2_D$), triggers an excitation state ($ChR2_{ex}$) before the channel can become open ($ChR2_O$). When open, ChR2 shift from a P^{480} to a P^{520} spectral intermediate. At the end of the red-shifted intermediate state, ChR2 begins to close. Recovery of the ground state follows soon after.

Modified from (Bamann *et al.*, 2008)

Selective targeting of ChR2 into the ENS

Two methods are widely used to ensure selective delivery of ChR2 into the target cell: viral vectors and transgenic animals. Although they are different delivery systems, they often utilize the same genetic tools to achieve ChR2 expression into the targeted cell population, such as the Cre-loxP recombinase system.

AAV delivery

Adeno associated virus (AAV) is a small (25 μm) virus from the *Parvovoridae* family, that is a non-enveloped icosahedral protein structure (capsid) that surrounds and protects a small single-stranded DNA genome of approximately 4 Kb, which contains all the genes required for its

replication. It was discovered as a contaminant of an adenovirus preparation, hence its name adeno associated virus (AAV) but it was quickly realized that it had potential use as a tool to deliver proteins of interest (e.g. ChR2 to specific organs or tissues with high spatial and temporal resolution (Balakrishnan *et al.*, 2014; Hastie *et al.*, 2015)

Genetic studies are performed using recombinant AAVs (rAAV), which are engineered AAVs that lack the viral DNA, but are packaged with the desired transgenes (e.g., ChR2, fluorescent protein, floxed containing sequence). The transgene is inserted between two inverted terminal repeats (ITRs) of the AAV genome. ITRs are required in order for the transgene to be integrated into the host cell genome. However, attempts to exceed the packaging capacity of the rAAV (approximately 5 kb) could result in a considerable reduction in rAAV production yield or transgene recombination (Naso *et al.*, 2017).

Development of rAAV vectors is typically achieved by transient transfection assays, usually via the triple-transfection method (Lock *et al.*, 2010). During this process, a plasmid containing the AAV packaging genes (Rep and Cap genes) of the desired AAV serotype is co-transfected with a plasmid encoding for the adenoviral helper genes into a cell line (e.g. HEK 293 cells) together with a plasmid containing the transgene of interest (Gray *et al.*, 2011; Naso *et al.*, 2017). Presently, there are 12 serotypes of the AAV, where half have shown to be efficient in viral vector delivery of ChR2 into the CNS and the ENS (Gombash, 2015). AAVs are favored over other viral vectors due to their lack of pathogenicity, their capability to express proteins in mature non-dividing cells of multiple lineages, the short period of time (weeks) required to achieve transduction, and their sustained expression in tissues (Flotte, 2004; Mingozzi *et al.*, 2011). AAVs are safe and effective in preclinical and clinical settings (Naso *et al.*, 2017).

AAVs are very stable vectors as they can withstand wide temperatures and pH changes, with almost no effect on their activity. This stability provides ample opportunities to attempt different routes of administration and specialized delivery systems (Naso *et al.*, 2017). AAV

delivery can be achieved following intravenous, intramuscular, intraperitoneal, and intrathecal injections, and direct injection of the virus to specific tissues or organs (Gombash, 2015). The latter method provides a higher spatial resolution; however, it requires an invasive surgical procedure (Benskey *et al.*, 2015b). However, not all AAV serotypes are efficient in ENS transfection; in fact, the serotype AAV6 and AAV9 show the highest level of transduction in the ENS, with AAV6 being expressed in glia and neurons and AAV9 being expressed mostly in neurons (Benskey *et al.*, 2015b). The cell-type-specific capsid selection method (CREATE) developed by Chan expanded the capability to further genetically modified AAV vectors. This allowed to achieve relatively uniform and sparse expression in specific organs and cell populations within the CNS and ENS without recurring surgery (Chan *et al.*, 2017). Therefore, in the future AAV vectors developed by the CREATE method combined with optogenetic technology could be implemented as a gene therapy strategy to treat GI motility disorders, that in many cases require an invasive or life-threatening procedure.

Transgenic animal models

A standard method used to express ChR2 in specific cells is by generating a transgenic animal model, usually developed by conventional methods (e.g., homologous recombination), or more increasingly by Cre-loxP recombination. Compared to the AAV delivery method, the global expression of ChR2 is often achieved in these transgenic animal models, which decreases spatial resolution, but allows researchers to study multiple tissue and organ systems. An example of a ChR2 expressing transgenic mouse model developed by conventional homologous recombination is the ChAT-ChR2-EYFP-BAC transgenic mouse. These mice were developed by inserting the enhanced ChR2/eYFP fused protein sequence (also called hChR2-H134R-EYFP) into the mouse choline acetyltransferase (Chat or ChAT) locus of the RP23-246B12 bacterial artificial chromosome (BAC), which was then injected into fertilized eggs of B6SJLF1 mice (Zhao *et al.*, 2011). Crossbreeding of the litters with C57BL/6J mice finally gave birth to ChAT-

ChR2/eYFP transgenic mice which express the ChR2-eYFP fused protein in cholinergic neurons. ChAT-ChR2/eYFP transgenic mice have been successfully used to study motor endurance, attention deficit, and other cognitive behavior changes in the CNS (Kolisnyk *et al.*, 2013), and maybe useful for studying ENS cholinergic neurotransmission.

Conversely, many transgenic mice that express ChR2 in specific cell populations in the ENS have been developed with potential applications for GI motility studies by using the Cre-loxP recombination method (Jiang *et al.*, 2017; Rakhilin *et al.*, 2016; Stamp *et al.*, 2017). For example, transgenic mice that express ChR2 in calretinin neurons (CAL-ChR2 Cre+ mice) have been useful for *ex vivo* and *in vivo* colonic motility assays showing optical control of GI patterns of motility following exposure to focal stimuli of blue light (Hibberd *et al.*, 2018). Hence, due to the advancement in transgenic technology, it is anticipated that more sophisticated transgenic animals with new opsin channel capabilities will be available for studies of ENS circuitry (Wang, 2018).

The optogenetic light delivery system

In general, the duration, intensity, frequency, and the on/off cycle of the light source control the kinetic activity of the opsin molecule. Therefore, controlling these parameters is key when designing an optogenetic experiment, which can be easily manipulated by existing software. Moreover, the light source used in a study can have an impact on the results. Therefore, choosing the ideal light source is as essential as the light stimulation parameters. LEDs and lasers are commonly used light sources for optogenetics. LEDs are inexpensive, easier to control, and can produce a focal light stimulus with a light spot diameter of 2-3 mm. This provides stability and better delivery of the light stimulus. In contrast, lasers coupled to optic fibers can achieve a smaller light spot diameter of several hundred micrometers. The laser light spot can even reach a diameter small enough, which is capable of focally stimulating individual cells (Wang, 2018). LEDs, however, are easily attached to wireless devices and have been implemented for free

animal moving experiments. These devices can weigh about 20 mg, and are easily implanted in peripheral locations, making them ideal tools to study GI motility (Montgomery *et al.*, 2015; Wentz *et al.*, 2011),for instance for *ex vivo* CMMC motility assays.

Cre-loxP recombination

Cre-loxP recombination is a site-specific recombination tool use to carry out genetic modifications (e.g., deletions, insertions, translocations, and inversions) at specific locations in the DNA of cells. It is a particularly useful method to develop transgenic animals with inducible knock-out and knock-in characteristics. It was developed by Brian Sauer as a method to control site-specific DNA recombination in the swine kidney cell line PK15 by utilizing the Cre enzyme and lox sequence derived from the bacteriophage P1 (Sauer *et al.*, 1988). However, it was not until John Tsien established Cre-loxP recombination as a gene knockout technology to study neuronal gene mutations and animal behavior that it gained popularity in the neuroscience scientific community. In this groundbreaking study, Dr. Tsien and colleagues showed that deletion of a predefined gene of interest can be spatially and temporally restricted in the brain. They determine that the major factor that controls specificity is the transcription promoter that initiates expression of the Cre gene. For instance, by utilizing the transgenic αCaMKII promoter, which is specific for cells in the forebrain after postnatal day 16 (e.g., pyramidal cells), gene deletion was restricted to cells in the forebrain only after the third postnatal week. This was noteworthy because by knocking out the gene of interest at the third postnatal week one can avoid most of the developmental effects due to gene deletion, and would also provide better interpretation of the gene function during adulthood (Tsien *et al.*, 1996).

The Cre-lox recombination system consists of the Cre recombinase, which is a DNA splicing enzyme, and a specific sequence of DNA in which the enzyme targets the lox sequence. The Cre (an abbreviation for Causes recombination) enzyme is a 343 residue protein consisting of 4 subunits and two domains with a large C-terminus and a small N-terminal domain. This C-

terminal contains the catalytic site of the enzyme (Sternberg *et al.*, 1981a; Sternberg *et al.*, 1981b; Sternberg *et al.*, 1981c). Conversely, the lox (or locus of X-over P1) sequence is composed of an 8 bp spacer region flanked by two identical 13 bp inverted repeats (recognition region), which in total sums a 34 bp target sequence. However, other synthetic loxP mutants can be used to enhance or alter the recombination process (Hoess *et al.*, 1986).

The mechanism of action for this system requires the loxP sites and the enzyme to be expressed in the same cell. A standard method to achieve this site-specific recombination (SSR) is by breeding heterozygous transgenic mice that contain a loxP-flanked allele with hemizygous/heterozygous transgenic mice that express the Cre recombinase gene in a specific cell promoter. As a result, cells that only express the loxP sequence or the Cre recombinase gene will not exhibit site-specific recombination, but cells that contain both components will. Henceforth, once Cre enzyme is synthesized, it binds to the 13 bp recognition regions of each loxP site forming a tetramer structure. Next, the double-stranded DNA located at the loxP sites is excised by the Cre enzyme and then quickly rejoined by DNA ligase. Nevertheless, the orientation of the loxP sites will further define the results for the recombination process. For instance, in cases for which both loxP repeats have the same orientation, it will cause deletion of a transgene that is being flanked by these loxP sites (floxed). Conversely, if a stop cassette (loxP-flanked “stop” sequence) is positioned after a promoter but before a transgene of interests, Cre recombinase will cleave the stop cassette and drive insertion of that transgene. For this reason, the development of inducible knockout and knocking transgenic animals via the cre-lox recombination protocol is dependent not only on the orientation, but also the location of the loxP sites relative to the transgene of interest (Sauer *et al.*, 1988)

FUNCTIONAL GASTROINTESTINAL MOTILITY DISORDERS

General description

Functional gastrointestinal (GI) disorders (FGIDs) are disorders of gut-brain interaction. FGIDs include any combination of the following: motility disturbance, visceral hypersensitivity, altered mucosal and immune function, altered gut microbiota, and altered central nervous system (CNS) processing of visceral sensations. FGIDs include irritable bowel syndrome (IBS) and functional dyspepsia. The FGID definition is based on Rome IV diagnosis criteria developed by the non-profit organization called the Rome foundation, which mission is to create scientific data and educational information to assist in the diagnosis and treatment of FGIDs (Drossman *et al.*, 2016). Rome IV improves upon Rome III criteria published more than 10 years ago, which takes into account early life factors (e.g. genetics, culture and environment), psychosocial factors (e.g. life stress, personality traits, psychological state), physiology (e.g. motility, sensation, immune dysfunction, altered microbiota, diet), and all other gut-brain interactions that could affect FGIDs onset. Although the diagnosis of FGIDs is based primarily on the patient's report of symptoms, FGIDs also exhibit motility dysfunction, and inflammation, which are hallmarks of organic (structural) disorders such as inflammatory bowel disease (IBD). Hence, the diagnosis of FGIDs is difficult. Other motility disorders include gastroparesis and intestinal pseudo-obstruction, which are based on organ function persistent motility disturbances. These changes in motility are linked to neurodegeneration, and functional impairment of the ENS. Therefore, ENS dysfunction causes the motor activity to become uncoordinated, which, as a result, it halts the transit of as intestinal content (De Giorgio *et al.*, 2004; Goyal *et al.*, 1996). In the following paragraphs, I will discuss some of the most common types of FGIDs and motility disorders in the GI tract.

Gastroparesis

Gastroparesis or delayed gastric emptying is a motility disorder in which food content contained in the stomach is not able to be propelled down to the small intestine. During normal conditions, food received in the stomach is pushed from the upper region of the stomach, fundus, and corpus, down to the bottom end region of the stomach, antrum, before reaching the pyloric antrum. Once here, muscles in the pyloric antrum contract to empty the food content into the duodenum. Yet, during gastroparesis, the stomach muscles do not contract properly, causing food content to remain stagnant, and hence emptying of the content towards the small intestine is delayed. This can lead to a lot of complications such as infections, blockages due to the formation of solid mass (bezoar), dehydration due to excessive vomiting, malnutrition due to lack of nutrient absorption, and weight loss. Patients that suffer from other health problems such as diabetes mellitus, scleroderma, hypothyroidism, gastroesophageal reflex disease (GERD), Parkinson's disease, multiple sclerosis, and eating disorders are more prone to develop gastroparesis complications. Symptoms of gastroparesis include early satiety, poor appetite, nausea, vomiting, bloating, belching, abdominal pain, and heart burn. The cause of gastroparesis ranges from viral infections, side effects of narcotics and antidepressants, scleroderma, amyloidosis, and impairment of the vagus nerve during gastric surgery. The vago-vagal reflexes coordinate the relaxation and contraction of the gastric muscles (Bulbring *et al.*, 1968; Desai *et al.*, 1991; Hennig *et al.*, 1997; Tack *et al.*, 2002; Wilbur *et al.*, 1973), hence, it is no surprise that damage to the vagus nerve due to high blood sugar (e.g., Diabetes) is one of the most known causes of gastroparesis (Chandrasekharan *et al.*, 2007; Patrick *et al.*, 2008; Samsom *et al.*, 2009). Diagnosis of gastroparesis requires a medical examination (e.g., upper GI endoscopy, blood testing, measurement of gastric emptying, imaging for gastric blockage) and looking into the patient's medical history. The physicians tailor the treatment based on the cause, symptoms, and severity of the condition. Treatment could consist of changing eating habits (e.g., foods low on fat and

fiber), controlling blood sugar levels (e.g., regulate insulin levels), and medication (e.g., gut motility stimulators, antidepressants, pain medication). In some instances, physicians may recommend a feeding tube that connects to the small intestine, this to ensure that the patient is getting the right amount of nutrients and calories (National Institute of Diabetes and Diagestive and Kidney Disease, January 2018).

Functional Dyspepsia

From the Greek word dys and pepse meaning “difficult digestion”, dyspepsia is a medical term used to describe several symptoms located in the upper abdomen. However, dyspepsia is also broadly defined as pain or discomfort centered in the upper abdomen (upset stomach or indigestion), but may also include other symptoms such as nausea, vomiting, belching, abdominal bloating, early satiety, heartburn, regurgitation, and uncomfortable fullness after a meal. It is common for patients with dyspepsia report several of these symptoms. There is, however, heterogeneity of the symptoms among patients; therefore, the ROME III consensus committee defined dyspepsia as the presence of symptoms considered by the physician to originate from the gastroduodenal region. Henceforth, the patient must exhibit no evidence of structural disease following endoscopy and must have one or more of the following symptoms to be diagnosed with dyspepsia: postprandial fullness, early satiation, epigastric pain, and/or epigastric burning. Following publication of ROME IV, the definition for dyspepsia was slightly modified, yet the symptoms used for diagnosis were unchanged (Futagami *et al.*, 2018).

Despite popular belief, the cause of dyspepsia is not due to ingestion of specific foods, or excessive food consumption. In fact, the etiology of dyspepsia is still not well understood. Nonetheless, excessive ingestion of foods (e.g., excessive capsaicin) and certain medications (e.g., antibiotics, narcotics, oral contraceptives, levodopa, and theophylline) may aggravate or trigger the symptoms. Non-steroidal anti-inflammatory drugs (NSAIDs) have received the most attention due to their capacity to induce ulceration in the GI tract; in fact, the chronic use of aspirin

has shown to provoke dyspeptic symptoms in 20% of people. The most common identifiable causes underlying these dyspeptic symptoms are erosive esophagitis GERD (gastroesophageal reflux disease) and peptic ulcers (PUD), which are ulcers that originate either inside the lining of the stomach or the upper portion of the small intestine. However, when no apparent cause is found, the condition is known as functional dyspepsia. Functional dyspepsia, also known as non-ulcer dyspepsia or non-ulcer stomach pain, is diagnosed when no apparent cause can be found for the persistent symptoms of dyspepsia. Hence, diagnosis is only achieved once all other conditions (e.g., stomach ulcers, stomach cancers, GERD, PUC, gallstones, Helicobacter pylori infection) come up negative following testing (e.g., blood test, endoscopy) (Qayed, 2017). Functional dyspepsia is incurable but is not life-threatening; moreover, symptoms are manageable. Changes in lifestyle (e.g., diet restrictions, eating small meals, managing stress, losing weight) and medication (e. acid-suppressive drugs, prokinetic agents, antidepressants, pain medication, and anti-histamine drugs) or eradication the *H. pylori* infection that causes dyspepsia can help improve quality of life. (Qayed, 2017).

Intestinal pseudo-obstruction

Intestinal pseudo-obstruction (IPO) is a rate condition in which the patient exhibits symptoms that resemble intestinal blockage or delay (paralysis) in intestinal transit of content. However, examination reveals no blockage. IPO can develop during infancy (e.g., congenital intestinal pseudo-obstruction), or during adulthood, mainly in the elderly, are both either acute or chronical, or alternatively, IPO can develop as a complication of another medical condition (e.g., Parkinson's disease, certain cancers). IPO symptoms include any alterations that cause GI dysfunction (e.g., abdominal distension and pain, nausea, vomiting, constipation, and diarrhea. Intestinal paralysis, or intestinoparesis, affects the small intestine (e.g., Ileus), although the stomach function (e.g., gastroparesis) and colon (e.g., colonoparesis, acute colonic pseudo-obstruction or Ogilvie's syndrome) may be similarly affected. In addition to medical conditions, other factors that can

contribute to IPO includes infections (e.g. abscess, sepsis), inflammation (e.g. local tissue trauma, peritonitis), the use of pharmacologic agent (e.g. anticholinergic agents, general anesthetics, opioids, tricyclic antidepressants), and surgical procedures (e.g. abdominal or retroperitoneal surgery). Although not well understood, the direct cause for IPO has been linked to defects or injury to the ENS nerves and networks, smooth muscle cells, interstitial cells of Cajal (ICC), the autonomic nervous system (ANS), and to the central nervous system (CNS), all which have shown to influence the patterns of intestinal motility and secretion in the GI tract. Physical examinations, imaging studies (e.g., abdominal x-rays), biopsy during endoscopy or surgery, blood test, gastric emptying test, and medical history are all considered by the physician when diagnosing. Treatment varies across the different classes of IPO. They typically require patients to change their diet dramatically and prescribe a medication regimen tailored to the type of IPO. A person may need surgery to remove a section of the intestine, but this only happens in severe cases of IPO (Qayed, 2017) (National Institute of Diabetes and Diagestive and Kidney Disease, 2014).

Irritable Bowel Syndrome (IBS)

IBS is the most common FGID with high prevalence, substantial morbidity, and enormous cost. IBS affects approximately 11% of the world population, with women reporting the symptoms more than men (Chang *et al.*, 2014). The Manning criteria (Manning *et al.*, 1978), the Kruis scoring system (Kruis *et al.*, 1984) along with the ROME III criteria (Thompson, 2006) and finally the physician's assessment are all used during the physical examination as a way to diagnose patients with IBS (Qayed, 2017). Off note, the new ROME IV criteria expand on Rome IIII by improving its diagnostic tests and considering gut-brain interactions (Drossman, 2016; Drossman *et al.*, 2016).

Overall, IBS is characterized by the presence of abdominal discomfort or pain associated with disturbed defecation (constipation and diarrhea), bloating and visible distention, and non-

colonic symptoms that include headache, backache, impaired sleep, chronic fatigue, and frequent urination. Because IBS patients exhibit constipation or diarrhea, or a mixture of both, some authors have then attempted to classify IBS patients based on their predominant symptoms: constipation (IBS-C), diarrhea (IBS-D), mixed (IBS-M), or unsubtyped IBS (Chang *et al.*, 2014). The stool pattern of IBS patients can change over time and alternate between IBS types. Nevertheless, stool form is routinely used in clinical trials, as changes in stool form roughly correlate with changes in colonic transit time.

IBS is the sixth leading physician diagnosis in outpatients in the United States, where 12% of the outpatients are diagnosed with IBS. The percentage of affected patients is, however, suspected to be underestimated. IBS is a financial burden as costs due to missed days of work, excess physician visits, diagnostic testing, and use of medications add up to a substantial loss of income. A comprehensive burden-of-illness study in the United States estimated that IBS cost almost $1 billion in direct costs and another $50 million in indirect costs (Everhart *et al.*, 2009). Moreover, patients with IBS consume over 50% more health care resources than matched controls without IBS (Inadomi *et al.*, 2003)

The prevalence of IBS increases with age, and are higher in women compared to men. Although not life-threatening, IBS does decrease quality of life and increases the risk for development of GI diseases (e.g., ischemic colitis). IBS is a life-long disorder, therefore establishing a strong physician-patient relationship will be key for getting the best clinical care. Treatment for IBS first consists of diet and lifestyle changes. For instance, a high-fiber diet or fiber supplements, avoiding certain types of foods such as milk products, gluten-containing products, or food with high fermentable oligosaccharides, disaccharides, monosaccharides, and polyols can help treat symptoms of constipation and can sometimes firm up loose stools. However, changes in lifestyle or a better diet do not always ameliorate the pain associated with IBS. Therefore, anticholinergic antispasmodic agents (e.g., dicyclomine, propantheline, belladonna, and hyoscyamine) are

continually used in the United States to treat abdominal pain. Other drugs such as laxatives, antidiarrheal agents (e.g. loperamide), serotonin-receptor drugs (e.g. Alosetron), (only effective on women), antibiotics (e.g. rifaximin), probiotics, and other drugs acting on pain receptors (e.g. pregabalin, gabapentin) have been prescribed by physicians or used in clinical trials as alternatives to treat IBS symptoms (Chang *et al.*, 2014; Qayed, 2017).

CHAPTER 2: HYPOTHESIS & SPECIFIC AIMS

OVERALL GOAL

Gastrointestinal (GI) motility is controlled by the enteric nervous system (ENS)consist of an intrinsic neural circuit of afferent neurons, interneurons, and excitatory and inhibitory motor neurons. Its main objective is to regulate GI motility. GI motility results from the synchronized contraction and relaxation of the GI smooth muscles. Acetylcholine (ACh) is the main excitatory neurotransmitter released by excitatory motor neurons (EMN) at the neuromuscular junction to induce contractility of the gut muscles. Conversely, inhibitory motor neurons (IMN) co-release a purine transmitter (possibly ATP) and nitric oxide (NO) to cause inhibitory junction potentials (IJPs) and muscle relaxation (Furness, 2000; LePard *et al.*, 1999). ATP mediates fast IJPs (fIJP, purinergic component) and NO generates slow IJPs (sIJP, nitrergic component) (Crist *et al.*, 1992; Gallego *et al.*, 2008a). However, recent publications suggest that both purinergic and nitrergic components engage their response on separate populations of interstitial cells during GI motility. NO, as well as ACh, positive nerve fibers innervate ICC cells, mainly in the myenteric plexus ICC cells (ICC_{MY}). Purinergic nerve fibers innervate adjacent fibroblast-like intestinal cells at the muscle. In addition, previous studies of neurogenic relaxation of the longitudinal muscle suggest that NO and ATP release requires activation of R-type and N-type voltage-gated Ca^{2+} channel (VGCC), respectively (Bywater *et al.*, 1989; Rodriguez-Tapia *et al.*, 2017). This suggests that purine release and nitric oxide synthesis are controlled via separate subclasses of VGCCs. Overall, the data suggest two competing models for the mechanism of inhibitory smooth muscle relaxation in the gut. The first competing model suggests that purinergic and nitrergic components are held in separate populations of inhibitory motor neurons. The second competing model follows the current model that one population of inhibitory motor neuron co-releases ATP and NO, however, both components are compartmentalized in separate nerve terminals. These compartmentalized nerve terminal then innervate different populations of interstitial cells leading to the biphasic IJP recordings observed following smooth muscle relaxation.

Similarly, electrophysiological studies suggest that myenteric descending interneurons co-release ACh and ATP to adjacent interneuron and IMN populations in the myenteric plexus, leading to the recording of mixed cholinergic/purinergic excitatory postsynaptic potentials (EPSP). However, studies performed in the presence of VGCC antagonist reveal that the mechanisms that induce both neurotransmitters release are not likely driven by activation of the same classes of VGCC (Bywater *et al.*, 1989; Rodriguez-Tapia *et al.*, 2017). Hence, this further supports the presence of a distinct subpopulation of cholinergic and purinergic descending interneurons. Overall, the following thesis provides evidence for the existence of subpopulation of myenteric neurons that govern GI motility, which if correct could prompt in the discovery of novel drug targets for the treatment of GI related diseases. For this reason, research in this area is of great importance.

OVERALL HYPOTHESIS & AIMS

Overall Hypothesis

These studies tested the hypothesis that purinergic and nitrergic neurotransmission to the muscle layers and purinergic and cholinergic neurotransmission in GI myenteric ganglia are mediated by distinct subpopulations of cholinergic, nitrergic, and purinergic neurons. This overall hypothesis was tested through completion of the following specific aims.

Specific Aim 1

To establish the different subpopulations of purinergic myenteric neurons in the GI tract and their relative relationship to other known myenteric cell populations.

Specific Aim 2

Test the hypothesis that NO and a purine are released from different inhibitory motor neurons supplying GI muscles.

Specific Aim 3

Test the hypothesis that a subpopulation of descending myenteric interneurons is purinergic.

CHAPTER 3: IDENTIFICATION OF PURINERGIC NERVES IN THE MOUSE MYENTERIC PLEXUS

ABSTRACT

Evidence supports that purinergic neurotransmission controls an overwhelming number of GI functions in the enteric nervous system (ENS), and are a link to some GI-related diseases. However, scarcity of specific purinergic markers has dampened the effort to identify and classify such populations in the ENS. In this study, we performed immunohistochemistry (IHC) in mouse GI tissue preparations and compared the novel discovered purinergic marker, known as the vesicular nucleotide transporter (VNUT, SLC17A9), with a repertoire of acknowledged immunological markers. Our results reveal that VNUT is only expressed in the form of punctate varicosities at the nerve fibers and that endogenous expression of VNUT in the soma is non-existing in any of the tested cell populations. VNUT pericellular baskets were also visible surrounding choline acetyltransferase (ChAT), neuronal nitric oxide synthase (nNOS), and calretinin-positive cells but were absent in tyrosine hydroxylase (TH), and calbindin labeled cell populations. Overall, VNUT is not co-localized with any of the tested immunoreactive markers in nerve fibers within the myenteric plexus, the tertiary plexus, or circular smooth muscle layer of all tested tissue preps. Our findings suggest an exclusive subclass of myenteric neurons that could be responsible for driving purinergic neurotransmission in the ENS. These results differ from the current models of neurotransmission, which state that a single population of inhibitory motor neurons co-releases ATP along with nitric oxide (NO) to cause the muscles to relax. Other studies suggest that the descending pathway of colonic motility is controlled by a single population of cholinergic descending interneurons that also co-releases ATP. Nonetheless, further experimentation is needed to underline the purinergic pathway of neurotransmission in the ENS.

INTRODUCTION

Purine nucleosides and nucleotides control many physiological functions in the GI tract, such as promoting GI motility (Antonioli *et al.*, 2013; Bornstein, 2008; Burnstock, 2014b). Electrophysiological data have shown that presynaptic release of a purine, most likely ATP, induces fast and slow postsynaptic activation of myenteric cells (Galligan *et al.*, 1994), initiates fast inhibitory junction potentials (fIJPs) from circular smooth muscle cells (Crist *et al.*, 1992; Furness, 2000; Gallego *et al.*, 2008a; Gil *et al.*, 2010), and arguably induces excitatory junction potentials (EJPs) at the longitudinal smooth muscle layer (Ivancheva *et al.*, 2000; Zizzo *et al.*, 2007). Moreover, abnormal purinergic neurotransmission has been implicated in many GI-related diseases (Burnstock, 2014b). Hence, the development of potential therapeutic drugs tailored for the modulation of specific purinergic receptors could benefit the treatment of GI dysmotility/constipation, other motility disorders (Galligan *et al.*, 2004). Novel therapies may also help ameliorate some symptoms of slow transient constipation that comes with inflammatory bowel diseases (IBD) and is observed in patients with colitis (Burnstock, 2014b; Gibbons *et al.*, 2009; Gulbransen *et al.*, 2012a).

Nevertheless, despite the overwhelming evidence, attempts to identify purinergic cell populations have been unsuccessful. Approximately 90% of the enteric neuron population in the GI tract has been identified and classified by its morphology and neurochemical repertoire (Brookes, 2001; Qu *et al.*, 2008a). One exception, however, is purinergic neurons, as lack of suitable purinergic markers has made this task difficult. For instance, the conventional adenosine triphosphate (ATP) marker, quinacrine dihydrochloride, indiscriminately binds to adenine-containing molecules, therefore it is unable to distinguish between ATP as a neurotransmitter and the many endogenously expressed adenosine substances whose function is unrelated to neurotransmission, (Irvin *et al.*, 1954; White *et al.*, 1995). In order to underline the etiology of purinergic neurotransmission, the recent identification of the vesicular nucleotide transporter

(VNUT, SLC17A9), has ramped up the efforts to characterize these purinergic neuronal populations. VNUT is a 430 amino acid, 12 transmembrane spanning nucleotide transporter that transports and accumulates purines, including ATP, into vesicles, and is ubiquitously expressed in the CNS (Sawada *et al.*, 2008). ATP transport into vesicles by VNUT is inhibited by DIDS, Evans blue, and atractyloside which are all well-known inhibitors of vesicular neurotransmitter transporters (Sawada *et al.*, 2008). In the CNS, ATP neurotransmitter is a stimulant of neuropathic pain via specific purinergic receptor activation as blockade of $P2X_4$ and $P2Y_{12}$ purinergic receptors has been shown to ameliorate nociceptive pain during induced peripheral nerve injury (PNI) (Inoue *et al.*, 2004; Tozaki-Saitoh *et al.*, 2008). More importantly, decreased expression of VNUT in spinal dorsal horn neurons of SC17A9-/- mice, has been shown to diminish neuropathic pain after PNI, this when compared to control animals. Moreover, storage vesicular storage of ATP, and depolarization-evoked ATP release from isolated hippocampal neurons is absent in SC17A9-/- mice (Sakamoto *et al.*, 2014). Hence, these results highlight the critical role of the VNUT-dependent exocytotic ATP release mechanism in the nervous system. (Masuda *et al.*, 2016). VNUT, therefore, is a valuable tool that can be used to characterize the purinergic neuronal populations of the gut.

In this study, we use the VNUT primary antibody to determine the morphological characteristic this purinergic marker with other neuronal markers in the myenteric plexus, tertiary plexus, and circular smooth muscle tissue, this using tissue preparation obtained from the large intestine, small intestine, and stomach of mice.

MATERIALS AND METHODS

C57BL/6 mice of either sex (8-13 weeks old) were euthanized by cervical dislocation. All procedures were done under the animal use form guidelines of Michigan State University.

After euthanization, colon, ileum, jejunum, duodenum, and stomach tissue were harvested and fixed for immunohistochemistry. Tissue was cleaned, pinned mucosa facing up, and set overnight at 4°C with Zamboni's fixative (4% formaldehyde with 5% picric acid in 0.1M sodium phosphate buffer, pH 7.2).

The fixative was later removed, and tissue was washed with 0.1M phosphate buffer (PB) solution, pH 7.2, 3x 10 min, or until yellow coloring was removed. Whole-mount longitudinal muscle myenteric plexus (LMMP) was achieved by microdissection of the mucosa, submucosa plexus and circular muscle layers of the tissue. Circular muscle (CM) strips were also kept for some immunohistochemical tests. LMMP preps and CM strips were then incubated overnight at 4°C with primary antibodies (table 3.1). The tissue preps were then washed 3X 10 min, and then incubated with the secondary antibody (table 3.2) for 1 hour at room temperature. Double-staining consisted of pairing the VNUT with another primary antibody found in table1 and labeled each with different fluorophore containing secondary antibodies. Lastly, after three 10 min washes in PB, preps were transfer to a glass slide with ready-to-use mounting medium (ProlongTM Gold Antifade Mountant, Thermofisher, Cat No: P36961). All LMMP and CM preps were examined by conventional microscopy using a Nikon TE2000-U Inverted Microscope (Nikon TE2000-U series, Nikon Corporation, Tokyo, Japan) with MetaMorph® image acquisition and analysis software. All figures were taken with a CFI Plan Fluor 20X NA: 0.50 (air) and CFI Plan Fluor 40X NA: 0.75 (air) objectives. Epitopes tagged with Cyanine 3 (Cy3), or fluorescein isothiocyanate (FITC) fluorophores were visualized with Nikon green excitation fluorescent filters (Filter cubes Cy GFP and B-2E/C).

Confocal images were taken by Olympus Confocal Laser Scanning microscope (Olympus FV1000 series, Olympus Corporation, Tokyo, Japan) with FV1000 software). Images were taken with a UPLFLN 40X NA: 1.30 (oil) objective. Images were taken in sequential mode, Z-depth images, sample speed of 4.0 µs/pixel, zoom x2.5. A 488nm laser was used to excite FITC, and a

543nm laser excited the Cy3 synthetic chromophore. Emission Filters: SDM560 and mirror, and excitation filters: DM405/488/543.

The term co-localization was used to describe when the VNUT fluorescent epitope expressed in neurons and nerves overlapped with the non-VNUT fluorescent epitopes during microscopy examination. Z-depth confocal imaging of the colon tissue preps were assessed to fully assess co-localization of the VNUT and nNOS immunological markers.

1 AB	**Host**	**Catalog #**	**Lot #**	**Dilution**	**Source**
VNUT	Rabbit	Sc-86312	G-1812	1/200	Santa Cruz
NOS	Sheep	AB1529	2728417	1/300	Merck Millipore
ChAT	Goat	AB144P	2736715	1/100	Merck Millipore
Calbindin	Mouse	300	07(F)	1/1000	Swant
Calretinin	Goat	CG1	1§.1	1/500	Swant
TH	Sheep	AB1542	2896740	1/500	Merck Millipore
2 AB		**Catalog #**	**Lot #**	**Dilution**	**Source**
Donkey anti-rabbit-Cy3		711-166-152	131954	1/200	Jackson
Donkey anti-rabbit-FITC		711-096-152	125792	1/100	Jackson
Donkey anti-sheep-FITC		713-096-147	123217	1/100	Jackson
Donkey anti-goat-Cy3		705-166-147	131306	1/200	Jackson
Donkey anti-mouse-FITC		715-096-150	128992	1/100	Jackson

Table 3.1: Primary antibodies (1 AB), secondary antibodies (2 AB), dilutions and suppliers of reagents used for immunohistochemical studies of neuronal markers.

As proof of concept, the specificity of the VNUT antibody was tested by incubating the VNUT antibody with the blocking peptide (Figure 3.1), and by measuring SLC7A9 (VNUT) protein levels post siRNA knockdown of endogenously expressed VNUT in a PC-12 cell line (ATTC® CRL-1721, Manassas, VA). SLC7A9 siRNA (catalog # sc-141874, Lot # 10712, Santa Cruz biotechnologies) and scramble siRNA (catalog # sc-36869, Lot # B0919, Santa Cruz biotechnologies) were transfected into undifferentiated PC-12 cells using HiPerFect transfection reagent (Cat # 301704, Qiagen company) as described by Sawada et al., 2008. PC-12 culture medium (DMEM high glucose with pyruvate (catalog # 11995073), 10% horse serum, 2.5% fetal

bovine serum, and 1% pen strep), containing a final concentration of 75nM of either siRNA was applied each to 6 well plates already containing PC-12 cells (2.5 X10^5 cells/ml) for 48hrs. The medium was replaced every 24hrs, following the first transfection. Following transfection, cells were lysed, and total protein concentration was determined via standard BCA assay. Later 40 µg/µL of protein was loaded into a 2% agarose gel for western blot analysis. Each sample protein was then imaged at 800nm and normalized to the lane normalization factor (LNF) obtained from the total protein staining (700nm image) (LI-COR-Revert-Total protein stain Normalization Protocol) (Fig. 3.2).

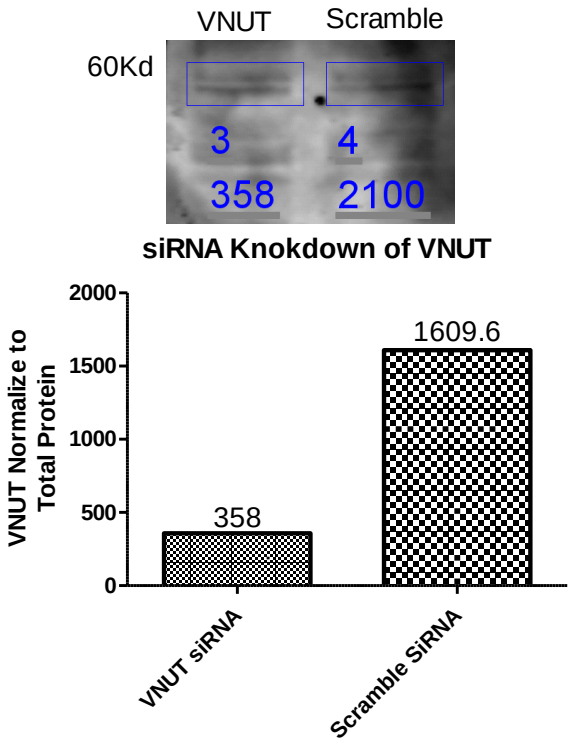

Figure 3.1: siRNA knockdown of endogenously expressed SLC7A9 (VNUT) in PC-12 cell line. Results show a decrease in VNUT protein after SLC7A9 siRNA (catalog # sc-141874, Lot # 10712, Santa Cruz biotechnologies) transfection of PC-12 cell line, this compared to our scramble siRNA (catalog # sc-36869, Lot # B0919, Santa Cruz biotechnologies). Each sample protein was imaged at 800nm and normalized the lane normalization factor (LNF) obtained from the total protein staining (700nm image) as explained by the LI-COR-Revert-Total protein stain Normalization Protocol.

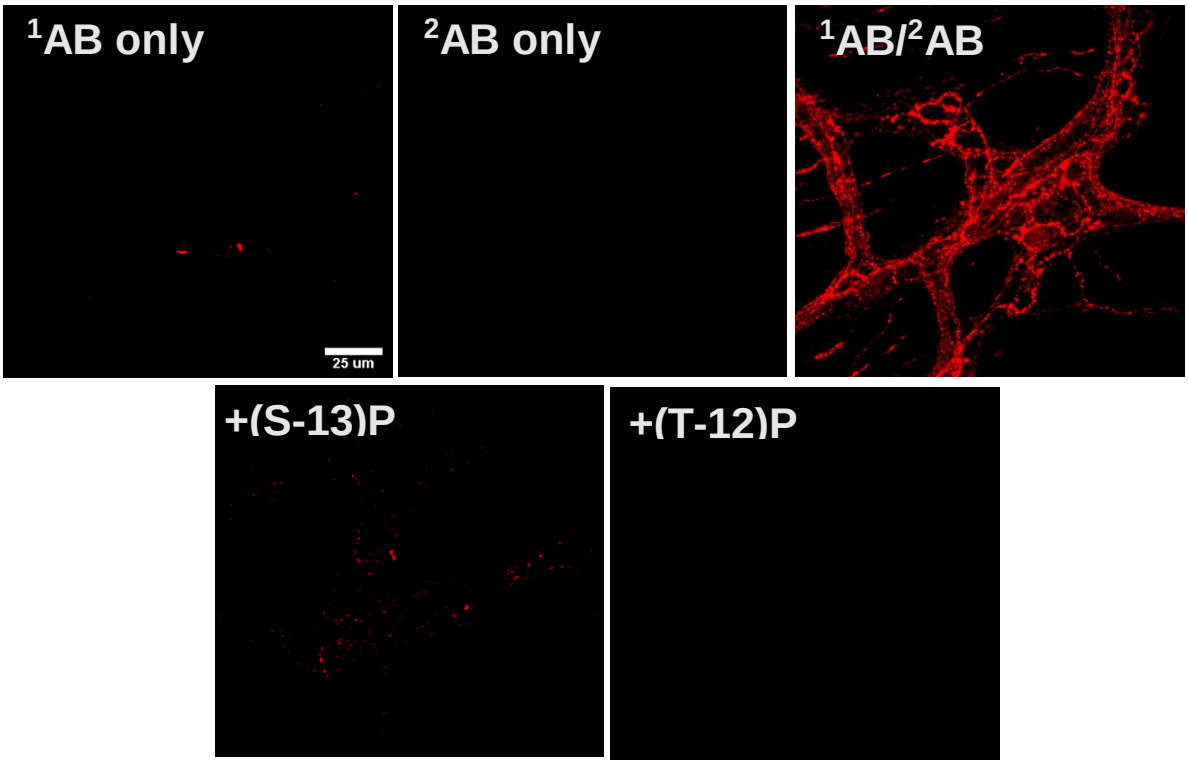

Figure 3.2: VNUT epi-fluorescence labeling in the colon myenteric plexus is reduced by VNUT blocking peptides. Immunohistochemistry for the purinergic marker, VNUT (SLC7A9) is decreased following overnight incubation of the primary antibody ([1]AB) with the N-terminal ((S-13)P, catalog # sc-86312, Lot # J3112, Santa Cruz biotechnologies) and Internal ((T-12)P, catalog # sc-86313, Lot # C2513, Santa Cruz biotechnologies) SLC7A9 competing peptides.
Images were taken using the same excitation/emission parameters under a conventional Nikon TE2000-U Inverted Microscope (Nikon TE2000-U series, Nikon Corporation). Abbreviations, [1]AB; primary antibody, [2]AB; secondary antibody,

RESULTS

The following results are a composite of the histological findings used to compare the purinergic marker, VNUT, and additional immunological markers in an attempt to examine the purinergic cell population and distribution in the enteric nervous system.

VNUT and nNOS are co-expressed in nerve bundles innervating smooth muscle

Neuronal nitric oxide synthase (nNOS) immunoreactive (ir) cell bodies and nerve fibers were observed in the myenteric plexus (Fig. 3.3), tertiary plexus (Fig. 3.4), and in the circular smooth muscle (Fig. 3.5) of all mice tested tissues. VNUT formed pericellular baskets that surround the

majority of nNOS-immunoreactive neurons. Only a small number of nerve fibers in the myenteric plexus co-expressed both VNUT and nNOS (Fig. 3.3A-E), A significant number of the VNUT only nerve fibers innervate non-nNOS positive cells. VNUT only, nNOS only, and NOS/VNUT mixed nerve fibers can be observed in the tertiary plexus (Fig. 3.4A-E). However, all nerve bundles that innervate the circular smooth muscle of the gut co-express VNUT and nNOS (Fig. 3.5A-E). These results were observed in all LMMP and CM tissue dissections of mice small intestine, large intestine, and the stomach.

Confocal Z-depth images reveal that VNUT and nNOS do not co-localize in nerve fibers in myenteric plexus, tertiary plexus and circular smooth muscle of the mouse colon. Co-localization in the small intestine and stomach was not assessed in this study (Fig. 3.18).

VNUT$^+$ nerve fibers innervate ChAT$^+$ neurons in the large and small intestine.

In the myenteric plexus of the mouse colon and ileum, VNUT$^+$ only nerve fibers innervate some ChAT$^+$ neurons (Fig. 3.6A-B). However the jejunum, duodenum and stomach tissues show little VNUT/ChAT interaction (Fig. 3.6C-E). In addition, rarely the two markers are co-expressed in nerve fibers at the tertiary plexus (Fig. 3.7A-E). Finally, VNUT and ChAT are contained within the same nerve bundles at the circular muscle yet do not seem to co-localize (Fig. 3.8A-E)

Calbindin$^+$ neurons and nerves do not express VNUT ir.

Calbindin ir is restricted to the myenteric plexus. VNUT$^+$ nerves rarely innervated calbindin$^+$ cell bodies or nerves of any tissue preps (Fig. 3.9A-E). Also, VNUT and calbindin were only observable in separate populations of enteric nerve fibers within the myenteric plexus. This is more evident in the tertiary plexus and CM, as mentioned before, only VNUT+ varicose nerve fibers could be observed in the tertiary plexus (Fig. 3.10A-E) and circular smooth muscle (Fig. 3.11A-E).

VNUT ir nerve fibers innervate calretinin^{+} neurons in the large intestine.

The calretinin ir marker is highly visible in the myenteric plexus (Fig. 3.12A-D), tertiary plexus (Fig. 3.13A-D), and circular smooth muscle (Fig. 3.14A-D) of the colon and small intestine, but little is observed in stomach tissue preps (Fig. 3.12E, 3.13E and 3.14E). In colon tissues, purinergic nerve varicosities innervate a small portion of calretinin ir cell bodies and nerve fibers (Fig 3.12A). VNUT can also be found innervating some calretinin cell bodies but at a lower frequency in the small intestine and stomach (Fig. 3.12 B-E). With exception of the stomach, myenteric nerve bundles that projected to the tertiary plexus (Fig. 3.13A-D) and circular smooth muscles (Fig. 3.14A-D) of colon and small intestine contained both VNUT and calretinin; however, they do not co-localize.

TH and VNUT do not co-localize in the ENS

TH immunoreactivity can be observed in the myenteric plexus (Fig. 3.15A-E), tertiary plexus (Fig. 3.16A-E), and circular smooth muscle (Fig. 3.17A-E) of all tissues. However, TH and VNUT do not co-localize in any of the tested tissues. Only a few VNUT nerve varicosities were observed to innervate cell bodies also targeted by TH immunoreactive nerves, but, in no instance did they co-localize. Finally, VNUT only and TH only nerve fibers were overwhelmingly observed in the myenteric plexus, tertiary plexus, and circular muscle.

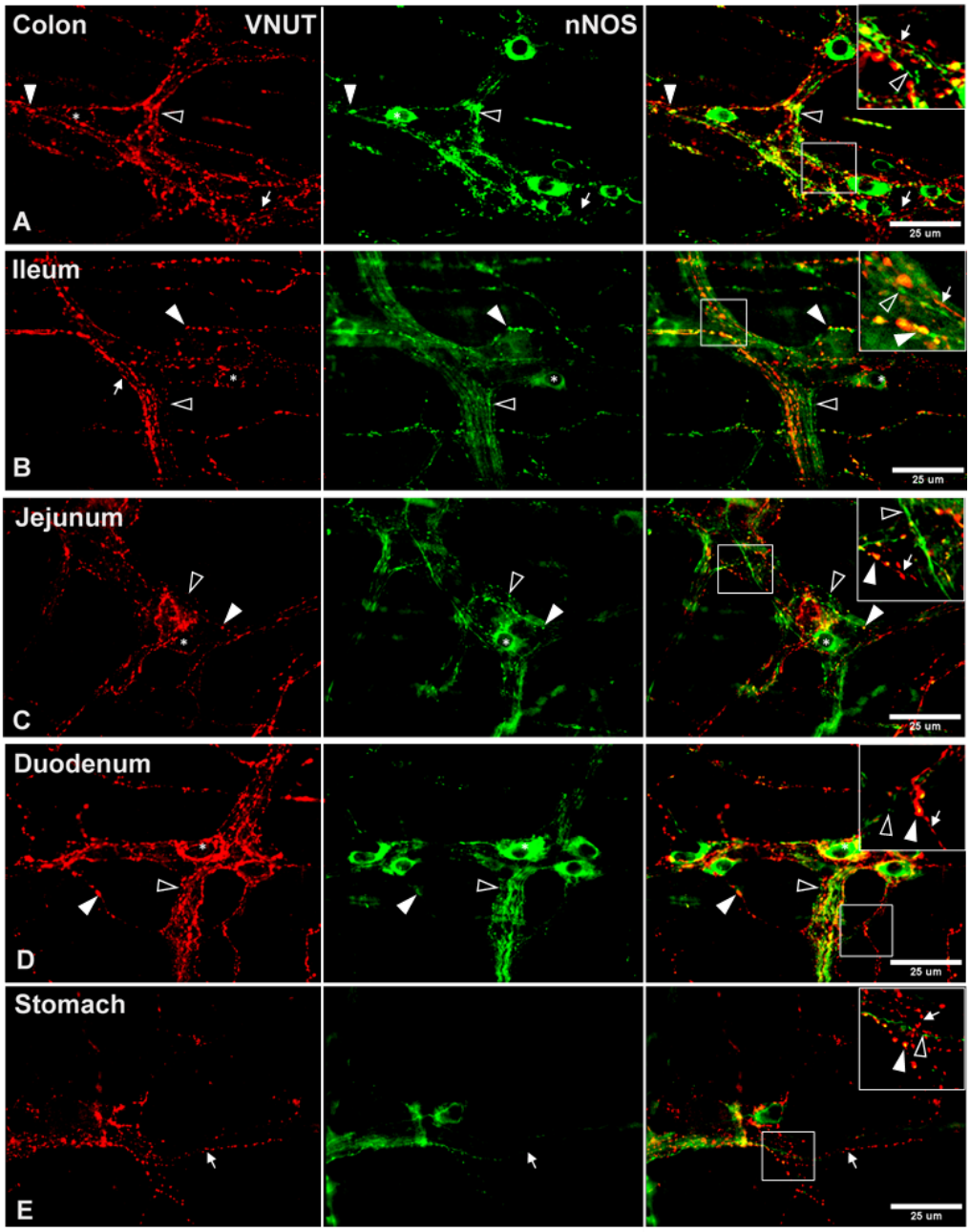

Figure 3.3: nNOS and VNUT co-expression in the myenteric plexus. $VNUT^+$ (red) only varicosities (full arrows), $nNOS^+$ (green) only varicosities (open arrowheads), and $VNUT^+/NOS^+$ varicosities (closed arrowheads) in the myenteric plexus of the colon, ileum, jejunum, duodenum, and stomach LMMP preps, A-E. FITC-conjugated donkey anti-sheep IgG (H+L) was used to labeled nNOS, and Cy3-conjugated donkey anti-rabbit label for VNUT. Images were taken using a conventional Nikon TE2000-U Inverted Microscope (Nikon TE2000-U series, Nikon Corporation).

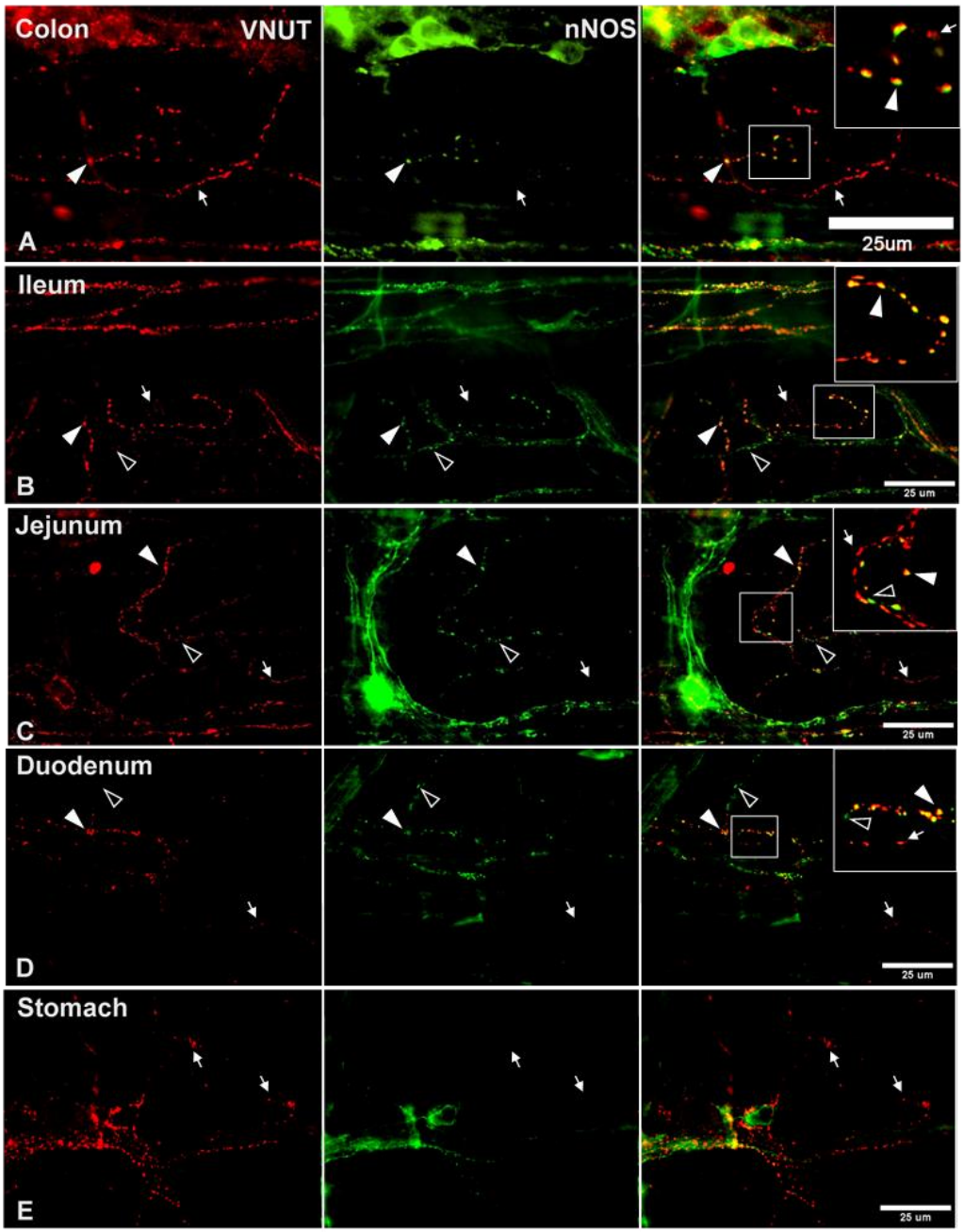

Figure 3.4: nNOS and VNUT co-expression in the tertiary plexus. $VNUT^+$ (red) only varicosities (full arrows), $nNOS^+$ (green) only varicosities (open arrowheads), and $VNUT^+/NOS^+$ varicosities (closed arrowheads) in the tertiary plexus of the colon, ileum, jejunum, duodenum, and stomach LMMP preps, A-E. FITC-conjugated donkey anti-sheep IgG (H+L) was used to labeled nNOS, and Cy3-conjugated donkey anti-rabbit label for VNUT. Images were taken using a conventional Nikon TE2000-U Inverted Microscope (Nikon TE2000-U series, Nikon Corporation).

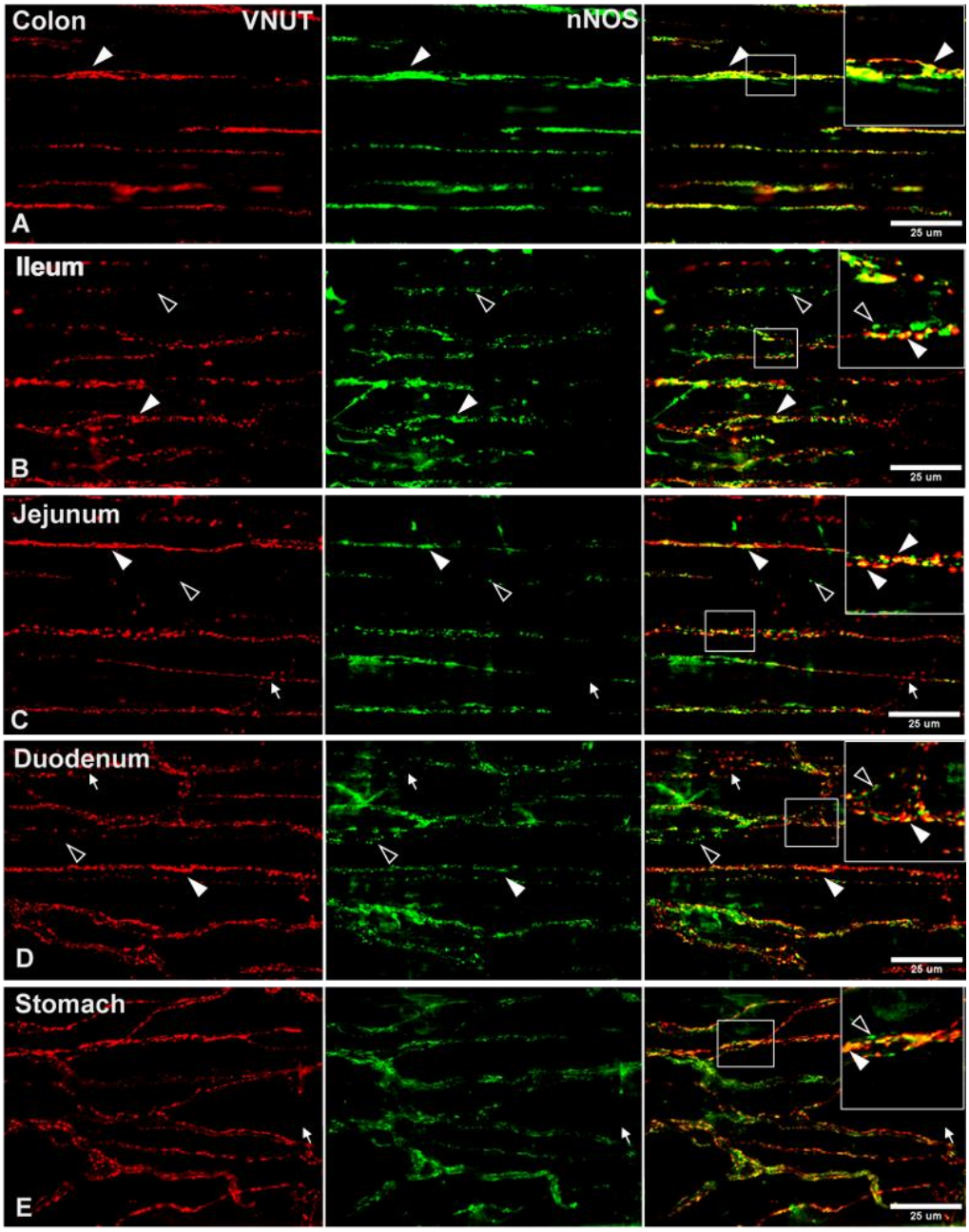

Figure 3.5: nNOS and VNUT co-expression in circular smooth muscle. $VNUT^+$ (red) only varicosities (closed arrowheads), $nNOS^+$ (green) only varicosities (open arrowheads), and $VNUT^+/NOS^+$ varicosities (full arrows) in circular smooth muscle strips of the colon, ileum, jejunum, duodenum, and stomach, A-E. FITC-conjugated donkey anti-sheep IgG (H+L) was used to labeled nNOS, and Cy3-conjugated donkey anti-rabbit label for VNUT. Images were taken using a conventional Nikon TE2000-U Inverted Microscope (Nikon TE2000-U series, Nikon Corporation).

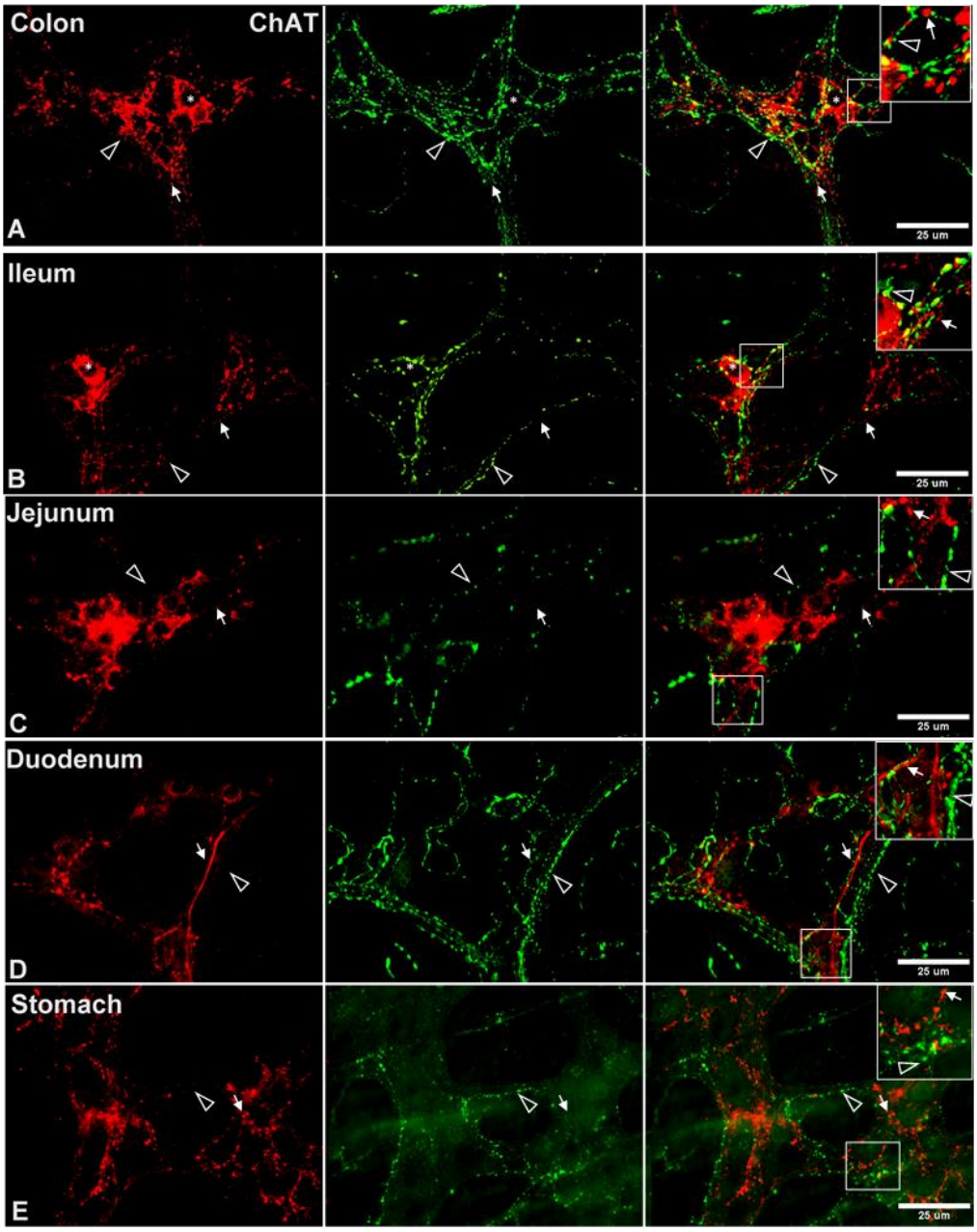

Figure 3.6: VNUT and ChAT are located in a separate subset of nerves in the myenteric plexus. ChAT^{+} (red), nerves in the myenteric ganglia (arrows), do not show the VNUT (green) immune marker (arrowheads), vice versa, of colon, ileum, jejunum, duodenum, and stomach, A-E. The asterisk (*)reveals ChAT^{+} cell bodies surrounded by VNUT varicose nerve fibers most predominantly in colon and ileum tissue preps. FITC-conjugated donkey anti-rabbit IgG (H+L) was used to label VNUT, and Cy3-conjugated donkey anti-goat label for ChAT. Images were taken using a conventional Nikon TE2000-U Inverted Microscope (Nikon TE2000-U series, Nikon Corporation).

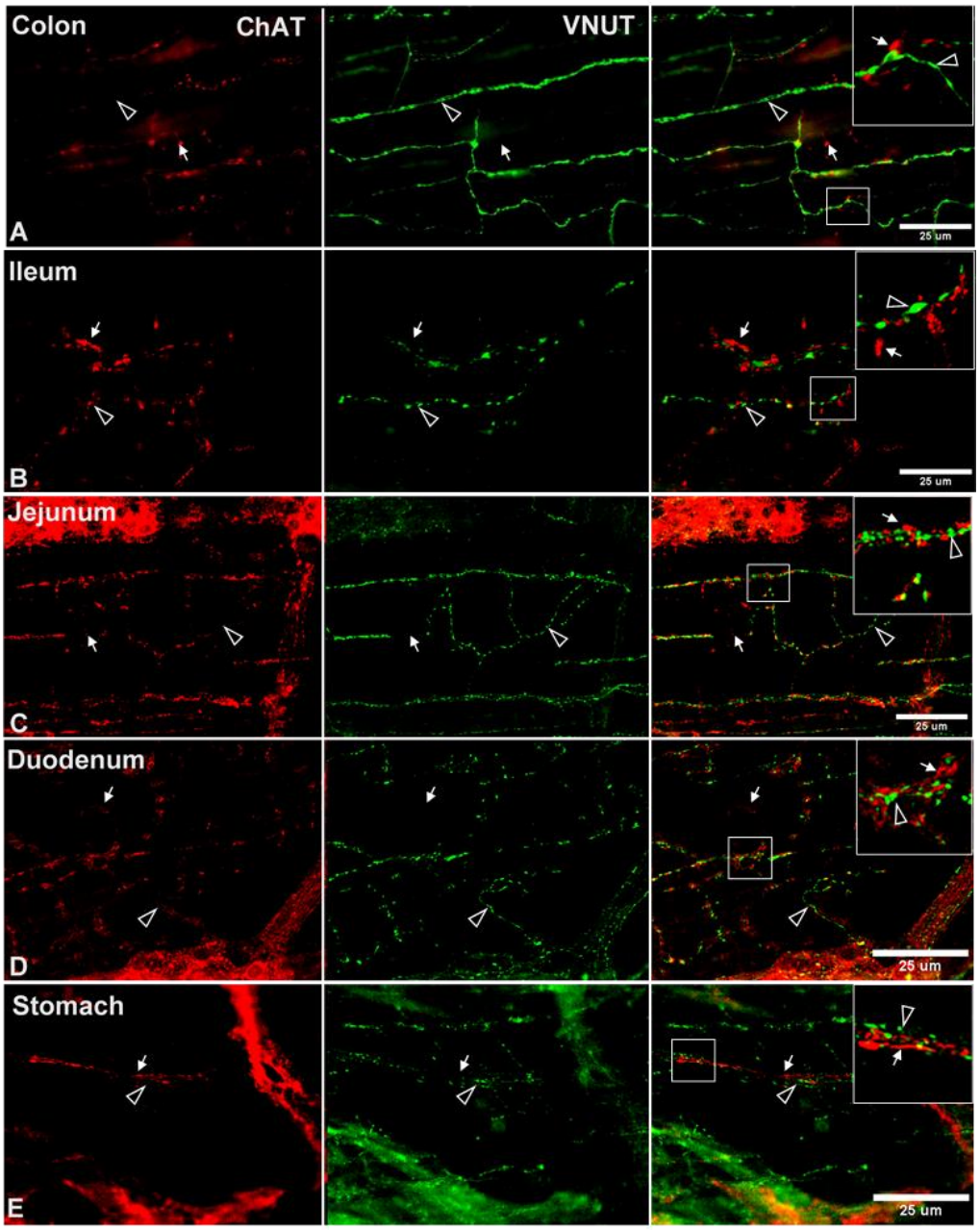

Figure 3.7: VNUT and ChAT are located in a separate subset of nerves in the tertiary plexus. ChAT^{+} (red) positive nerves in the tertiary plexus (arrows), do not show the VNUT (green) immune marker (arrowheads), vice versa, of colon, ileum, jejunum, duodenum, and stomach, A-E. FITC-conjugated donkey anti-rabbit IgG (H+L) was used to label VNUT, and Cy3-conjugated donkey anti-goat label for ChAT. Images were taken using a conventional Nikon TE2000-U Inverted Microscope (Nikon TE2000-U series, Nikon Corporation).

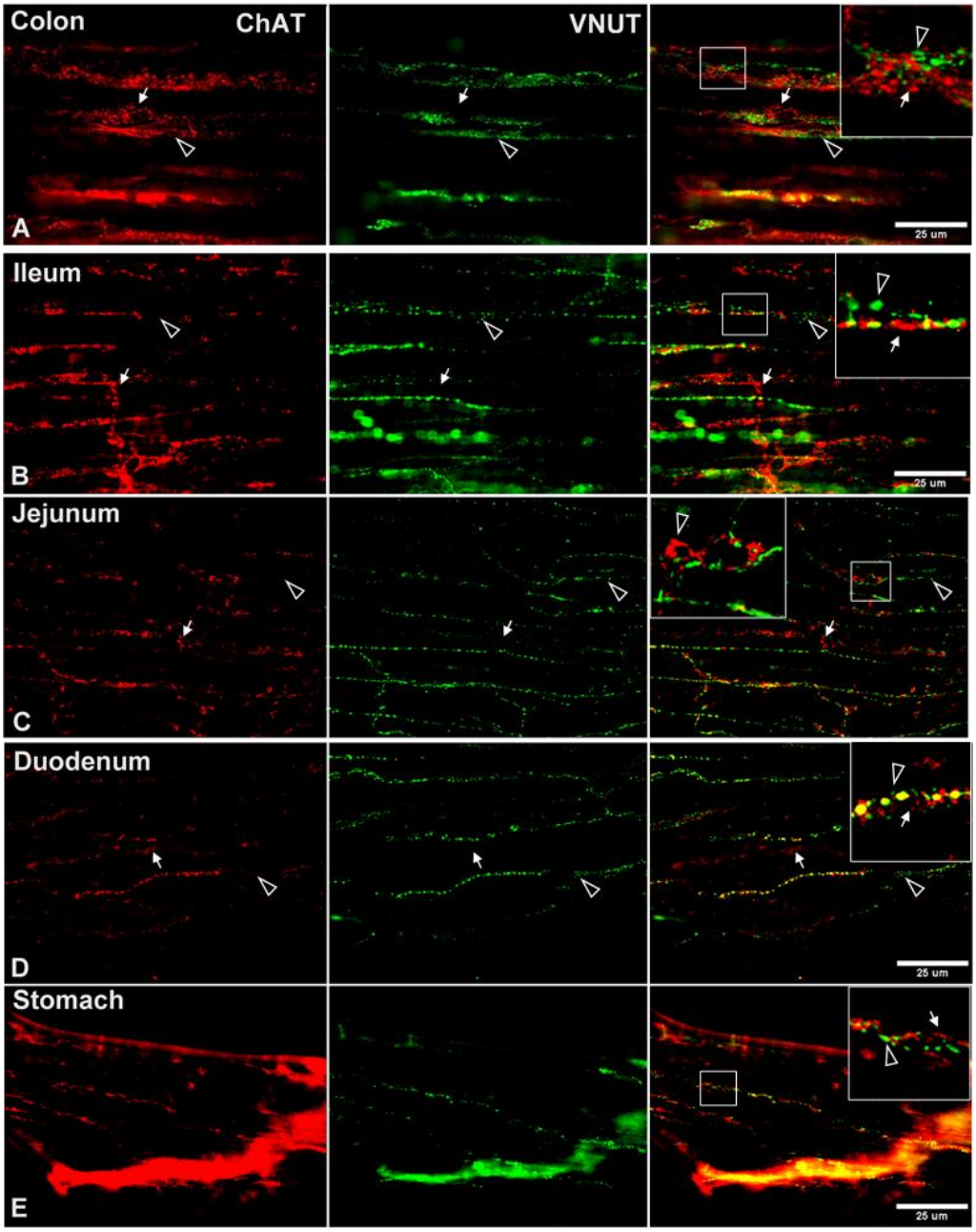

Figure 3.8: VNUT and ChAT are located in a separate subset of nerves in the circular smooth muscle. ChAT^{+} (red) nerves in circular smooth muscle (arrows), do not show the VNUT (green) immune marker (arrowheads), vice versa, of colon, ileum, jejunum, duodenum, and stomach, A-E. Co-localization was rarely observed in any of the examined tissue preps (D), however, this outcome is potentially false due to one of the stained nerves laying on top of the other as they are located at different focal planes. FITC-conjugated donkey anti-rabbit IgG (H+L) was used to label VNUT, and Cy3-conjugated donkey anti-goat label for ChAT. Images were taken using a conventional Nikon TE2000-U Inverted Microscope (Nikon TE2000-U series, Nikon Corporation).

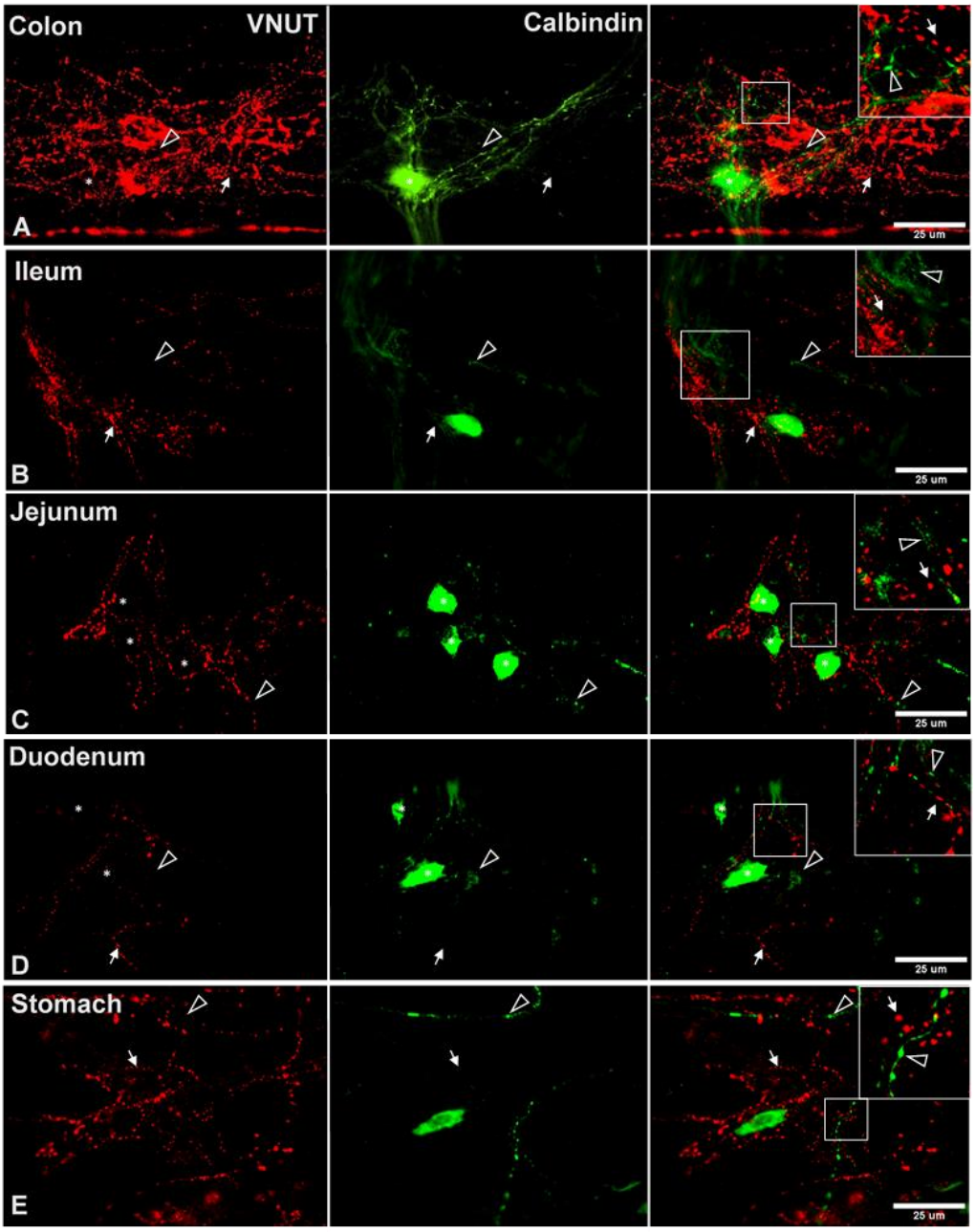

Figure 3.9: VNUT and calbindin are located in a separate subset of nerves in the myenteric plexus. VNUT^{+} (red) nerves in the myenteric ganglia (arrows), do not show the calbindin (green) immune marker (arrowheads), vice versa, of the colon, ileum, jejunum, duodenum, and stomach, A-E. The asterisk (*) reveals calbindin^{+} cell bodies, which in this case do not receive any innervation from VNUT varicose nerve fibers of all the tested tissue preps. FITC-conjugated donkey anti-mouse IgG (H+L) was used to label calbindin and Cy3-conjugated donkey anti-rabbit label for VNUT. Images were taken using a conventional Nikon TE2000-U Inverted Microscope (Nikon TE2000-U series, Nikon Corporation).

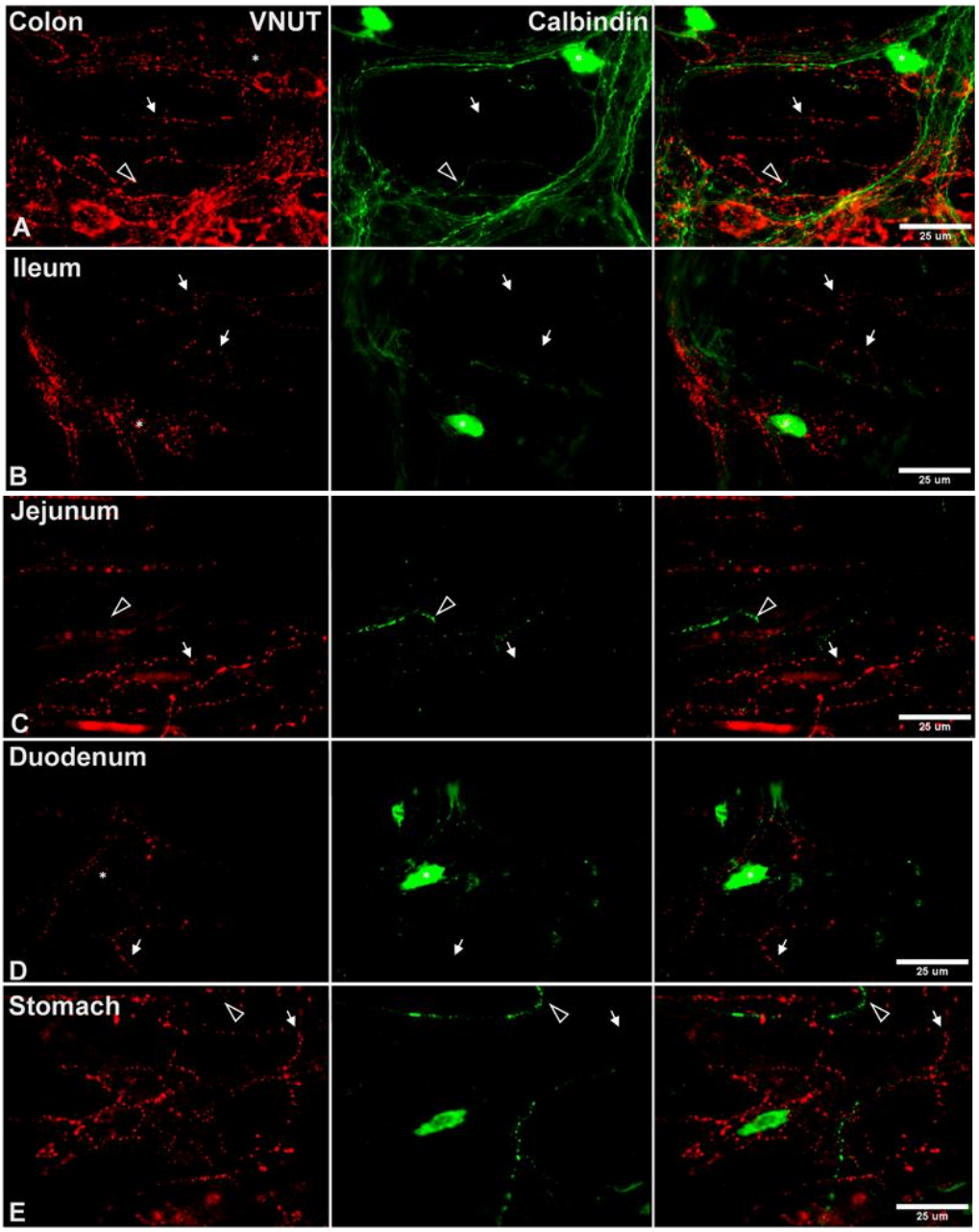

Figure 3.10: **VNUT and calbindin are located in a separate subset of nerves in the tertiary plexus.** VNUT^{+} (red) varicose nerves in the myenteric ganglia (arrows), do not show the calbindin (green) immune marker (arrowheads), in the colon, ileum, jejunum, duodenum, and stomach, A-E. The asterisk (*) reveals calbindin^{+} cell bodies in the myenteric plexus. Calretinin^{+} nerves fibers are rarely observed in the mouse tertiary plexus, C & E, as calretinin immunostaining is mainly restricted to the myenteric plexus. FITC-conjugated donkey anti-mouse IgG (H+L) was used to label calbindin and Cy3-conjugated donkey anti-rabbit label for VNUT. Images were taken using a conventional Nikon TE2000-U Inverted Microscope (Nikon TE2000-U series, Nikon Corporation).

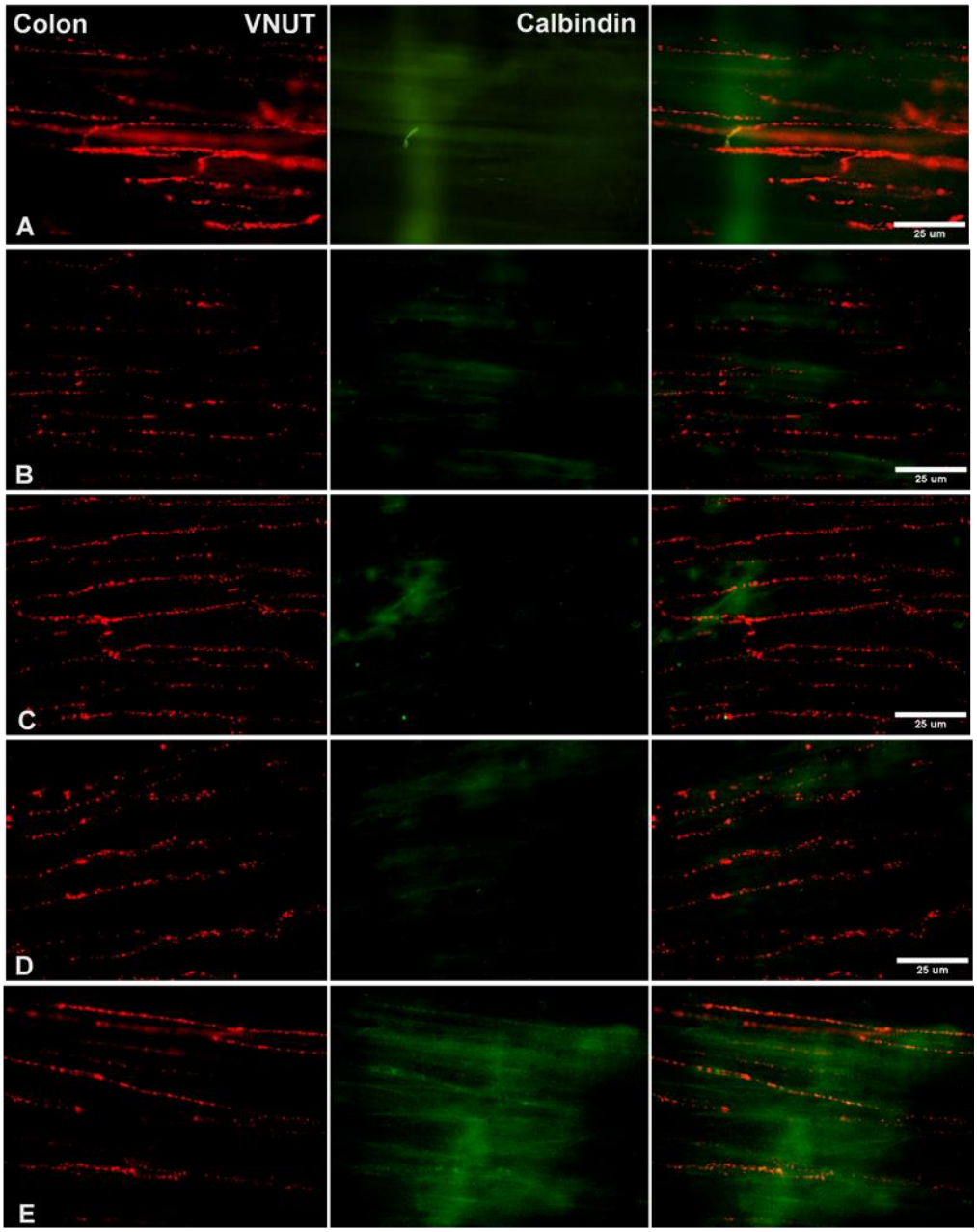

Figure 3.11: VNUT and calbindin are located in a separate subset of nerves in the circular smooth muscle. VNUT^{+} (red) varicose nerves in circular smooth muscle tissue preps do not show the calbindin (green) immune marker in the colon, ileum, jejunum, duodenum, and stomach, A-E.. Calretinin^{+} nerves fibers are never observed in the circular smooth muscle, as calretinin immunostaining is mainly restricted to the myenteric plexus. FITC-conjugated donkey anti-mouse IgG (H+L) was used to label calbindin and Cy3-conjugated donkey anti-rabbit label for VNUT. Images were taken using a conventional Nikon TE2000-U Inverted Microscope (Nikon TE2000-U series, Nikon Corporation).

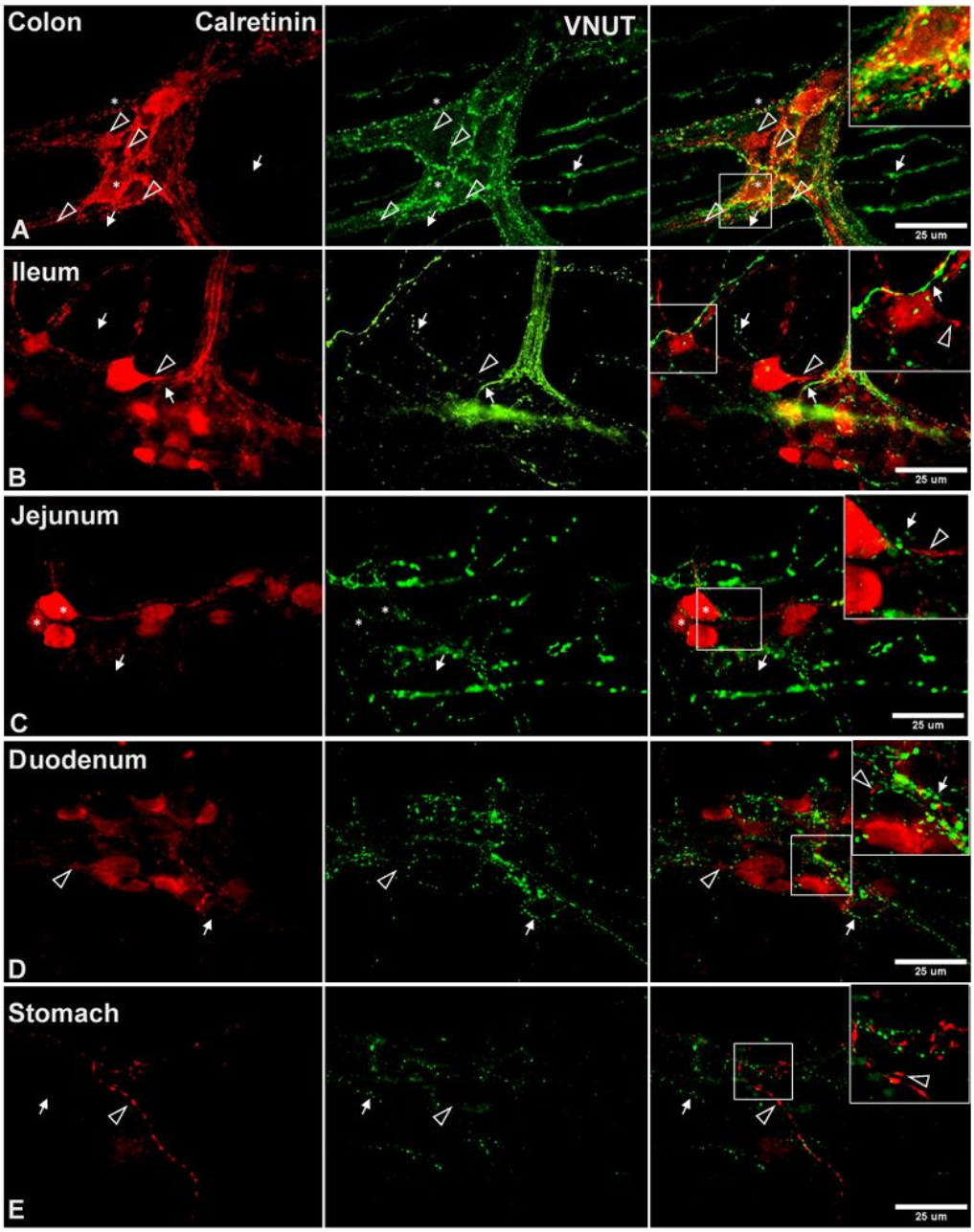

Figure 3.12: VNUT and calretinin are located in a separate subset of nerves in the myenteric plexus. VNUT^{+} (green) nerves in the myenteric ganglia (arrows), do not show the calretinin (red) immune marker (arrowheads), vice versa, of the colon, ileum, jejunum, duodenum, and stomach, A-E. The asterisk (*) reveals calretinin^{+} cell bodies surrounded by VNUT perivascular baskets in the colon, however, calretinin^{-} cells showed to be more likely to be targeted by VNUT varicose fibers within the myenteric plexus. FITC-conjugated donkey anti-rabbit IgG (H+L) was used to label VNUT, and Cy3-conjugated donkey anti-goat label for calretinin. Images were taken using a conventional Nikon TE2000-U Inverted Microscope (Nikon TE2000-U series, Nikon Corporation).

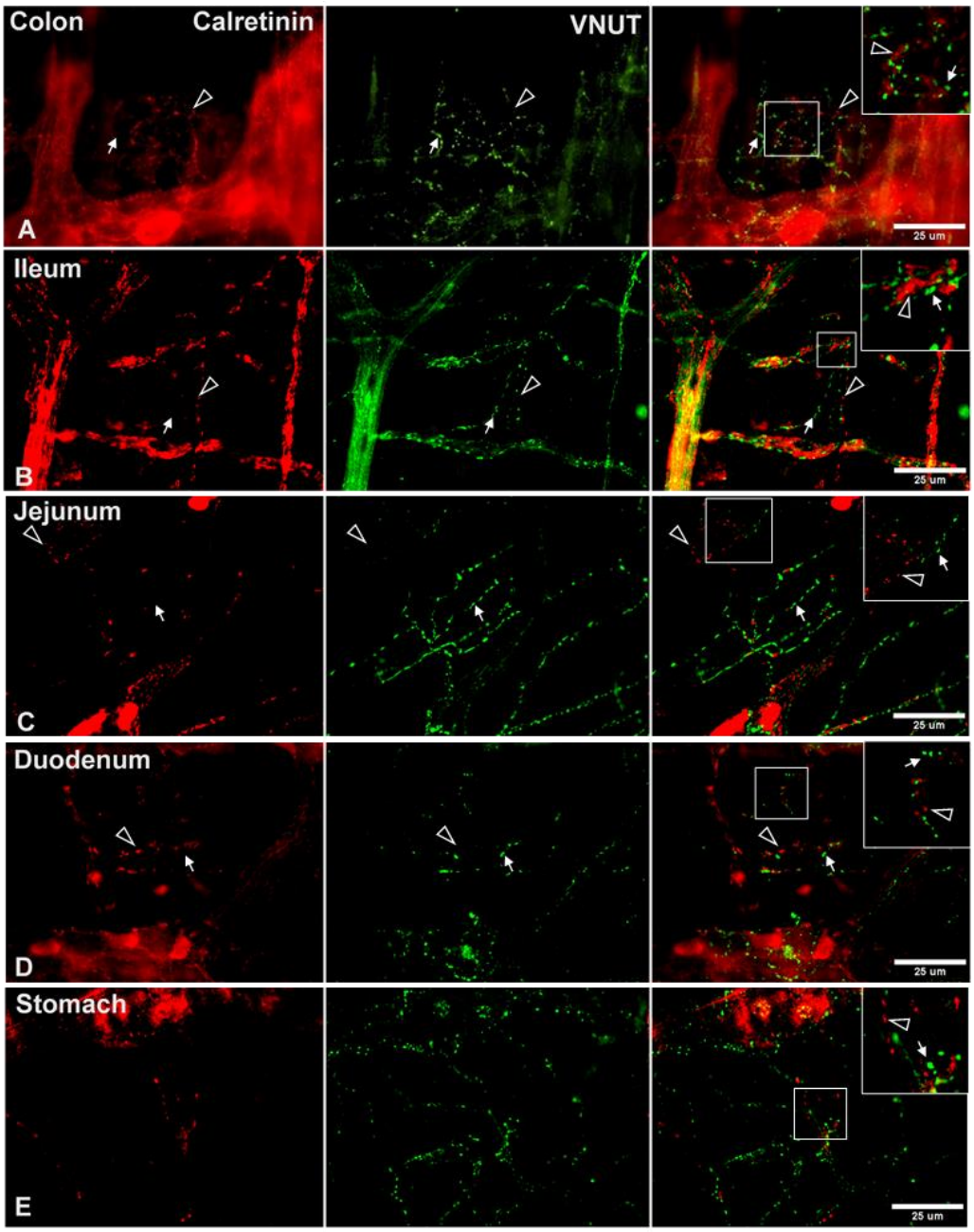

Figure 3.13: VNUT and calretinin are located in a separate subset of nerves in the tertiary plexus. VNUT^{+} (green) positive nerves in the tertiary plexus (arrows), do not show the calretinin (red) immune marker (arrowheads), vice versa, of colon, ileum, jejunum, duodenum, and stomach LMMP preps, A-E. FITC-conjugated donkey anti-rabbit IgG (H+L) was used to label VNUT, and Cy3-conjugated donkey anti-goat label for calretinin. Images were taken using a conventional Nikon TE2000-U Inverted Microscope (Nikon TE2000-U series, Nikon Corporation).

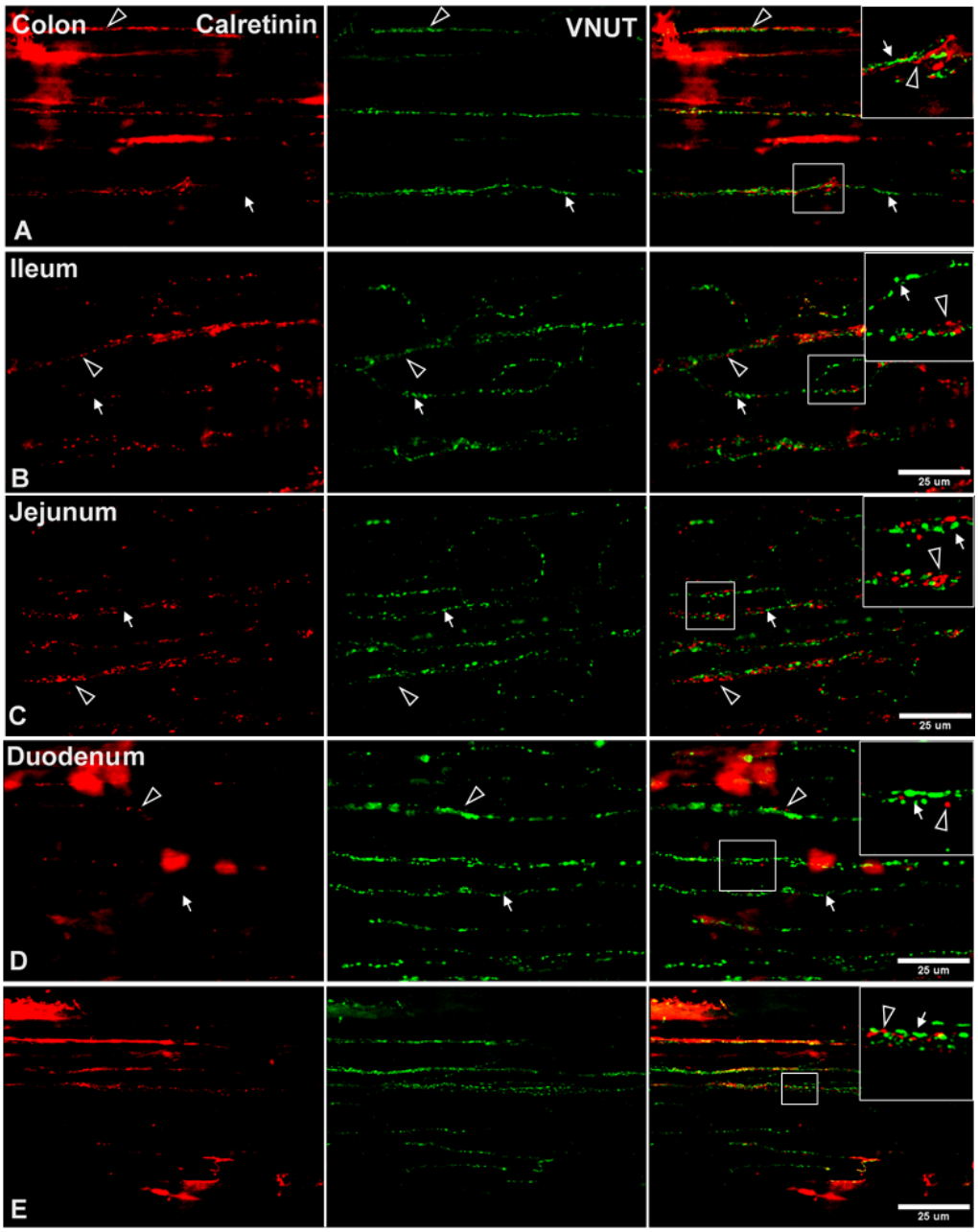

Figure 3.14: VNUT and calretinin are located in a separate subset of nerves in the circular smooth muscle. VNUT^{+} (green) nerves in the tertiary plexus (arrows), do not show the calretinin (red) immune marker (arrowheads), vice versa, of the colon, ileum, jejunum, duodenum, and stomach circular smooth muscle preps, A-E. FITC-conjugated donkey anti-rabbit IgG (H+L) was used to label VNUT and Cy3-conjugated donkey anti-goat label for calretinin. Images were taken using a conventional Nikon TE2000-U Inverted Microscope (Nikon TE2000-U series, Nikon Corporation).

.

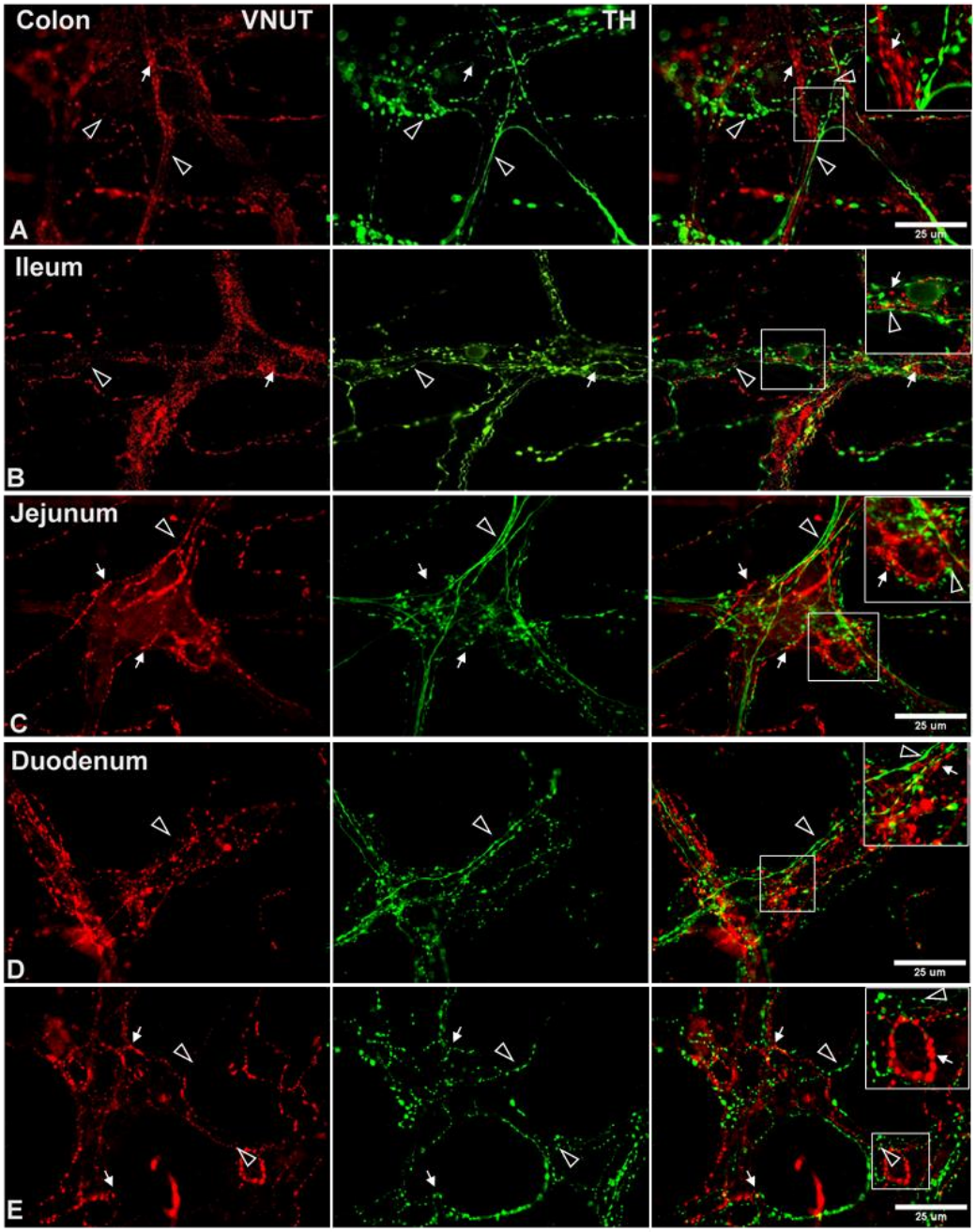

Figure 3.15: VNUT and TH are located in a separate subset of nerves in the myenteric plexus. VNUT^{+} (red) varicose nerves in the myenteric plexus (arrows) tissue preps do not show the TH (green) immune marker (arrowheads) in the colon, ileum, jejunum, duodenum, and stomach, A-E. FITC-conjugated donkey anti-sheep IgG (H+L) was used to label TH and Cy3-conjugated donkey anti-rabbit label for VNUT. Images were taken using a conventional Nikon TE2000-U Inverted Microscope (Nikon TE2000-U series, Nikon Corporation).

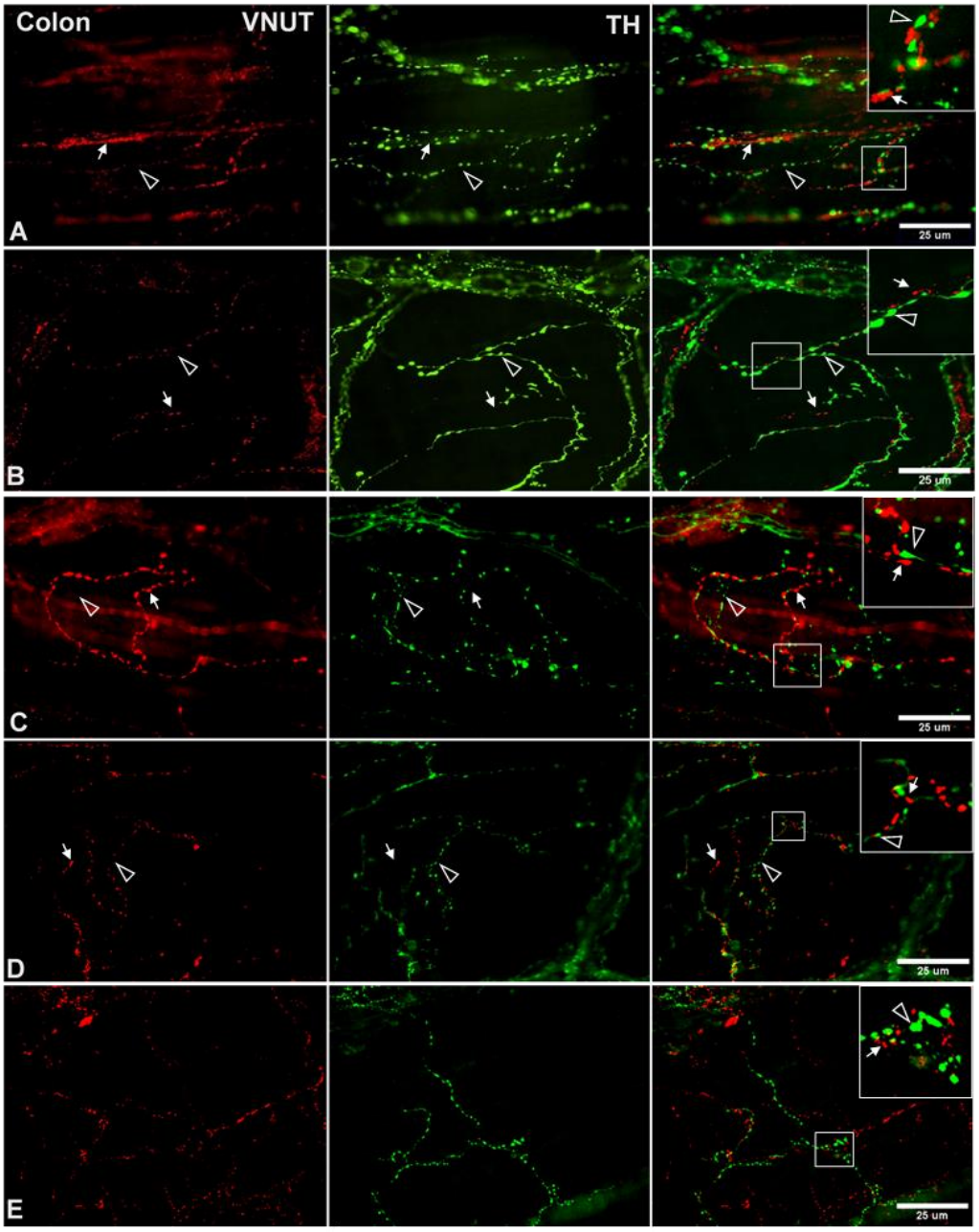

Figure 3.16: VNUT and TH are located in a separate subset of nerves in the tertiary plexus. $VNUT^{+}$ (red) varicose nerves in the tertiary plexus (arrows) tissue preps do not show the TH (green) immune marker (arrowheads) in colon, ileum, jejunum, duodenum, and stomach, A-E. FITC-conjugated donkey anti-sheep IgG (H+L) was used to label TH and Cy3-conjugated donkey anti-rabbit label for VNUT. Images were taken using a conventional Nikon TE2000-U Inverted Microscope (Nikon TE2000-U series, Nikon Corporation).

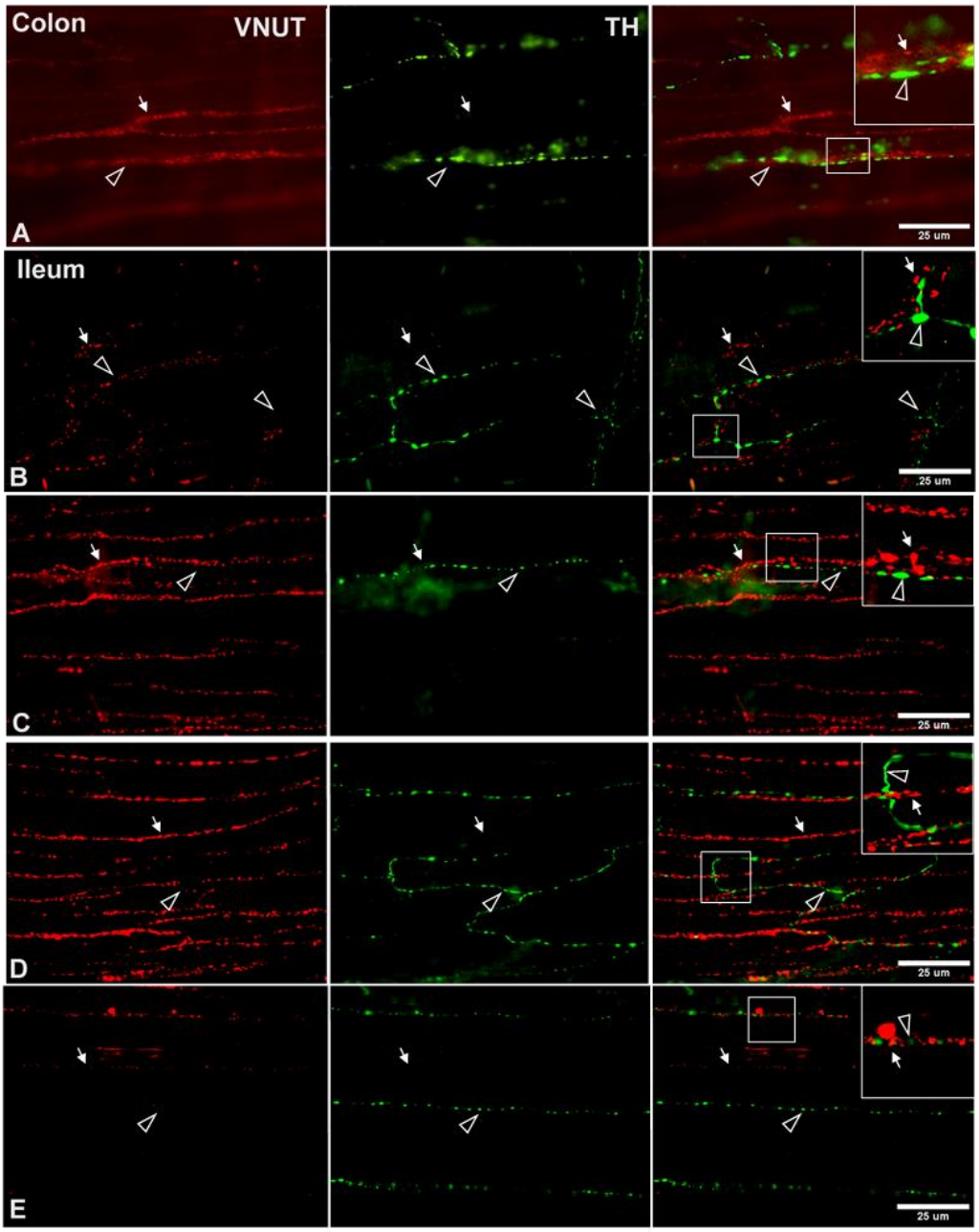

Figure 3.17: VNUT and TH are located in separate nerve bundles in circular smooth muscle. VNUT^{+} (red) varicose nerves in the circular smooth muscle (arrows) tissue preps do not show the TH (green) immune marker (arrowheads) in the colon, ileum, jejunum, duodenum, and stomach, A-E. FITC-conjugated donkey anti-sheep IgG (H+L) was used to label TH, and Cy3-conjugated donkey anti-rabbit label for VNUT. Images were taken using a conventional Nikon TE2000-U Inverted Microscope (Nikon TE2000-U series, Nikon Corporation).

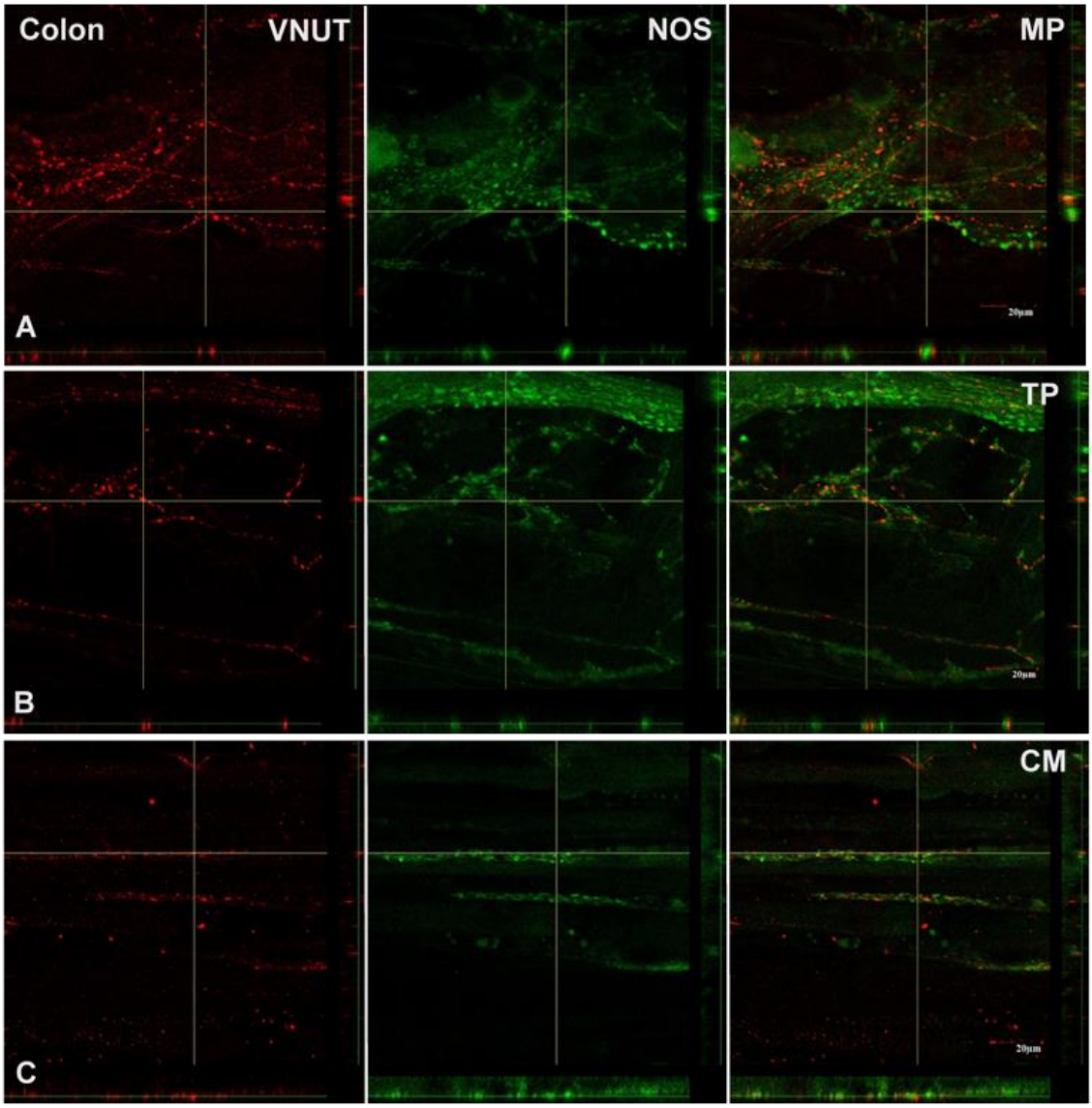

Figure 3.18: VNUT and NOS immunological markers do not co-localize. Confocal Z-depth images reveal that VNUT and NOS do not co-localize in the same nerve fibers located in the myenteric plexus (MP),A, tertiary plexus (TP),B, and circular smooth muscle (CM),C. FITC-conjugated donkey anti-sheep IgG (H+L) was used to labeled NOS and Cy3-conjugated donkey anti-rabbit label for VNUT. Confocal images were taken by an Olympus Confocal Laser Scanning Microscope (Olympus FV1000 series, Olympus Corporation, Tokyo, Japan) with FV1000 software).

DISCUSSION

The following observations along with previously published data are used to provide a characterization of the purinergic neuronal population in the myenteric plexus, and their nerve projections to the tertiary plexus and circular smooth muscle layers of the mice. We studied colon, ileum, jejunum, duodenum, and stomach tissue preps from the C57BL/6 mouse model. The resulting discussions take into account the relationship between the novel identified purinergic marker (VNUT, SLC17A9), and the already well defined immunological markers listed in Table 3.1.

Purinergic and nitrergic components are expressed in separate nerve fibers in the ENS.

Neuronal nitric oxide synthase (nNOS) is the enzyme that catalyzes nitric oxide (NO) from L-arginine amino acid: one of the two primary inhibitory transmitters found in the enteric nervous system (Brookes, 1993; Furness, 2000). nNOS is expressed in most species ENS, most evidently in the cell bodies and nerve terminals of a subclass of motor neurons that innervate the smooth muscle layers of the GI tract to promote muscle relaxation. (Costa *et al.*, 1992; Nurgali *et al.*, 2004; Porter *et al.*, 1997; Sanders *et al.*, 1992; Timmermans *et al.*, 1994). nNOS immunoreactivity may vary among species as well as in different segments of the GI tract. In the mouse small intestine, $nNOS^+$ neurons comprise 29% of all neurons in the mouse ileum none contains Dogiel type II (AH neurons) morphology. They are expressed in a small percentage of descending interneurons, but mainly in inhibitory motor neurons (IMNs), (Brookes, 2001; Qu *et al.*, 2008a). These motor neurons show immunoreactivity for the vasoactive intestinal peptide (VIP), and some additional markers such as neuropeptide Y (NPY), yet NPY is absent in the mouse large intestine (Sang *et al.*, 1996). In, contrast guinea pig ileum and caecum IMNs are primarily nNOS/VIP immunoreactive. It is also assumed to be the case in the large intestine (Costa *et al.*, 1996; Furness *et al.*, 1992; Qu *et al.*, 2008a). This is translatable to human tissues, as studies that

looked at human gastric fundus and colon tissue showed NOS and VIP co-localization (Guo *et al.*, 1997; Tonini *et al.*, 2000).

Nevertheless, the current model of inhibitory neurotransmission argues that adenosine 3',5'-triphosphate (ATP), or similar purine, and NO are the primary neurotransmitters co-released by IMNs, and are sufficient to drive GI smooth muscle relaxation (Burnstock, 2009). When activated, nerve processes from IMNs that innervate the muscle layers of the gut, release ATP and trigger the fast inhibitory junction potential (IJP) (purinergic component) of muscle relaxation via P2Y1 receptor activation. This acts through a PLC/DAG/IP3 mechanism (Gallego *et al.*, 2012; Gallego *et al.*, 2008b; Gil *et al.*, 2010; Serio *et al.*, 2003), while in these same processes, Ca^{2+}-dependent activation of NOS, synthesizes NO and produces the slow IJP (nitrergic component) muscle relaxation, but by a sGC/PKG driven mechanism (Dhaese *et al.*, 2008; Zhang *et al.*, 2010).

Consistent with these articles, we found that VNUT varicose fibers projected from the myenteric plexus to the tertiary plexus and circular smooth muscles. Additionally, a significant portion of these purinergic nerve bundles showed co-localization with the nNOS immunological marker. However, in some instances, VNUT and nNOS can be observed in separate nerve fibers in the myenteric plexus (MP), circular muscle (CM) and tertiary plexus. Hence, Z-depth confocal imaging was used to confirm co-localization of the immunological markers in the same nerve fiber. Our findings showed that VNUT and NOS immunological markers are in fact expressed in separate populations of nerve fibers and co-localization was not observed in any MP, CM and tertiary plexus tissue preparations of the mouse colon. This finding does not align with the current model that one population of IMNs co-releases ATP and NO to mediate smooth muscle relaxation, and thus suggests an alternative model, which consist of two separate populations of IMNs. This hypothesis is not novel (Bridgewater *et al.*, 1995), as studies performed on all three populations of muscle cells have shown to exhibit different levels of receptor expression as well as distinct inhibitory responses in the presence of receptors agonist. For instance, W/W^{v} mutant mice, that

lack intramuscular intestinal cells of Cajal (ICC_{IM}), exhibit loss of the nitrergic component, but retain the fast IJP (Suzuki *et al.*, 2003), while platelet-derived growth factor receptor-α- positive ($PDGFR\alpha^{+}$) smooth muscle cells are thought to be the true targets of purinergic neuromuscular transmission (Kurahashi *et al.*, 2014). Both ICC_{IM} and $PDGFR\alpha^{+}$ interstitial cells then relay their elicited responses following ligand-receptor activation onto smooth muscle cells via gap junction communication.

LMMP preparations of the colon, small intestine, and stomach also revealed that VNUT varicose fibers formed pericellular baskets that surround most myenteric cells labeled with the nNOS primary antibody. Pericellular baskets are indicative of synaptic sites of neurotransmitter release to the cells they surround (Mann *et al.*, 1997; Pompolo *et al.*, 1995). This finding is not surprising as $nNOS^{+}$ neurons are known to express many subtypes of purinergic receptors involved in mediating both inhibitory (Giaroni *et al.*, 2002; Ren *et al.*, 2007), and excitatory effects, (Antonioli *et al.*, 2013; Bornstein, 2008; Ren *et al.*, 2003).

Purinergic neurotransmission drives cholinergic myenteric neuron activity.

Along with Substance P, acetylcholine (ACh) contributes to the vast majority of the excitatory input that promotes GI contraction (Okasora *et al.*, 1986; Unekwe *et al.*, 1991). Choline acetyltransferase (ChAT) is the enzyme that synthesizes ACh and hence is considered an ideal marker to study cholinergic populations in the ENS (Brookes, 2001). Our results showed that VNUT varicosities formed pericellular baskets around the soma of ChAT immunoreactive cells predominantly in the colon and ileum of mice tissue. It is likely that VNUT varicose fibers innervated both Dogiel type I (S neurons) and Dogiel type II (AH Neurons) neurons, because ChAT immunoreactivity is present in both these classes of myenteric neurons (Furness *et al.*, 2004a; Li *et al.*, 1998; Qu *et al.*, 2008b). Dogiel type I cholinergic neurons make up half of the total myenteric neuron population, which includes interneurons or excitatory motor neurons (ENS). Conversely, type II cholinergic neurons, such as intrinsic primary afferent neurons

(IPANs), have immunoreactivity for the calcium-binding protein calbindin-D28K, however, in mice, some Dogiel type I are immunoreactive for calretinin, another class of calcium-binding protein (Brookes, 2001; Qu *et al.*, 2008b). As a final point, both Dogiel types have been shown to mediate fast synaptic excitation in response to ATP and other purinergic agonists. That is $P2X_2$ receptors having a predominant role in controlling fast synaptic excitation in S neurons, and $P2X_3$ in AH neurons of $P2X2^{-/-}$ knockout mice, thus making them likely targets of purinergic innervation (Galligan *et al.*, 1994; Ren *et al.*, 2003).

In contrast to these findings, myenteric VNUT nerve fibers that project from one ganglion to another, or the tertiary plexus, only contain VNUT immunoreactivity. A subpopulation of descending interneurons is suggested to mediate mixed cholinergic/purinergic fEPSP responses (LePard *et al.*, 1999; LePard *et al.*, 1997). However, our finding indicates only the existence of a separate purinergic population of descending interneurons. There does, however, appear to be fiber bundles of the circular smooth muscles that co-expressed VNUT and ChAT, yet, they do not appear to co-localize. Our results support the current model of GI motility, in which excitatory motor neurons induce muscle contraction by releasing ACh (Eglen *et al.*, 1996; Sawyer *et al.*, 1998) and a subpopulation of inhibitory motor neurons that synapses on the circular smooth muscle releases a purine that mediates relaxation at the neuromuscular junction (Bornstein, 2008). These patterns of GI motility are synchronized: contraction of the muscles is followed by relaxation. Therefore it is conceivable to have both ChAT and VNUT markers expressed in the same nerve bundles.

Myenteric Intrinsic primary afferent neurons receive no purinergic signaling

Calbindin immunoreactivity is visible on cell bodies and nerve fibers in the myenteric plexus, but not in the circular muscle or the tertiary plexus. These observations were consistent with past descriptions of calbindin immunoreactivity in the mouse ileum (Qu *et al.*, 2008b; Sang *et al.*, 1996). Also, nerve fibers that were ir for VNUT were not identified with the calbindin marker. Calbindin is

mainly found in Dogiel type II neurons (AH neurons), hence assumed to be intrinsic primary afferent neurons (IPANs). IPANs are ir for P1 and P2 receptors (Antonioli *et al.*, 2013; Castelucci *et al.*, 2002; Galligan *et al.*, 1994; Li *et al.*, 1998; Ren *et al.*, 2003), yet our findings suggest that VNUT varicose fibers are less likely to innervate these cells population. One explanation could be that control of gut motility requires fast purine release. Thus Dogiel type I cells (S neurons) are more likely to be involved with this fast activation mechanism, and hence receive synaptic input from purinergic myenteric neurons. Conversely, IPANs possess lengthy processes that extend to the intestinal milieu. Activation of these fibers results from changes in luminal chemistry and mechanical distortion of the mucosa (Furness *et al.*, 2004a). This suggests that purinergic receptor activation may play a more modulatory role on Dogiel type II neurons as opposed to more direct activation of the IPAN activity. However, this scenario is unlikely, as the $P2X_3$ receptor agonist, α,β-methylene ATP (α,β-mATP) depolarizes myenteric AH neurons in the mouse small intestine of $P2X_2^{-/-}$ knockout mice (Ren *et al.*, 2003). A more plausible explanation could be that purinergic activation of Dogiel type II neurons come from ATP release channels, also known as pannexin and connexin channels. Pannexin-1 (Panx1) is expressed in the cell body and processes of enteric neurons but not in glial cells (Gulbransen *et al.*, 2012b), whereas pannexin-2 (Panx2) is widely expressed in extrinsic as well as intrinsic neurons in the human colon (Diezmos *et al.*, 2015). In contrast, connexin-43 (CX43) channels are predominantly found at the smooth muscle layer and enteric glial cells. Regardless, both channel types transport ATP from the cytosol to the extracellular space by purinergic receptor activation, mechanical stress, and alter action of intracellular concentrations of Ca^{2+} (Diezmos *et al.*, 2016). This could lead some neuron populations, including myenteric Dogiel type II neurons, to depolarize from the increased concentrations of extracellular ATP.

Longitudinal excitatory motor neurons receive purinergic signaling

The calcium-binding protein calretinin is used as an immunological marker for longitudinal cholinergic EMNs and a small population of descending interneurons that are also immunoreactive for the growth hormone inhibitor somatostatin (SOM). Calretinin, can also be expressed in nerve fibers located at the myenteric plexus, tertiary plexus, and circular smooth muscle ((Brookes *et al.*, 1991; Giaroni *et al.*, 2002; Sang *et al.*, 1996). Double immunolabeling of calretinin with VNUT however, revealed no co-localization of the ir makers in nerve fibers within the mouse myenteric plexus, which suggests that EMNs are less likely to be purinergic. Nevertheless, electrophysiological studies have revealed that purines may work as an excitatory neurotransmitter in the longitudinal muscle layer of guinea pig colon and ileum via an unidentified G-protein mediated P2Y receptor (Ivancheva *et al.*, 2000; Rodriguez-Tapia *et al.*, 2017; Zizzo *et al.*, 2007). This further supports the idea that purinergic neurotransmission could potentially play additional roles that differ from the conventional models of smooth muscle relaxation. As a result, we cannot dismiss the idea that some of the observed VNUT varicose nerve fibers that project to the tertiary plexus may, in fact, induce smooth muscle contractility.

More on our findings, purinergic varicose fibers did innervate a population of calretinin cell bodies. Calretinin$^+$ cells express purinergic receptors, such as ionotropic $P2X_2$ receptors (Furness *et al.*, 2004a; Xiang *et al.*, 2005). VNUT varicose fibers could make synapses with EMNs to generate fEPSPs via P2X receptor activation, which would then result in the excitability of the longitudinal GI muscles. Another possibility is that purinergic nerves could depolarize ChAT/SOM/Calretinin descending interneurons, triggering a chain of events that ends with the hyperpolarization of the intestinal smooth muscles via depolarization of IMNs (LePard *et al.*, 1997; Serio *et al.*, 2003).

Calretinin is not detected in Dogiel type II neurons in guinea pigs, yet 15% of the calretinin$^+$ cells in mice ileum have Dogiel type II morphology, which suggests that VNUT varicose fibers may also innervate some IPANS (Brookes, 2001; Qu *et al.*, 2008a). But then again, our calbindin and VNUT

staining refute this idea. Incidentally, VNUT and calretinin do not co-localize in nerve fibers found in the tertiary plexus and circular smooth muscle layer. This finding is not surprising as purines main role in the circular muscle is to promote GI smooth muscle relaxation along with NO (Furness *et al.*, 2004a).

The purinergic component is absent in catecholaminergic nerves.

Tyrosine hydroxylase (TH) is the rate-limiting enzyme that produces catecholamines, such as dopamine. TH^+ cell bodies represent less than 1% of the entire cell populations in the ENS. (Qu *et al.*, 2008b), however, TH is abundantly present in varicose nerve fibers in the myenteric ganglia. Our results show that TH and VNUT immunoreactivity were found in separate nerve fibers in the myenteric plexus, tertiary plexus, and circular smooth muscle, yet occasionally we saw both innervating the same myenteric cells. Their roles in the ENS is still uncertain, yet evidence suggests they contribute to dopaminergic neurotransmission, plus may play a role in ENS development and inflammatory enteric neuropathies (Chevalier *et al.*, 2008; Li *et al.*, 2004). Regardless, results suggest that the VNUT mechanism of action in GI motility may not be directly influenced by TH.

CONCLUSION

The purinergic marker, VNUT (SLC17A9) is exclusively expressed in varicose nerve fibers but not in the cell body of myenteric neurons. Dual immunohistochemical analysis of VNUT with the other cell markers listed in table 3.1 showed that VNUT is not likely to be co-expressed with any other known myenteric cell populations along the tested GI tissue sections. Although VNUT is suggested to behave as a co-transmitter with NO, NOS IMNs cell body and nerve fibers exhibited no colocalization with the purinergic markers. Although both ir markers did show expression in the same nerve bundles that project to the CM and TP, confocal microscopy confirmed no colocalization. A subpopulation of descending interneurons are also suggested to co-release ACh

and ATP to mediate fEPSP. Then again, co-localization between VNUT and the cholinergic marker, ChAT, revealed that the ir markers are not expressed in the same nerve fibers. Based on this evidence we suggest that purinergic myenteric neurons are likely a distinct subpopulation of myenteric neuron. As a result, isolating the purinergic pathway of neurotransmission, and studying its mechanistic response could aid in the discovery of new drugs targets or the discovery of hallmarks that will aid in the treatment of FGIDs and GI related diseases. Isolating the purinergic pathway of neurotransmission could be possible with the implementation of optogenetic technology. For instance, VNUT could potentially be used as a promoter to drive cell-specific expression of the light-sensitive optogenetic actuator ChR2 into purinergic myenteric neurons. Therefore light activation of purinergic neurons using BLS could potentially help us understand better the purinergic pathway of neurotransmission in the ENS.

CHAPTER 4: OPTOGENETIC ANALYSIS OF INHIBITORY NEUROMUSCULAR TRANSMISSION IN THE MOUSE COLON AND GASTRIC ANTRUM

ABSTRACT

Gut propulsion requires contraction and relaxation of smooth muscles. Myenteric excitatory motorneurons (EMNs) cause contractions, while inhibitory motorneurons (IMNs) cause relaxation. Acetylcholine is released by EMNs and a purine, likely ATP, and nitric oxide (NO) are released by IMNs. Electrical stimulation of *ex vivo* gut tissues activates all neurons. In order to stimulate selectively subsets of neurons, we injected AAV9-floxed channelrhodopsin-2 (ChR2) fused with the enhanced yellow fluorescent protein (eYFP) into the proximal colon of *Nos1*$^{tm1(cre)Mgmj}$/J (Nos1^{Cre}) mice to express ChR2-eYFP in nNOS neurons (AAV9-Nos1-ChR2-eYFP). We also bred Nos1^{Cre} mice with B6;129S-Gt(ROSA)26Sor$^{tm32(CAG-COP4*H134R/EYFP)Hze}$/J mice to establish Nos1-ROSA-eYFP mice expressing ChR2-eYFP in all nNOS neurons. Colon and gastric antrum myenteric plexus/muscle preparations were used *ex vivo* to study neuromuscular transmission using electrophysiological methods. We measured inhibitory junction potentials (IJPs) evoked by blue light stimulation (BLS, 470 nm, 20 mW/mm^2) compared to electrically-evoked responses. Electrical stimulation and BLS evoked fast and slow IJPs in colon tissues from AAV9-Nos1-ChR2-eYFP and Nos1-ROSA-eYFP mice. Fast IJPs were blocked by MRS 2179 (P2Y1 antagonist) and slow IJPs were blocked by ω-nitro-L-arginine (NLA, NOS inhibitor). BLS inhibited contractions in CMMC recordings. Antral electrical and BLS evoked IJPs were blocked by MRS 2179 and NLA leaving a slow excitatory junction potential (EJP) that was not blocked by tetrodotoxin or ω-conotoxin-GVIA. Our data indicate that BLS activates purinergic/nitrergic neurons. eYFP was detected in nNOS$^+$ and some nNOS$^-$ neurons of AAV9 injected mice, yet was confined to nerve fibers in Nos1-ROSA-eYFP mice. Ectopic expression of ChR2 in non-nNOS$^-$ neurons could explain biphasic IJPs.

INTRODUCTION

Gastrointestinal (GI) motility is controlled largely by the myenteric plexus, a division of the enteric neuron system (ENS) located within the gut wall (Furness, 2012). Myenteric motor neurons and interneurons coordinate contraction and relaxation of GI smooth muscle to produce mixing and propulsive motor patterns (Sanders *et al.*, 2012). Smooth muscle contraction is mainly caused by acetylcholine (ACh) released from myenteric motor neurons and acting at postjunctional muscarinic (M2 and M3) acetylcholine receptors found in the muscles (see chapter 5). Conversely, neurogenic smooth muscle relaxation is biphasic with a fast component mediated by purinergic activation of metabotropic $P2Y_1$ receptors (Gallego *et al.*, 2012; Gallego *et al.*, 2006; Grasa *et al.*, 2009; Palmer *et al.*, 1998; Zhang *et al.*, 2010). Activation of the $P2Y_1$ receptor triggers a PLC_β/IP3/DAG mechanism that causes hyperpolarization of the smooth muscle via Ca^{2+} activation of small conductance Ca^{2+} activated potassium (SK) channels (Burnstock, 2014a; France *et al.*, 2012; Kurahashi *et al.*, 2014). The second component is NO mediated, and requires Ca^{2+} activation of neuronal nitric oxide synthase (nNOS) (Dhaese *et al.*, 2008). NO diffuses across cell membranes to bind to the soluble guanylate cyclase (sGC) enzyme causing activation of a cGMP/PKG dependent mechanism, and this lowers intracellular Ca^{2+} concentrations causing muscle relaxation. (Dhaese *et al.*, 2008; Lucas *et al.*, 2000). Combined purine and NO release from motor neurons, cause a biphasic inhibitory junction potential (IJP) in which the purinergic component is the initial fast IJP followed by a nitrergic slow IJP in smooth muscle cells (Gallego *et al.*, 2012). Neurogenic smooth muscle relaxation in the gut is suspected to be due to the purine and NO co-release by the same inhibitory motor neurons (IMNs) (Mane *et al.*, 2014). Nitrergic, as well cholinergic, nerve fibers are shown to predominantly innervate ICC cells (Alberti *et al.*, 2007; Kito *et al.*, 2003). More recently, ICC specific deletion of a key mediator of the NO/cGMP signaling pathway, PRKG1, abolished the NO dependent sIJP, but had no effect on the fIJP in these interstitial cell population (Klein *et al.*, 2013). Conversely, purinergic mediated P2Y1 receptors induce smooth muscle relaxation is suspected to be exclusively mediated by purinergic

innervation of adjacent PDGRFα+ interstitial cells, also known as fibroblast-like cells (Gallego *et al.*, 2012; Iino *et al.*, 2009a; Kurahashi *et al.*, 2011). These fibroblast-like cells show a purinergic mediated fast transient hyperpolarization during whole-cell recordings and do not express nNOS immunoreactivity (Kurahashi *et al.*, 2014). Moreover, qRT-PCR revealed that such genes that encode for the $P2Y_1$ receptor and SK_3 channels are highly expressed in PDGRFα^+ cells when compared to ICC and smooth muscle cells (Peri *et al.*, 2013). Hence, a competing model suggests that purinergic or nitrergic neurotransmitter release is mediated by separate inhibitory motor neuron subpopulations. This idea was first introduced by Bridgewater et al.,1995, who showed that presynaptic inhibition of the N-type (α1B; $Ca_v2.2$; CACNA1B) voltage-gated Ca^{+2} channel (VGCC) blocked the fIJP, but not the sIJP guinea pig longitudinal smooth muscle (Bridgewater *et al.*, 1995). It has since been shown that R-type (α1E; $Ca_v2.3$; CACNA1E) VGCCs provides Ca^{+2} for activation of nNOS in longitudinal muscle motorneurons in the guinea pig ileum (Rodriguez-Tapia *et al.*, 2017). An alternative scenario is that both inhibitory components are compartmentalized in the same varicosities; yet by an unknown neurodevelopmental mechanism, they form junctions with separate populations of ICC or PDGFα+ cells to drive relaxation.

Most of the knowledge we have about the function of nerve pathways in the ENS has been obtained using intracellular microelectrodes to record membrane potential changes in neurons and smooth muscle cells following transmural or focal electrical stimulation. However, electrical stimulation activates all neurons simultaneously and complicates data interpretation. In this study, we used cell-specific expression of the light-activated ion channel, channelrhodopsin-2 (ChR2) (Boyden *et al.*, 2005; Kolisnyk *et al.*, 2013; Nagel *et al.*, 2003). We expressed ChR2 in nNOS neurons to determine if NO and a purine were released from the same myenteric neurons or separate populations of inhibitory motor neurons. We hypothesized that blue-light stimulation (BLS) of $NOS^{(ChR2\text{-}eYFP)}$ containing tissues would generate overwhelming nitrergic only responses.

MATERIALS AND METHODS

Mice

We used the cre/lox recombinase system to express the ChR2-eYFP construct protein into nNOS expressing neurons via two distinct methods. In the first method, ChR2-eYFP expression in nNOS neurons (nNOS$^{(ChR2\text{-}eYFP)}$) was achieved by cross breeding homozygote B6;129S-Gt(ROSA)26Sor$^{tm32(CAG\text{-}COP4*H134R/EYFP)Hze}$/J mice (ROSA) (Jackson Laboratories; Stock No: 012569) with founder homozygous B6.129-NOS1$^{tm1(cre)Mgmj}$/J mice (Nos1^{cre}), which express Cre-recombinase in the neuronal nitric oxide synthase (Nos1) locus (Jackson Laboratory Stock no. 017526)). In the second method, ChR2 expression in mice proximal colon was also achieved by injecting a Cre-inducible AAV9-EF1a-DIO-hChR2(H134R)-eYFP between the muscle layers of the proximal colon of Nos1^{cre} mice (Fig.4.1).

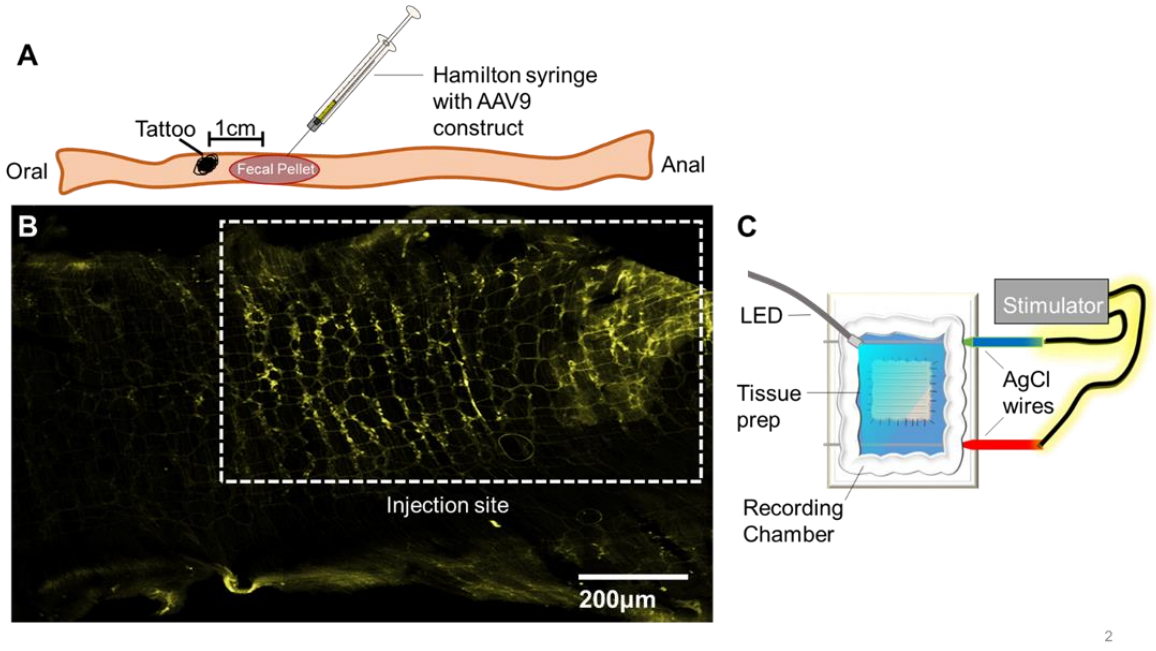

Figure 4.1: ChR2-eYFP expression contained at surgical injection sites of homozygous Nos1^{cre} mice proximal colon. (A) The pAAV9-Ef1α-DIO-ChR2-eYFP construct was injected 1 cm distal to the tattoo in the proximal colon of homozygous Nos1^{cre} mice. Injections were mainly performed at the location of fecal pellets, which enhance the injectability of the AAV9 virus. (B) Four weeks postsurgical injections, IHC revealed that ChR2-eYFP expression (Yellow) was contained only at injection site (boxed rectangle). C. Illustration depicting the paired EFS and BL stimulation experimental paradigm.

AVV9 Vector construction

The AAV9 vectors (Benskey *et al.*, 2015a) used in this study were encoded with a double-floxed inverted (DIO) construct that contained the sequence for channelrhodopsin 2 (ChR2) fused with the sequence for enhanced yellow fluorescent protein (eYFP), all under the control of the human elongation factor-1α (Ef1) promoter (pAAV9-Ef1α-DIO-ChR2-eYFP). AAV9 vectors that lacked the ChR2-eYFP construct were also used to test the specificity of the virus.

Colonic AVV9 injections

The surgical procedure and AAV9 injections followed the protocol developed by Benskey et al., (Benskey *et al.*, 2015a). Surgeries were performed on homozygous $Nos1^{cre}$ male mice (12 weeks old). All surgical procedures were performed under the guidelines of the Michigan State University Animal Care & Use Committee. Mice were anesthetized using 2% isoflurane via inhalation. Then 6 X 10 µl injections of the AAV9 virus were injected into the muscle layers of the proximal colon. Injections were performed using a 50 µl Hamilton syringe connected to a Harvard Apparatus foot-operated pump (Harvard Apparatus, Holliston, MA). Flow rate of microinjections was 10 µl/ min. After the injections were completed, a small tattoo (AIMS tattoo ink) was made proximal to the AAV9 injection sites in order to identify the injected colonic segment. The abdominal incision was closed with silk sutures and wound clips. Mice were then treated with piperacillin (60 mg/kg; ip) to avoid infections and rimadyl (5 mg/Kg; ip) to treat discomfort. The mice were monitored each morning post-surgery and given additional analgesia for 3 additional days. Colon tissues were harvested from euthanized mice 4 weeks after surgery in order to allow full expression of ChR2-eYFP at the injection sites (Benskey *et al.*, 2015a)**.**

Intracellular IJP recordings of circular smooth muscle cells

Following euthanasia 1 cm of the colon located distal to the tattoo was isolated and placed on a petri dish containing prewarmed (37 ºC) and oxygenated (95% O_2-5% CO_2) 1X Krebs solution (117 mM NaCl, 4.7mM KCl, 2.5 mM $CaCl_2$, 1.2 mM $MgCl_2$, 1.2 mM NaH_2PO_4, 25 mM $NaHCO_3$, and 11 mM dextrose). Colon segments were cut along the mesenteric border and pinned flat on the petri dish with the mucosal layer facing upward. Mucosal and submucosal layers were removed using fine forceps to expose the circular smooth muscle layer. A 0.5 cm^2 section was then transferred to a 5 ml silicone elastomer-lined recording chamber. Tissues were gently stretched and pinned to the recording chamber with small stainless steel pins. The chamber was then mounted on the stage of an inverted microscope and perfused with Krebs solution at a flow rate of 4 ml/min at 37 ºC. The preparations were allowed to acclimate for 30 min before the study.

Borosilicate 1.0 mm x 0.5 mm ID w/fiber glass (FHC Inc., Bowdoin, ME) microelectrodes were filled with 2M KCl (tip resistance, 60-120 MΩ) and were then used to impale circular smooth muscle cells. Transmural stimulation was performed using a pair of 1 mm diameter Ag/AgCl wire (A-M Systems, Seattle, WA) in the recording chamber. The electrodes were connected to a Grass S88 stimulator and stimulus isolator constant current unit (Grass Technologies, West Warwick, RI). In some experiments, focal stimulation was also performed using a two-barrel 1.5 mm x 0.84 ID borosilicate glass capillaries (WPI Inc., Sarasota, FL). To compare BLS with electrical stimulation, we set the number of pulses delivered by each stimulation method adjusting the stimulus train duration. The electrical stimulation paradigm consisted of a 10 Hz train, 0.5 ms pulse duration, and 80 V with train durations of 100-700 ms to determine the number of stimuli (1, 3, 5 and 7 stimuli).

Conversely, BLS was achieved by placing a fiber-optic tube connected to a blue light-emitting diode (470 nM; 20 mW/mm2) with the LED tip (2.5 mm dia) positioned 10 mm from the tissue surface and ~1 cm directly above the microelectrode muscle impalement site. Light pulses were triggered using a Grass S48 stimulator (Grass Technologies, West Warwick, RI). Stimulus-

response curves were obtained using a train duration of 300 ms, at 10 Hz with the light pulse duration ranging between 1 to 20 ms. Maximum peak amplitude and area under the curve (AUC) was achieved at a pulse duration of 10 ms (figure 4.2). Hence, BLS evoked responses using homozygous NOS^{cre} mice injected with the AAV9 virus construct performed using the following paradigm (10 Hz, 10 ms light pulse duration, with train durations of 100-700 ms which determined the number of stimuli (1, 3, 5 and 7 stimuli). However, to ensure maximum activation of ChR2, later experiments at the distal colon and antrum segments were performed using a pulse duration of 20 ms.

All membrane potential recordings were obtained using an Axoclamp-2A amplifier, a Digidata 1440A analog-digital converter, and Axoscope 10.6 software (Molecular Devices, Sunnyvale, CA). The amplified signal was sampled at 2 kHz and filtered at 1 kHz.

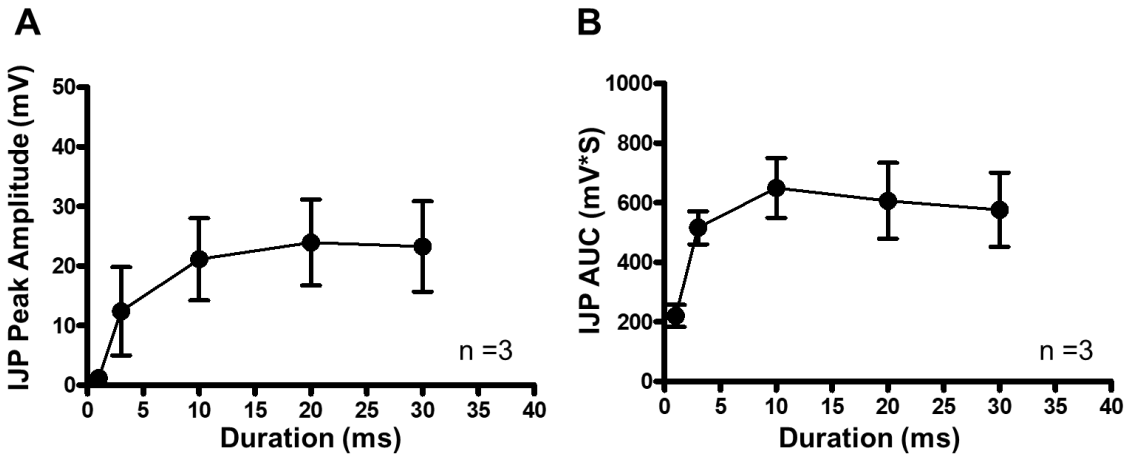

Figure. 4.2: Duration response curves following blue light (BL) evoked stimulation. The IJP (A) peak amplitude and (B) AUC reveals that the IJP response plateau at a pulse duration of 10ms.

Colonic migrating motor complex (CMMC)

Colonic segments for CMMC recordings were obtained from $Nos1^{(ChR2\text{-}eYFP)}$ mice and $Nos1^{(-/-)}$ control mice. After euthanasia, 5-6 cm long segments of colon were flushed with Krebs solution and a stainless steel rod was inserted into the lumen and surgical silk thread was used

to secure the oral and anal ends of the segment. Silk thread with reverse cutting needles (size 3-0 (CP medical), were bent to a 45 degree angle and secured to the proximal and distal ends of tissue 2.5 cm apart. Both ends of the threads were attached to separate force transducers. The preparation was then secured in a 60 ml bath that contained Krebs solution that was oxygenated and kept at 37°C. The tissues were then stretched at the site of attachment to the force transducers until reaching an initial tension of 2 g. The colonic segments were allowed to equilibrate for 1 hour during which time waves of propagating contractions (CMMC) developed. Inhibition of the propagating CMMC was accomplished by focal BLS using a micromanipulator mounted laser (480 nm) for 10 s and calculating the percent inhibition. Percent inhibition equals the peak amplitude of the migrating contraction measured prior to BLS, divided by the lowest peak amplitude response measured within the 10 s window of stimulation. The CMMC frequency, latency, and propagation speed were also analyzed and we compared the time periods 20 min before and 20 min after laser stimulation. In each experiment the laser was positioned within 5 cm of the proximal or distal recording site. Two Grass Instruments CP122A strain gauge amplifiers recorded the CMMC activity, and the signal was passed to an analog/digital converter (Minidigi 1A, Molecular Devices, Sunnyvale, CA) and then to a computer containing the LabChart software 8 (AD Instruments, Colorado Springs, CO).

Drug Application

To limit spontaneous smooth muscle contractions during intracellular recordings the L-type Ca^{2+} channel antagonist, nifedipine (1 μM) (Sigma-Aldrich, St. Louis, MO) was added to the superfusing Krebs solution for the duration of each experiment. Additional drugs were added to the superfusing Krebs solution using multiple drug-containing syringes and a 3-way tap system. MRS2179 (10 μM), ω-nitro-L-arginine (ω-NLA; 100 μM), scopolamine (SCOP; 1 μM), CP96345 (3 and 10 μM), ω-conotoxin GVIA (ω-CTX-GVIA; 0.3 μM), and tetrodotoxin (TTX; 0.3 μM) were obtained from Sigma-Aldrich. The extracellular Ca^{2+} chelating agent ethylene glycol-bis-(β-

aminoethyl ether)- N,N,N',N'-tetraacetic acid (EGTA ; 20 µM) in Ca^{2+} free Krebs solution was also used in the gastric antrum IJP recordings.

Immunohistochemistry

Proximal colon, distal colon, and gastric antrum were harvested from euthanized mice and fixed overnight at 4°C with Zamboni's fixative (4% formaldehyde with 5% picric acid in 0.1 M sodium phosphate buffer, pH 7.2) for immunohistochemistry. Mucosal and submucosal layers of the gut tissue were removed before fixing.

The fixative was later washed with 0.1 M phosphate buffer (PB) solution (PBS) (84 mM Na_2HPO_4, 18 mM Na H_2PO_4, pH 7.2) until yellow coloring was removed. The myenteric plexus was exposed by removing circular muscle (CM) strips using fine forceps. Whole mount longitudinal muscle myenteric plexus (LMMP) preparations were then incubated overnight at 4°C with primary antibodies (Table 1). Tissues were then washed 3 time at 10 minute intervals and then incubated with secondary antibodies (Table 1) for 1 hour at room temperature.

Lastly, after three, 10-minute washes in PBS, tissues were transferred onto a glass slide with ready-to-use mounting medium (ProlongTM Gold Antifade Mountant, Thermofisher, Cat No: P36961). All LMMP preps were examined using conventional microscopy and a Nikon TE2000-U Inverted Microscope (Nikon TE2000-U series, Nikon Corporation, Tokyo, Japan) with MetaMorph® image acquisition and analysis software. All images were acquired using CFI Plan Fluor 20X NA: 0.50 (air) and CFI Plan Fluor 40X NA: 0.75 (air) objectives. Cyanine 3 (Cy3) secondary antibody and enhanced YFP (eYFP) fluorescence were visualized with Nikon excitation fluorescent filters (Filter cubes Cy GFP and YFP-2427B-NTE-ZERO). Co-localization of eYFP fluorescence with NOS was also tested (Table 4.1).

1 AB	Host	Catalog #	Lot #	Dilution	Source
NOS	Sheep	AB1529	2728417	1/300	Merck Millipore
2 AB		**Catalog #**	**Lot #**	**Dilution**	**Source**
Donkey anti-rabbit-Cy3		711-166-152	131954	1/200	Jackson

Table 4.1: Primary antibody (1 AB), secondary antibody (2 AB), dilutions and suppliers of reagents used for immunohistochemical study of neuronal markers.

Statistical Analysis

Successful impalement of circular smooth muscle cells was verified by a rapid drop in the resting membrane potential. Only cells that had a stable resting membrane potential of -40mV or more hyperpolarized were considered for statistical analysis. Data are presented as mean $\pm$ SEM with n values representing the number of mice used for this study. The mean average was determined by averaging the total number of cells recorded from all animal per treatment. Statistical differences between groups were determined using two-way ANOVA followed by Bonferroni's post hoc test, or when applicable a two-tailed unpaired Student's t-test was used. Statistical significance was given to values with a $P<0.05$.

RESULTS

BLS activation of NOS$^{(ChR2\text{-}eYFP)}$ neurons evokes biphasic IJPs

AAV9-Ef1α-DIO-ChR2-eYFP injections into the colon produced ChR2-eYFP labeled neurons in myenteric ganglia near the sites of injection (Fig. 4.1). Immunohistochemical studies using an nNOS antibody confirmed that ChR2-eYFP expression occurred in nNOS immunoreactive (nNOS-ir) neurons and nerve fibers (Fig 4.3A). No fluorescent signal was detected in the colon of mice treated with the control AAV9 construct. Occasional ChR2-eYFP fluorescence was detected nNOS negative neurons (Fig 4.4).

EFS and BLS (pulse duration of 10 ms) evoked biphasic IJPs. The early fast IJP was inhibited by the $P2Y_1$ receptor antagonist MRS2179 (10 μM), and the later, slow IJP was blocked

by ω-NLA (100 μM). Both responses were abolished by the sodium channel antagonist TTX (0.3 μM) (Fig 4.3C). The EFS evoked IJP peak amplitude was significantly greater than BLS evoked IJPs (Fig 4.3D') (2- way ANOVA and Bonferroni post hoc test, $P < 0.05$). There was no difference between EFS and BLS evoked IJP amplitude in the presence of MRS 2179 and NLA (Fig 4.3E'). Conversely, the IJP AUC was similar for both stimulus controls (Fig. 4.3D").

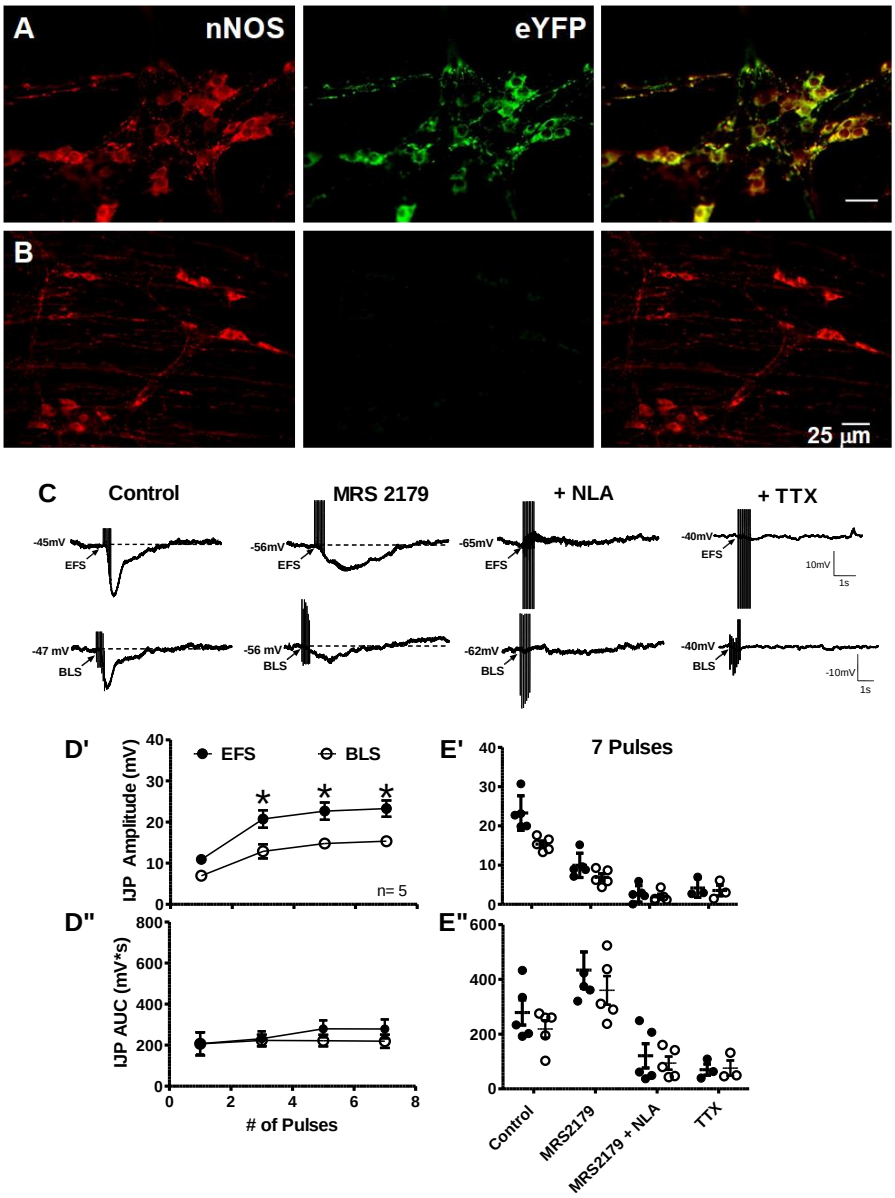

Figure 4.3: Light evoked a biphasic IJP response at site of AAV injection of Homozygous Nos1^{cre} mice. Epi-fluorescence microscopy reveals ChR2-eYFP expression in nNOS-IR myenteric cell populations in homozygous Nos1^{cre} mice injected with the (A) pAAV9-Ef1α-DIO-

Figure 4.3 (cont'd)

ChR2-eYFP construct, but not in tissue injected with the (B) control AAV9 construct. (C) Paired electrical field stimulation (EFS) and blue light (BL) evoked IJP representative traces in the absence (control) and presence of drugs. Control IJP peak amplitude (D') and area under the curve (E') response following an increase in the number of pulses. Scatter plot diagram comparing control IJP peak amplitude (E') and AUC (E") with IJP responses in the presence of MRS2179 (10μM), $_{L}$-NLA (100μM), combined MRS2179 + $_{L}$-NLA, and TTX (0.3μM).

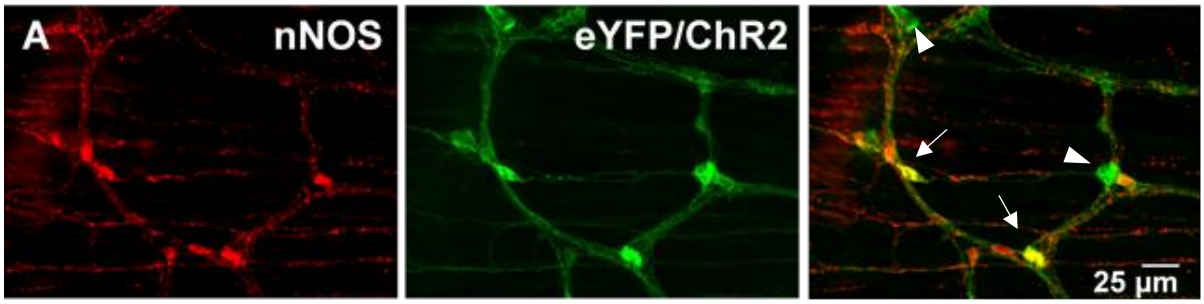

Figure. 4.4: Homozygous Nos1^{cre} mice injected with pAAV9-Ef1α-DIO-ChR2-eYFP construct reveals ChR2-eYFP ectopic expression. (A) Epi-fluorescence microscopy shows ChR2/eYFP expression in nNOS-IR cell bodies (arrows), but also in non-NOS-IR myenteric cell populations (Arrow heads).

Application of MRS 2179 (10 μM), unmasked the nitrergic response as an increase in the AUC compared to control recordings. However, there was no significant difference between EFS and BLS responses measured during drug application. These results suggest that BLS stimulation of ChR2-containing nNOS neurons in the proximal colon mimics electrically evoked IJPs.

We were able to evoke a biphasic IJP response in distal colon circular smooth muscle preparations from NOS$^{(ChR2/eYFP)}$ mice (Fig. 4.5B). EFS and BLS evoked IJP peak amplitude were similar in the absence or in the presence of drugs that block the IJP (Fig 4.5 C', 4.5D'). The BLS -evoked IJP AUC was significantly smaller compared to EFS evoked IJPs (Fig 4.5C") (two way ANOVA and Bonferroni post-hoc test, $P < 0.05$) although it was unmasked following blockade of the purinergic response. Nevertheless, no significant differences were observed between EFS and BLS evoked IJPs in the presence of MRS 2179 (10 μM), MRS 2179 plus NLA (100 μM), followed by TTX (0.3 μM). Comparison of the proximal and distal colon BLS -evoked IJPs showed a significant difference in IJP peak amplitude but not AUC. Moreover, the IJP AUC in the proximal

colon in the presence of MRS 2179 was significantly larger than to that in the distal colon (Fig. 4.6). These data are comparable to those obtained in the pAAV9-Efla-DIO-ChR2-eYFP injected mice, as both methods of inducing ChR2-eYFP expression can produce a similar purinergic/nitrergic biphasic IJP response after BLS. (Fig. 4.3).

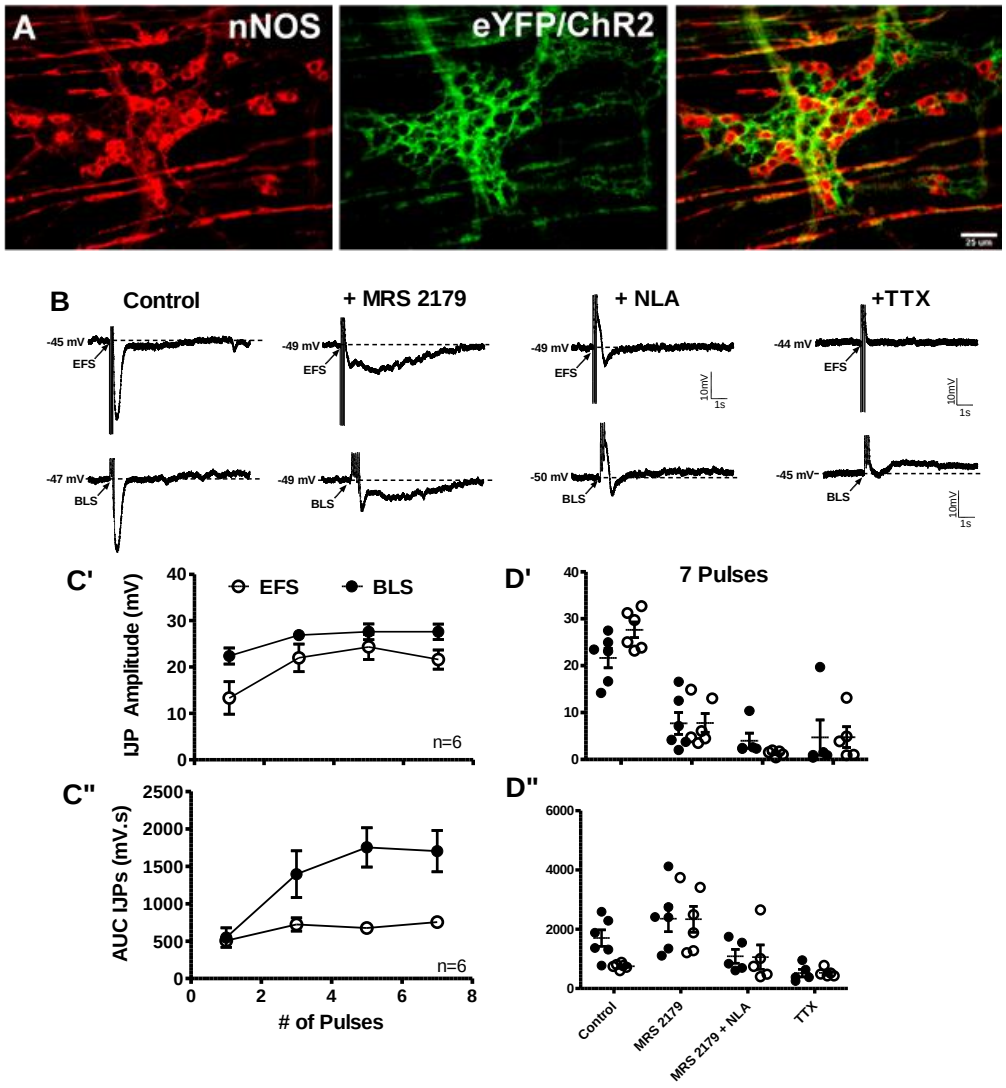

Figure. 4.5: Light evoked a biphasic IJP response in bred homozygous NOS$^{(ChR2/eYFP)}$ mice. (A) Epi-fluorescence microscopy reveals ChR2/eYFP expression in nerve fibers, but not in cell bodies, with little to no co-localization in NOS-IR myenteric cell populations. Epifluorescence images resemble glial staining in the myenteric plexus, unfortunately, glial markers were not used to address this question. (B) Paired electrical field stimulation (EFS) and blue light (BL) evoked IJP representative traces in the absence (control) and presence of drugs. Control IJP peak amplitude (C') and area under the curve (C") response following an increase in the number of pulses. Scatter plot diagram comparing control IJP peak amplitude (D') and AUC (D") with IJP responses in the presence of MRS2179 (10μM), $_{L}$-NLA (100μM), combined MRS2179 + $_{L}$-NLA, and TTX (0.3μM).

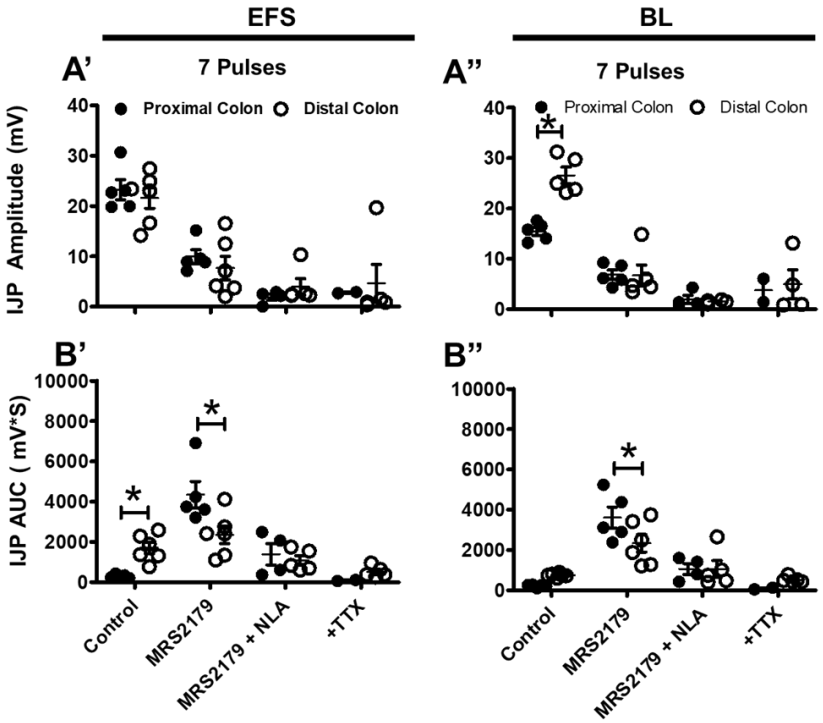

Figure. 4.6: Comparison of proximal and distal colon electrical and light-evoked IJP response. Scatter plot diagram shows no significant difference between the proximal and distal colon (A') electrical induced IJPs, however recordings at the distal colon reveal a significant larger BL-evoke IJP peak amplitude (A"). Both EFS and BL evoke IJP AUC recordings at the proximal colon were significantly bigger in the presence of MRS2179 (10μM), and were abolished following the application of $_{L}$-NLA (100μM).

BLS inhibition of the CMMC in NOS$^{(ChR2\text{-}eYFP)}$ mice

The effects of BLS on the CMMC were tested in nNOS$^{(ChR2\text{-}eYFP)}$ mice. During the peak of the CMMC, a reduction in the slow-wave response was observed in our ChR2/YFP/ NOS mouse model following 10 seconds of constant blue light (480nm) exposure (Fig 4.7A). The percent inhibition of the CMMC contraction was greater in the proximal colon (75% $\pm$ 6) than in the distal colon (36% $\pm$ 14), yet it was not significant (Fig 4.7B) (two-tailed paired student's t-test, $P < 0.05$). We next tested the frequency and latency of the proximal colon CMMC, as well as the propagation speed. CMMC recordings before and after giving a 10 second BLS stimulus were compared. No changes in the CMMC frequency (Fig 4.7C), latency (Fig 5D) or propagation speed (Fig 4.7E) was observed between NOS$^{(ChR2\text{-}eYFP)}$, and control (Nos1^{cre}) mice. These results show that light-

activation of NOS$^{(ChR2\text{-}eYFP)}$ neurons has no modulatory effect on the spontaneous activity of the CMMC, except to cause transient inhibition of the contraction.

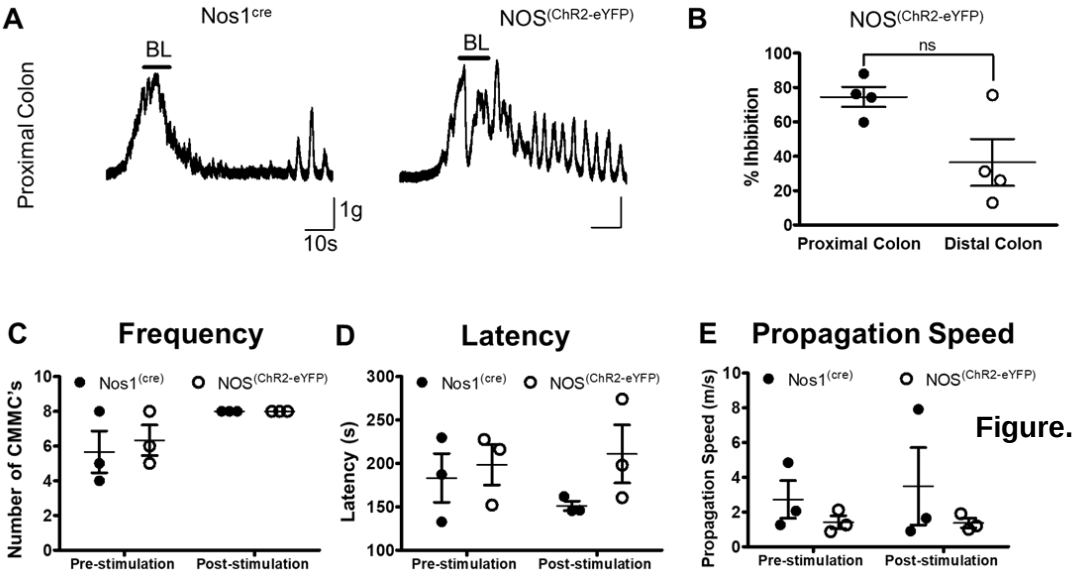

Figure.

4.7. Light-induced relaxation does not affect CMMC frequency, latency, and propagation speed. (A) CMMC representative traces of Nos1^{cree} (control) and NOS$^{(ChR2/eYFP)}$ mouse models. (B) Scatter plot graph depicting the percent (%) inhibition of the CMMC observed in the proximal and distal colon after light-evoked stimulation. Scatter plot graphs showing the changes in CMMC (C) frequency, (D) latency, and (E) propagation speed before (pre) and after (post) light evoke stimulation at the peak of the CMMC in the proximal colon.

BLS evokes a slow EJP in the antrum

The peak amplitude of the IJP was not significantly different between electrical and light stimulus (Fig 4.8A). However, the IJP AUC during EFS was higher than the light-evoked response, yet again was not significantly different (Fig 4.8B). Also, a slow excitatory junction potential (EJP) was evoked by BLS but not by EFS. MRS2179 (10 μM) blocked the IJP but not the EJP. Addition of NLA (100 μM), unmasked an EFS-evoked EJP and further enhanced the BLS evoked EJP. Scopolamine (SCOP; 1 μM) inhibited the EFS-evoked EJP but not the BLS-evoked EJP. Addition of TTX (0.3 μM) had no additional effect. Tachykinin peptides mediate some non-cholinergic contractions in the GI tract. However, treatment with the NK1 receptor antagonist CP96345 (3 μM) did not inhibit the BLS evoked slow EJP (Fig 4.9B). Bath application of ω-CTX-

GVIA (0.3 µM) did not affect the EJP (Fig 4.9C) and using physiological solution containing 0 Ca^{+2} with the Ca^{2+} chelating agent EGTA (20 µM) did not affect the EJP (Fig 4.9D). These results suggest that BLS stimulation of ChR2 in $NOS^{(ChR2\text{-}eYFP)}$ myenteric neurons produce an EJP that is independent of cholinergic and tachykinin transmission. Moreover, the data indicate that an unknown mechanism is influencing smooth muscle contraction in the antrum of our mouse model that is only triggered when the ChR2 channel is open.

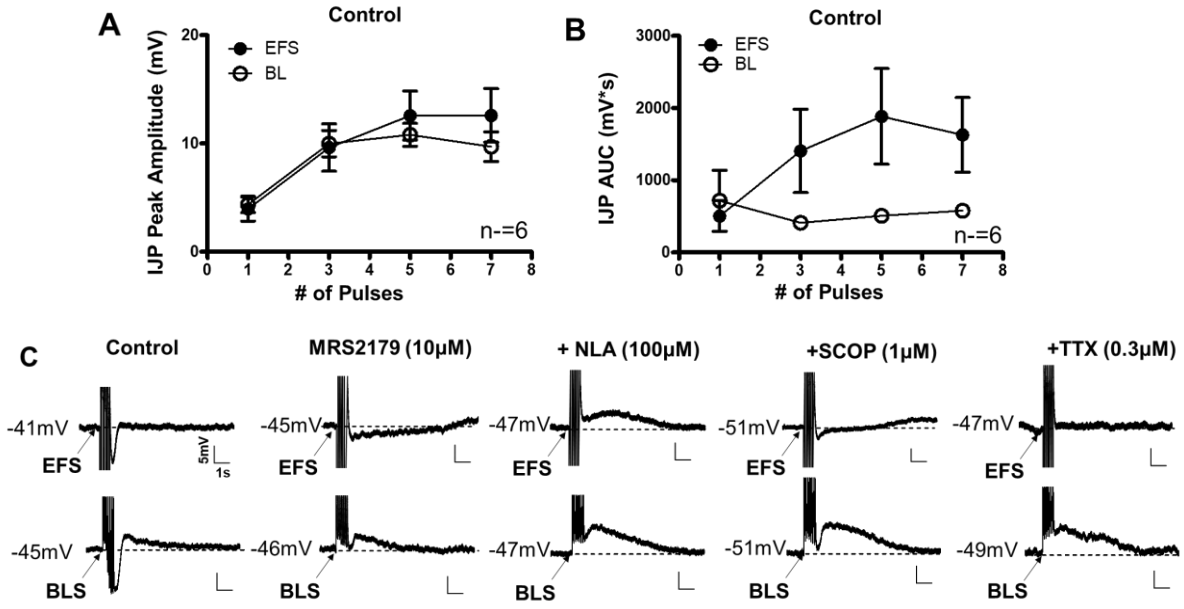

Figure. 4.8: Light-evoked stimulation at the gastric antrum mediates a drug-resistant slow synaptic response (SSR). Control IJP (A) peak amplitude (B) and area under the curve responses following electrical field stimulation (EFS) and blue light stimulation, given at an incrementing number of pulses. (C) Gastric antrum IJP representative traces in the absence (control) and presence of drugs**.**

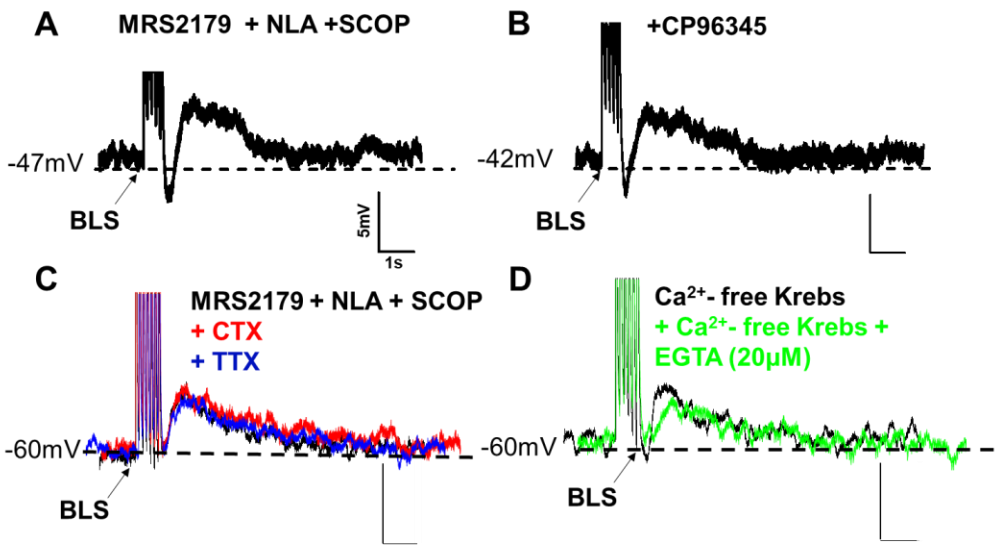

Figure. 4.9: Light-evoked slow synaptic responses (SSR) are resistant to cholinergic and tachykinin receptor antagonist and Ca^{2+} free Krebs solution. (A-D) Bath perfusion of MRS2179 (10 µM), L-NLA (100 µM), scopolamine (1µM), CP96345 (3 µM) antagonist, or adding Ca^{2+} free Krebs physiological solution to the bath was not sufficient to block the SSR following light evoke stimulation.

DISCUSSION

One population of IMNs mediates the slow and fast IJP components

We show that BLS evokes a biphasic IJP in circular muscle cells in the colon and antrum of NOS^{Cre} mice following cre/loxP expression of ChR2. We used the cre/lox recombinase system with 1) surgical injections of pAAV9-Ef1α-DIO-ChR2-eYFP into the proximal colon wall of $Nos1^{Cre}$ mice (Benskey *et al.*, 2015a) and 2) by cross-breeding of homozygous $Nos1^{Cre}$ mice with the ROSA transgenic mice (Jackson Laboratories; Stock No: 012569) which express "floxed" sequence for ChR2-eYFP in all nNOS neurons. More importantly, these results support the current model of inhibitory neurotransmission that one population of inhibitory motor neurons drives mediates purinergic and nitrergic neuromuscular transmission in the GI tract (Brookes, 2001; Burnstock, 2009). However, ChR2-eYFP was detected in non-nitrergic myenteric neurons following pAAV9-Ef1α-DIO-ChR2-eYFP injection into the colon of $Nos1^{cre}$ animals, and ChR2-eYFP expression was detected in some nerve fibers that were nNOS negative. Therefore, we still

can't rule out the existence of separate purinergic and nitrergic inhibitory subpopulation in the myenteric plexus, especially when evidence is also likely to support a two subpopulation IMN model. For instance, data suggest that purinergic IMNs innervate fibroblast-like interstitial cells and nitrergic IMNs innervate ICC cells. Moreover, evidence shows that both neurotransmitter release mechanisms are driven by different subclasses of VGCC. (Bridgewater *et al.*, 1995; Gallego *et al.*, 2012; Iino *et al.*, 2009b; Kurahashi *et al.*, 2014; Kurahashi *et al.*, 2011; Peri *et al.*, 2013; Rodriguez-Tapia *et al.*, 2017). These differences in ChR2-eYFP expression can be attributed to our use of two different methods to express ChR2 in $Nos1^{cre}$ mice via the Cre/loxp system. AAV9 viral expression of ChR2-eYFP was achieved using a double-floxed inverted (DIO) construct, while ChR2 expression in our breeding paradigm was successful following Cre recombinase removal of the LSL cassette position upstream of the ChR2-eYFP (Smedemark-Margulies *et al.*, 2013). Also, each loxP sequence contains different promotors which have been shown in the past to lead to the undesired expression of proteins of interest (Allen *et al.*, 2015). Regardless of the outcome, AAV9 viral expression of ChR2 showed to be the most favorable technique to achieve ChR2 expression. Therefore further studies should really focus on enhancing the AVV constructs delivery to specific region of the ENS, such as shown previously where modification of the AAV-PHP.B heptamer targeting sequence via the in vivo viral-capsid selection method CREATE, allowed researchers to further target specific myenteric neurons and possibly limiting off-target expression of ChR2 (Chan *et al.*, 2017).

Regardless of which method was used to express ChR2 in homozygous $Nos1^{cre}$ mice, a biphasic IJP was consistently evoked in the colon of $NOS^{ChR2\text{-}eYFP}$ mice. BLS -evoked IJPs recorded from the proximal colon were stimulated at a pulse duration of 10 ms, while distal colon and antrum IJP recordings were emitted at a pulse duration of 20ms. Our preliminary findings show that the light-evoked IJP peak amplitude and AUC plateau at a pulse duration of 10 ms (Supplemental fig 1), however, a low pulse duration could explain why the light-evoked IJP peak amplitude and AUC in the proximal colon were significantly smaller to the electrical response.

This is further evidence after comparing EFS and BLS-evoked IJPs in the proximal and distal colon (Fig 4). The AUC of IJPs evoked by EFS and BLS in the proximal colon responses was significantly larger following isolation of the nitrergic component with MRS2179. These results follow the findings that NOS-immunoreactivity and nitrergic mediated relaxation is more prominent in the proximal colon than in the distal colon (Takahashi *et al.*, 1998).

BLS of IMNs transiently inhibits the CMMC slow wave response.

CMMCs are repetitive spontaneous migrating contractions that propagate along the colon and propel fecal pellets in a proximal to distal directions (Bush *et al.*, 2000). NO is released constitutively from IMNs to suppress CMMC contractions in the mouse colon (Spencer, 2001) (Dickson *et al.*, 2010a; Powell *et al.*, 2001). Inhibition of NOS produces similar effects in the human colon by increasing colonic propagating contractions (Dinning *et al.*, 2006), as occurs in the mouse colon (Spencer, 2001). Conversely, ACh release from EMNs enhances ICC pacemaker activity to induce slow depolarizations that stimulate CMMC contractions (Bush *et al.*, 2000; Dickson *et al.*, 2010a). Moreover a recent study showed that BLS of the colon from CAL-ChR2 cre+ mice stimulated circular muscle contractions (Hibberd *et al.*, 2018). Our data show that BLS of the colon from $NOS^{(ChR2\text{-}eYFP)}$ mice transiently inhibited CMMC contraction and that this response was stronger in the proximal colon. However, BLS did not change CMMC frequency, latency, or propagation speed. More prolonged duration stimuli or multiple sites of BLS may have more sustained effects on the CMMC.

An unidentified neurotransmitter-receptor complex induces a slow EJP in the gastric antrum.

In the gastric antrum, EFS and BLS evoke a biphasic IJP, followed by a slow EJP. (Suzuki *et al.*, 2003). However, in most of our EFS-evoked IJPs recordings, the SWD was only present following inhibition of the fast and slow IJP with MRS 2179 and NLA respectively. The muscarinic

receptor antagonist scopolamine blocked slow EJP as previously shown (Suzuki *et al.*, 2003). Moreover, both the slow IJP and EJP were absent in W/W^{v} mice suggesting that both the nitrergic (inhibitory) and cholinergic (excitatory) components target intramuscular ICC in the gastric antrum circular muscle layer (Suzuki *et al.*, 2003). BLS evoked IJPs consistently revealed the slow EJP that was enhanced following inhibition of the IJPs. In addition, neither bath application of scopolamine, followed by TTX or the N-type Ca2+ channel blocker ω-CTX GVIA or Ca^{2+}-free Krebs solution was able to inhibit the slow EJP. Further studies with the NK1 receptor antagonist, CP96345 did not block the slow EJP, eliminating tachykinin contribution to the slow EJP. Ectopic expression of ChR2 in non-cholinergic/tachykinin and non-nitrergic populations of enteric neurons could explain the persistent slow EJP. Therefore, we suspect that neurotransmitter-receptor complex that we have yet to identify may also play a role in the slow EJP in the gastric fundus, at least in our transgenic mouse model.

CONCLUSION

We used optogenetic techniques and electrophysiology to expand our understanding of the enteric circuit that governs GI motility, this to enhance the discovery of novel therapeutics that could help treat GI-related diseases. Our hypothesis was to test if BLS of $NOS^{(ChR2\text{-}eYFP)}$ containing tissues would generate overwhelming nitrergic only responses to determine if multiple subpopulations of IMNs are responsible for the relaxation of the GI smooth muscles. The results, however, showed that BLS evokes a biphasic IJP in AAV injected NOS^{cre} mice and in $NOS^{(ChR2/eYFP)}$ bred mice. BLS of the gastric antrum generated slow EJPs that were not blocked by any of the drugs in our repertoire. Finally, BLS stimulation of ChR2 at the peak of the CMMC response caused a transient inhibition of the slow wave response, yet did not affect the CMMC frequency, latency, and propagation speed. Overall the findings suggest that one population of IMNs innervate the smooth muscles and co-release ATP and NO. However, ectopic expression of ChR2 was present in non-NOS neurons and nerve fibers in the myenteric plexus. Therefore,

multiple subpopulations of IMNs that control different patterns of GI motility is still a plausible scenario that needs further study.

CHAPTER 5: OPTOGENETIC ANALYSIS OF NEUROMUSCULAR TRANSMISSION IN THE COLON OF CHAT-CHR2-YFP BAC TRANSGENIC MICE

ABSTRACT

Propulsion of luminal content along the length of the gut requires coordinated contractions and relaxations of gastrointestinal smooth muscles controlled by the enteric nervous system (ENS). Activation of excitatory motor neurons (EMNs) causes muscle contractions while inhibitory motor neuron (IMN) activation causes muscle relaxation. EMNs release acetylcholine (ACh) which acts at muscarinic receptors on smooth muscle causing excitatory junction potentials (EJPs). INMs release a purine (ATP for example) and nitric oxide (NO) to induce inhibitory junction potentials (IJPs) and muscle relaxation. We used commercially available ChAT-ChR2-YFP-BAC transgenic mice, which expressed channelrhodopsin-2 (ChR2) in cholinergic neurons to study cholinergic neuromuscular transmission in the colon. Intracellular microelectrode recordings were used to measure IJPs and EJPs from circular muscle cells. We used blue light stimulation (BLS) (470 nm) (20 mW/mm^2), electrical field stimulation (EFS), and focal electrical stimulation (FES) to activate myenteric neurons. EFS evoked IJPs only while BLS evoked EJPs and IJPs. Mecamylamine (10 µM, nicotinic ACh receptor antagonist) reduced BLS evoked IJPs by 50% but had no effect on electrically evoked IJPs. MRS2179 (10 µM, a P2Y1 receptor antagonist) blocked BLS-evoked IJPs. Immunohistochemistry revealed that choline acetyltransferase (ChAT), was expressed in ~88% of eYFP expressing neurons, while 12% of eYFP neurons expressed nitric oxide synthase (NOS). These data show that cholinergic interneurons synapse with excitatory and inhibitory motor neurons to cause contraction and relaxation of colonic smooth muscle.

INTRODUCTION

The enteric nervous system (ENS) controls gastrointestinal motility and absorption and secretion by mucosal epithelial cells. Combined electrophysiological, pharmacological and immunohistochemical approaches have enabled identification of the electrical properties, neuronal subtypes and synaptic pathways in the ENS responsible for the control of gut function. Excitatory junction potentials (EJPs) are caused by activation of excitatory motor neurons and inhibitory junction potentials (IJPs) are caused by activation of inhibitory motor neurons. EJPs are associated with smooth muscle contraction, and IJPs are associated with smooth muscle relaxation. Coordinated contractions and relaxations of the muscle layers are responsible for the propulsion of intraluminal content along the length of the gut (Okasora *et al.*, 1986; Zagorodnyuk *et al.*, 1993).

EJPs are mediated by acetylcholine acting at M_2 and M_3 type muscarinic receptors expressed by intestinal smooth muscle cells (Matsuyama *et al.*, 2013). M_3 receptors mediate contraction via a PLC-β/DAG/IP3 mechanism that induce a burst of Ca^{2+} release from intracellular stores (Matsuyama *et al.*, 2013; Unno *et al.*, 2005), while M_2 receptors coupled to inhibition of adenyl cyclase/cAMP-mediated smooth muscle relaxation (Candell *et al.*, 1990; Ehlert *et al.*, 1997; Sawyer *et al.*, 1998). IJPs are biphasic hyperpolarizations with an early fast phase mediated by a purine, and a slower smaller amplitude-phase mediated by nitric oxide (NO). Vesicular release of purines mediate the fast IJP by activating the Gq/11 purinergic $P2Y_1$ receptors promoting a PLC/DAG/IP3 pathway (Zhang *et al.*, 2010) while NO, synthesized on demand by neuronal nitric oxide synthase (nNOS), mediates the slow IJP which is a GC/cGMP/PKG driven mechanism that lowers intracellular Ca^{2+} levels (Dhaese *et al.*, 2008; Gallego *et al.*, 2008a; Gallego *et al.*, 2012; Gallego *et al.*, 2008b; Grasa *et al.*, 2009).

Most studies of neuromuscular transmission in the gastrointestinal tract have used electrical field stimulation (EFS) or focal electrical stimulation (FES) of myenteric nerves to evoke

EJPs or IJPs recorded with intracellular microelectrodes. EFS and FES activate multiple types of nerve fibers which can complicate data interpretation. Drugs which may selectively block the action of excitatory or inhibitory neurotransmitters can help to isolate responses mediated by subtypes of myenteric neurons, but many drugs do not have the needed selectivity to isolate one kind of response, and this complicates data interpretation. To address this issue, we used an optogenetic approach to activate selectively cholinergic neurons in the myenteric plexus of the mouse colon. Optogenetics takes advantage of selective expression of the light-sensitive protein channelrhodopsin-2 (ChR2) in specific neurons by linking a neuron-specific promoter to the ChR2 gene sequence (Kolisnyk *et al.*, 2013; Nagel *et al.*, 2003). As a result, only neurons expressing the light-sensitive protein ChR2 molecule will be activated when stimulated with blue light (470 nm) flash. We studied excitatory and inhibitory neuromuscular transmission in the gastrointestinal tract of transgenic mice expressing ChR2 and enhanced yellow fluorescent protein (eYFP) in cholinergic neurons. Our data reveal that light-evoked EJPs were cholinergically-mediated, while light-evoked IJPs were mainly purinergic. We also show that blocking ganglionic neurotransmission inhibited light-evoked purinergic IJPs indicating that cholinergic interneurons synapse with inhibitory motor neurons. These data suggest that cholinergic interneurons synapse with purinergic, but not nitrergic inhibitory motor neurons.

MATERIALS AND METHODS

Mice.

We purchased two female ChAT-ChR2-YFP BAC mice (Stock number: 014546 | ChAT-ChR2-EYFP line 6) from Jackson Laboratories (Bar Harbor, ME) and bred these mice with male C57BL/6J mice. Heterozygote male and female offspring were then bred together, and male and female mice homozygous for the ChAT-ChR2-YFP-BAC were used for the analysis of neuromuscular transmission. Mice were anesthetized via isoflurane inhalation and were

euthanized following cervical dislocation. All animal use protocols were approved by the Institutional Animal Use and Care Committee at Michigan State University (AUF #02/16-014-00).

Immunohistochemistry.

The distal colon, ileum, and gastric antrum tissue was harvested and fixed overnight at 4°C with Zamboni's fixative (4% formaldehyde with 5% picric acid in 0.1M sodium phosphate buffer, pH 7.2) for immunohistochemical analysis. Mucosal and submucosal layers were removed before fixing. After fixation tissues were washed with 0.1M phosphate buffer (PB) solution (84 mM Na_2HPO_4, 18 mM NaH_2PO_4, pH 7.2) until yellow coloring (picric acid) was removed. The myenteric plexus was exposed by removing circular muscle (CM) strips using fine forceps. Whole-mount longitudinal muscle myenteric plexus (LPPM) preps were then incubated overnight at 4°C with primary antibodies (Table 1). Tissues were then washed 3X at 10-minute intervals and then incubated with secondary antibodies (Table 1) for 1 hour at room temperature. Lastly, after three washes using PB at 10-minute intervals, the tissues were transferred to glass slides with ready-to-use mounting medium (ProlongTM Gold Antifade Mountant, Thermofisher, Cat No: P36961). All LMMP preps were examined by conventional microscopy using a Nikon TE2000-U Inverted Microscope (Nikon TE2000-U series, Nikon Corporation, Tokyo, Japan) with MetaMorph image acquisition and analysis software. All images were obtained using CFI Plan Fluor 20X NA: 0.50 and CFI Plan Fluor 40X NA: 0.75 dry objectives. Fluorescence images were obtained using Nikon filter cubes Cy GFP and YFP-2427B-NTE-ZERO. Colocalization of eYFP fluorescence with ChAT and NOS was quantified for all tested tissues. Confocal microscopy was also used to assess co-localization of eYFP and the purinergic marker protein SLC17A9 (vesicular nucleotide transporter, VNUT).

1 AB	Host	Catalog #	Lot #	Dilution	Source
ChAT	Goat	AB144P	2736715	1/100	Merck Millipore
NOS	Sheep	AB1529	2728417	1/300	Merck Millipore
2 AB		**Catalog #**	**Lot #**	**Dilution**	**Source**
Donkey anti-rabbit-Cy3		711-166-152	131954	1/200	Jackson
Donkey anti-goat- Cy3		705-166-147	131306	1/200	Jackson

Table 5.1: Primary antibodies (1 AB), secondary antibodies (2 AB), dilutions and suppliers of reagents used for immunohistochemical studies of neuronal markers.

Intracellular recordings of excitatory & inhibitory junction potentials at the circular smooth muscle.

Intracellular microelectrodes were used to record IJPs and EJPs from the circular muscle layer of the distal colon of ChAT-ChR2-TG mice. A 1 cm segment of tissue was isolated and placed on a petri dish containing pre-warmed (37 ºC) and oxygenated (95% O_2-5% CO2) Krebs' solution (117 mM NaCl, 4.7mM KCl, 2.5 mM $CaCl_2$, 1.2 mM $MgCl_2$, 1.2 mM NaH_2PO4, 25 mM $NaHCO_3$, and 11 mM dextrose). Segments of the colon were cut open along the mesenteric border and pinned flat on the petri dish with the mucosal layer facing upward. Mucosal and submucosal layers were removed using fine forceps to expose the circular smooth muscle layer. A 0.5cm^2 section was then transferred to a 5-ml silicone elastomer-lined recording chamber. Tissue was then gently stretched and pinned to the recording chamber with small steel pins. The chamber was then mounted on the stage of an inverted microscope, and the chamber was perfused with Krebs solution at a flow rate of 4ml/min at 37 ºC. The preparations were allowed to acclimate for 30 min before the initiation of the electrophysiological measurements. Borosilicate glass microelectrodes (1.0 mm OD x 0.5 mm ID with filament, cat.# 27-30-1; FHC Inc., Bowdoin, ME) with a tip resistance of 60-120 MΩ were filled with 2M KCL and then used to impale circular smooth muscle cells. Electrical field stimulation (EFS) was performed using a pair of 1 mm diameter Ag/AgCl wire (A-M Systems, Seattle, WA) in the recording chamber connected to a Grass S88 stimulator and stimulus isolator constant current unit (Grass Technologies, West

Warwick, RI). EFS was performed using a double-barreled glass electrode with Ag/AgCl wires inserted into each barrel. The electrode was mounted on a micromanipulator and positioned near recording sites. For both simulation methods, the protocol consisted of a 10 Hz train of stimulation with a 0.5 ms pulse duration, 80 V, and train durations of 100-700 ms with 1, 3, 5 and 7 stimuli. Optogenetic stimulation was achieved by using a 470 nm blue light-emitting diode (LED, Thorlabs, Newton, NJ, USA) linked to a fiber optic tube (Thorlabs) with the tip (2.5 mm dia) placed ~1 cm directly above the microelectrode muscle impalement site. The blue light stimulation (BLS) paradigm consisted of a 10 Hz train with a 20 ms light pulse duration, with train durations of 100-700 ms which determined the number of stimuli (1, 3, 5 and 7 stimuli). Intracellular recordings were obtained from circular muscle cells with the LED tip positioned directly above the site of impalement. Light pulses (20 mW/mm^2) were triggered using a Grass S88 stimulator. An Axoclamp-2A amplifier, a Digidata 1440A analog-digital converter, and Axoscope 10.6 software (all from Molecular Devices, Sunnyvale, CA) were as used to record membrane potential changes. The amplified signal was sampled at 2 kHz and filtered at 1 kHz. Tissues from mice expressing ChR2/eYFP in cholinergic neurons were used in our experiments. Negative control tissues obtained from WT mice showed no changes in resting membrane potential following BLS. Only paired EFS and BLS recordings obtained from the same smooth muscle cells were analyzed for this study.

Drug Application.

To limit spontaneous smooth muscle contractility and enhance muscle impalement, the L-type Ca^{2+} channel antagonist, nifedipine (1 μM) (Sigma-Aldrich, St. Louis, MO) was applied to a physiological solution for the duration of each experiment. Additional drugs were perfused into the recording chamber to study the drug effects on the EJP and IJP when comparing group populations. MRS2179, ω-nitro-L-arginine ($_{\omega}$-NLA), mecamylamine, scopolamine, and tetrodotoxin (TTX) were all obtained from Sigma-Aldrich.

Statistical Analysis.

Successful impalements of a circular smooth muscle cell were determined by a rapid drop in the resting membrane potential, and only cells that sustain a resting membrane potential bellow -40mV were considered for statistical analysis. Data are presented as mean $\pm$ SEM with the n values representing the number of mice used for this study. The mean average was determined by averaging the total number of cells recorded from all animal per treatment. Statistical differences between groups was analyzed with one way or two-way ANOVA followed by a Bonferroni post hoc test, or when applicable a two-tailed unpaired Student's t-test was used. Statistical significance was determined if values had a $P< 0.05$.

RESULTS

Distribution of ChAT-ChR2-eYFP neurons in the colon, ileum, and gastric antrum.

The eYFP was detected in myenteric nerve cell bodies and varicose nerve fibers in the colon (Fig. 5.1A) ileum and antrum and the eYFP fluorescence overlapped with ChAT labeling. This overlap ranged from 91% in the ileal myenteric plexus to 81% in the gastric antrum (Fig. 5.1C; n=4 mice). We also detected a small population of eYFP positive neurons that also expressed NOS-ir ranging from 18% of eYFP neurons in the antrum to 9% in the proximal colon (Fig 5.1B,C). In contrast, ChAT-ir overlapped with eYFP expression in 77% of myenteric neurons in the proximal colon to 62% of ileal myenteric neurons. (Fig. 5.1D). The overlap of NOS-ir with eYFP ranged from 38% of ileal myenteric neurons to 23% of myenteric neurons in the proximal colon.

BLS does not evoke neuromuscular transmission in the ileum or gastric antrum.

Blue light stimulation (BLS, 470 nm) did not activate cholinergic motorneurons or interneurons in the ileum or the antrum even though eYFP was detected in many neurons in the antral and ileal myenteric plexus (Fig. 5.1C-E). Neither IJPs nor EJPs could be evoked by electrical field stimulation (EFS) or BLS in ileal circular muscle cells, although these cells showed

robust slow waves (Fig. 5.2A). Intracellular recordings from circular muscle cells in the antrum revealed slow wave activity while EFS but not BLS elicited IJPs (Fig. 5.2B).

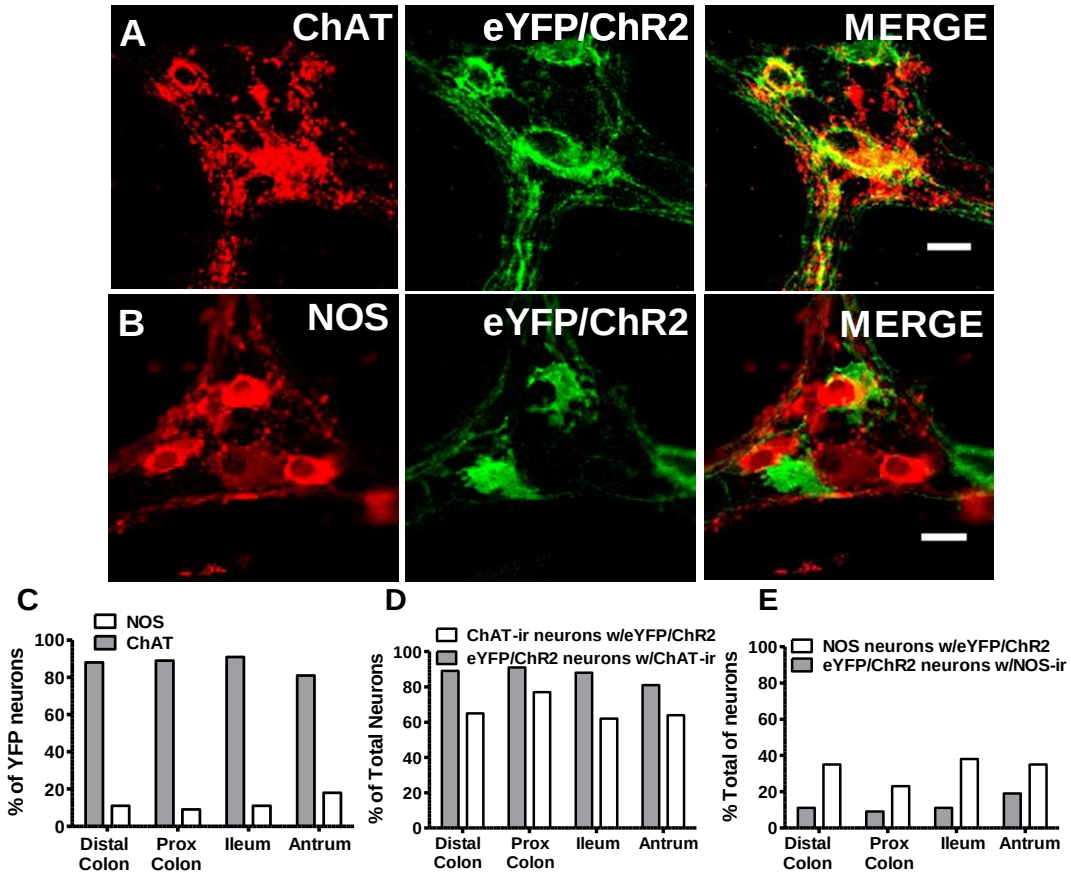

Figure. 5.1: Expression of eYFP/ChR2 myenteric neurons in the gastrointestinal tract of ChAT-ChR2-YFP BAC transgenic mice. *A*, Immunohistochemical labeling of cholinergic neurons in the colon myenteric plexus using an antibody raised against choline acetyltransferase (ChAT), these neurons also expressed enhanced yellow fluorescence protein (eYFP) as shown in the merged image on the right. *B*, Immunohistochemical labeling of nitric oxide synthase (NOS) myenteric neurons showed little overlap with eYFP as shown in the merged image. *C*, Histograms showing the percentage of eYFP expressing neurons that also expressed ChAT or NOS. Greater than 80% of eYFP neurons expressed ChAT while NOS was expressed in fewer than 20% of eYFP positive neurons. *D*, Histograms showing the percentage of eYFP expressing neurons that also express ChAT-ir and the percentage of ChAT-ir neurons that also express eYFP. *E*, Histograms showing the percentage of NOS-ir neurons that also express eYFP and the percentage of eYFP expressing neurons that express NOS-ir.

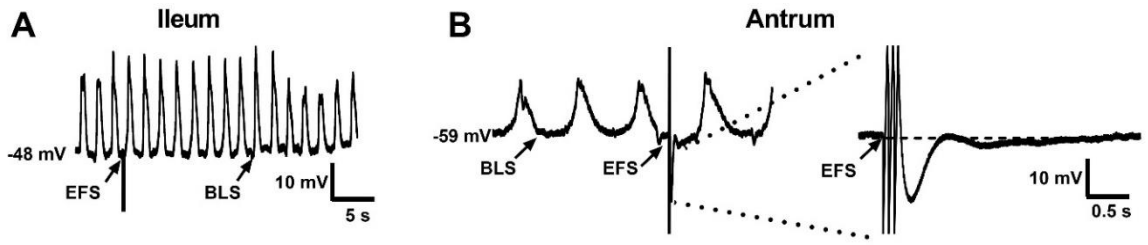

Figure. 5.2: BLS does not produce junction potentials in the circular muscle layer of the mouse ileum or antrum, and EFS stimulation evoked IJPs in the circular muscle of the mouse distal colon. *A,* Intracellular recording of large-amplitude slow waves from the circular muscle layer of the mouse ileum. EFS and BLS failed to evoked junction potentials. *B*, Low-frequency slow waves recorded from the circular muscle in the mouse antrum. EFS but not BLS evoked an IJP.

BLS evokes IJPs in colon circular smooth muscle plateau at a pulse duration of 10ms.

BLS duration response curves for IJPs were obtained using distal colon preparations to establish the stimulation parameters to be used in the remainder of the study. We first tested increasing light pulse durations to determine the peak response and the data show that 3 pulses of BLS at 10 or 20 ms caused responses that peaked 14 $\pm$ 2 mV and 17 $\pm$ 2 mV, respectively (Fig. 5.3A) The IJP area under the curve (AUC) plateaued at a pulse duration of 5 ms (Fig. 5.3B). Therefore, we used 20 ms of BLS for the remaining studies. We next determine the number of BLS pulses need to evoke a maximum response IJP amplitude and duration. We found that 3 BLS pulses (20 ms duration) produced the maximum amplitude and duration IJP, and additional stimuli did not further increase these responses (Fig. 5.3C, D). EFS (0.5 ms pulse duration) produced a maximum amplitude IJP at 3 pulses while the AUC of the IJP increased in duration with an increase in the number of stimuli (Fig. 5.3C, D, Table 5.2). Therefore, in the remaining studies, we used 3 stimuli when using EFS and BLS.

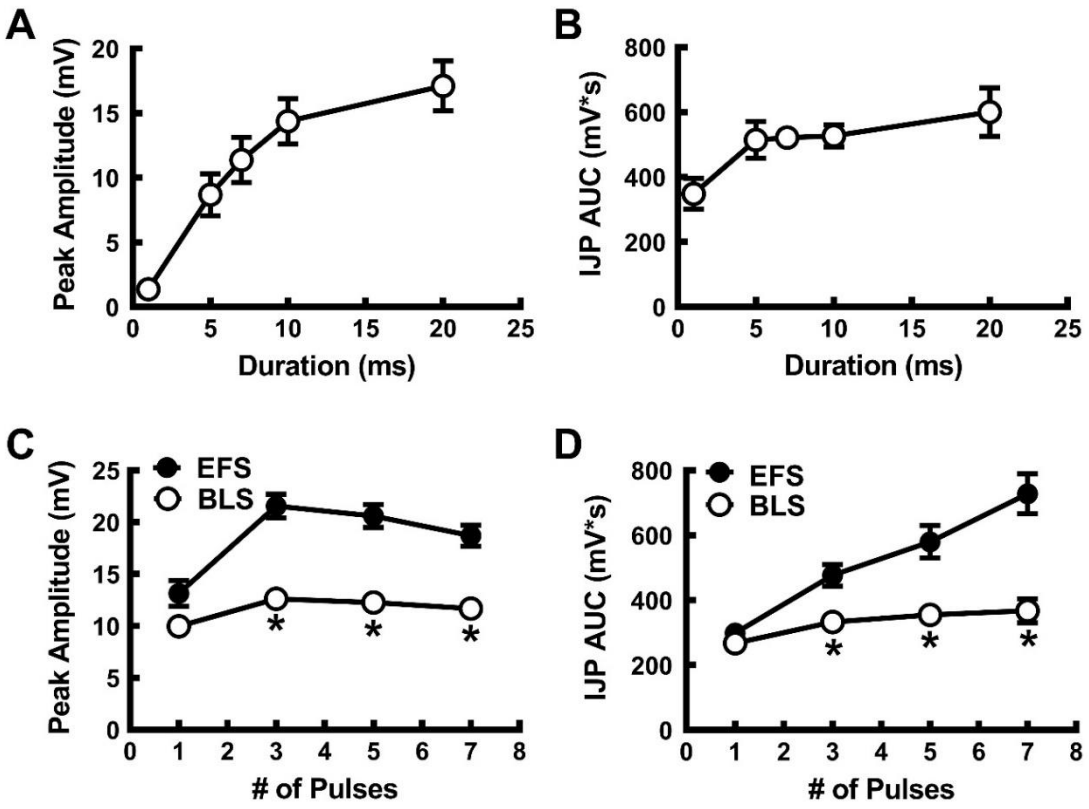

Figure. 5.3: Optimization of the stimulation parameters for BLS evoked IJPs in the distal colon of ChAT-ChR2-YFP BAC transgenic mice. *A*, Increasing the duration of BLS pulses increases IJP amplitude. *B,* Duration of the BLS pulse also increases the area under the curve of the IJP. Subsequent studies used a 20 ms light pulse to evoke junction potentials. *C*, IJP amplitude for responses caused by the increasing number of stimuli (0.5 ms) using electrical field stimulation (EFS) or BLS pulses (20 ms duration. IJP amplitude peaked at 3 pulses. 3 BLS pulses at the indicated pulse duration were used to elicit IJPs. *D*. IJP area under the curve (AUC) evoked by EFS and BLS at the indicated number of pulses. The AUC plateaued beginning at 3 BLS pulses while the AUC curve for EFS increased up to 7 stimuli. Three 20 ms BLS pulses and 3 0.5 ms EFS stimuli were used in all subsequent studies. *Indicates significantly different from EFS evoked responses ($P<0.05$; 2-way ANOVA followed by Bonferroni's multiple comparison's test).

	EFS					BLS					
	# of Pulses	# of Animals	# of Cells	Mean	SEM	# of Pulses	# of Animals	# of Cells	Mean	SEM	P Value
IJP Amplitude (mV)	1	7	43	13.1	1.24	1	7	43	9.96	0.9	> 0.05
	3	7	43	21.6	1.15	3	7	43	12.6*	1.0	< 0.001
	5	7	43	20.6	1.09	5	7	43	12.3*	1.0	< 0.001
	7	7	43	18.7	1.03	7	7	43	11.6*	1.0	< 0.001
	# of Pulses	# of Animals	# of Cells	Mean	SEM	# of Pulses	# of Animals	# of Cells	Mean	SEM	P Value
IJP AUC (mV*s)	1	7	43	124.7	18.0	1	7	43	267.6	13.1	> 0.05
	3	7	43	230.7	33.3	3	7	43	333.1*	15.4	< 0.05
	5	7	43	346.2	50.0	5	7	43	354.7*	20.4	< 0.001
	7	7	43	727.7	61.4	7	7	43	367.5*	36.6	< 0.001

Table 5.2: Comparison of peak amplitude and area under the curve (AUC) of IJPs activated by EFS and BLS. *Indicates a significant difference between responses evoked by EFS and BLS (*P< 0.05; two-tailed paired Student's t-test).

BLS, but not EFS, evokes EJP and IJP responses at the colon circular smooth muscle.

EFS evoked only IJPs which were biphasic with a large amplitude fast hyperpolarization followed by a slower developing, longer last hyperpolarization (Fig. 5.4A, B, C, *left*). BLS (470 nm) evoked three types of responses: EJPs only (Fig. 5.4A *right*), an EJP followed by a small amplitude IJP (Fig. 5.4B, right) and a large amplitude IJP (Fig 5.4C, *right*). BLS-evoked IJPs were the most common response. These results suggest that BLS activates cholinergic interneurons which synapse with inhibitory motorneurons to produce IJPs and cholinergic motorneurons which produce EJPs.

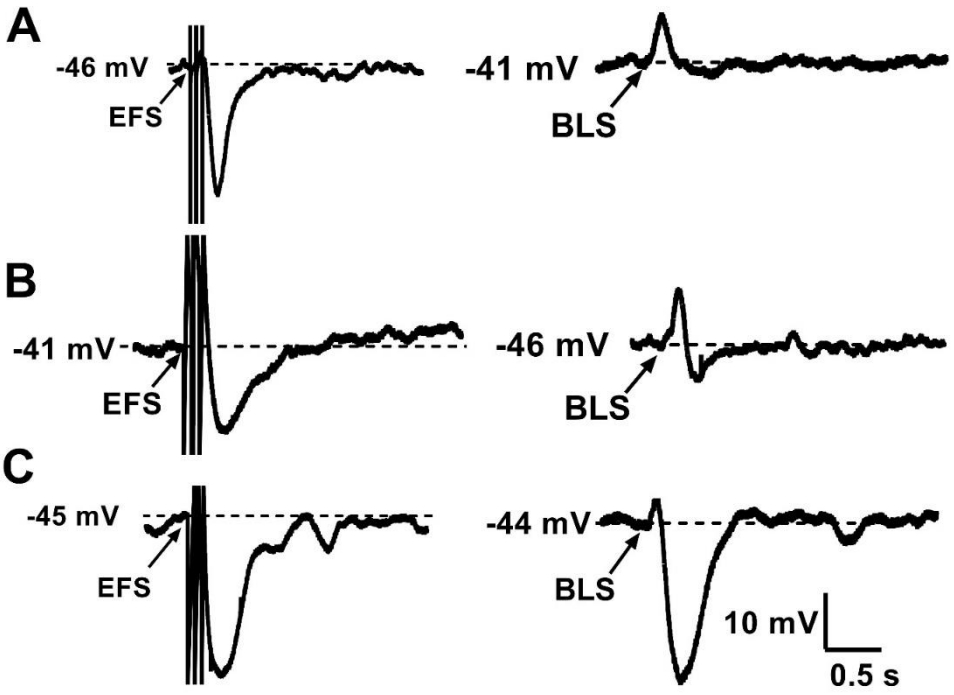

Figure. 5.4: Comparison of EFS- and BLS-evoked junction potentials recorded from circular muscle cells in the distal colon of ChR2-YFP BAC transgenic mice. *A*, EFS elicited an IJP while in the same cell BLS evoked an EJP. *B, In* another recording, EFS elicited an IJP while BLS evoked a biphasic EJP/IJP. *C, In* a third recording EFS and BLS both evoked an IJP.

MRS2179, but not NLA, significantly inhibit the BLS-evoked IJP.

As EFS and BLS elicited IJPs most frequently, we used the nitric oxide synthase (NOS) inhibitor, nitro-L-arginine (NLA, 100 μM) to inhibit the IJP. NLA did not change significantly the peak amplitude or the area under the curve (a measure of the NO-mediated response) (Fig. 5.5). Addition of MRS 2179 (10 μM), a P2Y1 receptor antagonist blocked the IJP (Fig. 5.5B, C) and EFS and BLS now caused an EJP (Fig. 5.5A). These results suggest that most BLS-evoked IJPs are driven by purinergic neurotransmission. Tetrodotoxin (TTX; 0.3 μM) alone reduced the peak IJP amplitude (Fig. 5.6A,B) while subsequent addition of the N-type Ca^{2+} channel blocker ω-conotoxin GVIA (ω-CTX GVIA; 0.3 μM) inhibited the peak IJP and the IJP AUC (Fig. 5.6A,B,C). These results suggest that activation of ChR2 at nerve terminals (TTX resistant but CTX sensitive) is sufficient to drive cholinergic neurotransmission (Fig. 5.6).

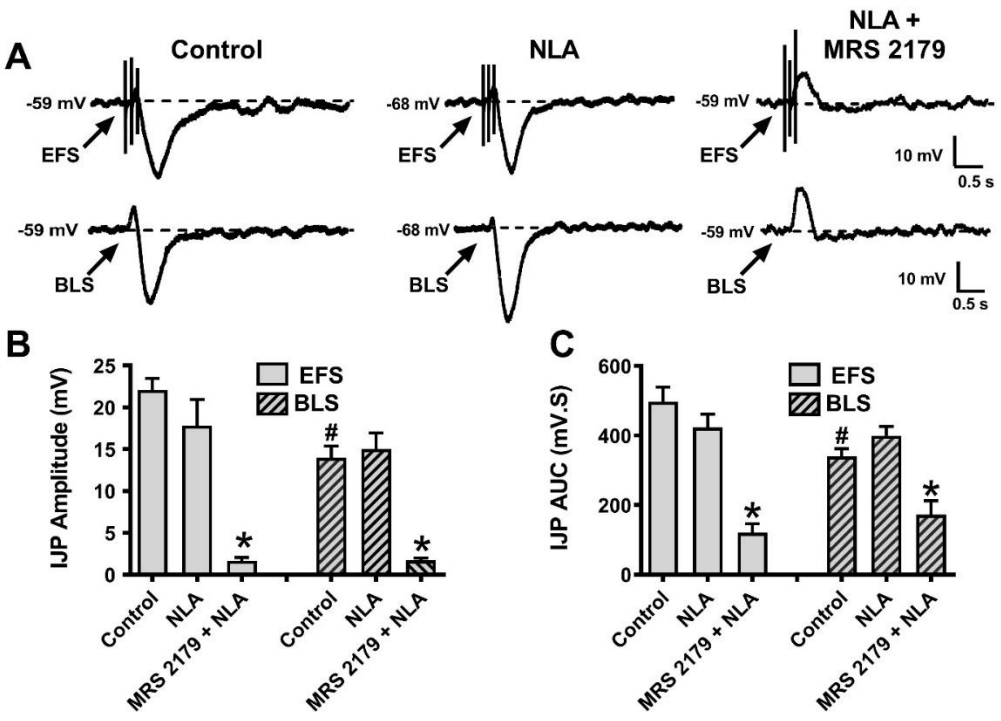

Figure. 5.5: EFS and BLS evoked IJPs in the distal colon. *A*, EFS, and BLS evoke IJPs that are not inhibited by the NOS inhibitor, nitro-L-arginine (NLA, 100 μM). Addition of the P2Y1 receptor antagonist MRS 2179 (10 μM) blocked the IJP, and now EFS evokes and EJP. *B*, NLA did not affect the peak IJP amplitude or AUC (*C*), evoked by either EFS or BLS. Addition of MRS 2179 blocked significantly decreased the peak amplitude and AUC of the IJP. *Significantly different from Control and NLA, P< 0.05, 2 way ANOVA, Bonferonni's multiple comparison test. #Significantly different from the Control EFS IJP, P <0.05.

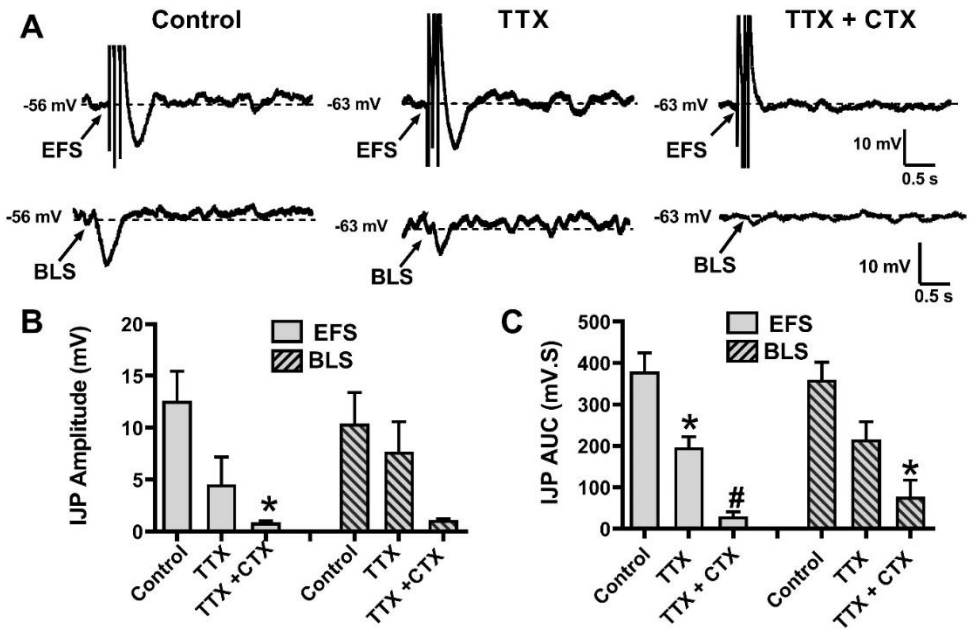

Figure. 5.6: EFS and BLS evoked IJPs are inhibited by the Na^+ channel blocker tetrodotoxin (TTX) and the N-type Ca^{2+} blocker ω-conotoxin GVIA (CTX). *A,* Representative recordings of IJPs evoked by EFS (upper) and BLS (lower). TTX (0.3 μM) reduces IJP amplitude while subsequent addition of CTX (0.1 μM) blocks the IJP. *B*, Pooled data showing that TTX reduces the EFS evoked IJP while the addition of CTX completely inhibits the EFS evoked IJP (P<0.05). *C*, TTX and TTX with CTX reduced the AUC of the EFS evoked IJP while only the combined application of TTX and CTX reduced significantly the AUC of the BLS evoked IJP. (*P< 0.05 vs. Control; #P<0.05 vs TTX only).

Mecamylamine significantly inhibited the BLS, but not the EFS, evoked IJP.

We next determined if ACh is the excitatory neurotransmitter released from interneurons onto inhibitory motor neurons in response to EFS and BLS in the colon of ChAT-ChR2-YFP BAC transgenic mice. We tested EFS and BLS in the absence and presence of the nicotinic acetylcholine receptor antagonist mecamylamine (10 μM). Mecamylamine did not significantly affect the peak amplitude, or AUC of EFS evoked IJPs, but it did significantly reduce the peak amplitude, and AUC of the BLS evoked IJP (Fig. 5.7). Addition of scopolamine (1 μM) increased the amplitude and AUC of the IJP evoked by EFS and BLS and subsequent addition of TTX only reduced the AUC of EFS evoked IJPs. Based on these results, we suggest that ACh released from interneurons during BLS is the main neurotransmitter that drives the IJP activated by ChR2.

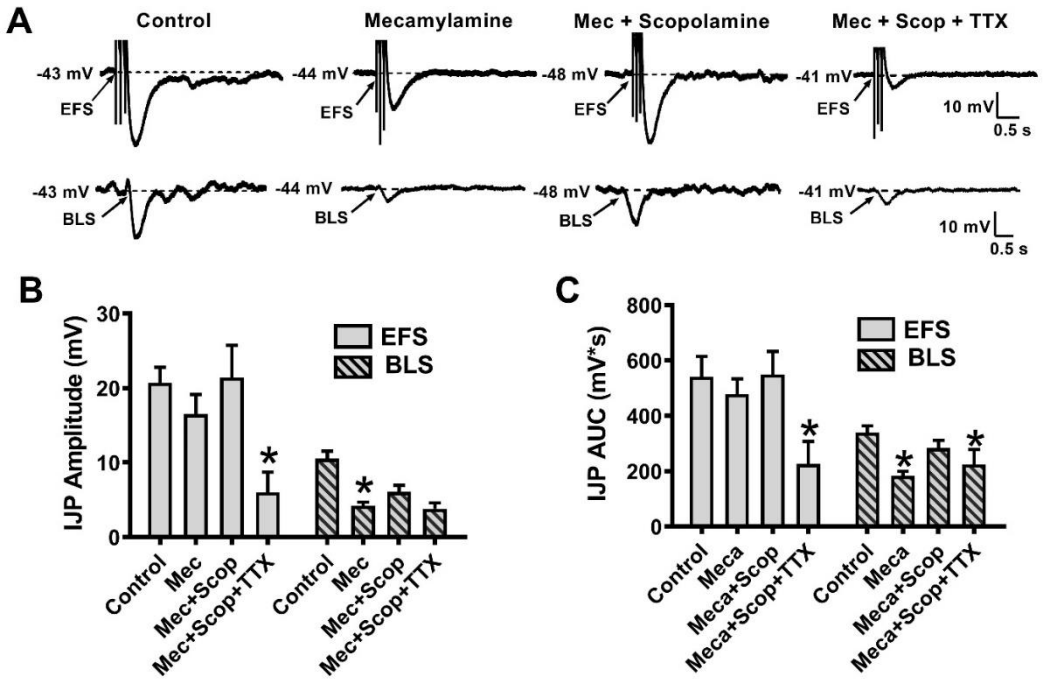

Figure. 5.7: EFS and BLS evoked IJPs recorded from the circular muscle in the distal colon of ChR2-YFP BAC transgenic mice. *A*, Representative IJPs evoked by EFS and BLS. EFS and BLS evoked IJPs were reduced in amplitude by the nicotinic acetylcholine receptor antagonist, mecamylamine (10 μM). Addition of the muscarinic receptor antagonist, scopolamine (1 μM), restores IJP amplitude and subsequent treatment with TTX (0.3 μM) inhibited the EFS and BLS evoked IJPs. *B*, Effects of drugs on the peak amplitude of IJPs evoked by EFS and BLS. The peak amplitude of EFS evoked IJPs was not significantly reduced by mecamylamine or mecamylamine plus scopolamine but the addition of TTX reduced significantly IJP amplitude. Mecamylamine reduced significantly the BLS-evoked IJP while the addition of scopolamine and TTX did not further inhibit the IJP. *C*, The AUC of the IJP evoked by EFS was not affected by mecamylamine and scopolamine but was reduced by TTX. The AUC of the IJP evoked by BLS was reduced by mecamylamine ($P<0.05$) while the addition of scopolamine and TTX did not further reduce the IJP.

MRS2179 & NLA unmask the BLS-evoke EJP

To test if purinergic neurotransmission is responsible for the BLS-evoked IJP, the P2Y1 receptor antagonist, MRS 2179 (10 μM) was used. MRS 2179 reduced significantly IJP peak amplitude evoked by EFS and BLS (Fig. 5.8A,B). A small amplitude IJP persisted in the presence of MRS 2179, and further addition of NLA (100 μM) reduced peak IJP amplitude, and AUC evoked

by EFS and BLS (Fig 8B, C) and this unmasked fast EJPs (Fig. 5.8A). Subsequent addition of the muscarinic receptor antagonist, scopolamine (1 μM), blocked the fast EJP (Fig. 5.8A).

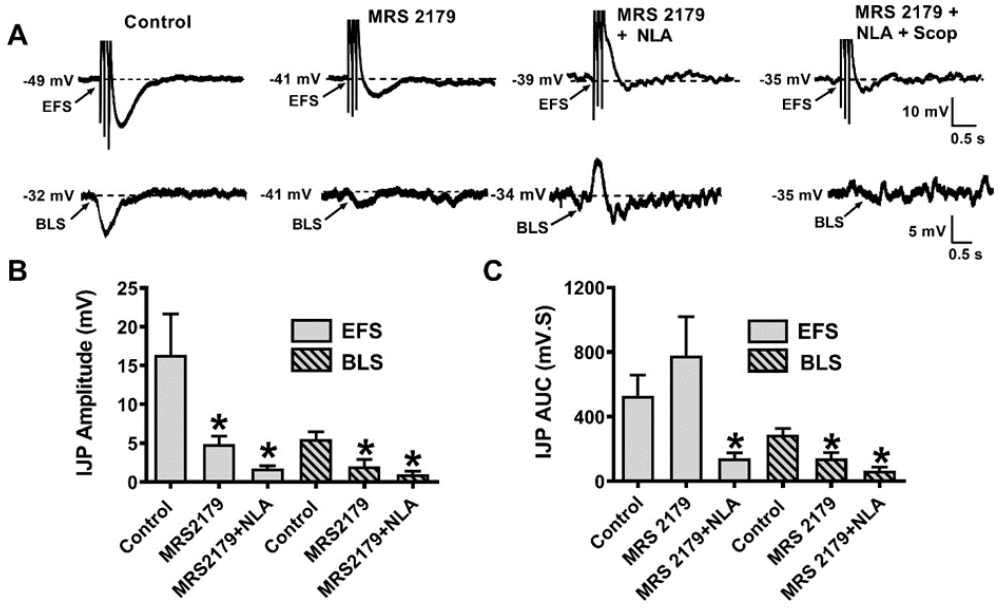

Figure. 5.8: Purinergic EFS and BLS evoked IJP in the distal colon of ChR2-YFP BAC transgenic mice. *A*, Representative EFS and BLS evoked IJP recordings. Co-application of MRS2179 (10 μM) + NLA (100 μM) unmasked the BLS evoke EJP that was later blocked by Scop (1 μM). B, Bath application of MRS 2179 was sufficient to block the peak IJP mediated by EFS and BLS stimulation, which was further inhibited with NLA. C, the AUC of the IJP evoked by BLS, but not by EFS, was significantly decreased by MRS2179 ($P<0.05$). Further application of NLA abolishes all EFS and BLS evoke AUC IJP responses.

BLS-evoked biphasic IJPs and EJPs were recorded from 23 out of 29 circular smooth muscle cells (Fig. 5.9A) while only 3 out of 14 cells that exhibited BLS-evoked EJPs also yielded EFS evoked EJPs. The control EJP amplitude was 6.5 $\pm$ 0.8 mV, and when MRS 2179 and NLA blocked the IJP, the EJP amplitude increased to 8.1 $\pm$ 1 mV ($P>0.05$). Although the peak amplitude did not increase (Fig. 5.9B), there was a significant increase in the AUC of the EJP (Fig. 5.9C). TTX (0.3 μM) blocked completely the EJP evoked by BLS (Fig. 5.9B, C).

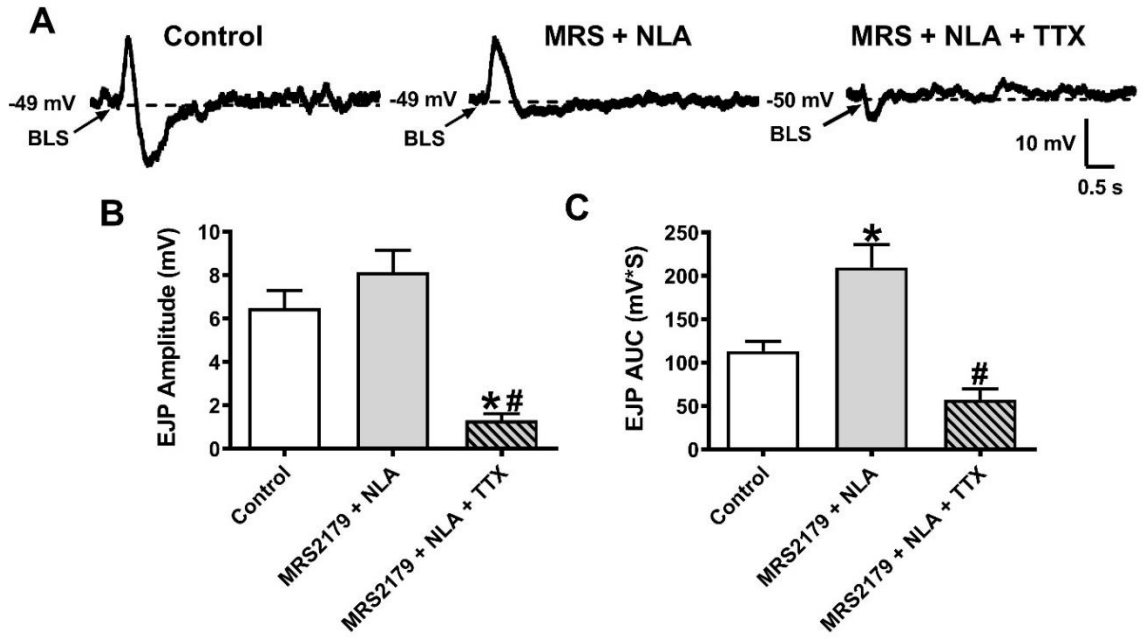

Figure. 5.9: IJP and EJP recordings from circular muscle in the distal colon of ChR2-YFP BAC transgenic mice. *A*, Representative BLS evoked EJP/IJP recording in the absence of drugs. Addition of MRS 2179 (10 μM) and NLA (100 μM) blocked the IJP and addition of TTX (0.3 mM) blocked the remaining IJP. *B*, Combined application of MRS 2179 and NLA did not affect significantly EJP amplitude while the addition of TTX blocked the EJP (*significantly different from control; #significantly different from MRS2179 + NLA ($P<0.05$, one-way ANOVA). MRS2179 plus NLA increased the AUC of BLS evoked EJP (*significantly different from control; #significantly different from MRS2179 + NLA; $P<0.05$, one-way ANOVA followed by Bonferroni's test).

DISCUSSION

Light stimulation of cholinergic neurons induces circular muscle contraction and relaxation.

We used intracellular microelectrodes to record from the circular muscle layer of the gastrointestinal tract of ChAT-ChR2-YFP BAC transgenic mice which express ChR2 in cholinergic neurons. We found that BLS produces 3 types of responses: EJPs, IJPs, and biphasic EJP/IJPs. EJPs were infrequently detected while biphasic EJP/IJP responses were the most common. We were unable to elicit BLS-induced junction potentials in the ileum or antrum for reasons that are not clear. We were able to record electrically evoked IJPs in the antrum but not ileum. The ileum

and antrum generate slow waves initiated interstitial cells of Cajal (ICCs) that are located near the myenteric plexus (ICC_{MY}) (Suzuki *et al.*, 2003; Ward *et al.*, 1994). Hence, the slow wave activity may mask BLS-evoked responses in the ileum and antrum.

Cholinergic neurotransmission elicits the purinergic component of smooth muscle relaxation

Variations in responses (EJP, IJP, or EJP/IJP) recorded in the colon can be attributed to several factors. The relationship between the focal area of BLS relative to the intracellular microelectrode is one factor. For example, BLS of myenteric ganglia could activate selectively cholinergic excitatory motor neurons producing EJPs whereas BLS of an inter-ganglionic fiber tract could activate cholinergic axons that synapse with excitatory and inhibitory motor neurons. Similarly, ChR2 expression in myenteric nerve cell bodies would also produce overlapping EJPs and IJPs. Nonetheless, the majority of the eYFP/ChR2 cell myenteric population are cholinergic, with a small percent of NOS-IR myenteric neurons expressing eYFP/ChR2. In the mouse intestine, about 10% of NOS-ir neurons express ChAT; hence, these neurons are likely to be excitatory interneurons (Qu *et al.*, 2008b). Cholinergic interneurons synapse with inhibitory motor neurons, and this would account for the IJPs elicited by BLS. Our data show that NLA (NOS inhibitor) alone does not block completely BLS-evoked IJPs while combined application of MRS 2179 ($P2Y_1$ receptor antagonist) and NLA blocked the IJP completely. We also found that MRS 2179 alone blocked BLS-evoked IJPs, but not EFS-evoked IJPs. These findings suggest that activation of nicotinic cholinergic receptors on inhibitory motorneurons elicits purinergic but not the nitrergic component of the IJP. This is due to BLS of cholinergic descending interneurons that predominantly synapse with purinergic inhibitory motorneurons to elicit the fast component of the IJP.

ChR2 activation at the nerve terminals induces neuromuscular transmission

Not all BLS-evoked IJPs were inhibited by TTX. TTX blocks the axonal propagation of action potentials by blocking Na^+ channels, most likely TTX-sensitive Nav1.3 and Nav1.7 α subunit-containing channels (Sage *et al.*, 2007). It is possible that BLS activates ChR2 expressed in nerve terminals, and this is sufficient to activate transmitter release to cause IJPs and smooth muscle relaxation. This conclusion is supported by our data showing that bath application of ω-CTX GVIA blocked TTX-resistant junctional potentials. ω-CTX GVIA blocks N-type VGCCs, which contribute to Ca^{+2} entry at the nerve terminal, causing neurotransmitter release (Bian *et al.*, 2007).

Increase expression of VAChT enhances the BLS evoke a neuromuscular response

Co-application of MRS 2179 and NLA enhanced EFS and BLS-induced EJPs. However, BLS-evoked EJPs were more common than EFS evoked EJPs as they are frequently masked by the IJP (Wang *et al.*, 2007). The ChAT-ChR2-YFP BAC transgenic mice also have increased expression of the vesicular acetylcholine transporter (VAChT) which is responsible for a 3-fold increase in ACh release from neurons in the hippocampus (Kolisnyk *et al.*, 2013; Nagy *et al.*, 2012). As a result, the increased BLS-evoked EJPs seen in our studies could be attributed to this increase in ACh release.

BLS induce cholinergic neurotransmission implicates purinergic descending interneurons

In addition to excitatory motor neurons (EMNs), ACh is also released by interneurons (ascending and descending) and by intrinsic primary afferent neurons (IPANs) (Qu *et al.*, 2008b). Neuronal release of ACh activates myenteric neurons that express ionotropic nicotinic ACh receptors (nAchR), and activation of these receptors is the primary mechanism of excitatory neurotransmission in the ENS (Galligan, 2002). Nevertheless, studies suggest that contingent on the myenteric cell population, other types of neurotransmitters such as substance P, 5-HT, or purines work in collaboration with ACh to stimulate GI motility (Furness, 2000; Zagorodnyuk *et al.*, 2000). Tachykinins, such as substance P (SP) are co-released with ACh to induce smooth

muscle contraction (Costa *et al.*, 1985; Grider, 1989). Bath application of the muscarinic cholinergic receptor antagonist, scopolamine, was sufficient to block the EJP as it is commonly used to block spontaneous contractions of the muscle layer during intracellular recordings (Abazov *et al.*, 2006; Matsuyama *et al.*, 2013). These data suggest that SP, may not contribute to excitatory responses evoked by BLS. Conversely, purinergic P2X receptors and nAChRs control most of the descending inhibitory reflexes, while the ascending pathway is predominantly cholinergic (Galligan *et al.*, 1994; Johnson *et al.*, 1999b; Zhou *et al.*, 1996). However, our data reveal that BLS of ChAT/ChR2 neurons causes IJPs and further application of mecamylamine blocked the BLS-evoked IJP. This suggests that the descending inhibitory is mainly driven by descending cholinergic interneurons rather than a cholinergic/purinergic population. Abolishing the excitatory component by further application of scopolamine recovered more than half of the BL-evoked IJP. Recovery of BLS evoked IJPs in the presence of mecamylamine and scopolamine support a role for purinergic P2X receptors in myenteric neurotransmission (Galligan *et al.*, 1994; Johnson *et al.*, 1999b). Homomeric $P2X_2$ receptors have been shown to mediate the non-cholinergic fast synaptic response in S neurons in the mouse small intestine and is suspected of doing the same in the large intestine (Ren *et al.*, 2008; Ren *et al.*, 2003). Nevertheless, the lack of a specific $P2X_2$ receptor antagonist limited further studies to better define purinergic contributions to the inhibitory pathway activity (Antonioli *et al.*, 2013).

***Conclusions*.**

We recorded IJPs and EJPs from the circular smooth muscle layer of the distal colon of the ChAT-ChR2-YFP BAC transgenic mouse model following light-evoke stimulation of cholinergic myenteric cell populations in the ENS. Hence, our data confirm that cholinergic neurotransmission controls excitatory and inhibitory smooth muscle reflexes in the GI tract. Moreover, our data support the idea that a subpopulation of descending cholinergic interneurons are responsible for controlling the purinergic, but not the nitrergic, IMNs which initiate smooth muscle relaxation. Despite these findings, further electrophysiological studies are needed to

identify cholinergic pathways in the myenteric plexus. Future studies should be done using optogenetic stimulation of interganglionic nerve fibers to answer these questions. This technique has the potential of becoming a powerful tool in enhancing the discovery novel therapeutic targets to treat GI motility disorders but can also be shaped as a therapeutic tool of itself for treating patients with GI-related diseases, such as irritable bowel disease (IBS).

CHAPTER 6: GENERAL DISCUSSION AND CONCLUSION

SUMMARY AND GENERAL CONCLUSION

Motor impairment is a common symptom found in motility disorders and functional gastrointestinal disorders (FGIDs) which typically results from damage to the ENS circuitry. These disorders affect ¼ of the United States population and comprise about 40% of the diagnosed GI disorders by physicians and therapists (Parkman *et al.*, 2006). Motility disorders (e.g., gastroparesis, intestinal pseudo-obstruction) are GI disorders where the patterns of contraction and relaxation of the GI muscles behave abnormally, leading to detectable motility disturbances (e.g., delayed gastric emptying). Conversely, FGIDs are defined as disorders of the gut-brain interaction, which takes into account a combination of symptoms: motility disturbance, visceral hypersensitivity, altered mucosal and immune function, altered gut microbiota, and altered central nervous system (CNS) processing (Drossman *et al.*, 2016). In addition, most FGIDs display no pathological anomalies. Hence, the term "functional" in FGIDs is not used to describe how the disease affects normal gut functions, but to construe that the direct cause of gut dysfunction is unknown. This is because in many cases, examination (e.g., endoscopy, x-rays, blood tests) reveals no structural or chemical abnormalities, yet symptoms persist. These classes of GI disorders are life-long conditions, and because surgical procedures are rarely needed or represent a considerable risk to the patient's health, a pharmacological approach is often the only available option for many patients.

Although drug treatments may improve the symptoms of patients that suffer from some form of a GI disorder, their efficacy is often limited: they offer temporary relief, patients often exhibit tolerance or side effects, they only have a therapeutic effect on specific demographics, and they often don't improve the patient's quality of life (Di Nardo *et al.*, 2008). For instance, Alosetron, brand name Lotronex ®, is a $5HT_4$ receptor antagonist that is used to treat diarrhea symptoms in patients with severe IBS-D. However, this drug only provides relief to some women, and those that take the medication are at risk of developing severe complications such as severe constipation or could develop ischemic colitis (Chang *et al.*, 2014), hence the Food and Drug

Administration (FDA) limits its widespread use (Vannucchi *et al.*, 2018). Other receptors such as corticotropin-releasing factor receptors (CRFr), TK receptors (NK1, NK2, and NK3 receptors), and Ca^{+2} channels have been linked to IBD. However, no modulators, antagonist, or drugs of any kind have reached the pharmaceutical market. Plus, only a handful of recent drugs such as lubipotone and linactotide have been approved to treat symptoms of constipation in IBS. Hence an alternative approach to conventional pharmacology that would improve the quality of life of patients that suffer from GI dysfunction or disease is desperately needed. The use of AAV virus vectors and optogenetic technology could help aid in the discovery of new therapeutic drugs, but may also be considered itself as an alternative gene therapy strategy to treat GI disorders.

Optogenetic gene therapy: a potential strategy for the treatment of FGID and motility disorders

The discovery of DNA as the biomolecule of genetic inheritance and disease opened up the prospects of therapies in which mutations and damaged genes could be genetically modified to improve the human condition. In addition, sequencing of the human genome provided identification of the gene or genes that might be driving the disease state. Hence, this means that if the sequence of the mutant gene could be normalized or "fixed," potentially the disease could be treated at a molecular level, or, in a best-case scenario, cured (Naso *et al.*, 2017). However, strategies to safely deliver transgenes into the targeted cell/tissue/organ of disease without degradation of the genetic material has been challenging. Viruses became the ideal vectors for this purpose as they are naturally occurring biological agents that have evolved to deliver nucleic acid (RNA or DNA) into host cells for its replication. However, their immunologic profiles or their tendency to induce tumor growth made them unsuitable for clinical gene therapy application. Nevertheless, the discovery of adeno associated virus (AAV), followed by the engineering of the recombinant AAV (rAAV) (see chapter 1), allowed scientists to traffic and deliver non-virulent genetic material (transgene) into the nucleus of target cells without exhibiting off-target effects.

For instance, rAAV have shown to be less immunogenic than other viruses due to their inefficiency to transduce antigen-presenting cells (APCs) (Mays *et al.*, 2014), and because they don't carry any viral genes that could trigger or amplify the immune response (Basner-Tschakarjan *et al.*, 2014). There is also limited genotoxicity with rAAV because the transgene it carries does not integrate into the host genome following transfection but instead remains episomal or in plasmid form (Chandler *et al.*, 2017; Nakai *et al.*, 2003). Also, AAVs are very stable vectors capable of withstanding a wide range of temperatures and pH changes, which provides ample opportunities to attempt different routes of administration: systemic, intramuscular, intrathecal, or direct injection of the virus into the tissue.

Overall, there are many characteristics that make rAAV an ideal vector for gene therapy to an extent that rAAV as a delivery vector for gene therapy has been rapidly gaining interest in the last 5-7 years, with many novel rAAV therapeutics designed to treat a range of diseases (e.g., Hemophilia, Alzheimer's disease, Parkinson's disease, corneal disease) are currently being evaluated in preclinical and clinical trials (Colella *et al.*, 2018; Naso *et al.*, 2017; Rodrigues *et al.*, 2018). However, several issues need to be addressed before AAV can be fully exploited as a potential strategy for human gene therapy. Some of these issues involve the immunogenicity, potency and efficacy, genotoxicity, and the manufacturing/development process of AAV vectors.

Although AAV has shown to be less immunoreactive, a significant portion of individuals already develop a pre-existing adaptive immune response to AAV due to exposure to the wild-type AAV during the first 2 years of age, or via acquired immunity during gestation (Balakrishnan *et al.*, 2014; Calcedo *et al.*, 2011; Sonntag *et al.*, 2010). Either way, anti-AAV neutralizing antibodies (Nabs) can have a profound impact on the efficacy of the gene transfer. As a result, careful prior assessments, such as screening for Nabs, immunosuppressant strategies, or development of AAVs that don't mediate an immunogenic response should be taken into consideration prior to commencement of gene therapy clinical trials.

To achieve long-term stable transgene expression at levels that are therapeutic, AAV vectors must be administered at a dosage that would provide optimum therapeutic effects. In clinical trials designed to treat patients with hemophilia B, therapeutic levels of expression of the transgene of interest were achieved using different AAVs in a dose-dependent manner. However, these AAV doses were also correlated with unwanted Nab responses, which could potentially counteract, decrease or even abolish the transgene expression (Manno *et al.*, 2006; Mingozzi *et al.*, 2007; Mingozzi *et al.*, 2009; Nathwani *et al.*, 2014; Nathwani *et al.*, 2011b). Moreover, the efficacy of AAV transfection could also vary depending on the severity of the disease state, the nature of the transgene product, and the route at which the AAV is being administered. Therefore additional steps should be taken when optimizing the design of the vector (capsid and genome), the transgene expression cassette (sequence and regulatory elements), as well the method of delivery. By optimizing the AAV design, it would increase cell infection/transduction and transgene levels and would decrease the dose/response ratio needed to achieve therapeutic efficacy, reducing the risk of unwanted Nabs and toxicity (Colella *et al.*, 2018).

An advantage that AAV vectors possess as a vehicle for gene therapy mentioned earlier is that they remain extra-chromosomal following transfection, and only on rare occasions, they integrate into the host cell genome. Integration of the transgene into the host genome could lead to genotoxic effects resulting in loss- or gain-of-function mutations that end in altered cell function and homeostasis, or more severe cases lead to the development of cancer. For instance, systemic AAV administration to neonatal mice predisposes them to hepatocellular carcinoma (HCC) because the viral genetic material becomes inserted into the host genome causing dysregulation of genes that trigger tumor growth and formation (Chandler *et al.*, 2015; Donsante *et al.*, 2007; Russell, 2003). However, in long-term studies performed in larger animals such as dogs (Niemeyer *et al.*, 2009)and non-human primates (NHP) (Gil-Farina *et al.*, 2016; Nathwani *et al.*, 2011a), there were no observed concerns over genotoxicity risk of AAV vectors in the liver,

with similar results obtained in human clinical trial studies (Nathwani *et al.*, 2014). In this same human trial study, no tumor formation was documented in more than seven years post-gene transfer with an AAV design to treat hemophilia B (Nathwani *et al.*, 2014). Nevertheless, monitoring AAV vector insertion and genotoxicity in preclinical trials should be taken seriously. That is long-term monitoring of tumor formation in tissues of patients that were transfected with the AAV, and extensive evaluation of the AAV vector genome to determine its potential capacity for genome integration should always be monitor.

Another technology that is exploding in popularity as a tool to study and treat diseases is optogenetics (see chapter 1). Optogenetics is a technique that allows the control of excitable cells (e.g., smooth muscle, skeletal muscle, neurons) by activating light-sensitive optogenetic actuators (e.g., halorhodopsin, channelrhodopsin (ChR2)) that are expressed in specific tissue/cells, typically via utilization of site-specific recombination technology (e.g., Cre-loxP, Tet-On/Off, and Gal4-UAS) (Wang, 2018). As a result, optogenetics is a powerful tool currently used to elucidate the CNS, PNS, and ENS neuronal circuits (Wang, 2018). However, site-specific injections of AAV constructs containing these optogenetic actuators could significantly serve a more clinical purpose (Wrobel *et al.*, 2018). A study by Wrobel et al. and colleagues shows the potential clinical application of optogenetics for treating patients that have acute hearing loss. In their research, AAV constructs containing the light-sensitive Ca^{+2} translocating channelrhodopsin (CatCh) was injected into the cochlea of adult deaf gerbils. In control adult gerbils, light-evoked activation of CatCh elicited cued avoidance behaviors that are similarly induced by acoustic stimuli. More importantly, auditory responses and cued avoidance behavior were also induced in adult deaf gerbils injected with the AAV construct following light stimulation, suggesting the partial restoration of the rodent's auditory functions. AAV delivery of optogenetic actuators into the optic nerve has also shown to restore vision responses in mice (Bi *et al.*, 2006; Doroudchi *et al.*, 2011), and in non-human primates (NHP) (Chaffiol *et al.*, 2017). The development of the ChR2

therapeutic agent RST-001 developed by the pharmaceutical company Allegan is currently being tested in phase 1 clinical trials for the treatment of the genetic eye disease retinitis pigmentosa (Rodriguez et al. 2019). It is, therefore, no surprise that other optogenetic gene therapies will soon follow as it's evident that optogenetics and AAV technology is becoming increasingly more sophisticated and useful in treating diseases that once were deemed incurable. As a result, novel optogenetic gene therapy strategies tailored for the treatment of FGID or motility disorders may become a reality in the following decades.

The challenges of optogenetic gene therapy

Optogenetic control of the activity of the enteric neurons, muscle cells, and potentially glia cells can provide a great new strategy to treat ENS disease and disorders. However, many challenges require addressing before optogenetics can be potentially utilized for clinical purpose. Some of these challenges include identifying specific promoters, lack of firm surfaces, and the relative motion of the gut.

What makes optogenetic gene therapy a potential tool to treat FGID and motility disorders in the ENS, is its capacity to deliver the optogenetic actuators to the target cell population via AAV delivery. However, to ensure accurate targeting of the optogenetic actuator, the AAV vector must be encoded with the specific promoter that will provide cell-specific expression. For instance, it has been shown that ChAT promoter drives ChR2/YFP expression exclusively in enteric cholinergic neurons of ChAT-ChR2-YFP BAC mice, while the nNOS promoter in nNOS ERT2 mice induces Cre expression solely in NOS-positive neurons in the ENS (Jiang *et al.*, 2017). Excitatory motor neurons (EMNs) are predominately cholinergic, and nNOS is predominately expressed in inhibitory motor neurons (IMNs) (Gallego *et al.*, 2008a; Matsuyama *et al.*, 2013). Both enteric neuron types are essential modulators of GI motility in the Gut. As a result, optogenetic gene therapeutics in which both cell populations are targeted via their respective promoters and controlled via different optogenetic actuators can potentially be used to control

patterns of motility in the gut. Optogenetic control of these cell populations in the ENS could serve to alleviate symptoms of constipation or diarrhea observed in patients suffering from different forms of IBS (e.g., IBS-D, IBS-C, and IBS-M), or to relieve gastrointestinal obstruction in motility disorders. Other promoters such as the human dopamine β-hydroxylase promoter (Thy1) (Taylor-Clark *et al.*, 2015), and the glial fibrillary acid protein (GFAP) (Hoque *et al.*, 2016) have been used to drive expression in GABAergic and enteric glial cells in the ENS. Optogenetic therapeutic strategies could be tailored to treat some symptoms of neuropathic pain (Belle *et al.*, 2007) or glia related disease. Nevertheless, identification of new specific promoters, as well as better opsin actuators and AAV constructs are equally important, to ensure spatial and temporal expression of this therapeutic strategy. Off note, one alternative therapeutic approach using optogenetics to treat FGID and motility disorders, would be expressing optogenetic actuators directly into smooth muscle cells as they are also excitable cells. This could be a more viable approach to treating these diseases, in particular to FGIDs such as IBS as little is known about the exact origin of its pathogenicity. Hence, direct optogenetic manipulation of the gastrointestinal smooth muscle would disregard any need to comprehend the disease mechanism of action entirely. Yet again, underlining that the different SMCs, ICCs, and PDGFα cells, in addition to their specific promoters is fundamental. This is assuming that there are different subpopulations of each these cell types that reside within or near the gut muscle layers.

The CNS contains firm surfaces such as the skull and spine that would allow installment of devices such as light fibers (e.g., small LEDs) for optogenetic stimulation, and electrodes for recordings. Conversely, the ENS lacks any firm surface, which would make it difficult to maintain consistent optogenetic stimulation and as well as recordings of the same groups of enteric neurons. However, the use of integrated graphene sensors placed close to the intestine can be used to overcome this problem. In a study by Rakhilin et al., researchers were able to develop an implantable abdominal window integrated with a graphene sensor. The graphene sensor was

integrated into the small intestine of Pirt-GCaMP3 mice to observer neuronal firing *in vivo*, and at the same time perform optical and electrical recording in the ENS. This technique also showed to provide high spatial and temporal resolution allowing single waveform detection of action potentials. Although the apparatus does not include any light source, modifications can be made so that both recording electrodes and light source (small LED) can be integrated into the device (all-in-one device) (Rakhilin *et al.*, 2016). The power supply, on the other hand, can also be strategically placed under the skin, such as shown by Montgomery et al. In this study by Montgomery et al they were able to develop a wireless LED device that weighted only 20mg with a size of $10mm^3$, making it easier to implant it under the skin of mice (Montgomery *et al.*, 2015). In a similar study, a LED device was implanted under the skin of Advilin-ChR2 mice. Wireless activation of the LED lead to ChR2 triggering pain behavior responses in these mice (Il Park *et al.*, 2015). As a result, an implantable abdominal window integrated with a graphene sensor with wireless LED could help alleviate symptoms of constipation, diarrhea, and most importantly pain present in patients that suffer from a type of FGIDs or motility disorder. The downside of this strategy, however, is that transplantation of the device will require surgery. Therefore this therapeutic alternative should only be used when non-surgical therapeutic strategies have been exhausted. Another problem to this strategy is that FGIDs exhibit no organic etiology, as a result determining a site or sites of treatment would be difficult. Hence, identification of FGID biomarkers would help narrow down the potential areas of the gut that requires treatment. However, typical animal models used to study FGIDs such as IBS can only mimic aspects of the disease pathophysiology, without exhibiting any markers of the disease (Wang, 2018). The lack of suitable animal models and the absence of organic markers for FGIDs can almost entirely be attributed to our lack of understanding of gastrointestinal physiology and ENS circuitry. As a result, basic science research using optogenetic could further uncover some of these unknown pathways in the ENS.

Dissecting the enteric neuronal circuits that control GI motility

The discovery of novel drug targets and the development of new therapeutic alternatives are desperately needed to treat patients that suffer from some form of FGID or motility disorders. To accomplish this, we must first fully understand the nerve circuit physiology that coordinates patterns of GI motility, so that we can then identify the hallmarks of the diseases state.

Motility in the gastrointestinal tract is manipulated by three central populations of myenteric neuron populations: intrinsic primary afferent neurons (IPANs), interneurons, and motor neurons (MN) (Qu *et al.*, 2008b). Moreover, EMN and IMNs are the two subclasses of myenteric motor neurons that innervate the smooth muscles that trigger the contraction and relaxation, respectively, observed during patterns of motility. EMNs predominately release ACh, while IMNs co-releases a purine and NO as the main neurotransmitters. Neuronal nitric oxide synthase (nNOS) is the immunological marker used to target the cell body and nerves of nitrergic neurons (Matini *et al.*, 1995) , while the vesicular nucleotide transporter (VNUT, SLC17A9) (Sawada *et al.*, 2008) is a synaptic vesicle transporter located in the synaptic terminals, and is used to identify purinergic nerve fibers during immunolabeling. Despite belief, in chapter 3, my findings show that nNOS and VNUT do not co-localize in myenteric ganglia, tertiary plexus, or circular smooth muscle nerve fibers of different tissue sections of the GI tract (e.g., stomach, small intestine, and large intestine). These findings question the current understanding of inhibitory neurotransmission in the GI tract, which states that one population of IMNs is responsible for the co-release of NO and a purine during smooth muscle relaxation. Moreover, sharp-electrode electrophysiology recordings show the postsynaptic activation of some myenteric neurons are triggered by the presynaptic release of a purine along with ACh (Galligan and Bertrand 1994). However, VNUT does not colocalize with any of the tested neuronal markers used to stain for other subclasses of myenteric neurons (e.g. calretinin, calbindin, and TH), including the immunomarker for cholinergic

cells, ChAT. This suggested that a particular subclass of myenteric neurons is responsible for driving purinergic neurotransmission.

Nevertheless, VNUT has also been shown to be expressed in C6 glioma cells and primary culture of cortical astrocytes, where is mainly associated to lysosomes (Oya *et al.*, 2013).Therefore, VNUT-dependent ATP exocytosis from enteric glial cells could also regulate purinergic mediated functions in the GI tract. ATP can also be released from cells into the extracellular space via pannexin and connexin hemichannel (Locovei *et al.*, 2006; Lohman *et al.*, 2014). Pannexin hemichannels (e.g., Panx1 and Panx2) are abundantly expressed enteric neurons (Diezmos *et al.*, 2013; Diezmos *et al.*, 2015), while connexin (e.g., Cx43) hemichannels are highly expressed in glia, SMC, ICC cells, and cell bodies and processes of enteric neuronal (McClain *et al.*, 2014; Nemeth *et al.*, 2000). Deletion of the Cx43 hemichannel resulted in a 29% decrease in GI intestinal transit (Doring *et al.*, 2007). Therefore, it's essential to keep in mind that in addition to the vesicular release of ATP, pannexin and connexin hemichannels may also play an important role in regulating purinergic neurotransmission in the gastrointestinal tract.

To further test if purinergic neurotransmission is mediated by an exclusive enteric neuron subpopulation we set out to used various optogenetic mouse models that express the enhance optogenetic actuator Channelrhodopsin-2 (ChR2) in specific populations of enteric neurons. In chapter 4, we injected AAV9-floxed channelrhodopsin-2 (ChR2) fused with eYFP (ChR2-eYFP) into the proximal colon of *Nos1*$^{tm1(cre)Mgmj}$/J (Nos1^{Cre}) mice to express ChR2-eYFP in nNOS neurons (AAV9-Nos1-ChR2-eYFP). However, we also bred Nos1^{Cre} mice with B6;129S-Gt(ROSA)26Sor$^{tm32(CAG-COP4*H134R/EYFP)Hze}$/J mice to establish Nos1-ROSA-eYFP mice expressing ChR2-eYFP in all nNOS neurons. Overall the recordings obtained from our AAV9 injected mice and bred mice exhibited similar results. That is, EFS and BLS were able to evoke a biphasic IJP response in both AAV9-Nos1-ChR2-eYFP and Nos1-ROSA-eYFP mice. Following application of the P2Y1 receptor antagonist and the nNOS inhibitor, MRS 2179 and NLA respectively, the fast

and slow IJP responses were abolished. The data hence suggested that both neurotransmitters are in fact, released by the same populations of IMNs. Nevertheless, after further immunological inspection of the eYFP tag ChR2 in tissue, we observed significant expression of ChR2 in non-nNOS positive cells. Hence, the ectopic expression of ChR2 could explain the observed biphasic IJP responses. Studies using double-reporter-mice that expresses two fluorescent reporter strains for ChAT and nNOS showed a small percentage of neurons were positive for both nNOS and ChAT (Jiang *et al.*, 2017) when compared to the immunostaining method. In this study, mice expressing Cre-ERT2 recombinase under the control of the nNOS promoter (B6;129S-Nos1$^{tm1.1(cre/ERT2)Zjh}$/; nNOS-CreER; Stock No: 014541) were crossbred with Cre reported mice that are positive for the red fluorescent protein, Td-Tomato. The Cre-ERT2 fusion gene activity was then induced by administration of tamoxifen, a selective estrogen receptor modulator used to treat breast cancer. As a result, only cells that expressed Cre (e.g., nNOS cells) produced the fluorescence reporter. Hence, the crossbreed of nNOS-CreER mice with the available ROSA mouse model (B6;129S-Gt(ROSA)26Sor$^{tm32(CAG-COP4*H134R/EYFP)Hze}$/J; Stock No: 024109) could be used to develop a more reliable optogenetic mouse model to underline the circuitry of inhibitory neurotransmission.

In chapter 5, we used commercially available ChAT-ChR2-YFP-BAC transgenic mice which express ChR2 in cholinergic neurons to study the cholinergic neurotransmission in the colon. Similar to our AAV9-Nos1-ChR2-eYFP and Nos1-ROSA-eYFP mice, we measured neurogenic EFS and BLS IJP responses, but also EJP responses from circular smooth muscle of transgenic mice. Compared to EFS that predominately evoked IJPs, BLS elicit an array of different responses including EJPs only, IJP only, and mixed EJP and IJP responses. Application of the nicotinic acetylcholine receptor inhibitor, mecamylamine, causes inhibition of the IJP response by more than 50%, while only use of MRS 2179 was sufficient to inhibit the full IJP response. Off note, mecamylamine is the most potent nAChR antagonist in the ENS affecting α3, α5, β2, and β4

containing nicotinic ACh receptors (nAChR), while none of the myenteric nAChRs express the α7 subunit, this as intracellular recordings were unaffected by α-bungarotoxin (Zhou et al., 2002). These results suggest that cholinergic interneurons are predominately responsible for activation of nAChR located postsynaptically on purinergic IMNs. Hence cholinergic activation of nAChRs of purinergic IMNs results in a purine only IJP response or a fast IJP. The inhibitor of the nNOS, NLA, had little to no effect on the light-evoke IJP response. Based on this evidence, we suggest that a population of cholinergic only interneurons innervate purinergic only IMNs to drive the fast component of relaxation in muscle. Purines are also released by descending interneurons and are suggested to activate P2X receptors located on the cell body of IMNs (LePard *et al.*, 1999). (). Hence it is possible that some nitrergic IMNs receive exclusive input from subpopulations of purinergic interneurons in the myenteric plexus. However, further studies are needed to uncover this mystery. Electrophysiological recordings from myenteric neurons populations following paired electrical and light evoke stimulation of the interconnecting fiber tract, as well using a pharmacological approach, could help uncover this conundrum. We suggest that these studies should be performed with recording electrodes containing an intracellular dye marker such as neurobiotin (Huang *et al.*, 1992) to trace the impaled neuron following a successful electrophysiological recording (Clerc *et al.*, 1998). That is, once this marker dye is injected into a cell, immunohistochemistry can be performed to analyze the morphology and projections of the impaled cell following EFS and BLS. Also, using our ChAT-ChR2-eYFP transgenic mouse, one can study the correlation of eYFP/ChR2 nerve projections relative to the cell injected with the marker dye. This will allow us to confirm if the light-evoked response recoded from an impaled myenteric cell is due to direct or indirect innervation of eYFP/ChR2 nerve projections that originate from a subpopulation of cholinergic interneuron.

Regardless, similar to the discussion portion regarding AAV vectors, as more cell-specific promoters are discovered, and used to drive optogenetic actuators expression in enteric cell

populations either by viral delivery or the use of transgenic animal models, the closer we will get to deciphering the enteric circuit of the gut. Figure 6.1 shows a summary of the findings.

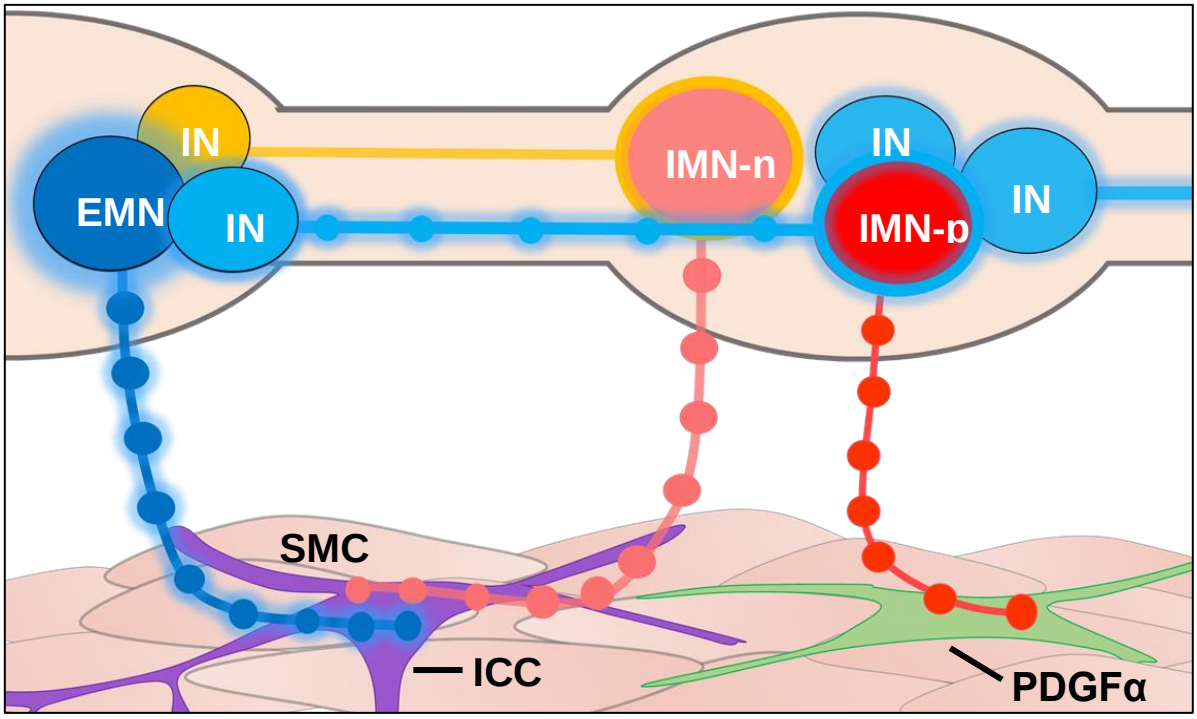

Figure 6.1: Alternative model of GI motility. The purinergic ir marker, VNUT, resides in nerve fibers and not inside the soma of cells, and is not observed co-localized with any other myenteric cell population in the GI tract (Chapter 3). Optogenetic stimulation of neurons using established AAV9-Nos1-ChR2-eYFP and Nos1-ROSA-eYFP mice revealed a biphasic IJP response. However, IHC analysis shows that ChR2 is ectopically expressed in non-NOS ir neurons (Chapter 4). Conversely, optogenetic stimulation of cholinergic neurons using ChAT-ChR2-YFP-BAC transgenic mice induced both EJP and IJP responses that were predominately cholinergic and purinergic-mediated responses, respectively (Chapter 5). Thus, completion of the studies discussed in this dissertation provides an alternative model of myenteric neurotransmission: Cholinergic EMNs (dark blue) and nitrergic IMNs (IMN-n; rose) predominately innervate ICCs (e.g. ICC_{DMP} and ICC_{IM}; purple) (Wang *et al.*, 2003), while purinergic IMNs (IMN-p; red) innervate PDGFα+ cells (light green) which abundantly express the purinergic $P2Y_1$ receptor (Kurahashi *et al.*, 2014). Together, SMCs, PDGFα+ cells, and ICC-IM cells make up the SIP syncytium and are electrically coupled via gap junctions (Figure 1.9). As a result, conductive changes in any of these interstitial cells leads to changes in syncytial input resistance and regulation of smooth muscle excitability (Kurahashi *et al.*, 2014). In addition, cholinergic descending interneurons (light blue) predominantly innervate and activate IMN-p to induce an fIJP, while the sIJP response could result from purinergic or mixed cholinergic/purinergic descending interneuron activity (LePard *et al.*, 1999)

REFERENCES

REFERENCES

Aad G, Abajyan T, Abbott B, Abdallah J, Khalek SA, Abdinov O*, et al.* (2014). Electron reconstruction and identification efficiency measurements with the ATLAS detector using the 2011 LHC proton-proton collision data. *The European physical journal. C, Particles and fields* **74**(7)**:** 2941.

Abazov VM, Abbott B, Abolins M, Acharya BS, Adams M, Adams T*, et al.* (2006). Measurement of the Bs(0) lifetime using semileptonic decays. *Physical review letters* **97**(24)**:** 241801.

Aeberhard PF, Magnenat LD, Zimmermann WA (1980). Nervous control of migratory myoelectric complex of the small bowel. *The American journal of physiology* **238**(2)**:** G102-108.

Alberti E, Mikkelsen HB, Wang XY, Diaz M, Larsen JO, Huizinga JD*, et al.* (2007). Pacemaker activity and inhibitory neurotransmission in the colon of Ws/Ws mutant rats. *American journal of physiology. Gastrointestinal and liver physiology* **292**(6)**:** G1499-1510.

Allen BD, Singer AC, Boyden ES (2015). Principles of designing interpretable optogenetic behavior experiments. *Learn Mem* **22**(4)**:** 232-238.

Alvarez WC, Mahoney LJ (1922). Action currents in stomach and intestine. *American Journal of Physiology* **58**(3)**:** 476-493.

Andrae J, Gallini R, Betsholtz C (2008). Role of platelet-derived growth factors in physiology and medicine. *Genes & development* **22**(10)**:** 1276-1312.

Andrews PL, Grundy D, Scratcherd T (1980). Reflex excitation of antral motility induced by gastric distension in the ferret. *The Journal of physiology* **298:** 79-84.

Antonioli L, Colucci R, Pellegrini C, Giustarini G, Tuccori M, Blandizzi C*, et al.* (2013). The role of purinergic pathways in the pathophysiology of gut diseases: pharmacological modulation and potential therapeutic applications. *Pharmacology & therapeutics* **139**(2)**:** 157-188.

Balakrishnan B, Jayandharan GR (2014). Basic biology of adeno-associated virus (AAV) vectors used in gene therapy. *Current gene therapy* **14**(2)**:** 86-100.

Bamann C, Gueta R, Kleinlogel S, Nagel G, Bamberg E (2010). Structural guidance of the photocycle of channelrhodopsin-2 by an interhelical hydrogen bond. *Biochemistry* **49**(2)**:** 267-278.

Bamann C, Kirsch T, Nagel G, Bamberg E (2008). Spectral characteristics of the photocycle of channelrhodopsin-2 and its implication for channel function. *Journal of molecular biology* **375**(3)**:** 686-694.

Basner-Tschakarjan E, Mingozzi F (2014). Cell-Mediated Immunity to AAV Vectors, Evolving Concepts and Potential Solutions. *Frontiers in immunology* **5:** 350.

Bassotti G, Gaburri M (1988). Manometric investigation of high-amplitude propagated contractile activity of the human colon. *The American journal of physiology* **255**(5 Pt 1)**:** G660-664.

Bayliss WM, Starling EH (1899). The movements and innervation of the small intestine. *The Journal of physiology* **24**(2)**:** 99-143.

Belle MD, Pattison EF, Cheunsuang O, Stewart A, Kramer I, Sigrist M*, et al.* (2007). Characterization of a thy1.2 GFP transgenic mouse reveals a tissue-specific organization of the spinal dorsal horn. *Genesis* **45**(11)**:** 679-688.

Benskey MJ, Kuhn NC, Galligan JJ, Garcia J, Boye SE, Hauswirth WW*, et al.* (2015a). Targeted gene delivery to the enteric nervous system using AAV: a comparison across serotypes and capsid mutants. *Molecular Therapy* **23**(3)**:** 488-500.

Benskey MJ, Kuhn NC, Galligan JJ, Garcia J, Boye SE, Hauswirth WW*, et al.* (2015b). Targeted gene delivery to the enteric nervous system using AAV: a comparison across serotypes and capsid mutants. *Molecular therapy : the journal of the American Society of Gene Therapy* **23**(3)**:** 488-500.

Bertrand PP (2004). Real-time detection of serotonin release from enterochromaffin cells of the guinea-pig ileum. *Neurogastroenterology and motility : the official journal of the European Gastrointestinal Motility Society* **16**(5)**:** 511-514.

Bertrand PP, Bornstein JC (2002). ATP as a putative sensory mediator: activation of intrinsic sensory neurons of the myenteric plexus via P2X receptors. *The Journal of neuroscience : the official journal of the Society for Neuroscience* **22**(12)**:** 4767-4775.

Bertrand PP, Kunze WA, Bornstein JC, Furness JB, Smith ML (1997). Analysis of the responses of myenteric neurons in the small intestine to chemical stimulation of the mucosa. *The American journal of physiology* **273**(2 Pt 1)**:** G422-435.

Bertrand PP, Kunze WA, Furness JB, Bornstein JC (2000). The terminals of myenteric intrinsic primary afferent neurons of the guinea-pig ileum are excited by 5-hydroxytryptamine acting at 5-hydroxytryptamine-3 receptors. *Neuroscience* **101**(2)**:** 459-469.

Bharucha AE (2012). High amplitude propagated contractions. *Neurogastroenterology and motility : the official journal of the European Gastrointestinal Motility Society* **24**(11)**:** 977-982.

Bi A, Cui J, Ma YP, Olshevskaya E, Pu M, Dizhoor AM*, et al.* (2006). Ectopic expression of a microbial-type rhodopsin restores visual responses in mice with photoreceptor degeneration. *Neuron* **50**(1)**:** 23-33.

Bian X, Galligan JJ (2007). Alpha2-adrenoceptors couple to inhibition of R-type calcium currents in myenteric neurons. *Neurogastroenterology and motility : the official journal of the European Gastrointestinal Motility Society* **19**(10)**:** 845-855.

Blair PJ, Bayguinov Y, Sanders KM, Ward SM (2012). Relationship between enteric neurons and interstitial cells in the primate gastrointestinal tract. *Neurogastroenterology and motility : the official journal of the European Gastrointestinal Motility Society* **24**(9)**:** e437-449.

Boesmans W, Hao MM, Vanden Berghe P (2015). Optical Tools to Investigate Cellular Activity in the Intestinal Wall. *Journal of neurogastroenterology and motility* **21**(3)**:** 337-351.

Bornstein JC (2008). Purinergic mechanisms in the control of gastrointestinal motility. *Purinergic signalling* **4**(3)**:** 197-212.

Bornstein JC (2012). Serotonin in the gut: what does it do? *Frontiers in neuroscience* **6:** 16.

Bornstein JC, Costa M, Furness JB, Lees GM (1984). Electrophysiology and enkephalin immunoreactivity of identified myenteric plexus neurones of guinea-pig small intestine. *The Journal of physiology* **351:** 313-325.

Bornstein JC, Furness JB, Costa M (1989). An electrophysiological comparison of substance P-immunoreactive neurons with other neurons in the guinea-pig submucous plexus. *Journal of the autonomic nervous system* **26**(2)**:** 113-120.

Bornstein JC, Furness JB, Smith TK, Trussell DC (1991). Synaptic responses evoked by mechanical stimulation of the mucosa in morphologically characterized myenteric neurons of the guinea-pig ileum. *The Journal of neuroscience : the official journal of the Society for Neuroscience* **11**(2)**:** 505-518.

Boyden ES, Zhang F, Bamberg E, Nagel G, Deisseroth K (2005). Millisecond-timescale, genetically targeted optical control of neural activity. *Nature neuroscience* **8**(9)**:** 1263-1268.

Brehmer A, Schrodl F, Neuhuber W (1999). Morphological classifications of enteric neurons--100 years after Dogiel. *Anatomy and embryology* **200**(2)**:** 125-135.

Bridgewater M, Cunnane TC, Brading AF (1995). Characteristic features of inhibitory junction potentials evoked by single stimuli in the guinea-pig isolated taenia caeci. *The Journal of physiology* **485 (Pt 1):** 145-155.

Brookes SJ (2001). Classes of enteric nerve cells in the guinea-pig small intestine. *The Anatomical record* **262**(1)**:** 58-70.

Brookes SJ, Meedeniya AC, Jobling P, Costa M (1997). Orally projecting interneurones in the guinea-pig small intestine. *The Journal of physiology* **505 (Pt 2):** 473-491.

Brookes SJ, Steele PA, Costa M (1991). Calretinin immunoreactivity in cholinergic motor neurones, interneurones and vasomotor neurones in the guinea-pig small intestine. *Cell and tissue research* **263**(3)**:** 471-481.

Brookes SJH (1993). Neuronal Nitric-Oxide in the Gut. *J Gastroen Hepatol* **8**(6)**:** 590-603.

Bruegmann T, van Bremen T, Vogt CC, Send T, Fleischmann BK, Sasse P (2015). Optogenetic control of contractile function in skeletal muscle. *Nature communications* **6:** 7153.

Bueno L, Praddaude F, Ruckebusch Y (1979). Propagation of electrical spiking activity along the small intestine: intrinsic versus extrinsic neural influences. *The Journal of physiology* **292:** 15-26.

Bulbring E, Gershon MD (1968). Serotonin participation in the vagal inhibitory pathway to the stomach. *Advances in pharmacology* **6**(Pt A)**:** 323-333.

Burnstock G (2009). Purinergic cotransmission. *Experimental physiology* **94**(1)**:** 20-24.

Burnstock G (2014a). Purinergic signalling in endocrine organs. *Purinergic signalling* **10**(1)**:** 189-231.

Burnstock G (2014b). Purinergic signalling in the gastrointestinal tract and related organs in health and disease. *Purinergic signalling* **10**(1)**:** 3-50.

Bush TG, Spencer NJ, Watters N, Sanders KM, Smith TK (2000). Spontaneous migrating motor complexes occur in both the terminal ileum and colon of the C57BL/6 mouse in vitro. *Autonomic neuroscience : basic & clinical* **84**(3)**:** 162-168.

Bywater RA, Small RC, Taylor GS (1989). Neurogenic slow depolarizations and rapid oscillations in the membrane potential of circular muscle of mouse colon. *The Journal of physiology* **413:** 505-519.

Calcedo R, Morizono H, Wang L, McCarter R, He J, Jones D*, et al.* (2011). Adeno-associated virus antibody profiles in newborns, children, and adolescents. *Clinical and vaccine immunology : CVI* **18**(9)**:** 1586-1588.

Candell LM, Yun SH, Tran LL, Ehlert FJ (1990). Differential coupling of subtypes of the muscarinic receptor to adenylate cyclase and phosphoinositide hydrolysis in the longitudinal muscle of the rat ileum. *Molecular pharmacology* **38**(5)**:** 689-697.

Cannon WB (1911). The Mechanical Factors of Digestion. *Edward Arnold, London*.

Cannon WB (1898). The movements of the stomach studied by means of the Roentgen rays. *Am. J. Physiol* **1:** 359-382.

Caprette DR (1995). Chlamydomonas as a Model Organism Vol. 2019. Rice university Website.

Castelucci P, Robbins HL, Poole DP, Furness JB (2002). The distribution of purine P2X(2) receptors in the guinea-pig enteric nervous system. *Histochemistry and cell biology* **117**(5)**:** 415-422.

Castrichini M, Lazzerini PE, Gamberucci A, Capecchi PL, Franceschini R, Natale M*, et al.* (2014). The purinergic P2x7 receptor is expressed on monocytes in Behcet's disease and is modulated by TNF-alpha. *European journal of immunology* **44**(1)**:** 227-238.

Chaffiol A, Caplette R, Jaillard C, Brazhnikova E, Desrosiers M, Dubus E*, et al.* (2017). A New Promoter Allows Optogenetic Vision Restoration with Enhanced Sensitivity in Macaque Retina. *Molecular therapy : the journal of the American Society of Gene Therapy* **25**(11)**:** 2546-2560.

Chan KY, Jang MJ, Yoo BB, Greenbaum A, Ravi N, Wu WL*, et al.* (2017). Engineered AAVs for efficient noninvasive gene delivery to the central and peripheral nervous systems. *Nature neuroscience* **20**(8)**:** 1172-1179.

Chandler RJ, LaFave MC, Varshney GK, Trivedi NS, Carrillo-Carrasco N, Senac JS*, et al.* (2015). Vector design influences hepatic genotoxicity after adeno-associated virus gene therapy. *The Journal of clinical investigation* **125**(2)**:** 870-880.

Chandler RJ, Sands MS, Venditti CP (2017). Recombinant Adeno-Associated Viral Integration and Genotoxicity: Insights from Animal Models. *Human gene therapy* **28**(4)**:** 314-322.

Chandrasekharan B, Srinivasan S (2007). Diabetes and the enteric nervous system. *Neurogastroenterology and motility : the official journal of the European Gastrointestinal Motility Society* **19**(12)**:** 951-960.

Chang L, Lembo A, Sultan S (2014). American Gastroenterological Association Institute Technical Review on the pharmacological management of irritable bowel syndrome. *Gastroenterology* **147**(5)**:** 1149-1172 e1142.

Chevalier J, Derkinderen P, Gomes P, Thinard R, Naveilhan P, Vanden Berghe P*, et al.* (2008). Activity-dependent regulation of tyrosine hydroxylase expression in the enteric nervous system. *The Journal of physiology* **586**(7)**:** 1963-1975.

Christensen J, Anuras S, Hauser RL (1974). Migrating spike bursts and electrical slow waves in the cat colon: effect of sectioning. *Gastroenterology* **66**(2)**:** 240-247.

Clerc N, Furness JB, Bornstein JC, Kunze WA (1998). Correlation of electrophysiological and morphological characteristics of myenteric neurons of the duodenum in the guinea-pig. *Neuroscience* **82**(3)**:** 899-914.

Colella P, Ronzitti G, Mingozzi F (2018). Emerging Issues in AAV-Mediated In Vivo Gene Therapy. *Mol Ther-Meth Clin D* **8:** 87-104.

Cornelissen W, De Laet A, Kroese AB, Van Bogaert PP, Scheuermann DW, Timmermans JP (2000). Electrophysiological features of morphological Dogiel type II neurons in the myenteric plexus of pig small intestine. *Journal of neurophysiology* **84**(1)**:** 102-111.

Costa M, Brookes SJ, Steele PA, Gibbins I, Burcher E, Kandiah CJ (1996). Neurochemical classification of myenteric neurons in the guinea-pig ileum. *Neuroscience* **75**(3)**:** 949-967.

Costa M, Furness JB, Pompolo S, Brookes SJ, Bornstein JC, Bredt DS*, et al.* (1992). Projections and chemical coding of neurons with immunoreactivity for nitric oxide synthase in the guinea-pig small intestine. *Neuroscience letters* **148**(1-2)**:** 121-125.

Costa M, Furness JB, Pullin CO, Bornstein J (1985). Substance P enteric neurons mediate non-cholinergic transmission to the circular muscle of the guinea-pig intestine. *Naunyn-Schmiedeberg's archives of pharmacology* **328**(4)**:** 446-453.

Crist JR, He XD, Goyal RK (1992). Both ATP and the peptide VIP are inhibitory neurotransmitters in guinea-pig ileum circular muscle. *J Physiol* **447:** 119-131.

De Giorgio R, Sarnelli G, Corinaldesi R, Stanghellini V (2004). Advances in our understanding of the pathology of chronic intestinal pseudo-obstruction. *Gut* **53**(11)**:** 1549-1552.

Desai KM, Sessa WC, Vane JR (1991). Involvement of nitric oxide in the reflex relaxation of the stomach to accommodate food or fluid. *Nature* **351**(6326)**:** 477-479.

Dhaese I, Vanneste G, Sips P, Buys E, Brouckaert P, Lefebvre RA (2008). Involvement of soluble guanylate cyclase alpha(1) and alpha(2), and SK(Ca) channels in NANC relaxation of mouse distal colon. *Eur J Pharmacol* **589**(1-3)**:** 251-259.

Dhaese I, Vanneste G, Sips P, Buys ES, Brouckaert P, Lefebvre RA (2009). Small intestinal motility in soluble guanylate cyclase alpha1 knockout mice: (Jejunal phenotyping of sGCalpha1 knockout mice). *Naunyn-Schmiedeberg's archives of pharmacology* **379**(5)**:** 473-487.

Di Nardo G, Blandizzi C, Volta U, Colucci R, Stanghellini V, Barbara G*, et al.* (2008). Review article: molecular, pathological and therapeutic features of human enteric neuropathies. *Alimentary pharmacology & therapeutics* **28**(1)**:** 25-42.

Dickens EJ, Edwards FR, Hirst GD (2001). Selective knockout of intramuscular interstitial cells reveals their role in the generation of slow waves in mouse stomach. *The Journal of physiology* **531**(Pt 3)**:** 827-833.

Dickson EJ, Heredia DJ, McCann CJ, Hennig GW, Smith TK (2010a). The mechanisms underlying the generation of the colonic migrating motor complex in both wild-type and nNOS knockout mice. *American journal of physiology. Gastrointestinal and liver physiology* **298**(2)**:** G222-232.

Dickson EJ, Heredia DJ, Smith TK (2010b). Critical role of 5-HT1A, 5-HT3, and 5-HT7 receptor subtypes in the initiation, generation, and propagation of the murine colonic migrating motor complex. *American journal of physiology. Gastrointestinal and liver physiology* **299**(1)**:** G144-157.

Diezmos EF, Bertrand PP, Liu L (2016). Purinergic Signaling in Gut Inflammation: The Role of Connexins and Pannexins. *Frontiers in neuroscience* **10:** 311.

Diezmos EF, Sandow SL, Markus I, Shevy Perera D, Lubowski DZ, King DW*, et al.* (2013). Expression and localization of pannexin-1 hemichannels in human colon in health and disease. *Neurogastroenterology and motility : the official journal of the European Gastrointestinal Motility Society* **25**(6)**:** e395-405.

Diezmos EF, Sandow SL, Perera DS, King DW, Bertrand PP, Liu L (2015). Pannexin-2 is expressed in the human colon with extensive localization in the enteric nervous system. *Neurogastroenterology and motility : the official journal of the European Gastrointestinal Motility Society* **27**(5)**:** 672-683.

Dinning PG, Szczesniak M, Cook IJ (2006). Removal of tonic nitrergic inhibition is a potent stimulus for human proximal colonic propagating sequences. *Neurogastroenterology and motility : the official journal of the European Gastrointestinal Motility Society* **18**(1)**:** 37-44.

Dogiel A (1985). 1895b) Zur Frage über die Ganglion der Darmgefl echte bei den Säugetieren. *Anat. Anz.* **10:** 517-528.

Dogiel A (1989). Über den Bau der Ganglien in den Gefl echten des Darmes und der Gallenblase des Menschen und der Säugetiere. *Arch. Anat. Physiol. Leipzig Anat Abt Jg* **1899:** 130–158.

Donsante A, Miller DG, Li Y, Vogler C, Brunt EM, Russell DW*, et al.* (2007). AAV vector integration sites in mouse hepatocellular carcinoma. *Science* **317**(5837)**:** 477.

Doring B, Pfitzer G, Adam B, Liebregts T, Eckardt D, Holtmann G*, et al.* (2007). Ablation of connexin43 in smooth muscle cells of the mouse intestine: functional insights into physiology and morphology. *Cell and tissue research* **327**(2)**:** 333-342.

Doroudchi MM, Greenberg KP, Liu J, Silka KA, Boyden ES, Lockridge JA*, et al.* (2011). Virally delivered channelrhodopsin-2 safely and effectively restores visual function in multiple mouse models of blindness. *Molecular therapy : the journal of the American Society of Gene Therapy* **19**(7)**:** 1220-1229.

Drossman DA (2016). Functional gastrointestinal disorders: what's new for Rome IV? *The lancet. Gastroenterology & hepatology* **1**(1)**:** 6-8.

Drossman DA, Hasler WL (2016). Rome IV-Functional GI Disorders: Disorders of Gut-Brain Interaction. *Gastroenterology* **150**(6)**:** 1257-1261.

Dukowicz AC, Lacy BE, Levine GM (2007). Small intestinal bacterial overgrowth: a comprehensive review. *Gastroenterology & hepatology* **3**(2)**:** 112-122.

Dusdieker NS, Summers RW (1980). Longitudinal and Circumferential Spread of Spike Bursts in Canine Jejunum Invivo. *American Journal of Physiology* **239**(4)**:** G311-G318.

Eglen RM, Hegde SS, Watson N (1996). Muscarinic receptor subtypes and smooth muscle function. *Pharmacological reviews* **48**(4)**:** 531-565.

Ehlert FJ, Ostrom RS, Sawyer GW (1997). Subtypes of the muscarinic receptor in smooth muscle. *Life sciences* **61**(18)**:** 1729-1740.

Ehrlein HJ, Schemann M, Siegle ML (1987). Motor patterns of small intestine determined by closely spaced extraluminal transducers and videofluoroscopy. *The American journal of physiology* **253**(3 Pt 1)**:** G259-267.

El-Sharkawy TY, Markus H, Diamant NE (1982). Neural control of the intestinal migrating myoelectric complex. A pharmacological analysis. *Canadian journal of physiology and pharmacology* **60**(6)**:** 794-804.

el-Sharkawy TY, Morgan KG, Szurszewski JH (1978). Intracellular electrical activity of canine and human gastric smooth muscle. *The Journal of physiology* **279:** 291-307.

Evans RJ, Jiang MM, Surprenant A (1994). Morphological properties and projections of electrophysiologically characterized neurons in the guinea-pig submucosal plexus. *Neuroscience* **59**(4)**:** 1093-1110.

Everhart JE, Ruhl CE (2009). Burden of digestive diseases in the United States part II: lower gastrointestinal diseases. *Gastroenterology* **136**(3)**:** 741-754.

Fida R, Lyster DJ, Bywater RA, Taylor GS (1997). Colonic migrating motor complexes (CMMCs) in the isolated mouse colon. *Neurogastroenterology and motility : the official journal of the European Gastrointestinal Motility Society* **9**(2)**:** 99-107.

Flotte TR (2004). Gene therapy progress and prospects: recombinant adeno-associated virus (rAAV) vectors. *Gene therapy* **11**(10)**:** 805-810.

France M, Bhattarai Y, Galligan JJ, Xu H (2012). Impaired propulsive motility in the distal but not proximal colon of BK channel beta1-subunit knockout mice. *Neurogastroenterology and motility : the official journal of the European Gastrointestinal Motility Society* **24**(9)**:** e450-459.

Furness J (2006). *The enteric nervous system* edn.

Furness JB (2012). The enteric nervous system and neurogastroenterology. *Nature reviews. Gastroenterology & hepatology* **9**(5)**:** 286-294.

Furness JB (2000). Types of neurons in the enteric nervous system. *Journal of the autonomic nervous system* **81**(1-3)**:** 87-96.

Furness JB, Alex G, Clark MJ, Lal VV (2003). Morphologies and projections of defined classes of neurons in the submucosa of the guinea-pig small intestine. *The anatomical record. Part A, Discoveries in molecular, cellular, and evolutionary biology* **272**(2)**:** 475-483.

Furness JB, Costa M (1982). Neurons with 5-hydroxytryptamine-like immunoreactivity in the enteric nervous system: their projections in the guinea-pig small intestine. *Neuroscience* **7**(2)**:** 341-349.

Furness JB, Costa M, Keast JR (1984). Choline acetyltransferase- and peptide immunoreactivity of submucous neurons in the small intestine of the guinea-pig. *Cell and tissue research* **237**(2)**:** 329-336.

Furness JB, Jones C, Nurgali K, Clerc N (2004a). Intrinsic primary afferent neurons and nerve circuits within the intestine. *Progress in neurobiology* **72**(2)**:** 143-164.

Furness JB, Kearney K, Robbins HL, Hunne B, Selmer IS, Neylon CB*, et al.* (2004b). Intermediate conductance potassium (IK) channels occur in human enteric neurons. *Autonomic neuroscience : basic & clinical* **112**(1-2)**:** 93-97.

Furness JB, Pompolo S, Shuttleworth CW, Burleigh DE (1992). Light- and electron-microscopic immunochemical analysis of nerve fibre types innervating the taenia of the guinea-pig caecum. *Cell and tissue research* **270**(1)**:** 125-137.

Furness JB, Robbins HL, Xiao J, Stebbing MJ, Nurgali K (2004c). Projections and chemistry of Dogiel type II neurons in the mouse colon. *Cell and tissue research* **317**(1)**:** 1-12.

Futagami S, Yamawaki H, Agawa S, Higuchi K, Ikeda G, Noda H*, et al.* (2018). New classification Rome IV functional dyspepsia and subtypes. *Translational gastroenterology and hepatology* **3:** 70.

Gallego D, Gil V, Aleu J, Auli M, Clave P, Jimenez M (2008a). Purinergic and nitrergic junction potential in the human colon. *American journal of physiology. Gastrointestinal and liver physiology* **295**(3)**:** G522-533.

Gallego D, Gil V, Martinez-Cutillas M, Mane N, Martin MT, Jimenez M (2012). Purinergic neuromuscular transmission is absent in the colon of P2Y(1) knocked out mice. *The Journal of physiology* **590**(8)**:** 1943-1956.

Gallego D, Hernandez P, Clave P, Jimenez M (2006). P2Y1 receptors mediate inhibitory purinergic neuromuscular transmission in the human colon. *American journal of physiology. Gastrointestinal and liver physiology* **291**(4)**:** G584-594.

Gallego D, Vanden Berghe P, Farre R, Tack J, Jimenez M (2008b). P2Y1 receptors mediate inhibitory neuromuscular transmission and enteric neuronal activation in small intestine. *Neurogastroenterology and motility : the official journal of the European Gastrointestinal Motility Society* **20**(2)**:** 159-168.

Gallegos B, Martinez R, Perez L, Del Socorro Pina M, Perez E, Hernandez P (2014). Lectins in human pathogenic fungi. *Revista iberoamericana de micologia* **31**(1)**:** 72-75.

Galligan JJ (2002). Ligand-gated ion channels in the enteric nervous system. *Neurogastroent Motil* **14**(6)**:** 611-623.

Galligan JJ, Bertrand PP (1994). ATP mediates fast synaptic potentials in enteric neurons. *The Journal of neuroscience : the official journal of the Society for Neuroscience* **14**(12)**:** 7563-7571.

Galligan JJ, Costa M, Furness JB (1985a). Gastrointestinal Myoelectric Activity in Conscious Guinea-Pigs. *American Journal of Physiology* **249**(1)**:** G92-G99.

Galligan JJ, Costa M, Furness JB (1985b). Gastrointestinal myoelectric activity in conscious guinea pigs. *The American journal of physiology* **249**(1 Pt 1)**:** G92-99.

Galligan JJ, Furness JB, Costa M (1986). Effects of cholinergic blockade, adrenergic blockade and sympathetic denervation on gastrointestinal myoelectric activity in guinea pig. *The Journal of pharmacology and experimental therapeutics* **238**(3)**:** 1114-1125.

Galligan JJ, North RA (2004). Pharmacology and function of nicotinic acetylcholine and P2X receptors in the enteric nervous system. *Neurogastroenterology and motility : the official journal of the European Gastrointestinal Motility Society* **16 Suppl 1:** 64-70.

Gershon MD (2012). Serotonin is a sword and a shield of the bowel: serotonin plays offense and defense. *Transactions of the American Clinical and Climatological Association* **123:** 268-280; discussion 280.

Giaroni C, Knight GE, Ruan HZ, Glass R, Bardini M, Lecchini S*, et al.* (2002). P2 receptors in the murine gastrointestinal tract. *Neuropharmacology* **43**(8)**:** 1313-1323.

Gibbons SJ, De Giorgio R, Faussone Pellegrini MS, Garrity-Park MM, Miller SM, Schmalz PF*, et al.* (2009). Apoptotic cell death of human interstitial cells of Cajal. *Neurogastroenterology and motility : the official journal of the European Gastrointestinal Motility Society* **21**(1)**:** 85-93.

Gil-Farina I, Fronza R, Kaeppel C, Lopez-Franco E, Ferreira V, D'Avola D*, et al.* (2016). Recombinant AAV Integration Is Not Associated With Hepatic Genotoxicity in Nonhuman Primates and Patients. *Molecular therapy : the journal of the American Society of Gene Therapy* **24**(6)**:** 1100-1105.

Gil V, Gallego D, Grasa L, Martin MT, Jimenez M (2010). Purinergic and nitrergic neuromuscular transmission mediates spontaneous neuronal activity in the rat colon. *American journal of physiology. Gastrointestinal and liver physiology* **299**(1)**:** G158-169.

Gombash SE (2015). Adeno-Associated Viral Vector Delivery to the Enteric Nervous System: A Review. *Postdoc journal : a journal of postdoctoral research and postdoctoral affairs* **3**(8)**:** 1-12.

Goyal RK, Hirano I (1996). The enteric nervous system. *The New England journal of medicine* **334**(17)**:** 1106-1115.

Grasa L, Gil V, Gallego D, Martin MT, Jimenez M (2009). P2Y(1) receptors mediate inhibitory neuromuscular transmission in the rat colon. *British journal of pharmacology* **158**(6)**:** 1641-1652.

Gray JT, Zolotukhin S (2011). Design and construction of functional AAV vectors. *Methods Mol Biol* **807:** 25-46.

Grider JR (2003). Reciprocal activity of longitudinal and circular muscle during intestinal peristaltic reflex. *American journal of physiology. Gastrointestinal and liver physiology* **284**(5)**:** G768-775.

Grider JR (1989). Tachykinins as transmitters of ascending contractile component of the peristaltic reflex. *The American journal of physiology* **257**(5 Pt 1)**:** G709-714.

Grider JR, Kuemmerle JF, Jin JG (1996). 5-HT released by mucosal stimuli initiates peristalsis by activating 5-HT4/5-HT1p receptors on sensory CGRP neurons. *Am J Physiol-Gastr L* **270**(5)**:** G778-G782.

Grote M, Engelhard M, Hegemann P (2014). Of ion pumps, sensors and channels - Perspectives on microbial rhodopsins between science and history. *Bba-Bioenergetics* **1837**(5)**:** 533-545.

Gulbransen BD, Bashashati M, Hirota SA, Gui X, Roberts JA, MacDonald JA*, et al.* (2012a). Activation of neuronal P2X7 receptor-pannexin-1 mediates death of enteric neurons during colitis. *Nature medicine* **18**(4)**:** 600-604.

Gulbransen BD, Bashashati M, Hirota SA, Gui XY, Roberts JA, MacDonald JA*, et al.* (2012b). Activation of neuronal P2X7 receptor-pannexin-1 mediates death of enteric neurons during colitis. *Nature medicine* **18**(4)**:** 600-604.

Guo R, Nada O, Suita S, Taguchi T, Masumoto K (1997). The distribution and co-localization of nitric oxide synthase and vasoactive intestinal polypeptide in nerves of the colons with Hirschsprung's disease. *Virchows Archiv : an international journal of pathology* **430**(1)**:** 53-61.

Gwynne RM, Bornstein JC (2007). Local inhibitory reflexes excited by mucosal application of nutrient amino acids in guinea pig jejunum. *American journal of physiology. Gastrointestinal and liver physiology* **292**(6)**:** G1660-1670.

Han X, Boyden ES (2007). Multiple-color optical activation, silencing, and desynchronization of neural activity, with single-spike temporal resolution. *PloS one* **2**(3)**:** e299.

Hastie E, Samulski RJ (2015). Adeno-associated virus at 50: a golden anniversary of discovery, research, and gene therapy success--a personal perspective. *Human gene therapy* **26**(5)**:** 257-265.

Hegemann P, Gartner W, Uhl R (1991). All-trans retinal constitutes the functional chromophore in Chlamydomonas rhodopsin. *Biophysical journal* **60**(6)**:** 1477-1489.

Hendriks R, Bornstein JC, Furness JB (1990). An electrophysiological study of the projections of putative sensory neurons within the myenteric plexus of the guinea pig ileum. *Neuroscience letters* **110**(3)**:** 286-290.

Hennig GW, Brookes SJ, Costa M (1997). Excitatory and inhibitory motor reflexes in the isolated guinea-pig stomach. *The Journal of physiology* **501 (Pt 1):** 197-212.

Heredia DJ, Dickson EJ, Bayguinov PO, Hennig GW, Smith TK (2009). Localized release of serotonin (5-hydroxytryptamine) by a fecal pellet regulates migrating motor complexes in murine colon. *Gastroenterology* **136**(4)**:** 1328-1338.

Heredia DJ, Gershon MD, Koh SD, Corrigan RD, Okamoto T, Smith TK (2013). Important role of mucosal serotonin in colonic propulsion and peristaltic reflexes: in vitro analyses in mice lacking tryptophan hydroxylase 1. *The Journal of physiology* **591**(23)**:** 5939-5957.

Heredia DJ, Grainger N, McCann CJ, Smith TK (2012). Insights from a novel model of slow-transit constipation generated by partial outlet obstruction in the murine large intestine. *American journal of physiology. Gastrointestinal and liver physiology* **303**(9)**:** G1004-1016.

Hibberd TJ, Feng J, Luo J, Yang P, Samineni VK, Gereau RWt*, et al.* (2018). Optogenetic Induction of Colonic Motility in Mice. *Gastroenterology* **155**(2)**:** 514-528 e516.

Hill RA, Tong L, Yuan P, Murikinati S, Gupta S, Grutzendler J (2015). Regional Blood Flow in the Normal and Ischemic Brain Is Controlled by Arteriolar Smooth Muscle Cell Contractility and Not by Capillary Pericytes. *Neuron* **87**(1)**:** 95-110.

Hirst GD, Holman ME, Spence I (1974). Two types of neurones in the myenteric plexus of duodenum in the guinea-pig. *The Journal of physiology* **236**(2)**:** 303-326.

Hirst GD, Johnson SM, van Helden DF (1985). The slow calcium-dependent potassium current in a myenteric neurone of the guinea-pig ileum. *The Journal of physiology* **361:** 315-337.

Hirst GD, Spence I (1973). Calcium action potentials in mammalian peripheral neurones. *Nature: New biology* **243**(123)**:** 54-56.

Hirst GD, Ward SM (2003). Interstitial cells: involvement in rhythmicity and neural control of gut smooth muscle. *The Journal of physiology* **550**(Pt 2)**:** 337-346.

Hoess RH, Wierzbicki A, Abremski K (1986). The role of the loxP spacer region in P1 site-specific recombination. *Nucleic acids research* **14**(5)**:** 2287-2300.

Hoque MR, Ishizuka T, Inoue K, Abe-Yoshizumi R, Igarashi H, Mishima T*, et al.* (2016). A Chimera Na+-Pump Rhodopsin as an Effective Optogenetic Silencer. *PloS one* **11**(11)**:** e0166820.

Horiguchi K, Komuro T (2000). Ultrastructural observations of fibroblast-like cells forming gap junctions in the W/W(nu) mouse small intestine. *Journal of the autonomic nervous system* **80**(3)**:** 142-147.

Huang Q, Zhou D, DiFiglia M (1992). Neurobiotin, a useful neuroanatomical tracer for in vivo anterograde, retrograde and transneuronal tract-tracing and for in vitro labeling of neurons. *Journal of neuroscience methods* **41**(1)**:** 31-43.

Huizinga JD, Thuneberg L, Kluppel M, Malysz J, Mikkelsen HB, Bernstein A (1995). W/kit gene required for interstitial cells of Cajal and for intestinal pacemaker activity. *Nature* **373**(6512)**:** 347-349.

Iino S, Horiguchi K, Horiguchi S, Nojyo Y (2009a). c-Kit-negative fibroblast-like cells express platelet-derived growth factor receptor alpha in the murine gastrointestinal musculature. *Histochemistry and cell biology* **131**(6)**:** 691-702.

Iino S, Horiguchi K, Nojyo Y, Ward SM, Sanders KM (2009b). Interstitial cells of Cajal contain signalling molecules for transduction of nitrergic stimulation in guinea pig caecum. *Neurogastroenterology and motility : the official journal of the European Gastrointestinal Motility Society* **21**(5)**:** 542-550, e512-543.

Iino S, Nojyo Y (2009c). Immunohistochemical demonstration of c-Kit-negative fibroblast-like cells in murine gastrointestinal musculature. *Archives of histology and cytology* **72**(2)**:** 107-115.

Il Park S, Brenner DS, Shin G, Morgan CD, Copits BA, Chung HU*, et al.* (2015). Soft, stretchable, fully implantable miniaturized optoelectronic systems for wireless optogenetics. *Nature biotechnology* **33**(12)**:** 1280-+.

Inadomi JM, Fennerty MB, Bjorkman D (2003). Systematic review: the economic impact of irritable bowel syndrome. *Alimentary pharmacology & therapeutics* **18**(7)**:** 671-682.

Inoue K, Tsuda M, Koizumi S (2004). ATP- and adenosine-mediated signaling in the central nervous system: chronic pain and microglia: involvement of the ATP receptor P2X4. *Journal of pharmacological sciences* **94**(2)**:** 112-114.

Irvin JL, Irvin EM (1954). The Interaction of Quinacrine with Adenine Nucleotides. *J Biol Chem* **210**(1)**:** 45-56.

Ishizuka T, Kakuda M, Araki R, Yawo H (2006). Kinetic evaluation of photosensitivity in genetically engineered neurons expressing green algae light-gated channels. *Neuroscience research* **54**(2)**:** 85-94.

Ivancheva C, Itzev D, Radomirov R (2000). Functional antagonism between nitric oxide and ATP in the motor responses of guinea-pig ileum. *Journal of autonomic pharmacology* **20**(3)**:** 147-156.

Iyer V, Bornstein JC, Costa M, Furness JB, Takahashi Y, Iwanaga T (1988). Electrophysiology of guinea-pig myenteric neurons correlated with immunoreactivity for calcium binding proteins. *Journal of the autonomic nervous system* **22**(2)**:** 141-150.

Jia Z, Valiunas V, Lu Z, Bien H, Liu H, Wang HZ*, et al.* (2011). Stimulating cardiac muscle by light: cardiac optogenetics by cell delivery. *Circulation. Arrhythmia and electrophysiology* **4**(5)**:** 753-760.

Jiang Y, Dong H, Eckmann L, Hanson EM, Ihn KC, Mittal RK (2017). Visualizing the enteric nervous system using genetically engineered double reporter mice: Comparison with immunofluorescence. *PloS one* **12**(2)**:** e0171239.

Johnson PJ, Bornstein JC, Yuan SY, Furness JB (1996). Analysis of contributions of acetylcholine and tachykinins to neuro-neuronal transmission in motility reflexes in the guinea-pig ileum. *British journal of pharmacology* **118**(4)**:** 973-983.

Johnson PJ, Shum OR, Thornton PD, Bornstein JC (1999a). Evidence that inhibitory motor neurons of the guinea-pig small intestine exhibit fast excitatory synaptic potentials mediated via P2X receptors. *Neuroscience letters* **266**(3)**:** 169-172.

Johnson PJ, Shum OR, Thornton PDJ, Bornstein JC (1999b). Evidence that inhibitory motor neurons of the guinea-pig small intestine exhibit fast excitatory synaptic potentials mediated via P-2X receptors. *Neuroscience letters* **266**(3)**:** 169-172.

Kellow JE, Borody TJ, Phillips SF, Tucker RL, Haddad AC (1986). Human interdigestive motility: variations in patterns from esophagus to colon. *Gastroenterology* **91**(2)**:** 386-395.

Kelly KACCFE, L.R. (1969). Patterns of canine gastric electrical activity. *Am. J. Physiol* **217:** 461-470.

Kirchgessner AL, Liu MT (1999). Differential localization of Ca2+ channel alpha1 subunits in the enteric nervous system: presence of alpha1B channel-like immunoreactivity in intrinsic primary afferent neurons. *The Journal of comparative neurology* **409**(1)**:** 85-104.

Kirchgessner AL, Liu MT, Raymond JR, Gershon MD (1996). Identification of cells that express 5-hydroxytryptamine1A receptors in the nervous systems of the bowel and pancreas. *The Journal of comparative neurology* **364**(3)**:** 439-455.

Kirchgessner AL, Tamir H, Gershon MD (1992). Identification and stimulation by serotonin of intrinsic sensory neurons of the submucosal plexus of the guinea pig gut: activity-induced expression of Fos immunoreactivity. *The Journal of neuroscience : the official journal of the Society for Neuroscience* **12**(1)**:** 235-248.

Kito Y, Suzuki H (2003). Pacemaker frequency is increased by sodium nitroprusside in the guinea pig gastric antrum. *The Journal of physiology* **546**(Pt 1)**:** 191-205.

Klein S, Seidler B, Kettenberger A, Sibaev A, Rohn M, Feil R*, et al.* (2013). Interstitial cells of Cajal integrate excitatory and inhibitory neurotransmission with intestinal slow-wave activity. *Nature communications* **4:** 1630.

Kohler N, Lipton A (1974). Platelets as a source of fibroblast growth-promoting activity. *Experimental cell research* **87**(2)**:** 297-301.

Kolisnyk B, Guzman MS, Raulic S, Fan J, Magalhaes AC, Feng G*, et al.* (2013). ChAT-ChR2-EYFP mice have enhanced motor endurance but show deficits in attention and several additional cognitive domains. *The Journal of neuroscience : the official journal of the Society for Neuroscience* **33**(25)**:** 10427-10438.

Komuro T, Seki K, Horiguchi K (1999). Ultrastructural characterization of the interstitial cells of Cajal. *Archives of histology and cytology* **62**(4)**:** 295-316.

Kruis W, Thieme C, Weinzierl M, Schussler P, Holl J, Paulus W (1984). A diagnostic score for the irritable bowel syndrome. Its value in the exclusion of organic disease. *Gastroenterology* **87**(1)**:** 1-7.

Kunze WA, Bornstein JC, Furness JB (1995). Identification of sensory nerve cells in a peripheral organ (the intestine) of a mammal. *Neuroscience* **66**(1)**:** 1-4.

Kurahashi M, Mutafova-Yambolieva V, Koh SD, Sanders KM (2014). Platelet-derived growth factor receptor-alpha-positive cells and not smooth muscle cells mediate purinergic hyperpolarization in murine colonic muscles. *American journal of physiology. Cell physiology* **307**(6)**:** C561-570.

Kurahashi M, Zheng H, Dwyer L, Ward SM, Koh SD, Sanders KM (2011). A functional role for the 'fibroblast-like cells' in gastrointestinal smooth muscles. *The Journal of physiology* **589**(Pt 3)**:** 697-710.

Langley JN (1921). *The Autonomic nervous system* edn. Cambridge, W. Heffer & Sons LTD.

Lawrentjew B (1931). Zur Lehre von der Cytoarchitektonik des peripheren autonomen Nervensystems. *Anat. Forsch.* **23:** 527–551.

Lawson MA, Zacks DN, Derguini F, Nakanishi K, Spudich JL (1991). Retinal analog restoration of photophobic responses in a blind Chlamydomonas reinhardtii mutant. Evidence for an archaebacterial like chromophore in a eukaryotic rhodopsin. *Biophysical journal* **60**(6)**:** 1490-1498.

LePard KJ, Galligan JJ (1999). Analysis of fast synaptic pathways in myenteric plexus of guinea pig ileum. *The American journal of physiology* **276**(2)**:** G529-538.

LePard KJ, Messori E, Galligan JJ (1997). Purinergic fast excitatory postsynaptic potentials in myenteric neurons of guinea pig: distribution and pharmacology. *Gastroenterology* **113**(5)**:** 1522-1534.

Li X, Gutierrez DV, Hanson MG, Han J, Mark MD, Chiel H*, et al.* (2005). Fast noninvasive activation and inhibition of neural and network activity by vertebrate rhodopsin and green algae channelrhodopsin. *Proceedings of the National Academy of Sciences of the United States of America* **102**(49)**:** 17816-17821.

Li ZS, Furness JB (1998). Immunohistochemical localisation of cholinergic markers in putative intrinsic primary afferent neurons of the guinea-pig small intestine. *Cell and tissue research* **294**(1)**:** 35-43.

Li ZS, Pham TD, Tamir H, Chen JJ, Gershon MD (2004). Enteric dopaminergic neurons: definition, developmental lineage, and effects of extrinsic denervation. *The Journal of neuroscience : the official journal of the Society for Neuroscience* **24**(6)**:** 1330-1339.

Liu J, Prosser CL, Job DD (1969). Ionic dependence of slow waves and spikes in intestinal muscle. *The American journal of physiology* **217**(5)**:** 1542-1547.

Liu X, Ramirez S, Pang PT, Puryear CB, Govindarajan A, Deisseroth K*, et al.* (2012). Optogenetic stimulation of a hippocampal engram activates fear memory recall. *Nature* **484**(7394)**:** 381-385.

Lock M, Alvira M, Vandenberghe LH, Samanta A, Toelen J, Debyser Z*, et al.* (2010). Rapid, simple, and versatile manufacturing of recombinant adeno-associated viral vectors at scale. *Human gene therapy* **21**(10)**:** 1259-1271.

Locovei S, Bao L, Dahl G (2006). Pannexin 1 in erythrocytes: function without a gap. *Proceedings of the National Academy of Sciences of the United States of America* **103**(20)**:** 7655-7659.

Lohman AW, Isakson BE (2014). Differentiating connexin hemichannels and pannexin channels in cellular ATP release. *FEBS letters* **588**(8)**:** 1379-1388.

Lomax AE, Bertrand PP, Furness JB (2001). Electrophysiological characteristics distinguish three classes of neuron in submucosal ganglia of the guinea-pig distal colon. *Neuroscience* **103**(1)**:** 245-255.

Lomax AE, Sharkey KA, Bertrand PP, Low AM, Bornstein JC, Furness JB (1999). Correlation of morphology, electrophysiology and chemistry of neurons in the myenteric plexus of the guinea-pig distal colon. *Journal of the autonomic nervous system* **76**(1)**:** 45-61.

Lucas KA, Pitari GM, Kazerounian S, Ruiz-Stewart I, Park J, Schulz S*, et al.* (2000). Guanylyl cyclases and signaling by cyclic GMP. *Pharmacological reviews* **52**(3)**:** 375-414.

Lyster DJ, Bywater RA, Taylor GS (1995). Neurogenic control of myoelectric complexes in the mouse isolated colon. *Gastroenterology* **108**(5)**:** 1371-1378.

Magnus R (1904). Versuche am überlebenden Dünndarm von Säugethieren. I.Miltheilung. *Pflüger's Archiv ges Physiol.* **102:** 123–151.

Mane N, Gil V, Martinez-Cutillas M, Clave P, Gallego D, Jimenez M (2014). Differential functional role of purinergic and nitrergic inhibitory cotransmitters in human colonic relaxation. *Acta Physiol (Oxf)* **212**(4)**:** 293-305.

Mann PT, Southwell BR, Young HM, Furness JB (1997). Appositions made by axons of descending interneurons in the guinea-pig small intestine, investigated by confocal microscopy. *Journal of chemical neuroanatomy* **12**(3)**:** 151-164.

Manning AP, Thompson WG, Heaton KW, Morris AF (1978). Towards positive diagnosis of the irritable bowel. *British medical journal* **2**(6138)**:** 653-654.

Manno CS, Pierce GF, Arruda VR, Glader B, Ragni M, Rasko JJ*, et al.* (2006). Successful transduction of liver in hemophilia by AAV-Factor IX and limitations imposed by the host immune response. *Nature medicine* **12**(3)**:** 342-347.

Marik F, Code CF (1975). Control of the interdigestive myoelectric activity in dogs by the vagus nerves and pentagastrin. *Gastroenterology* **69**(2)**:** 387-395.

Marlett JA, Code CF (1979). Effects of celiac and superior mesenteric ganglionectomy on interdigestive myoelectric complex in dogs. *The American journal of physiology* **237**(5)**:** E432-443.

Martinez FJ, Marquez A, Gallego S, Frances J, Pascual I, Belendez A (2014a). Retardance and flicker modeling and characterization of electro-optic linear retarders by averaged Stokes polarimetry. *Optics letters* **39**(4)**:** 1011-1014.

Martinez FJ, Marquez A, Gallego S, Ortuno M, Frances J, Belendez A*, et al.* (2014b). Averaged Stokes polarimetry applied to evaluate retardance and flicker in PA-LCoS devices. *Optics express* **22**(12)**:** 15064-15074.

Martinez R, Figueroa D, Calvo R, Conget P, Gallegos M, Figueroa F*, et al.* (2015). [Osteochodral lesion mouse model: an alternative for experimental work]. *Revista espanola de cirugia ortopedica y traumatologia* **59**(1)**:** 9-13.

Masuda T, Ozono Y, Mikuriya S, Kohro Y, Tozaki-Saitoh H, Iwatsuki K*, et al.* (2016). Dorsal horn neurons release extracellular ATP in a VNUT-dependent manner that underlies neuropathic pain. *Nature communications* **7:** 12529.

Matini P, Faussone-Pellegrini MS, Cortesini C, Mayer B (1995). Vasoactive intestinal polypeptide and nitric oxide synthase distribution in the enteric plexuses of the human colon: an histochemical study and quantitative analysis. *Histochemistry and cell biology* **103**(6)**:** 415-423.

Matsuyama H, Tanahashi Y, Kitazawa T, Yamada M, Komori S, Unno T (2013). Evidence for M2 and M3 muscarinic receptor involvement in cholinergic excitatory junction potentials through synergistic activation of cation channels in the longitudinal muscle of mouse ileum. *Journal of pharmacological sciences* **121**(3)**:** 227-236.

Mawe GM, Hoffman JM (2013). Serotonin signalling in the gut--functions, dysfunctions and therapeutic targets. *Nature reviews. Gastroenterology & hepatology* **10**(8)**:** 473-486.

Mays LE, Wang L, Lin J, Bell P, Crawford A, Wherry EJ*, et al.* (2014). AAV8 induces tolerance in murine muscle as a result of poor APC transduction, T cell exhaustion, and minimal MHCI upregulation on target cells. *Molecular therapy : the journal of the American Society of Gene Therapy* **22**(1)**:** 28-41.

McClain J, Grubisic V, Fried D, Gomez-Suarez RA, Leinninger GM, Sevigny J*, et al.* (2014). Ca2+ responses in enteric glia are mediated by connexin-43 hemichannels and modulate colonic transit in mice. *Gastroenterology* **146**(2)**:** 497-507 e491.

Mingozzi F, High KA (2011). Therapeutic in vivo gene transfer for genetic disease using AAV: progress and challenges. *Nature reviews. Genetics* **12**(5)**:** 341-355.

Mingozzi F, Maus MV, Hui DJ, Sabatino DE, Murphy SL, Rasko JE*, et al.* (2007). CD8(+) T-cell responses to adeno-associated virus capsid in humans. *Nature medicine* **13**(4)**:** 419-422.

Mingozzi F, Meulenberg JJ, Hui DJ, Basner-Tschakarjan E, Hasbrouck NC, Edmonson SA*, et al.* (2009). AAV-1-mediated gene transfer to skeletal muscle in humans results in dose-dependent activation of capsid-specific T cells. *Blood* **114**(10)**:** 2077-2086.

Montgomery KL, Yeh AJ, Ho JS, Tsao V, Mohan Iyer S, Grosenick L*, et al.* (2015). Wirelessly powered, fully internal optogenetics for brain, spinal and peripheral circuits in mice. *Nature methods* **12**(10)**:** 969-974.

Nagel G, Ollig D, Fuhrmann M, Kateriya S, Musti AM, Bamberg E*, et al.* (2002). Channelrhodopsin-1: a light-gated proton channel in green algae. *Science* **296**(5577)**:** 2395-2398.

Nagel G, Szellas T, Huhn W, Kateriya S, Adeishvili N, Berthold P*, et al.* (2003). Channelrhodopsin-2, a directly light-gated cation-selective membrane channel. *Proceedings of the National Academy of Sciences of the United States of America* **100**(24)**:** 13940-13945.

Nagy PM, Aubert I (2012). Overexpression of the vesicular acetylcholine transporter increased acetylcholine release in the hippocampus. *Neuroscience* **218:** 1-11.

Nakai H, Montini E, Fuess S, Storm TA, Grompe M, Kay MA (2003). AAV serotype 2 vectors preferentially integrate into active genes in mice. *Nature genetics* **34**(3)**:** 297-302.

Naso MF, Tomkowicz B, Perry WL, 3rd, Strohl WR (2017). Adeno-Associated Virus (AAV) as a Vector for Gene Therapy. *BioDrugs : clinical immunotherapeutics, biopharmaceuticals and gene therapy* **31**(4)**:** 317-334.

Nathwani AC, Reiss UM, Tuddenham EG, Rosales C, Chowdary P, McIntosh J*, et al.* (2014). Long-term safety and efficacy of factor IX gene therapy in hemophilia B. *The New England journal of medicine* **371**(21)**:** 1994-2004.

Nathwani AC, Rosales C, McIntosh J, Rastegarlari G, Nathwani D, Raj D*, et al.* (2011a). Long-term safety and efficacy following systemic administration of a self-complementary AAV vector encoding human FIX pseudotyped with serotype 5 and 8 capsid proteins. *Molecular therapy : the journal of the American Society of Gene Therapy* **19**(5)**:** 876-885.

Nathwani AC, Tuddenham EG, Rangarajan S, Rosales C, McIntosh J, Linch DC*, et al.* (2011b). Adenovirus-associated virus vector-mediated gene transfer in hemophilia B. *The New England journal of medicine* **365**(25)**:** 2357-2365.

National Institute of Diabetes and Diagestive and Kidney Disease (January 2018). Gastroparesis.

National Institute of Diabetes and Diagestive and Kidney Disease (2014). Intestinal Pseudo-obstruction.

Nemeth L, Maddur S, Puri P (2000). Immunolocalization of the gap junction protein Connexin43 in the interstitial cells of Cajal in the normal and Hirschsprung's disease bowel. *Journal of pediatric surgery* **35**(6)**:** 823-828.

Niemeyer GP, Herzog RW, Mount J, Arruda VR, Tillson DM, Hathcock J*, et al.* (2009). Long-term correction of inhibitor-prone hemophilia B dogs treated with liver-directed AAV2-mediated factor IX gene therapy. *Blood* **113**(4)**:** 797-806.

Nishi S, North RA (1973). Intracellular recording from the myenteric plexus of the guinea-pig ileum. *The Journal of physiology* **231**(3)**:** 471-491.

Nurgali K, Stebbing MJ, Furness JB (2004). Correlation of electrophysiological and morphological characteristics of enteric neurons in the mouse colon. *J Comp Neurol* **468**(1)**:** 112-124.

Okasora T, Bywater RA, Taylor GS (1986). Projections of enteric motor neurons in the mouse distal colon. *Gastroenterology* **90**(6)**:** 1964-1971.

Ormsbee HS, 3rd, Telford GL, Mason GR (1979). Required neural involvement in control of canine migrating motor complex. *The American journal of physiology* **237**(5)**:** E451-456.

Oya M, Kitaguchi T, Yanagihara Y, Numano R, Kakeyama M, Ikematsu K*, et al.* (2013). Vesicular nucleotide transporter is involved in ATP storage of secretory lysosomes in astrocytes. *Biochemical and biophysical research communications* **438**(1)**:** 145-151.

Palmer RK, Boyer JL, Schachter JB, Nicholas RA, Harden TK (1998). Agonist action of adenosine triphosphates at the human P2Y1 receptor. *Molecular pharmacology* **54**(6)**:** 1118-1123.

Park SA, Lee SR, Tung L, Yue DT (2014). Optical mapping of optogenetically shaped cardiac action potentials. *Scientific reports* **4:** 6125.

Parkman HP, Doma S (2006). Importance of Gastrointestinal Motility Disorders. *Pract Gastroenterol* **30**(9)**:** 23-40.

Patrick A, Epstein O (2008). The naked fat sign. *Gastrointest Endosc* **67**(1)**:** 158; commentary 159.

Peery AF, Crockett SD, Murphy CC, Lund JL, Dellon ES, Williams JL*, et al.* (2019). Burden and Cost of Gastrointestinal, Liver, and Pancreatic Diseases in the United States: Update 2018. *Gastroenterology* **156**(1)**:** 254-272 e211.

Peri LE, Sanders KM, Mutafova-Yambolieva VN (2013). Differential expression of genes related to purinergic signaling in smooth muscle cells, PDGFRalpha-positive cells, and interstitial cells of Cajal in the murine colon. *Neurogastroenterology and motility : the official journal of the European Gastrointestinal Motility Society* **25**(9)**:** e609-620.

Pompolo S, Furness JB (1995). Sources of inputs to longitudinal muscle motor neurons and ascending interneurons in the guinea-pig small intestine. *Cell and tissue research* **280**(3)**:** 549-560.

Pompolo S, Furness JB (1988). Ultrastructure and synaptic relationships of calbindin-reactive, Dogiel type II neurons, in myenteric ganglia of guinea-pig small intestine. *Journal of neurocytology* **17**(6)**:** 771-782.

Portbury AL, Pompolo S, Furness JB, Stebbing MJ, Kunze WA, Bornstein JC*, et al.* (1995). Cholinergic, somatostatin-immunoreactive interneurons in the guinea pig intestine: morphology, ultrastructure, connections and projections. *Journal of anatomy* **187 (Pt 2):** 303-321.

Porter AJ, Wattchow DA, Brookes SJH, Costa M (1997). The neurochemical coding and projections of circular muscle motor neurons in the human colon. *Gastroenterology* **113**(6)**:** 1916-1923.

Powell AK, Bywater RA (2001). Endogenous nitric oxide release modulates the direction and frequency of colonic migrating motor complexes in the isolated mouse colon. *Neurogastroenterology and motility : the official journal of the European Gastrointestinal Motility Society* **13**(3)**:** 221-228.

Qayed ES, S.; Shahnavaz, N. (2017). *Sleisenger and Fordtran's Gastrointestinal and Liver Disease*. 10 edn. Elsevier.

Qu ZD, Thacker M, Castelucci P, Bagyanszki M, Epstein M, Furness J (2008a). Immunohistochemical analysis of neuron types in the mouse small intestine. *Cell and tissue research* **334**(2)**:** 147-161.

Qu ZD, Thacker M, Castelucci P, Bagyanszki M, Epstein ML, Furness JB (2008b). Immunohistochemical analysis of neuron types in the mouse small intestine. *Cell and tissue research* **334**(2)**:** 147-161.

Rakhilin N, Barth B, Choi J, Munoz NL, Kulkarni S, Jones JS*, et al.* (2016). Simultaneous optical and electrical in vivo analysis of the enteric nervous system. *Nature communications* **7:** 11800.

Reed DE, Vanner SJ (2001). Converging and diverging cholinergic inputs from submucosal neurons amplify activity of secretomotor neurons in guinea-pig ileal submucosa. *Neuroscience* **107**(4)**:** 685-696.

Ren J, Bertrand PP (2008). Purinergic receptors and synaptic transmission in enteric neurons. *Purinergic signalling* **4**(3)**:** 255-266.

Ren J, Bian X, DeVries M, Schnegelsberg B, Cockayne DA, Ford AP*, et al.* (2003). P2X2 subunits contribute to fast synaptic excitation in myenteric neurons of the mouse small intestine. *The Journal of physiology* **552**(Pt 3)**:** 809-821.

Ren J, Galligan JJ (2007). A novel calcium-sensitive potassium conductance is coupled to P2X3 subunit containing receptors in myenteric neurons of guinea pig ileum. *Neurogastroenterology and motility : the official journal of the European Gastrointestinal Motility Society* **19**(11)**:** 912-922.

Rodrigues GA, Shalaev E, Karami TK, Cunningham J, Slater NKH, Rivers HM (2018). Pharmaceutical Development of AAV-Based Gene Therapy Products for the Eye. *Pharmaceutical research* **36**(2)**:** 29.

Rodriguez-Tapia ES, Naidoo V, DeVries M, Perez-Medina A, Galligan JJ (2017). R-Type Ca(2+) channels couple to inhibitory neurotransmission to the longitudinal muscle in the guinea-pig ileum. *Experimental physiology* **102**(3)**:** 299-313.

Ruckebusch Y, Pairet M, Becht JL (1985). Origin and Characterization of Migrating Myoelectric Complex in Rabbits. *Digestive diseases and sciences* **30**(8)**:** 742-748.

Ruckebush MF, J (1975). Electrical spiking activity and propulsion in small intestine in fed and fasted rats. *Gastroenterology* **68:** 1500-1508.

Rugiero F, Gola M, Kunze WA, Reynaud JC, Furness JB, Clerc N (2002). Analysis of whole-cell currents by patch clamp of guinea-pig myenteric neurones in intact ganglia. *The Journal of physiology* **538**(Pt 2)**:** 447-463.

Russell DW (2003). AAV loves an active genome. *Nature genetics* **34**(3)**:** 241-242.

Sage D, Salin P, Alcaraz G, Castets F, Giraud P, Crest M*, et al.* (2007). Na(v)1.7 and Na(v)1.3 are the only tetrodotoxin-sensitive sodium channels expressed by the adult guinea pig enteric nervous system. *J Comp Neurol* **504**(4)**:** 363-378.

Sakamoto S, Miyaji T, Hiasa M, Ichikawa R, Uematsu A, Iwatsuki K*, et al.* (2014). Impairment of vesicular ATP release affects glucose metabolism and increases insulin sensitivity. *Scientific reports* **4:** 6689.

Samsom M, Bharucha A, Gerich JE, Herrmann K, Limmer J, Linke R*, et al.* (2009). Diabetes mellitus and gastric emptying: questions and issues in clinical practice. *Diabetes/metabolism research and reviews* **25**(6)**:** 502-514.

Sanders KM, Koh SD, Ro S, Ward SM (2012). Regulation of gastrointestinal motility--insights from smooth muscle biology. *Nature reviews. Gastroenterology & hepatology* **9**(11)**:** 633-645.

Sanders KM, Koh SD, Ward SM (2006). Interstitial cells of cajal as pacemakers in the gastrointestinal tract. *Annual review of physiology* **68:** 307-343.

Sanders KM, Ward SM (1992). Nitric oxide as a mediator of nonadrenergic noncholinergic neurotransmission. *The American journal of physiology* **262**(3 Pt 1)**:** G379-392.

Sang Q, Young HM (1996). Chemical coding of neurons in the myenteric plexus and external muscle of the small and large intestine of the mouse. *Cell and tissue research* **284**(1)**:** 39-53.

Sarna SK, Condon R, Cowles V (1984). Colonic migrating and nonmigrating motor complexes in dogs. *The American journal of physiology* **246**(4 Pt 1)**:** G355-360.

Sauer B, Henderson N (1988). Site-specific DNA recombination in mammalian cells by the Cre recombinase of bacteriophage P1. *Proceedings of the National Academy of Sciences of the United States of America* **85**(14)**:** 5166-5170.

Sawada K, Echigo N, Juge N, Miyaji T, Otsuka M, Omote H*, et al.* (2008). Identification of a vesicular nucleotide transporter. *Proceedings of the National Academy of Sciences of the United States of America* **105**(15)**:** 5683-5686.

Sawyer GW, Ehlert FJ (1998). Contractile roles of the M2 and M3 muscarinic receptors in the guinea pig colon. *The Journal of pharmacology and experimental therapeutics* **284**(1)**:** 269-277.

Schemann M, Ehrlein HJ (1986). Mechanical characteristics of phase II and phase III of the interdigestive migrating motor complex in dogs. *Gastroenterology* **91**(1)**:** 117-123.

Scott LD, Summers RW (1976). Correlation of Contractions and Transit in Rat Small-Intestine. *American Journal of Physiology* **230**(1)**:** 132-137.

Serio R, Alessandro M, Zizzo MG, Tamburello MP, Mule F (2003). Neurotransmitters involved in the fast inhibitory junction potentials in mouse distal colon. *Eur J Pharmacol* **460**(2-3)**:** 183-190.

Smedemark-Margulies N, Trapani JG (2013). Tools, methods, and applications for optophysiology in neuroscience. *Frontiers in molecular neuroscience* **6:** 18.

Smith TK, Park KJ, Hennig GW (2014). Colonic migrating motor complexes, high amplitude propagating contractions, neural reflexes and the importance of neuronal and mucosal serotonin. *Journal of neurogastroenterology and motility* **20**(4)**:** 423-446.

Smith TK, Spencer NJ, Hennig GW, Dickson EJ (2007). Recent advances in enteric neurobiology: mechanosensitive interneurons. *Neurogastroenterology and motility : the official journal of the European Gastrointestinal Motility Society* **19**(11)**:** 869-878.

Soffer EE, Thongsawat S, Ellerbroek S (1998). Prolonged ambulatory duodeno-jejunal manometry in humans: normal values and gender effect. *The American journal of gastroenterology* **93**(8)**:** 1318-1323.

Song ZM, Brookes SJ, Costa M (1991). Identification of myenteric neurons which project to the mucosa of the guinea-pig small intestine. *Neuroscience letters* **129**(2)**:** 294-298.

Song ZM, Brookes SJ, Neild TO, Costa M (1997). Immunohistochemical and electrophysiological characterization of submucous neurons from the guinea-pig small intestine in organ culture. *Journal of the autonomic nervous system* **63**(3)**:** 161-171.

Song ZM, Brookes SJ, Steele PA, Costa M (1992). Projections and pathways of submucous neurons to the mucosa of the guinea-pig small intestine. *Cell and tissue research* **269**(1)**:** 87-98.

Sonntag F, Schmidt K, Kleinschmidt JA (2010). A viral assembly factor promotes AAV2 capsid formation in the nucleolus. *Proceedings of the National Academy of Sciences of the United States of America* **107**(22)**:** 10220-10225.

Spencer NJ (2001). Control of migrating motor activity in the colon. *Current opinion in pharmacology* **1**(6)**:** 604-610.

Spencer NJ, Dickson EJ, Hennig GW, Smith TK (2006). Sensory elements within the circular muscle are essential for mechanotransduction of ongoing peristaltic reflex activity in guinea-pig distal colon. *The Journal of physiology* **576**(Pt 2)**:** 519-531.

Spencer NJ, Kyloh M, Wattchow DA, Thomas A, Sia TC, Brookes SJ*, et al.* (2012). Characterization of motor patterns in isolated human colon: are there differences in patients with slow-transit constipation? *American journal of physiology. Gastrointestinal and liver physiology* **302**(1)**:** G34-43.

Spencer NJ, Smith TK (2001). Simultaneous intracellular recordings from longitudinal and circular muscle during the peristaltic reflex in guinea-pig distal colon. *The Journal of physiology* **533**(Pt 3)**:** 787-799.

Stach W (1981). [The neuronal organization of the plexus myentericus (Auerbach) in the small intestine of the pig. II. Typ II-neurone (author's transl)]. *Zeitschrift fur mikroskopisch-anatomische Forschung* **95**(2)**:** 161-182.

Stamp LA, Gwynne RM, Foong JPP, Lomax AE, Hao MM, Kaplan DI*, et al.* (2017). Optogenetic Demonstration of Functional Innervation of Mouse Colon by Neurons Derived From Transplanted Neural Cells. *Gastroenterology* **152**(6)**:** 1407-1418.

Stanton MP, Hutson JM, Simpson D, Oliver MR, Southwell BR, Dinning P*, et al.* (2005). Colonic manometry via appendicostomy shows reduced frequency, amplitude, and length of propagating sequences in children with slow-transit constipation. *Journal of pediatric surgery* **40**(7)**:** 1138-1145.

Sternberg N, Hamilton D (1981a). Bacteriophage P1 site-specific recombination. I. Recombination between loxP sites. *Journal of molecular biology* **150**(4)**:** 467-486.

Sternberg N, Hamilton D, Austin S, Yarmolinsky M, Hoess R (1981b). Site-specific recombination and its role in the life cycle of bacteriophage P1. *Cold Spring Harbor symposia on quantitative biology* **45 Pt 1:** 297-309.

Sternberg N, Hamilton D, Hoess R (1981c). Bacteriophage P1 site-specific recombination. II. Recombination between loxP and the bacterial chromosome. *Journal of molecular biology* **150**(4)**:** 487-507.

Suzuki H, Ward SM, Bayguinov YR, Edwards FR, Hirst GD (2003). Involvement of intramuscular interstitial cells in nitrergic inhibition in the mouse gastric antrum. *The Journal of physiology* **546**(Pt 3)**:** 751-763.

Szurszewski JH (1969). A migrating electric complex of canine small intestine. *The American journal of physiology* **217**(6)**:** 1757-1763.

Szurszewski JH, Ermilov LG, Miller SM (2002). Prevertebral ganglia and intestinofugal afferent neurones. *Gut* **51 Suppl 1:** i6-10.

Tack J, Demedts I, Meulemans A, Schuurkes J, Janssens J (2002). Role of nitric oxide in the gastric accommodation reflex and in meal induced satiety in humans. *Gut* **51**(2)**:** 219-224.

Takahashi T, Owyang C (1998). Regional differences in the nitrergic innervation between the proximal and the distal colon in rats. *Gastroenterology* **115**(6)**:** 1504-1512.

Tamura K, Wood JD (1989). Electrical and synaptic properties of myenteric plexus neurones in the terminal large intestine of the guinea-pig. *The Journal of physiology* **415:** 275-298.

Taylor-Clark TE, Wu KY, Thompson JA, Yang K, Bahia PK, Ajmo JM (2015). Thy1.2 YFP-16 Transgenic Mouse Labels a Subset of Large-Diameter Sensory Neurons that Lack TRPV1 Expression. *PloS one* **10**(3).

Thompson WG (2006). The road to rome. *Gastroenterology* **130**(5)**:** 1552-1556.

Thorneloe KS, Nelson MT (2005). Ion channels in smooth muscle: regulators of intracellular calcium and contractility. *Canadian journal of physiology and pharmacology* **83**(3)**:** 215-242.

Timmermans JP, Barbiers M, Scheuermann DW, Stach W, Adriaensen D, Mayer B*, et al.* (1994). Distribution Pattern, Neurochemical Features and Projections of Nitrergic Neurons in the Pig Small-Intestine. *Ann Anat* **176**(6)**:** 515-525.

Tonini M, De Giorgio R, De Ponti F, Sternini C, Spelta V, Dionigi P*, et al.* (2000). Role of nitric oxide- and vasoactive intestinal polypeptide-containing neurones in human gastric fundus strip relaxations. *British journal of pharmacology* **129**(1)**:** 12-20.

Tozaki-Saitoh H, Tsuda M, Miyata H, Ueda K, Kohsaka S, Inoue K (2008). P2Y12 receptors in spinal microglia are required for neuropathic pain after peripheral nerve injury. *The Journal of neuroscience : the official journal of the Society for Neuroscience* **28**(19)**:** 4949-4956.

Tsien JZ, Chen DF, Gerber D, Tom C, Mercer EH, Anderson DJ*, et al.* (1996). Subregion- and cell type-restricted gene knockout in mouse brain. *Cell* **87**(7)**:** 1317-1326.

Tuladhar BR, Kaisar M, Naylor RJ (1997). Evidence for a 5-HT3 receptor involvement in the facilitation of peristalsis on mucosal application of 5-HT in the guinea pig isolated ileum. *British journal of pharmacology* **122**(6)**:** 1174-1178.

Ueki N, Ide T, Mochiji S, Kobayashi Y, Tokutsu R, Ohnishi N*, et al.* (2016). Eyespot-dependent determination of the phototactic sign in Chlamydomonas reinhardtii. *Proceedings of the National Academy of Sciences of the United States of America* **113**(19)**:** 5299-5304.

Unekwe PC, Savage AO (1991). The Effects of Electrical-Stimulation, Adenosine and Adenosine-5'-Triphosphate (Atp) on Mouse Rectal Muscle. *Pharmacol Res* **23**(4)**:** 389-398.

Unno T, Matsuyama H, Sakamoto T, Uchiyama M, Izumi Y, Okamoto H*, et al.* (2005). M(2) and M(3) muscarinic receptor-mediated contractions in longitudinal smooth muscle of the ileum studied with receptor knockout mice. *British journal of pharmacology* **146**(1)**:** 98-108.

Vannucchi MG, Evangelista S (2018). Experimental Models of Irritable Bowel Syndrome and the Role of the Enteric Neurotransmission. *Journal of clinical medicine* **7**(1).

Wang GD, Wang XY, Hu HZ, Liu S, Gao N, Fang X*, et al.* (2007). Inhibitory neuromuscular transmission mediated by the P2Y1 purinergic receptor in guinea pig small intestine. *American journal of physiology. Gastrointestinal and liver physiology* **292**(6)**:** G1483-1489.

Wang W (2018). Optogenetic manipulation of ENS - The brain in the gut. *Life sciences* **192:** 18-25.

Wang XY, Paterson C, Huizinga JD (2003). Cholinergic and nitrergic innervation of ICC-DMP and ICC-IM in the human small intestine. *Neurogastroenterology and motility : the official journal of the European Gastrointestinal Motility Society* **15**(5)**:** 531-543.

Ward SM, Burns AJ, Torihashi S, Harney SC, Sanders KM (1995). Impaired development of interstitial cells and intestinal electrical rhythmicity in steel mutants. *The American journal of physiology* **269**(6 Pt 1)**:** C1577-1585.

Ward SM, Burns AJ, Torihashi S, Sanders KM (1994). Mutation of the proto-oncogene c-kit blocks development of interstitial cells and electrical rhythmicity in murine intestine. *The Journal of physiology* **480 (Pt 1):** 91-97.

Wattchow DA, Brookes SJ, Costa M (1995). The morphology and projections of retrogradely labeled myenteric neurons in the human intestine. *Gastroenterology* **109**(3)**:** 866-875.

Wattchow DA, Porter AJ, Brookes SJ, Costa M (1997). The polarity of neurochemically defined myenteric neurons in the human colon. *Gastroenterology* **113**(2)**:** 497-506.

Wentz CT, Bernstein JG, Monahan P, Guerra A, Rodriguez A, Boyden ES (2011). A wirelessly powered and controlled device for optical neural control of freely-behaving animals. *Journal of neural engineering* **8**(4)**:** 046021.

Westermark B, Wasteson A (1976). A platelet factor stimulating human normal glial cells. *Experimental cell research* **98**(1)**:** 170-174.

White PN, Thorne PR, Housley GD, Mockett B, Billett TE, Burnstock G (1995). Quinacrine Staining of Marginal Cells in the Stria Vascularis of the Guinea-Pig Cochlea - a Possible Source of Extracellular Atp. *Hearing Res* **90**(1-2)**:** 97-105.

Wilbur BG, Kelly KA (1973). Effect of proximal gastric, complete gastric, and truncal vagotomy on canine gastric electric activity, motility, and emptying. *Annals of surgery* **178**(3)**:** 295-303.

Wrobel C, Dieter A, Huet A, Keppeler D, Duque-Afonso CJ, Vogl C*, et al.* (2018). Optogenetic stimulation of cochlear neurons activates the auditory pathway and restores auditory-driven behavior in deaf adult gerbils. *Science translational medicine* **10**(449).

Xiang ZH, Burnstock G (2005). Distribution of P2Y(2) receptors in the guinea pig enteric nervous system and its coexistence with P2X(2) and P2X(3) receptors, neuropeptide Y, nitric oxide synthase and calretinin. *Histochemistry and cell biology* **124**(5)**:** 379-390.

Zagorodnyuk V, Santicioli P, Maggi CA (1993). Tachykinin NK1 but not NK2 receptors mediate non-cholinergic excitatory junction potentials in the circular muscle of guinea-pig colon. *British journal of pharmacology* **110**(2)**:** 795-803.

Zagorodnyuk VP, Brookes SJ (2000). Transduction sites of vagal mechanoreceptors in the guinea pig esophagus. *The Journal of neuroscience : the official journal of the Society for Neuroscience* **20**(16)**:** 6249-6255.

Zarate N, Spencer NJ (2011). Chronic constipation: lessons from animal studies. *Best practice & research. Clinical gastroenterology* **25**(1)**:** 59-71.

Zhang Y, Lomax AE, Paterson WG (2010). P2Y1 receptors mediate apamin-sensitive and -insensitive inhibitory junction potentials in murine colonic circular smooth muscle. *The Journal of pharmacology and experimental therapeutics* **333**(2)**:** 602-611.

Zhao S, Ting JT, Atallah HE, Qiu L, Tan J, Gloss B*, et al.* (2011). Cell type-specific channelrhodopsin-2 transgenic mice for optogenetic dissection of neural circuitry function. *Nature methods* **8**(9)**:** 745-752.

Zhou X, Galligan JJ (1996). P2X purinoceptors in cultured myenteric neurons of guinea-pig small intestine. *The Journal of physiology* **496 (Pt 3):** 719-729.

Zizzo MG, Mule F, Serio R (2007). Evidence that ATP or a related purine is an excitatory neurotransmitter in the longitudinal muscle of mouse distal colon. *British journal of pharmacology* **151**(1)**:** 73-81.